`

Deliverable 5.1: State-of-the-Art report on the understanding of radionuclide retention and transport in clay and crystalline rocks

Work Package 5

The project leading to this application has received funding from the European Union's Horizon 2020 research and innovation programme under grant agreement No 847593.

Document information

Project Acronym	**EURAD**
Project Title	**European Joint Programme on Radioactive Waste Management**
Project Type	**European Joint Programme (EJP)**
EC grant agreement No.	**847593**
Project starting / end date	**1st June 2019 – 30 May 2024**
Work Package No.	**5**
Work Package Title	**Fundamental understanding of radionuclide retention**
Work Package Acronym	**FUTuRE**
Deliverable No.	**D5.1**
Deliverable Title	State-of-the-Art report on the understanding of radionuclide retention and transport in clay and crystalline host rocks
Lead Beneficiary	**SCK CEN**
Contractual Delivery Date	**M6**
Actual Delivery Date	**M24**
Type	**Report**
Dissemination level	**public**
Authors	**Norbert Maes (SCK CEN), Martin Glaus (PSI), Bart Baeyens (PSI), Maria Marques Fernandes (PSI), Sergey Churakov (PSI), Rainer Dähn (PSI), Sylvain Grangeon (BRGM), Christophe Tournassat (BRGM), Horst Geckeis (KIT), Leurent Charlet (ISTERRE), Felix Brandt (FZJ), Jenna Poonoosamy (FZJ), Alwina Hoving (TNO), Vaclava Havlova (UJV), Andreas Scheinost (HZDR), Cornelius Fischer (HZDR), Ulrich Noseck (GRS), Susan Britz (GRS), Marja Siitari-Kauppi (UH), Tiziana Missana (CIEMAT)**

To be cited as:

Maes N., Glaus M., Baeyens B., Marques Fernandes M., Churakov S., Dähn R., Grangeon S., Tournassat C., Geckeis H., Charlet L., Brandt F., Poonoosamy J., Hoving A., Havlova V., Fischer C., Scheinost A., Noseck U., Britz S., Siitari-Kauppi M., Missana T. (2021): State-of-the-Art report on the understanding of radionuclide retention and transport in clay and crystalline rocks. Final version as of 30.04.2021 of deliverable D5.1 of the HORIZON 2020 project EURAD. EC Grant agreement no: 847593.

Disclaimer

Acknowledgement

This document is a deliverable of the European Joint Programme on Radioactive Waste Management (EURAD). EURAD has received funding from the European Union's Horizon 2020 research and innovation programme under grant agreement No 847593.

Status of deliverable		
	By	Date
Delivered (Lead Beneficiary)	Norbert Maes	29/10/2020
Verified (WP Leader)	Sergey V. Churakov	30/10/2020
Reviewed (Reviewers)	Pierre De Cannière	17/01/2021
Verified (Lead beneficiary and WP Leader)	Norbert Maes and Sergey V. Churakov	30/04/2021
Approved (PMO)	Bernd Grambow	05/05/2021
Submitted to EC (Coordinator)	ANDRA	05/05/2021

Executive Summary

After isolation of radioactive waste in deep geological formations, radionuclides can only enter the biosphere by slow migration. This process typically takes many thousands of years. The rate of transport depends on the distance of the repository from the biosphere and movement of the groundwater, and is mainly governed by the interaction of the dissolved radionuclides with minerals present in the host rock and engineered barrier systems.

The FUTURE project deals with fundamental understanding of retention and transport processes in clay and crystalline host rocks.

This state-of-the-art report aims at providing a comprehensive overview of our current understanding of the underlying processes contributing to the radionuclide retention and migration in clay and crystalline host rocks. For each process, a brief theoretical background is provided together with current methodologies used to study these processes as well as references to key data.

Despite that research on retention and migration has been intensive for some decades and the knowledge is extensive, the process understanding and insights are continuously improving, thanks to innovative research, prompting to adapt and refine conceptual descriptions towards safety assessments. Hence, uncertainties remain and the key uncertainties that presently need to be resolved are listed.

Table of content

List of figures

List of tables

1 Introduction to transport controlling processes in clay and crystalline host rocks

After isolation of radioactive waste in deep geological formations and design based repository closure, radionuclides are expected to only enter the biosphere by slow migration. This process typically takes many thousands of years. The rate of transport depends on the distance of the repository from the biosphere and movement of the groundwater, and is mainly governed by the interaction of the dissolved radionuclides with minerals present in the host rock and engineered barrier systems.

A geological disposal system (GDS) for radioactive waste has to fulfil three main "safety functions": Containment, Isolation and Retention (ONDRAF/NIRAS, 2013).

The host rock, as major part of this system, is expected to contribute to these functions by:

- Providing favourable and stable chemical and mechanical conditions to ensure a good containment on a geological time scale.
- Isolating the waste packages from man and the biosphere.
- Limiting the radionuclide release to the biosphere by a slow transport and sufficient retention in the host rock.

As deep clay and granitic formations offer the perspective to fulfil these three safety functions, they are intensively studied by several countries in Europe.

The FUTURE project deals with fundamental understanding of retention and transport processes of in clay and crystalline host rocks.

Retention processes, in general called "sorption or uptake", depend on the pore water chemistry, which controls the radionuclide speciation and on the reactive surface functional groups, present on the minerals. The most extensively studied "sorption" processes are surface complexation and ion-exchange. Other processes such as surface induced redox uptake, incorporation, surface precipitation and solid-solution formation are less studied. However, they can be important retention mechanisms for a variety of radionuclides and are therefore gaining more attention. Chapter 2 describes these retention processes.

The two main physical mechanisms by which radionuclides migrate in the host rock are diffusion and advection driven by chemical concentration and hydraulic pressure gradients, respectively. Which mechanism predominates depends on the host rock matrix and environmental conditions. This is described in detail in chapter 3 for clay and crystalline host rocks.

In clay host rocks, diffusion is the dominant transport process. The negatively charged clay mineral surfaces not only results in a high retention capacity for cationic radionuclides, but also in a distinct diffusion behaviour of anionic, cationic and neutral species. The most important retention processes are ion-exchange and surface complexation. As clay materials may exhibit strongly reducing properties (i.e., a negative redox potential), due to the presence of reducing mineral phases containing Fe(II) in their crystal structure, surface induced reduction-precipitation in clays has become a field of more intense studies.

In crystalline rocks, solute transport is mainly controlled by advection in open and connected fractures and by matrix diffusion. The latter may be enhanced in weathered/altered zones along the fracture. Moreover, the presence of fracture filling materials, which are composed by clay minerals, Fe-oxy-hydroxides, calcite, etc. may cause retention by different mechanisms such as ion-exchange, surface complexation, surface induced precipitation and solid solution formation.

EURAD Deliverable 5.1 – State-of-the-Art report on the understanding of radionuclide retention and transport in clay and crystalline host rocks

This state-of-the-art report aims at providing a comprehensive overview of our current understanding of the underlying processes that contribute to radionuclide retention and migration in clay and crystalline host rocks. For each process, a brief theoretical background is provided together with current methods used to study these processes as well as references to key data.

Despite that research on retention and migration has been intensive for some decades and the knowledge is extensive, the process understanding and insights are continuously improving, thanks to innovative research, prompting to adapt and refine conceptual descriptions towards safety assessments. Hence, uncertainties remain and the key uncertainties that presently need to be resolved are listed in chapter 4.

2 Retention processes

This chapter on retention processes is split in two sections. In a first section, so-called “classical” retention processes such as ion-exchange and surface complexation are discussed. These two processes are the dominant sorption phenomena and most extensively studied. These processes are described taking clay minerals as an example. In a second section, other relevant but less studied retention processes such as surface induced redox uptake, incorporation, surface precipitation and solid-solution formation are discussed.

2.1 Classical retention processes

To assess the suitability of geological formations as potential host rocks for the deep disposal of high-level radioactive waste world-wide, detailed long-term safety studies are carried out, *e.g.* NAGRA (2002); ONDRAF/NIRAS (2001); POSIVA (2012a); SKB (2011). Classical retention processes (adsorption) of radionuclides on the rock substrate (vs. colloids) in the near- and far-field of the repository are an important component in such safety studies. It is a common practice to treat adsorption in terms of a distribution ratio, R_d, or distribution coefficient, defined as

$$R_d = \frac{C_{sorbed}}{C_{eql}} \tag{2-1}$$

where C_{sorbed} is the radionuclide concentration retained on the solid phase (mol/kg) and C_{eql} is the equilibrium radionuclide concentration in the liquid phase [mol/L]. In the literature most often the term K_d is used (same relationship), but this term entails that the sorption on the solid has linear dependency on the concentration in the solution and is reversible. The sorption databases consisting of the selected K_d values for the safety relevant radionuclides are crucial for the performance assessments of a GDS.

Clay minerals such as montmorillonite and illite (including illite-smectite mixed layers) play an important role in the capacity of the engineered and geological barriers to retain radionuclides in many disposal concepts for radioactive waste, either as part of the host formation (argillaceous rocks), the engineered barrier system (bentonite), or as natural fracture filling materials in crystalline host rocks (see section 3.3.2.3.1). Besides clay minerals, also other minerals exhibit sorption properties. Especially for crystalline rocks, minerals like feldspars, quartz, mica, (hydr)oxides,… are important contributors to radionuclide sorption. The two most important sorption mechanisms are ion-exchange (especially for clays) and surface complexation.

In an ion-exchange process, adsorption of cations is occurring by Coulomb attraction at permanent, negatively charged surface sites. Ion-exchange sites are a typical feature of clay minerals (see also next section where the process of ion-exchange is explained based on the properties of clays). The interaction is electrostatic and mainly results in so-called “outer sphere” complexes. The maximum adsorption capacity by ion-exchange is denoted as cation exchange capacity (CEC) of the mineral or rock. Cation exchange is strongly dependent on the ionic strength through competitive adsorption of the background electrolyte.

Surface complexation is taking place on amphoteric surface groups (>SOH) present in minerals and it is strongly dependent on pH because of the protolysis behaviour of the amphoteric groups (Dzombak and Morel, 1990). In the example of clays, functional groups are either related to Si atoms in the tetrahedral sheets and Al atoms in the octahedral sheets (>SiOH, >AlOH, >Al_2OH, >AlSiOH). These groups are common to edge surfaces of clay minerals (broken bond). Generally, surface complexation leads to the formation of “inner sphere” surface complexes.

The main adsorption mechanisms ion-exchange and surface complexation are graphically illustrated for a 2:1 clay mineral in *Figure 2-1*. Ion-exchange takes place on the permanent charged planar sites in the interlayer and surface complexation takes place at amphoteric sites at the edges.

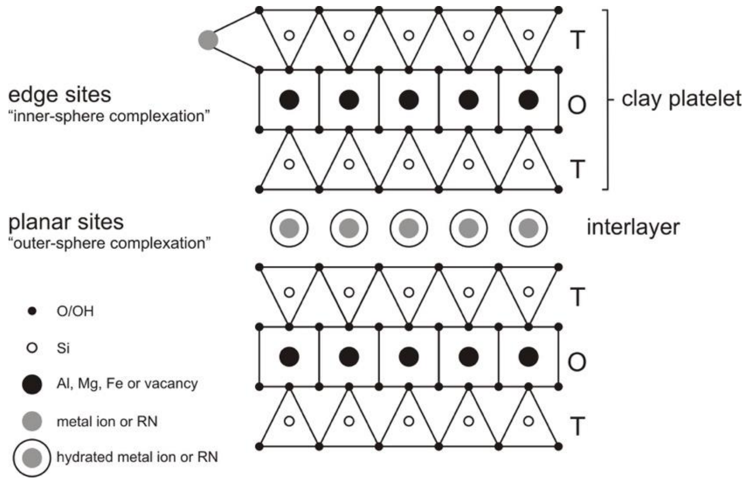

Figure 2-1 – Graphical representation of the structure of 2:1 clay minerals and the different adsorption sites. Taken from Marques Fernandes et al. (2012).

In the next section, the ion-exchange and surface complexation are discussed using clay minerals as example substrate because they prevail in argillaceous rocks and fracture fillings in crystalline rocks. The sorption of rock forming minerals is treated in section 3.3.2.3.1.

Various sorption-modelling approaches are discussed and information on the atomistic nature of these classical adsorption mechanisms is addressed.

2.1.1 Ion-exchange

2.1.1.1 Theory and current understanding

The surfaces of clay mineral platelets (see also 3.2.1 for more background on clay structural properties) carry a permanent negative charge arising from isomorphous substitution of the main lattice cations by another cations of a lower valency, e.g. Si(IV) by Al(III) in the tetrahedral layer and Al(III) by Mg(II) or Fe(II) in the octahedral layer (Liu et al., 2015b; Liu et al., 2012b; Liu et al., 2013; Liu et al., 2014b). Charge neutrality is maintained by the presence of an excess of cations in solution held electrostatically in close proximity of the clay surface. The electrostatically bound cations, which constitute the electrical double layer, can undergo stoichiometric exchange with the cations in solution. This permanent negative charge of a clay mineral gives rise to the so-called cation exchange capacity (CEC) (e.g. Grimm (1953); Van Olphen (1963)). The CEC of montmorillonites (smectitic or swelling clay, with full access to the interlayer) are ~1 equiv/kg, and of illites (non-swelling clay with only access to the outer surface) ~0.2 equiv/kg. Note that in the latter case a large part of the structural charge is neutralised by collapsed K which is not readily available for cation exchange. By expressing the CEC in equivalent per unit mass the value is independent of the charge of the exchangeable cations compensating for the negative surface charge arising from isomorphous substitution in the clay mineral matrix. On this convention the Gaines and Thomas formalism (Gaines and Thomas, 1953) is based. The description of the mass law action equations is expressed by a selectivity coefficient (K_c). Another well-known expression for the description of cation exchange processes is given by the Vanselow (Vanselow, 1932) selectivity coefficient (K_v). The main difference between the two approaches is that K_c is based on the equivalent fraction scale whereas K_v uses the molar fraction scale for the cations on the exchange complex. The current understanding of ion-exchange in clay minerals is high because it has been a subject of research since the end of the 19th century.

2.1.1.2 Ion-exchange models

Law of mass action models: Cation exchange reactions are often expressed in terms of a selectivity coefficient obtained by the application of the mass action law. The cation exchange reaction of a metal B, of valence z_B, exchanging with a metal A, of valence z_A, on a clay mineral in the A-form, can be written as:

$$z_B A^{z_A} - clay + z_A B^{z_B} \Leftrightarrow z_A B^{z_B} - clay + z_B A^{z_A} \qquad (2\text{-}2)$$

Following the convention given by Gaines and Thomas (1953), a selectivity coefficient, ${}_A^BK_c$ [-], for reaction (2-2) can be defined as:

$${}_A^BK_c = \frac{(N_B)^{z_A}}{(N_A)^{z_B}} \cdot \frac{[A]^{z_B}}{[B]^{z_A}} \cdot \frac{(\gamma_A)^{z_B}}{(\gamma_B)^{z_A}} \qquad (2\text{-}3)$$

Where N_A and N_B are the equivalent fractional occupancies, defined as the equivalents of A (or B) sorbed per kg of clay divided by the cation exchange capacity, CEC [equiv/kg]. [*A*] and [*B*] are the aqueous concentrations [mol/L], γ_A and γ_B represent the aqueous phase activity coefficients [-].

A selectivity coefficient can be derived from experimental data at trace *B* concentrations (N_A ~ 1), using:

$${}_A^BK_c = \left({}^BR_d\right)^{z_A} \frac{(z_B)^{z_A}}{(CEC)^{z_A}} . [A]^{z_B} . \frac{(\gamma_A)^{z_B}}{(\gamma_B)^{z_A}} \qquad (2\text{-}4)$$

where ${}^BR_d$ [m³/kg] represents the sorption of cation *B* by cation exchange defined as the number of moles of *B* sorbed by unit mass of the solid phase divided by the number of moles of *B* in the aqueous solution per unit volume.

An extensive literature review of cation exchange on clay minerals has been compiled by Bruggenwert and Kamphorst (1982). In their survey cation exchange constants K_c (Gaines and Thomas, 1953), or K_v (Vanselow, 1932) are listed and can be easily incorporated in geochemical computer codes to model cation exchange. A tabulation and evaluation of ion-exchange data on smectites have been carried out by Benson (1982). Data are presented as log(*K*) values and reflect very well the ranges found for some common ion equilibria on smectite.

More recent studies on cation exchange studies are from Charlet and Tournassat (2005); Tournassat et al. (2011); Tournassat et al. (2009); Tournassat et al. (2007); Tournassat et al. (2008).

In the case of illite there are very specific type of exchange sites, often called frayed edge sites (FES), which have a high affinity to (and are only accessible by) alkali metals because of their specific ionic size matching the surface structure. Brouwer et al. (1983) have developed a three-site (FES, type II and planar sites) cation exchange model for Cs and Rb sorption on illite. This model has been extended to a generalised Cs sorption model (Bradbury and Baeyens, 2000) to predict Cs sorption isotherms for argillaceous rocks. Recently, this three site cation exchange model could be implemented for Tl^+ adsorption on illite (Wick et al., 2018). Non-linear sorption of Cs has been also observed in some smectites, attributable to the presence of randomly interstratified illite–smectite mixed layers, providing highly selective sorption sites for alkaline metals. This behaviour could be modelled considering a two-site exchange model accounting for sorption on planar and FES-like sites (Missana et al., 2014).

An overview of cation exchange systems relevant to geological disposal is given in *Table 2-1* together with information on surface complexation (see section 2.1.2).

Atomistic cation exchange models: Atomistic simulations are widely used to elucidate the hydration and adsorption mechanisms of ions in the interlayer of clay particles and the structure of the electric double layer at the basal plane of clay minerals. Such simulations are performed using Molecular Dynamics and Monte Carlo approaches. In molecular dynamics simulations trajectories of ions and molecules are obtained by solving Newton's equation of motion for all atoms in the system. Thermodynamic averages are obtained by time and ensemble averaging of the simulated trajectory. In the Monte Carlo technique, the equilibrium distribution of ions is obtained by stochastic modification of atomic positions following Markov Chain stochastic process. The thermodynamic and structural parameters are obtained by averaging uncorrelated atomic configurations. The most important factor controlling the accuracy of the simulation are the underlying model for interatomic interactions and surface models used in the simulations. Most of the simulations are performed using so called empirical pair interaction potentials. Such an approach provides a compromise between accuracy and computational efficiency. Only a few studies are known using a quantum mechanical system description (see Churakov and Liu (2018) for an exhaustive review). Most popular and widely used force fields for the simulations of clay minerals are CLAYFF (Cygan et al., 2004), INTERFACE (Heinz et al., 2013) and OPLS (Jorgensen and Tirado-Rives, 1988). These empirical force fields can in principle be combined with a variety of models for water (Guillot, 2002) and ions (Aqvist, 1990). Several efforts are undertaken to develop, so-called polarisable force field, which take into account the electronic polarisation of electron shells depending on the instantaneous atomic configuration (Tesson et al., 2016).

The investigation of cation exchange in molecular simulations are based on calculations of equilibrium distributions of ions between the interlayer space and the bulk electrolyte in direct simulations with interface (Lammers et al., 2017) or by thermodynamic integration without interface (Rotenberg et al., 2009).

2.1.2 Surface complexation

2.1.2.1 Theory and current understanding

Different thermodynamic sorption models (TSM) have been introduced to describe the solid-solution interface during sorption processes (Ochs et al., 2012). Thermodynamic sorption models used to calculate defined surface complexation processes of e.g. metal cations (Me) are called surface complexation models (SCMs). Each SCM is characterized by an individual set of surface complexation parameters (SCPs) defining the mechanistic approach to describe retardation processes at the solid-solution interface. These parameters comprise surface complexation constants (logK_{Me}), the specific surface area (SSA), surface site density (SSD), and protolysis constants (logK_{prot}) that describe acid-base characteristics of each mineral surface (Britz, 2018). TSMs extend the ion-association theory of aqueous species to surface species through thermodynamic equilibrium reactions using measurements of SSAs and estimated SSDs. Besides the commonly applied diffuse double layer model (DDLM) and non-electrostatic models (noEDLM), more sophisticated model approaches exist such as the basic Stern model (BSM), triple layer models, and three plane models (TPMs) which are widely used thermodynamic sorption models. All thermodynamic sorption models are based on mass law equations and mole balance equations (Davis and Kent, 1990a), but involve different descriptions of the electric double layer, i.e. an electrostatic interaction term (Davis and Kent, 1990b; Westall and Hohl, 1980). In the noEDLM the electrostatic interaction term is not considered at all; thus, the diffuse double layer is neglected. Each thermodynamic sorption model (except noEDLMs) considers different electrostatic planes that are prone to sorption processes.

2.1.2.2 Surface complexation models

Acid base modelling of minerals:

The protolysis behaviour of the amphoteric surface hydroxyl sites are usually described by following protonation and deprotonation reactions with their corresponding mass action relationship:

$$\equiv SOH + H^+ \Leftrightarrow \equiv SOH_2^+ \qquad K^+ = \frac{[\equiv SOH_2^+]}{[\equiv SOH]\{H^+\}} \tag{2-5}$$

$$\equiv SOH \Leftrightarrow \equiv SOH^- + H^+ \qquad K^- = \frac{[\equiv SOH^-]\{H^+\}}{[\equiv SOH]} \tag{2-6}$$

where [ ] represents molar concentration and { } denotes activities.

Note that the above mass action equations are written without an electrostatic term. In electrostatic models (see *Table 2-2*) an additional electrostatic term is included in the equations, which accounts for the distribution of the ions in the double layer according to Maxwell-Boltzmann equation (e.g. (Dzombak and Morel, 1990)).

We like to refer to two comprehensive review papers on this subject related to clay minerals. The first by Duc et al. (2005) gives a substantial overview of the experimental difficulties/constraints regarding titration measurements and their influence on modelling. The second review is by Bourg et al. (2007) giving an overview of available protolysis models. This compilation contains *pK* data, site densities and specific edge surface areas from 12 different studies on acid-base titration models of Na-montmorillonite.

The site types, their density and the protolysis constants can vary in the various model approaches from one single site up to 27 sites (Tournassat et al., 2004a; Tournassat et al., 2004b). In general, two sites are considered and are associated to the tetrahedral silanol sites and the octahedral aluminol sites.

Table 2-1 lists a number of selected model approaches on the acid/base behaviour of clay minerals, which are isolated from metal sorption data and can only be used for describing the proton buffer capacity of clay minerals.

Sorption of anions:

Sorption of anionic species generally takes place via a ligand exchange mechanism. For example, the sorption of boron on the edge sites of montmorillonite, illite and kaolinite was modelled by Goldberg and Glaubig (1986) by means of the following reaction:

$$\equiv SOH + H_3BO_3 \Leftrightarrow \equiv SH_2BO_3 + H_2O \tag{2-7}$$

with associated mass action equation:

$$K = \frac{[\equiv SH_2BO_3]}{[\equiv SOH][H_3BO_3]} \tag{2-8}$$

In this study the boron sorption on the three clay minerals was modelled either by fitting protolysis constants to the tetrahedral silanol sites and the octahedral aluminol sites, and, by using protolysis constants from Al and Fe oxides (Goldberg and Sposito, 1984).

Modelled sorption data of anions on clay minerals are very sparse in the open literature. Most of the studies has been completed for B(III), Mo(VI), Se(IV) and As(V) uptake on montmorillonite and illite (Goldberg and Glaubig, 1986, 1988b, a; Manning and Goldberg, 1996; Motta and Miranda, 1989). More recently Bruggeman (2006) investigated the uptake of Se(IV/VI) on illite and was capable to apply a non-electrostatic model (NEM) to quantitatively describe the pH dependent adsorption of the anionic species using both wet chemistry and spectroscopic methods. Missana et al. (2009) investigated selenite sorption on smectite and illite and modelled the sorption behaviour on smectite/ illite mixtures with a two-site non-electrostatic model.

Sorption of cations:

The general form of the surface complexation equations used for surface binding of cations can be written as:

$$\equiv SOH + Me^{z+} + yH_2O \Leftrightarrow \equiv SOMe(OH)_y^{z-(y+1)} + (y+1)H^+ \quad (2\text{-}9)$$

where *Me* is a metal with valency *z*, *y* is an integer, and the corresponding surface stability constant is expressed as K_y. For $y = 0$ the surface complex is $\equiv SOMe^{(z-1)}$.

In a non-electrostatic model, the corresponding surface complexation constant, K_y can be expressed as:

$$K_y = \frac{\left[SOMe(OH)_y^{z-(y+1)}\right]}{[\equiv SOH]} \cdot \frac{f_{\equiv SOMe(OH)_y^{z-(y+1)}}}{f_{\equiv SOH}} \frac{\{H^+\}^{y+1}}{\{Me^{z+}\}} \quad (2\text{-}10)$$

where [ ] terms are surface concentrations, f terms are surface activity coefficients, and { } terms are aqueous activities. Following the discussions given in Dzombak and Morel (1990), the same assumption concerning surface activity coefficients is made here i.e. the ratio of the surface activity coefficients in the mass action equations describing the surface complexation reactions is taken to be unity.

The model developed for montmorillonite and illite, the 2 site protolysis non-electrostatic surface complexation and cation exchange, 2SPNE SC/CE, (Bradbury and Baeyens, 1997a; Bradbury and Baeyens, 2009a) can be used to illustrate the modelling approach using the following three data sets, i.e.:

- clay acid/base titration data,
- sorption edges (trace sorption as a function of pH at fixed ionic strength),
- sorption isotherms (concentration dependent sorption at fixed pH and fixed ionic strength).

A consequent iterative process was applied to model all three data sets until all experimental measurements were satisfactorily described (see *Figure 2-2*). The model results were described with site capacities (two weak protolysis sites ($\equiv S^{W1}OH$), ($\equiv S^{W2}OH$) and one strong site ($\equiv S^{S}OH$) for metal sorption at trace concentration), protolysis constants, cation exchange capacities, cation exchange selectivity's and surface complexation constants for strong and in some cases weak sites. Furthermore, there were enough elements investigated so that linear free energy relations could be derived for cation sorption (Bradbury and Baeyens, 2005b, a).

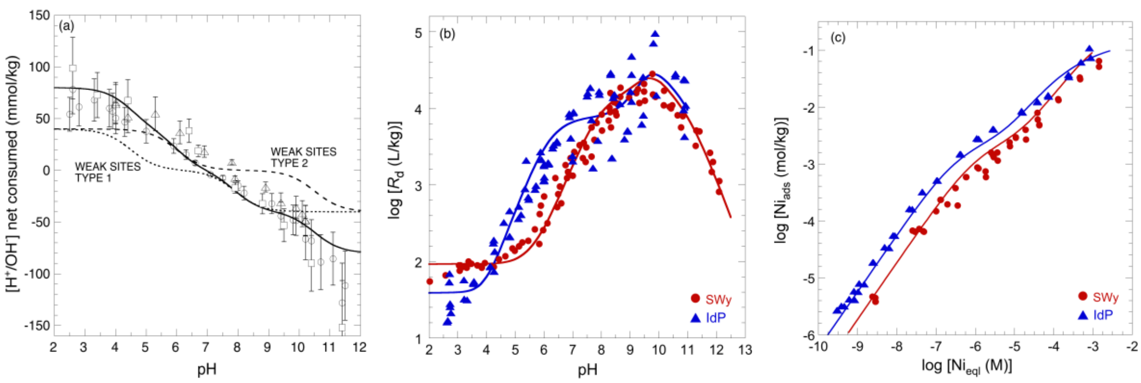

Figure 2-2 – Example of the non-electrostatic modelling of (a) acid/base behaviour of montmorillonite, (b) sorption edges and (c) isotherms of Ni on illite (IdP – illite du Puy) and montmorillonite (Swy – smectite Wyoming). Taken from Baeyens and Marques Fernandes (2018).

It is now well documented that montmorillonite edges have unique electrostatic potential characteristics, which are not similar to electrostatic potentials at simple oxide surfaces (Bourg et al., 2007; Tournassat et al., 2016b; Tournassat et al., 2013; Tournassat et al., 2018). In aqueous suspension, because of the large aspect ratio of montmorillonite layers and of the presence of a permanent basal surface charge, the edge surface potential is affected by the charge density at both edge and basal surfaces depending on ionic strength and on the number of stacked layers in a single particle (*Figure 2-3*). The influence of the basal surface charge on the edge surface potential is named the spillover effect (Chang and Sposito, 1994, 1996). The spillover effect has a significant influence on the adsorption properties of clay edges.

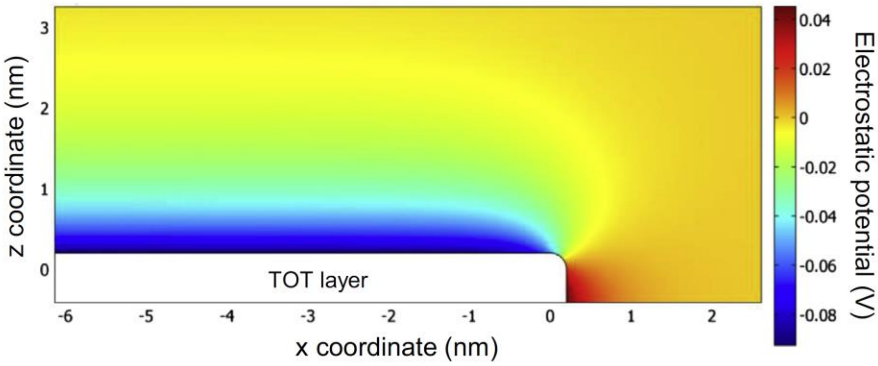

Figure 2-3 – Mutual influences of the edge and basal surface charge on the electrostatic potential developing in the vicinity of the edge surface of a montmorillonite layer. The colour scale corresponds to the potential value (in V) calculated at an ionic strength of 0.1 for a uniform basal charge density of -0.109 C/m² and an edge charge density of 0.1 C/m². Figure from Tournassat et al. (2013).

A more atomistic/crystallographic approach towards surface complexation phenomena on clay mineral edges has been recently proposed by various authors. The crystallographic orientation of the edge surfaces and the existence of various functional groups on these surfaces are also important parameters. Although there is some uncertainty about the crystallographic orientations of the edges, different analysis and measurements demonstrated that the most stable edge surfaces are perpendicular to [010] and [110] crystallographic directions (Bickmore et al., 2001; Churakov, 2006; Kraevsky et al., 2020; Newton and Sposito, 2015; Tournassat et al., 2016b). Functional groups are either associated with Si atoms in the tetrahedral sheets or Al atoms in the octahedral sheets (>SiOH, >AlOH, >Al_2OH, >AlSiOH). Tournassat et al. (2016b) developed a generic surface complexation model for the montmorillonite edge surfaces perpendicular to [010] and [110] in order to simulate the acid base chemistry of montmorillonite. On each surface, they defined five possible edge surface functional groups including two tetrahedral and one octahedral cation with their associated OH groups as following Si_T-Al_{Oc}-Si_T (S_aOH), Si_T-Mg_{Oc}-Si_T (S_bOH), Al_T-Al_{Oc}-Si_T (S_cOH), Si_T-Fe(II)$_{Oc}$-Si_T (S_dOH), Si_T-Fe(III)$_{Oc}$-Si_T (S_eOH) (*Figure 2-4*). Their site densities were calculated from reported clay unit cell formula and electrostatic potential of the edge surfaces (ψ_{edge}) were calculated by using the following formula (Bourg et al., 2007; Tournassat et al., 2016b):

$$\frac{F\psi_{edge}}{RT} = A_1 \operatorname{asinh}\left(A_2\left(Q_{edge} + A_3\right)\right) \qquad (2\text{-}11)$$

where F is the Faraday constant [96485 C/mol], R is the ideal gas constant [8.314 J/mol K], T is temperature [K], Q_{edge} is the surface potential [V], A_1, A_2 and A_3 are fitted parameters (A_1=1.4 -1.2 log I, A_2= 11 + log I and A_3= -0.02 × (-log I)$^{1.60}$ where I is the ionic strength (dimensionless)). The pK_a values of the surface functional groups were obtained from First Principle Molecular Dynamics calculations (Liu et al., 2012, 2013, 2014, 2015). Titration data were reproduced with this model without adjustment of parameters from ab initio simulations. This surface complexation model was then successfully applied to simulate the adsorption of U(VI) onto montmorillonite surfaces in a range of chemical conditions (Tournassat et al., 2018b).

An overview of cation exchange and surface complexation models of anionic and cationic species for geological disposal relevant elements on 2:1 clay minerals is given in *Table 2-1*.

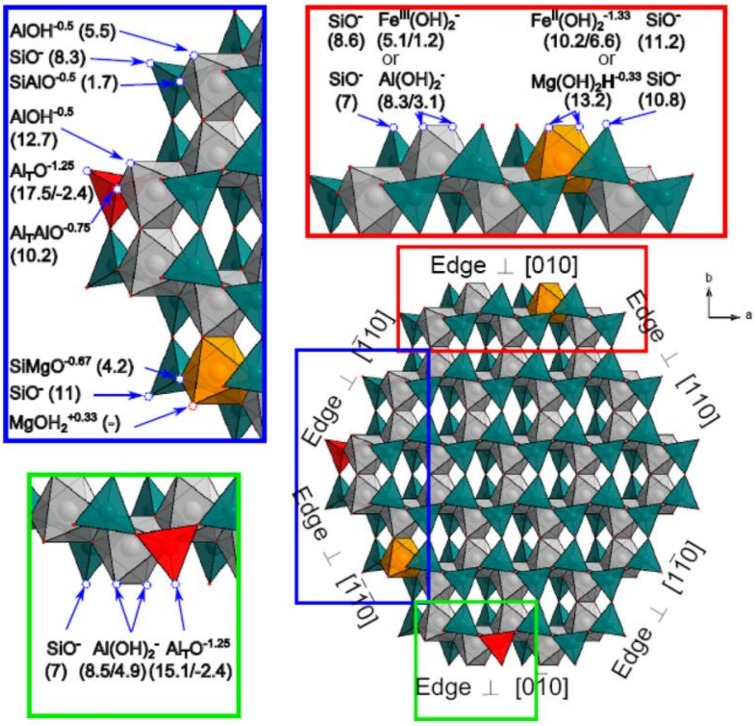

Figure 2-4 – Edge surface sites of a model montmorillonite particle. Insets with red and green borders describe sites on the B edge. The inset with a blue border describes sites on the AC edge. Grey octahedra, Al or Fe(III); orange octahedra, Mg or Fe(II); green tetrahedra, Si; red tetrahedra, Al. Isomorphic substitutions are only shown if they occur at the edge surface. The stoichiometry's of the deprotonated sites are written on the figure along with numbers corresponding to the log K values of the associated protonation reactions predicted by ab initio MD calculations. Figure from Tournassat et al. (2016).

Table 2-1 – Overview of cation exchange and surface complexation models on 2:1 clay minerals.

Clay	Model	Proto-lysis	SC	CE	Cations	Reference
bentonite, zeolites	CE	-	-	K_v	Na^+, K^+, NH_4^+, Ca^{2+}, Ba^{2+}	Vanselow (1932)
montmorillonite	CE	-	-	K_c	Cs^+, K^+, Sr^{2+}	Faucher and Thomas (1954); Gaines and Thomas (1955)
montmorillonite	CE	-	-	K_c	Na^+, Co^{2+}, Ni^{2+}, Cu^{2+}, Zn^{2+}, Cd^{2+}	Maes et al. (1975)
illite	CE	-	-	K_c	Na^+, Rb^+, Cs^+, Tl^+, Ca^{2+}, Sr^{2+}, Ba^{2+}	Brouwer et al. (1983); Poinssot et al. (1999); Wick et al. (2018)
montmorillonite	CE	-	-	K_c	Na^+, Fe^{2+}	Singhal and Kumar (1975)
montmorillonite	CCM		1 site	-	H^+	Wanner et al. (1994)
montmorillonite	DDLM		1 site	-	H^+	Kraepiel et al. (1998)
montmorillonite	MUSIC		4 sites	-	H^+	Tournassat et al. (2004b)
illite	GEMS		2 sites		H^+, Ln	Sinitsyn et al. (2000) Kulik et al. (2000)
montmorillonite illite	2SPNE SC/CE	2 pK_a	strong/ weak	K_c	Ni(II), Zn(II), Eu(III), Sn(IV), Am(III), Np(V), U(VI)	Baeyens and Bradbury (1997); Bradbury and Baeyens (1997a); Bradbury and Baeyens (2009a, 2009b)
montmorillonite	EM/CE SC	2 pK_a	strong/ weak	K_{ex}	Ni(II), Zn(II)	Kraepiel et al. (1999)
montmorillonite		4 pK_a	≡AlOH ≡SiOH	K_{ex}	UO_2^{2+}	McKinley et al. (1995)
montmorillonite	spillover				UO_2^{2+}	Tournassat et al. (2018)
montmorillonite	EM/CE SC	2 pK_a	1 site K_{SOM}	K_{ex}	Pb(II), Cd(II)	Barbier et al. (2000)
montmorillonite	DLM	3 pK_a (two ≡AlOH, ≡SiOH)	≡AlOH ≡SiOH	neglected I = 0.1	Np(V)	Turner et al. (1998)
montmorillonite silica alumina	EM CCM	3 pKa (K_{A1}, K_{Si1} and K_{Si2}	≡AlOH ≡SiOH	K_{ex}	Eu^{3+}; UO_2^{2+}	Kowal-Fouchard et al. (2004a); Kowal-Fouchard et al. (2004b)
bentonite	DLM	3 pK_a	1 site	n.i.	U(VI), Se(IV)	Boult et al. (1998)
beidellite	TLM		2 sites ≡AlOH ≡SiOH	K_{ex}	UO_2^{2+}	Pabalan and Turner (1996)

SC: surface complexation; CE: cation exchange; K_v: Vanselow constant; K_c: Gaines & Thomas selectivity constant; K_{ex}: cation exchange constant; CCM: Constant capacitance modelling; EM: Electrostatic modelling; DLM: Diffuse layer model (Dzombak and Morel, 1990); ECCM: (Extended) constant capacitance model (Nilsson et al., 1996); TLM: Triple-layer model (Hayes et al., 1991); MUSIC: Multi-site complexation model (Hiemstra et al., 1996); GEMS: Gibbs energy minimization selector (http://gems.web.psi.ch/).

2.1.2.3 Atomistic acid/base and surface complexation models

Intrinsic acidity of the surface OH groups is one of most important parameters controlling the development of surface charge on the edge sites of clay particles as a function of pH. The intrinsic acidity depends on the structural position of OH group and the isomorphic substitutions in the TOT sheet. Significant progress has been recently made in understanding the stability and structure of edge sites in clay minerals (Churakov, 2006; Churakov, 2007; Keri et al., 2020; Liu et al., 2012b; Okumura et al., 2017). These data were used to investigate the acidity of the surface groups using ab initio simulation techniques (Liu et al., 2015b; Liu et al., 2013; Liu et al., 2011; Liu et al., 2014b). The essence of the method is the calculation of free energy for the proton transfer reaction in the presence of explicit solvent molecules:

$$\equiv SOH_n^p + H_2O_{aq} \leftrightarrow \equiv SOH_{n-1}^{p-1} + H_3O_{aq}^+ \tag{2-12}$$

using thermodynamic integration techniques. The site acidities obtained in such a way represent, so-called intrinsic *pK*'s, corresponding to the deprotonation reaction of an isolated >SiOH site in pure water on an "ideal" charge neutral surface. To describe experimental data, these constants have to be combined together with an electrostatic model "analytical" or one based on molecular simulations, which accounts for interaction between the surface charge and the ions in the electrolyte solution using thermodynamic integration techniques.

Table 2-2 summarises currently available data obtained by ab initio simulations for different clay minerals.

Table 2-2 – pK_a's of edge sites for individual surfaces of phyllosilicates, modified and augmented after Churakov and Liu (2018).

Surfaces	Sites	p*K*a's	Reference
Pyrophyllite/Montmorillonite			
(110) Neutral	≡Si(OH$_2$)/≡Si(OH)	-6.8/8.3	(Liu et al., 2014b)
	≡AlSiOH	1.7	
	≡Al(OH$_2$)	5.5	
(110) Mg-sub	≡Si(OH$_2$)/≡Si(OH) (connecting Mg via O)	-2.5/11.0	
	≡MgSiOH	4.2	
(110) Al-sub	≡Al(OH$_2$)$_{Tetra}$ /≡Al(OH)$_{Tetra}$	-2.4/17.5	
	≡AlAlOH	10.2	
	≡Al(OH$_2$)$_{Octa}$	12.7	
(010) Neutral	≡Si(OH$_2$)/≡Si(OH)	-14.3/7.0 6.8	(Liu et al., 2013; Tazi et al., 2012)
	≡Al(OH$_2$)(OH$_2$)$_{Octa}$ /≡Al(OH$_2$)(OH)$_{Octa}$	3.1/8.3 7.6/22.01	(Liu et al., 2014b; Tazi et al., 2012)
(010) Mg-sub	≡Si(OH$_2$)/≡Si(OH) (connecting Mg via O)	-10.9/10.8	(Liu et al., 2013)
	≡Mg(OH$_2$)$_2$	13.2	
(010) Al-sub	≡Al(OH$_2$)$_{Tetra}$ /≡Al(OH)$_{Tetra}$	-2.4/15.1	(Liu et al., 2014b)
	≡Al(OH$_2$)(OH$_2$)$_{Octa}$ /≡Al(OH$_2$)(OH)$_{Octa}$	4.9/8.5	
(010) Fe(III)	≡Si(OH)	8.6	(Liu et al., 2015a)
	≡Fe(OH$_2$)(OH$_2$)/≡Fe(OH$_2$)(OH)	1.2/5.1	
(010) Fe(II)	≡Si(OH)	11.2	
	≡Fe(OH$_2$) [5-fold] /≡Fe(OH$_2$)(OH$_2$) [6-fold]	6.6/10.2	
Nontronite			
(010) Fe(III)	≡Si(OH)	8.7	(Liu et al., 2015a)
	≡Fe(OH$_2$)(OH$_2$) /≡Fe(OH$_2$)(OH)	1.2/4.4	
(010) Fe(II)	≡Si(OH)	9.9	
	≡Fe(OH$_2$) [5-fold]	8.4	

Ab initio simulations have been applied to reveal energetically favourable configuration of surface complexing ions on the edge surfaces of phyllosilicate minerals (*Table 2-3*). Most of the studies are performed for the simple structural prototype pyrophyllite (pyrophyllite has no structural charge). The general conclusions about the sorption mechanism should be transferable to other clay minerals, however. The extent and the distribution of the surface charge has a strong influence on the strength of the ion-surface interactions.

Thermodynamic sorption models described in previous sections rely on the existence of at least two sorption sites (Baeyens and Bradbury, 1997; Bradbury and Baeyens, 1997a). These sites are referred to as strong and weak sites, which can be related to the higher and lower affinity constants of the surface complexation reaction. The ab initio simulations combined with X-ray absorption spectroscopy (XAS) studies specifically address the molecular structure of such sorption sites. It could be shown that for divalent and trivalent transition metals the high affinity sites are represented by etch pits (single atom defects) on the edge of clay minerals. The weak sites in the thermodynamic sorption model are structurally related to the inner-sphere sorption complexes on the edge surfaces (Churakov and Daehn, 2012; Keri et al., 2020). The structure and site density of the cationic surface complexes obtained by ab initio simulations is consistent with the spectroscopic data and thermodynamic simulations, respectively.

Table 2-3 – Ab initio surface studies of sorption complexation mechanism of cation on edges of clay minerals.

Mineral	**Cation**	**References**
Montmorillonite	Zn^{2+}	(Churakov and Daehn, 2012)
Pyrophyllite	Fe^{2+}/Fe^{3+}	(Keri et al, 2020)
Pyrophyllite	Fe^{2+}	(Liu et al., 2014a; Liu et al., 2012a; Liu et al., 2013)
Pyrophyllite	Cd^{2+}/Ni^{2+}	(Zhang et al., 2016; Zhang et al., 2017)
Kaolinite / pyrophyllite / illite	UO_2^{2+}	(Kremleva et al., 2011; Kremleva et al., 2015a; Kremleva et al., 2015b; Kremleva et al., 2012)

2.1.2.4 Reversibility

The analysis of radionuclide desorption behaviour is essential for evaluating the (ir)reversibility of sorption processes in order to predict the long-term migration behaviour of radionuclides.

Desorption tests are typically performed following sorption tests. In the sorption step, after the selected contact time, the solid-to-liquid distribution coefficient, $R_{d,sorb}$ is determined. The solid in which the adsorbate is retained, can be suspended again in a fresh solution to determine the distribution coefficient for the desorption step $R_{d,desorb}$. When the sorption and desorption times are the same, and $R_{d,sorb}$ is identical to $R_{d,desorb}$, sorption is considered as "reversible", if not, as "irreversible".

The reasons why retention is reversible (or not) are multiple and must be evaluated in detail. In some of the cases, the irreversibility is only apparent because the sorption and desorption processes were not at equilibrium. However, the hysteretic behaviour might indicate that other reactions than sorption are taking place, which contribute to the overall retention in the system.

A hysteretic sorption behaviour does not necessarily mean that part of the contaminant is "fixed" and could not be desorbed at all from the solid, but just that its release will be kinetically controlled. The main mechanism leading to contaminant retention in a mineral surface is adsorption, which is generally rapid and reversible. However, several kinetically controlled processes also exist contributing to slower uptake, such as diffusion processes inside the solid where the formation of stronger bonds and the crystallization of new phases can occur (Sparks, 2003). In addition, aging can have a significant effect on contaminant release. These processes are usually not included in surface complexation modelling.

The importance of the “reaction time” and kinetically controlled processes increases when dynamic phenomena (diffusion, advective-dispersive transport) must be described. An apparently “irreversible” process for short residence times can be completely reversible on the long-time scales considered in safety assessment for radioactive waste repositories.

Amongst the most important processes contributing to irreversible sorption on clays is the formation of surface precipitates incorporating and sequestrating the contaminant (see also section 2.2, other uptake processes). The identification and characterization of surface precipitates is an important task which has to be accomplished by microscopic and spectroscopic techniques (Ford et al., 2001; Scheidegger et al., 1997).

Structural modifications within the layered structure of phyllosilicates (clays) can lead to irreversible retention of contaminants. Many recent studies have been devoted to the analysis of irreversible sorption of Cs into illite focusing on processes favouring its fixation caused by the collapse of the frayed edge sites, and their de-lamination favoured in the presence of divalent ions (Benedicto et al., 2014c; Durrant et al., 2018; Fuller et al., 2015).

One of the key parameters determining the reversibility of the surface complexation on edges of clay minerals on an atomistic scale is the structural evolution of the mineral surface as part of dissolution and precipitation processes. These processes determine the availability of high affinity sorption sites and the structural (irreversible) incorporation of cations. Ab initio simulations can provide direct information on the dissolution process for individual surface sites (Schliemann and Churakov, 2021). The macroscopic description of these data needs a global view of the temporal evolution of site density. Such information can be obtained using course grain models for clay particle dissolution and growth and the mineral-fluid interaction (Delhorme et al., 2010; Kurganskaya and Luttge, 2013; Yang et al., 2020).

2.1.2.5 Research methods

Different approaches exist to characterize mineral-specific and sorption relevant processes such as acid-base behaviour of surfaces and retardation of cations, e.g., cation exchange and surface complexation processes, in general. To examine sorption reactions at the solid-liquid interface, commonly applied methods are classical potentiometric titration experiments, so-called batch experiments to elucidate adsorption experiments and spectroscopic investigations.

2.1.2.5.1 Wet chemistry

Acid-base titrations

The wet chemistry investigations on dispersed systems are aimed to elucidate the nature of the radionuclide retention at the solid liquid interface, i.e. to characterise the different adsorption site types and capacities. Detailed knowledge of protonation and deprotonation processes (acid-base behaviour) of mineral surfaces are of great importance to realistically describe retardation processes at mineral-water interfaces since they are - for most radionuclides/contaminants - pH dependent.

Potentiometric acid-base titration experiments of mineral surfaces have been widely applied (e.g., Arnold et al. (2001), Lützenkirchen et al. (2012 a, b), Schwarz et al. (1983)) to characterize mineral electrostatic behaviour in terms of points of zero charge, surface charge densities, and net surface proton excess. A combination of discontinuous electrolyte and mass titration experiments with continuous potentiometric acid-base titrations offer even deeper insight into mineral surface protonation and deprotonation states as a function of e.g., pH, ionic strength, and solid-liquid ratio (e.g. Lützenkirchen et al. (2012 a), Preocanin and Kallay (1998), Noh and Schwarz (1988)). An alternative experimental approach followed by (Baeyens and Bradbury, 1995, 1997; Bradbury and Baeyens, 2009a; Tournassat et al., 2004b) is the batch titration technique with back-titration, as originally proposed by Schulthess and Sparks (1986) on aluminium oxides.

Adsorption experiments

The research methods for ion-exchange and surface complexation mainly target towards the elucidation of the nature of the uptake mechanism (inner sphere/outer sphere complexes) and the type and capacities of the adsorption sites of the sorbents investigated. Wet chemistry investigation on dispersed systems is the most common experimental method used.

Sorption experiments are carried out by equilibrating an adsorbate solution of known composition and volume with a known amount of adsorbent. The suspension is gently shaken/stirred for a certain period of time until sorption equilibrium is reached. After equilibrium, the solution is separated from the solid phase by centrifugation and/or filtration and analysed. From these experiments, the distribution coefficient R_d is calculated (see Eq. 2-1). When a series of experiments is conducted at a well-defined ionic strength and similar initial concentration but at varying pH values, so-called “sorption edges” are obtained. When a series of experiments is conducted at a well-defined ionic strength and constant pH but varying the initial concentration, so-called “adsorption isotherms” are determined.

2.1.2.5.2 Spectroscopic and atomistic techniques

Surface complexation studies of ionic species are generally carried out by batch sorption techniques similar to ion exchange studies. These methods are frequently complemented by a number of alternative techniques such as micro-calorimetry, infrared spectroscopy, etc., to elaborate the nature of the surface complex. X-Ray absorption spectroscopy techniques (EXAFS/XANES, see sections 0 and 2.2.2.3.3 for more details) have been applied to demonstrate the outer-sphere character of ions in the interlayer.

EXAFS has proven successful to gain a molecular understanding of sorption on edge sites (Dähn et al., 2011; Dähn et al., 2003; Schlegel et al., 2001b), uptake on interlayer sites via cation exchange (Chisholm-Brause et al., 1994; Muller et al., 1997; Sposito, 1984) and also uptake in newly formed lamellar phases such as layer silicates (Dähn et al., 2002; Schlegel et al., 2001a) and mixed layered double hydroxides (Scheidegger et al., 1998; Thompson et al., 1999a; Towle et al., 1997).

Molecular dynamics and Monte Carlo simulations are used to reveal the equilibrium distribution of ions in the interlayer of smectites minerals, cation exchange processes, and the structure of the electrical double layer at the solid/liquid interface. Surface complexation processes involve protonation and deprotonation reaction at edges of clay minerals. The surface complexation reactions result in direct interaction of ions with deprotonated oxygen sites. These processes lead to a significant change of the electron density between the interacting atoms and thus require a quantum mechanical description of the system. A recent review of quantum mechanical studies of adsorption processes on clay minerals is available in Churakov and Liu (2018).

2.2 Other uptake processes

2.2.1 Neo-formation/Surface precipitation

2.2.1.1 Theory and current understanding

Most of the studies on the uptake of contaminants in clay systems have been based on wet chemistry experiments and modelling at the macroscopic level. Batch studies (see also section 2.1.2.5) provide an efficient tool to determine distribution coefficients of metal ions and, under certain circumstances, they also allow differentiation between cation exchange and surface complexation processes occurring at the solid-water interface (Sposito, 1984). However, the ability of a particular surface complexation model to fit macroscopic data does not certify that the assumptions underlying the model are correct. For example, macroscopic data does not allow unambiguous discrimination between surface complexation and nucleation processes. A way to gain mechanistic information about metal interactions on solid surfaces is to combine batch studies with synchrotron-based spectroscopic investigations.

With increasing reaction time and metal concentrations, transition metal surface precipitates (neo formed phyllosilicate or Layered Double Hydroxides/LDH) can form on clay minerals. This process can irreversibly bind contaminants to mineral surfaces. Whereas, sorption models assume that adsorption of trace metals is reversible. Using extended X-ray absorption fine structure (EXAFS), it has been demonstrated that Ni-, Co- and Zn-containing precipitates can form when clay minerals and Al- and Si-(hydr)oxides are treated with Ni, Co and Zn, and this even when the initial metal concentration in solution is undersaturated relative to the pure (oxyhydr)oxide forms of the metal (Dähn et al., 2001; Dähn et al., 2002; Lee et al., 2004; Manceau et al., 1999; Morton et al., 2001; Scheidegger et al., 1998; Schlegel et al., 2001a; Thompson et al., 1999a, b; Towle et al., 1997). For example Scheidegger et al. (1998) observed the formation of a layered double hydroxide (LDH) phase when pyrophyllite (a 2:1 clay which lacks isomorphic substitution) was treated with Ni. A Ni-Al LDH phase formed after a contact time of only a few minutes between pyrophyllite and Ni, suggesting that nucleation can occur rapidly in metal clay sorption systems. LDH formation has been further reported for Co(II) and Zn(II) sorption on kaolinite and Al-(hydr)oxides (Thompson et al., 1999a, b; Towle et al., 1997). Similarly, the uptake of Co on quartz was shown to result in the neoformation of a trioctahedral clay-like structure (Manceau et al., 1999).

Using polarized-EXAFS (P-EXAFS) Dähn et al. (2002) and Schlegel et al. (2001a) showed the presence of neoformed phyllosilicates after treating di- and tri-octahedral 2:1 clay minerals (montmorillonite, hectorite) with Ni and Zn solutions at elevated pH and metal concentrations. The neoformed phases were oriented parallel to the octahedral smectite sheets. In the case of Schlegel et al. (2001a) a structural link of the neoformed phases to hectorite particles could be observed. The study of Dähn et al. (2002) indicates that neoformation processes of clay minerals have started already after one day of reaction time and continued as long as metal ions in solution are present.

2.2.1.2 Research methods

As mentioned in 2.1.2.5.2, EXAFS has proven successful to gain a molecular understanding of sorption on edge sites, uptake on interlayer sites via cation exchange and also by uptake in newly formed lamellar phases. In these studies, macroscopic wet chemistry investigations were combined with synchrotron-based spectroscopic analysis. Studies on the uptake of metals on mineral surfaces observed the formation of phyllosilicates upon the uptake of Co on quartz (Manceau et al., 1999), Zn on hectorite (Schlegel et al., 2001a), Ni on montmorillonite (Dähn et al., 2001) (Dähn et al., 2002), respectively the formation of LDH phases for Co uptake on Al-(hydr)oxides (Towle et al., 1997), Zn on kaolinite and Al-(hydr)oxides (Thompson et al., 1999a, b) and Ni on gibbsite, pyrophyllite and montmorillonite (Scheidegger et al., 1997; Scheidegger et al., 1998). The sensitivity of EXAFS measurements on clay minerals can be significantly improved by performing polarized-EXAFS. In P-EXAFS, neighbouring atoms along the polarization direction of the X-ray beam are preferentially probed, and atoms located in a plane perpendicular to this direction are attenuated. Applying P-EXAFS to clay self-supporting films has the advantage of minimizing the contributions from the out-of-plane Si atoms from the tetrahedral sheet, when the X-ray polarization vector is in the *ab* plane of the montmorillonite self-supporting film (Dähn et al., 2011; Dähn et al., 2003; Dähn et al., 2002; Manceau et al., 1998). Conversely, when the polarization vector is aligned normal to the film plane, the contribution from octahedral layer cation vanishes. The method allows determining the speciation of chemical entities at the atomistic scale, even when the element of interest is present at low concentrations (concentrations of X-ray absorber down to ~100 ppm in clay matrixes).

2.2.1.3 Remaining uncertainties

Research on the neoformation of minerals raises many questions, for example how can stable mineral clay phases generate sufficient soluble Al or Si to react with sorbed metals? None of these studies could gain a deep insight about what triggers the precipitation of a phyllosilicate or a LDH phase. In both cases, it was observed that higher pH, higher metal concentrations and prolonged reaction time favour the formation of phyllosilicates or LDH precipitates. In the past, most efforts in radioactive waste management studies focused on the understanding of sorption process at low metal concentrations, as it was assumed that precipitation processes are not relevant for the safety analyses, considering a conservative approach, of future radioactive waste disposal sites. However nowadays it has been accepted that, for example, high Fe concentrations arising from waste forms can occur (Soltermann et al., 2014b; Soltermann et al., 2013b; Soltermann et al., 2014c). In order to understand the neoformation of phyllosilicates or LDH phases from a thermodynamic perspective the solubility products needs to be determined in the future (Dähn et al., 2003). Presently, such information is lacking in thermodynamic databases. The heterogeneous formation of phyllosilicates has important geochemical implications because layer silicates are stable minerals in mild acidic to basic pH conditions and can irreversibly bound metals in waste and soil matrices, as demonstrated in Zn-smelter impacted soils (Manceau et al., 2000; Vespa et al., 2010).

For long duration sorption experiments, the development of microbial activity with time could interfere with sorption processes and neo-formation / surface precipitation. There is however not much documentation on the effect of a microbial perturbation on the results of a batch sorption tests. It is suggested to do a deeper check of the literature and to consider this in future studies.

2.2.2 Surface-induced redox uptake

2.2.2.1 Theory and current understanding

2.2.2.1.1 General definition of redox processes and selected examples

Reduction-oxidation (redox) reactions require the transfer of electrons between aqueous species (homogenous) or between aqueous species and mineral surfaces (heterogeneous) (Ahmed and Hudson-Edwards, 2017). Redox processes are key geochemical processes since they strongly influence the mobility of redox sensitive contaminants (e.g., elements such as Se, Tc, U, Np, Pu), which are abiotically reduced to often less toxic or less mobile forms (Guillaumont et al., 2003; Ma et al., 2019; Olin et al., 2005; Winkel et al., 2012). These include the tetravalent oxides of U, Np, Pu and Tc; Se(0) and FeSe; and sulphide phases like TcS, while notable exceptions to this rule include the Pu^{3+} aqueous complex and gaseous Se species (Kirsch et al., 2011; Winkel et al., 2012).

Minerals containing redox-active species such as Fe (II, III) or Mn (II, IV) can participate in a wide range of surface induced electron-transfer reactions. For instance, Fe bearing minerals cover a large range of redox potentials depending on the amount and location of Fe in the crystal lattice (Gorski et al., 2012a; Gorski et al., 2016; Gorski et al., 2012b; Gorski et al., 2013; Li et al., 2019a; Sander et al., 2015). The rates and extents of redox reactions are controlled by the physico-chemical properties (e.g., redox and sorption potential, or electron conductivity, depending in turn on factors like composition or particle size) of the minerals (Ilgen et al., 2019; Scheinost et al., 2008).

In the last two decades, many studies have addressed the influence of Fe bearing minerals on immobilization of redox sensitive nuclides such Se, Tc, U, Np and Pu. Studies on the relevant minerals are summarised below:

- **Clays:** (Alexandrov and Rosso, 2013; Boland et al., 2011; Brookshaw et al., 2015; Chakraborty et al., 2010; Charlet et al., 2007; Fox et al., 2013; Frohlich et al., 2012; Hoving et al., 2017; Ilton et al., 2010; Jaisi et al., 2009; Jeon et al., 2005; Joe-Wong et al., 2017; Jones et al., 2017; Latta et al., 2012; Latta et al., 2017; Liger et al., 1999; O'Loughlin et al., 2003; Pearce et al., 2017; Peretyazhko et al., 2008; Peretyazhko et al., 2012; Roberts et al., 2019; Schaefer et al., 2011; Soltermann et al., 2014a; Soltermann et al., 2013a; Stumm and Sulzberger, 1992; Tsarev et al., 2016; Yang et al., 2012; Zhu and Elzinga, 2014)
- **Iron oxides (including oxyhydroxides and hydroxides)**: (Bender and Becker, 2019; Börsig et al., 2018; Christiansen et al., 2011; Dumas et al., 2019; Emmanuel and Ague, 2009; Emmanuel et al., 2010; Huber et al., 2012; Kirsch et al., 2011; Kobayashi et al., 2013; O'Loughlin et al., 2003; O'Loughlin et al., 2010; Peretyazhko et al., 2008; Pidchenko et al., 2017; Roberts et al., 2017; Scheinost and Charlet, 2008; Scheinost et al., 2008; Um et al., 2011; Wylie et al., 2016; Yalçıntaş et al., 2016)
- **Fe(II) (hydroxo-) carbonates:** (Badaut et al., 2012; Ithurbide et al., 2009; Kirsch et al., 2011; Llorens et al., 2007; Scheinost and Charlet, 2008; Scheinost et al., 2016)
- **Fe(II) sulfides:** (Breynaert et al., 2008; Bruggeman et al., 2007; Finck et al., 2012; Han et al., 2011; Kirsch et al., 2011; Liu et al., 2008; Livens et al., 2004; Moyes et al., 2002; Pearce et al., 2018; Rodriguez et al., 2020; Scheinost and Charlet, 2008; Scheinost et al., 2008; Wharton et al., 2000; Yalçıntaş et al., 2016)

Element-specific reviews, for example those focusing on Tc (Meena and Arai, 2017; Pearce et al., 2020), can also be used as a state-of-the art introduction on the nature of the redox interactions between Fe minerals and redox-sensitive elements.

2.2.2.1.2 Redox relevant minerals in disposal systems

The following section is based on the mineralogical data available for clay formations, namely Boom Clay, Opalinus Clay, the clay-rich horizon of the Callovian-Oxfordian Formation in Bure and for the granitic formation of Aspö.

As discussed above, for a redox reaction at the mineral/aqueous solution interface to occur, the solid phase must contain a chemical element that can have different oxidation states in the considered chemical system, and it must be in a reduced state if the element with which it interacts is in the oxidized state, and vice versa. In the environment, the two main metallic elements that are reported to be capable of participating in redox reactions are Fe and Mn. In the following, Mn will not be discussed specifically. Although Mn oxyhydroxides are extremely reactive (Manceau et al., 1997; Means et al., 1978), the deep geological formations that are reviewed here contain little amounts of Mn, and no discrete Mn oxyhydroxides (Gaucher et al., 2004; Landstroem and Tullborg, 1995; Lerouge et al., 2014; Zeelmaekers et al., 2015). Interesting to note that Mn oxyhydroxides could play a role in the case of subsurface storage of low activity wastes (Debure et al., 2018).

Carbonate minerals, sulphide minerals and phyllosilicates in the pristine rock

Fe can be found in a variety of minerals from different groups, under the Fe(II), Fe(III), or in a mixed Fe(II)/Fe(III) oxidation states. In most deep clay-rich formations, three main mineralogical “groups” contain Fe: sulphide minerals, carbonate minerals, and phyllosilicates. The most frequent sulphide mineral bearing Fe is pyrite (FeS_2), but in spite of few reports possibly related to the difficulties to identify this poorly crystalline mineral, its precursor mackinawite may play a significant role due to its high redox reactivity (Breynaert et al., 2010; Bruggeman et al., 2007; Frohlich et al., 2012; Grambow, 2016; Zeelmaekers et al., 2015). Concerning carbonate minerals, siderite ($FeCO_3$), the pure Fe endmember is regularly observed in clay-rich formations, but Fe-containing calcite is also common, and ankerite is also regularly observed (Bossart et al., 2017; Kars et al., 2015; Zeelmaekers et al., 2015). In all carbonate minerals, Fe is present in the Fe(II) oxidation state. Finally, several phyllosilicates are known to host iron. Amongst them, the most common probably are chlorite, biotite, illite (including illite layers in mixed-layers minerals), and micas (see data compilation in Finck, 2020; Lerouge et al., 2017), the distinction between illite and mica being almost difficult to perform because of the close similarity in their crystal structure and because they are frequently mixed in a given sample (Grangeon et al., 2015). Thus, it is likely that the proportions of illite, illite/smectite mixed-layers minerals and micas presented in literature studies suffer from uncertainties. In the Callovian-Oxfordian level of the deep geological laboratory of Bure, di-octahedral interlayer-deficient micas (mainly illite and illite-rich illite/smectite mixed-layers minerals) represent 36-71 % of Fe-bearing minerals, and their FeO content ranges from 1.7-5.7 wt%. Chlorite typically represent 2 % of the Fe-bearing minerals, and their FeO content is ~20 wt%. Finally, other phyllosilicates are present at trace concentration, but their contribution to the total Fe abundance may not be negligible. For example, although biotite is present at trace concentration, its high FeO content of 13-22 wt% provides that it could contribute significantly to the total Fe content in a given sample where it would be enriched. Most of the Fe associated to phyllosilicates occurs in the Fe(II) oxidation state and is present in the phyllosilicate structure, but a minor fraction is in an exchangeable position, making that the amount of exchangeable Fe in the Callovian-Oxfordian formation, at the depth of the Bure laboratory, can reach ~1.2 mequiv/kg (Tournassat et al., 2008).

In granitic geological environments, phyllosilicates are rock-forming minerals. For example, at Aspö, biotite and chlorite are observed, with the latter possibly resulting from hydrothermal alteration (Morad et al., 2018). The presence of illite-rich illite/smectite mixed-layers minerals can also be observed as fracture-filling material, but their abundance as fracture-filling material is relatively low, typically less than 10 wt% (Stanfors et al., 1999).

(Oxyhydr)oxides in the pristine rock

In addition to the above-mentioned minerals, Fe (oxyhydr)oxides, hereafter referred to as "Fe oxides" can also be found. In most clay-rich formations, their abundance is low, therefore probably have a negligible role in contributing to the whole-rock sorption capacity. Yet, they are of great importance for the understanding of the rock geochemistry, since they control the Fe in the porewater, even if present at trace concentration. For example, in the Callovian-Oxfordian level of Bure, goethite (FeO(OH)) abundance is typically less than 0.1 wt%, a trace concentration that is however sufficient to control Fe in the pore water (Gailhanou et al., 2017; Kars et al., 2015).

In granitic rocks that are not subject to hydrothermal reactions, Fe oxides are commonly observed as part of the mineralogical assemblage that form fracture-filling material near the surface, but not in depth (Mathurin et al., 2014), coherent with their formation by alteration of Fe-rich phyllosilicates (e.g., biotite). The typical small size of Fe oxides makes that they are prone to be mobilized by an advective water flow, which would be coherent with the observation of Fe-rich colloids in open fractures (Degueldre et al., 1989).

Potential influence of construction and waste packages materials on the neoformation of Fe oxides

In many disposal concepts, construction materials will remain in the repository, either because it will be used to build access structures and galleries or because it will be part of the waste packages (metallic canisters and steel overpacks). Amongst these materials, steel in contact with either clay or cement will induce potential formation of Fe(II)-bearing minerals (Bildstein and Claret, 2015). In the case of corrosion of steel in contact with clays, the oxide like magnetite, the (hydroxy-)carbonates like siderite and chukanovite, Fe sulfides and Fe-rich phyllosilicates have been observed depending on the geochemical environment and redox conditions (El Hajj et al., 2013; El Mendili et al., 2014; Necib et al., 2016; Schlegel et al., 2010; Schlegel et al., 2014). In both freshwater and saline conditions, mixed Fe(II)/Fe(III) layered double hydroxides, termed green rusts, may form (Bach et al., 2014; Christiansen et al., 2011; Grambow et al., 1996). Contrastingly, when steel is corroded in cement pore water conditions, $Fe(OH)_2$ and $Fe(OH)_3$ can be stabilized (Ma et al., 2018).

In addition, cement in contact with a clay-rich formation can destabilize clay minerals and lead to the precipitation of new phases that are enriched in Mg as observed in the Cement-clay Interaction (CI) experiment in Opalinus Clay conducted at Mont Terri (Dauzères et al., 2016; Jenni et al., 2014; Lerouge et al., 2017; Mäder et al., 2018). These phases, often termed "M-S-H" are nanocrystalline defective Mg phyllosilicates that have a layer structure close to stevensite (Roosz et al., 2015) and which contain appreciable amounts of Fe(III) (Bonen, 1992; Lerouge et al., 2017).

The mixed Fe(II)/Fe(III) oxide magnetite is a common corrosion product under anoxic repository conditions, experimentally evidenced at the steel/clay rock interfaces of waste canisters embedded in clay backfill (El Hajj et al., 2013; El Mendili et al., 2014; Necib et al., 2016; Schlegel et al., 2010; Schlegel et al., 2014). Magnetite, especially as pristine nanoparticles formed under strictly anoxic conditions with near-ideal stoichiometry, rapidly reduces a suite of relevant radionuclides including Se, Tc, U, Np, and Pu (Bender and Becker, 2019; Börsig et al., 2018; Christiansen et al., 2011; Dumas et al., 2019; Emmanuel and Ague, 2009; Emmanuel et al., 2010; Huber et al., 2012; Kirsch et al., 2011; Kobayashi et al., 2013; O'Loughlin et al., 2003; O'Loughlin et al., 2010; Pidchenko et al., 2017; Roberts et al., 2017; Scheinost and Charlet, 2008; Scheinost et al., 2008; Um et al., 2011; Wylie et al., 2016; Yalçıntaş et al., 2016).

In case of Tc, Tc(VII) is reduced by magnetite to Tc(IV), which either forms small polymeric chains with $TcO_2.xH_2O$–like structure sorbed onto the magnetite surface, or is structurally incorporated by substituting for Fe in octahedral positions in magnetite structure (Kobayashi et al., 2013; McBeth et al., 2011; Peretyazhko et al., 2012; Zachara et al., 2007). Incorporated Tc is better protected against reoxidation (Marshall et al., 2014; Um et al., 2017), hence understanding the control between both processes is essential for the safety case of repositories. Earlier work suggests that structural incorporation of Tc might be favoured under pH conditions, where magnetite is less stable, offering a more dynamic surface with frequent Fe dissolution/reprecipitation events, through which Tc(IV) with similar ionic radius and coordination could be trapped into the magnetite structure (Yalçıntaş et al., 2016).

In case of Pu, Pu(V) is reduced to Pu(III) and forms highly symmetric tridentate sorption complexes at the {111} faces of magnetite (Kirsch et al., 2011). In case of neoforming magnetite from Pu-containing solutions, Pu(III) becomes also partly trapped by magnetite, but is increasingly released by Fe-enforced aging (Dumas et al., 2019). The mechanism behind this scenario seems to be the large size of the Pu(III) ion, which is largely incompatible with the magnetite structure; incorporation proceeds through the formation of pyrochlore-like islands in the 2-nm magnetite nanoparticles, which are energetically less favourable than the Pu(III) sorption complex, and hence form by kinetic entrapment rather than being thermodynamically stable. Analogous to the Tc case, the control between sorption and incorporation might be highly relevant for Pu mobility and hence the safety case.

2.2.2.2 Experimental methods to distinguish between total Fe and redox-active Fe

Fe can play an important role in reduction and oxidation of redox-sensitive radionuclides and thereby influence their migration and retention. Whether electron transfer between Fe and radionuclides indeed occurs, depends on various factors: i) the form in which Fe is present (e.g. redox state, aqueous, adsorbed, structural, coordination, mineral properties etc.), ii) the type and redox state of the radionuclide, and iii) chemical conditions in the solution (pH, ionic strength etc.). Measuring total Fe, or total Fe(II) and total Fe(III), does not necessarily lead to correct estimates of the actual redox interaction between Fe and the radionuclide. Examples are the incomplete reduction of Tc(VII) by structural Fe in various clay minerals (Bishop et al., 2011), the incomplete reduction of Se(IV) by Fe(II) sorbed to clay (Charlet et al., 2007), and the absence of Se(VI) reduction by pyrite (e.g. Bruggeman and Maes, 2010; Charlet et al., 2012).

The redox properties of both sorbed Fe as structural Fe have been investigated in a variety of Fe-minerals under different conditions (pH, E_h). Fe-minerals subjected to study include Fe-sulfides, siderite, magnetite, Fe associated to clay minerals and iron (oxyhydr-)oxides. Several methods have been used to distinguish between total Fe and Fe accessible to redox reactions and are explained in the following paragraphs.

2.2.2.2.1 Radionuclide-mineral batch experiments

This method uses batch experiments with the respective radionuclide and the Fe-containing mineral. To which extent the Fe in the mineral was redox-active is assessed by comparing the composition of solution and solid state before and after the batch experiment using spectroscopic measurements such as X-ray absorption spectroscopy (XAS) and Mössbauer spectroscopy or using (sequential) mineral dissolution methods. In these batch experiments, often small amounts of radionuclide are used and therefore the method does not necessarily assess the total amount of redox-active Fe. It does give the most reliable information on whether the Fe-mineral is reactive towards the specific radionuclide.

Examples of studies investigating the impact of redox-active Fe on the reduction/oxidation of radionuclides are:

- Fe associated to clay minerals and micas:
  - **Tc(VII)** (e.g. Bishop et al., 2011; Jaisi et al., 2009; Jaisi et al., 2005; Peretyazhko et al., 2008; Yang et al., 2012).
  - **U(VI)** (e.g. Burgos, 2016; Chakraborty et al., 2010; Ilton et al., 2010; Luan et al., 2014; Tsarev et al., 2016)
  - **Se(IV)** (e.g. Charlet et al., 2012; Scheinost et al., 2008).

- Fe-sulfides:
  - **Tc(VII)** (e.g. Huo et al., 2017; Liu et al., 2008)
  - **U(VI)** (e.g. Bruggeman and Maes, 2010; Livens et al., 2004).
  - **Se (IV, VI, -II)** (e.g. Bruggeman et al., 2012; Charlet et al., 2012; Curti et al., 2013; Han et al., 2011; Han et al., 2012; Kang et al., 2011; Kang et al., 2013; Naveau et al., 2007; Scheinost and Charlet, 2008)
  - **Pu(VI)** (e.g. Hixon et al., 2010)

- Magnetite:
  - **Tc(VII) and Np(V)** (e.g. Cui and Eriksen, 1996)
  - **U(VI)** (e.g. Grambow et al., 1996; Huber et al., 2012; Missana et al., 2003; Rovira et al., 2003)
  - **Se(IV)** (e.g. Scheinost and Charlet, 2008)
  - **Pu(V)** (e.g. Kirsch et al., 2011; Powell et al., 2005).

- Carbonates:
  - **U(VI)** (e.g. Ithurbide et al., 2009; Ithurbide et al., 2010)
  - **Se(IV)** (e.g. Badaut et al., 2012; Chakraborty et al., 2010; Scheinost and Charlet, 2008)
  - **Np(V)** (e.g. Scheinost et al., 2016)

- Fe(oxyhydr)oxides:
  - **Tc(VII)** (Peretyazhko et al., 2012; Um et al., 2011; Yalçıntaş et al., 2016; Zachara et al., 2007)
  - **Pu(V)** (e.g. Powell et al., 2005)

2.2.2.2.2 Using probe compounds – strong chemical reductants and oxidants

For this method, the redox-activity of the Fe-containing mineral is assessed by ‘probe compounds’. In batch experiments the probe compound (oxidant or reductant) reacts with the Fe-mineral and the redox-activity is assessed by loss of the probing compound and quantification of Fe(II) and Fe(III) in the mineral before and after reaction. Probe compounds used to assess the redox-activity of the Fe are often strong oxidants and reductants. The reduction and oxidation capacities that result from these reactions can be seen as a maximum redox-activity and may not be entirely representative for reaction with specific radionuclides.

Examples of such research are:

- **Clay minerals:**
  - Nitroaromatic compounds (e.g. Neumann et al., 2008; Neumann et al., 2011)
  - Dithionite and O_2 or H_2O_2 (e.g. Gorski et al., 2012a; Stucki, 2011).
- **Fe(oxyhydr)oxides:**
  - Ti-EDTA (Heron et al., 1994)
  - Ascorbate (e.g. Roden, 2003)

2.2.2.2.3 Biochemistry – microbial reduction

Anaerobic microbes are often used to study the redox-activity of e.g. structural Fe(III) in clay minerals. The Fe associated to the mineral is characterized before and after reduction by e.g. XAS or Mössbauer spectroscopy. This method is limited to certain electrolyte conditions that are suitable for the microbes. Electron mediators, such as Anthraquinone-2,6-disulfonate (AQDS), are often used to enhance the redox reaction occurring between the microbe and the structural Fe. Many redox reactions in nature occur via microbial interaction. Therefore, this method can give a good representation on which Fe is actually redox-active under natural conditions.

Examples of studies using microbial interaction to study redox-active Fe in minerals:

- **Clay minerals** (e.g. Bishop et al., 2011; Dong et al., 2009; Dong et al., 2003; Jaisi et al., 2009; Jaisi et al., 2005; Kostka et al., 1999; Luan et al., 2014; Pentráková et al., 2013; Seabaugh et al., 2006; Stucki, 2011; Yang et al., 2012)
- **Magnetite** (e.g. Byrne et al., 2016; Dong et al., 2000)
- **Fe(oxyhydr)oxides** (e.g. Roden, 2003)

2.2.2.2.4 (Mediated) Electrochemical oxidation and reduction

This method assesses redox-activity of Fe by measuring electron transfer (as electrical current) between an (Fe) mineral and the working electrode. An electric potential, reducing or oxidizing, high or low, is applied and any resulting redox reactions with the Fe-mineral are directly measured as electric current. This makes it possible to study both the extent and the kinetics of the redox reaction. The measurements can be performed under well-defined conditions such as pH, ionic strength, and redox potential.

Examples of studies using this method to characterize redox-activity in Fe-minerals are:

- **Clay minerals** (e.g. Gorski et al., 2012a; Gorski et al., 2012b; Hoving et al., 2017; Sander et al., 2015)
- **Fe(oxyhydr)oxides** (e.g. Aeppli et al., 2018)
- **Fe-sulfides** (e.g. Hoving et al., 2017).

2.2.2.3 Characterisation of redox reactions

2.2.2.3.1 Experiments to determine thermodynamic data and compilation of thermodynamic databases

The safety assessment of radioactive waste repositories needs a sound understanding of radionuclide (RN) migration behaviour. The study of RN aqueous speciation (i.e. its distribution among the different possible occurring chemical forms or species), determines the conditions under which contaminants can be mobile or can be retarded by (co)precipitation or sorption, being fundamental for understanding their environmental fate and transport.

The most important factors controlling aqueous speciation are: pH, redox (E_h), salinity, temperature, but the presence of solid phases, colloids, organic and inorganic ligands should also be accounted for.

Many experimental methods can be used for determining radionuclide speciation, from chemical analytical methods such as potentiometry; calorimetry, to different spectroscopic techniques especially as for example UV-Vis-NIR (Ultraviolet-Visual-Near Infrared); Raman; attenuated total reflectance Fourier-Transform infrared (ATR-FT-IR); fluorescence or optical spectroscopy; time-resolved laser fluorescence spectroscopy (TRLFS); nuclear magnetic resonance (NMR). Newest techniques such as extended X-ray absorption spectroscopy (EXAFS), small-angle X-ray scattering (SAXS) and high-energy X-ray scattering (HEXS) have been successfully applied to the scope, also in the case of actinides.

Some of the above-mentioned techniques provide indirect information on the formation of complexes in solution; other may give additional information on metal-ligand coordination modes, coordination numbers, ion distances, etc. Additional detailed information on the techniques used for actinides speciation can be found in a recent review (Batrice et al., 2016).

It is well accepted that speciation and solubility data should be obtained in well-defined solutions, with the knowledge of the nature (oxidation state, coordination environment) of the species involved in equilibrium reactions under consideration, and of the solid phases limiting the solubility. However, experimental studies cannot be performed under all the potential chemical conditions. Geochemical and thermodynamic modelling represents an important tool for the interpretation of empirical radionuclide speciation and solubility data and for predicting their behaviour under different environments.

Thus, the main objective of experimental studies is to derive stability constants and all those thermodynamic parameters needed to feed geochemical models. Laboratory analyses provide a direct measure of different forms of an element, but chemical modelling is needed to apply all known thermodynamic relationships among chemical forms and to predict the overall equilibrium distribution. The model based description of uptake thus includes several coupled physicochemical processes that are described by thermodynamic and kinetic laws.

The mathematical approach to the analysis of aqueous speciation, above all in natural systems, is quite complex and the development of dedicated software has ongoing since the ’80s. Far from being exhaustive, amongst the most known speciation software packages (and their updates) are: MINEQL (Westall et al., 1976); PHREEQE (Parkhurst et al., 1980) and PHREEQC (Parkhurst and Appelo, 2013); MINTEQA2 (Allison et al., 1991) and MINEQL+ (Schecher and McAvoy, 1992); EQ3/6 (Wolery and Daveler, 1992); CHESS and JCHESS (Van der Lee and de Windt, 2002); Geochemists’ Workbench (Bethke and Yeakel, 2016), GEMSs (http://gems.web.psi.ch/) (Kulik et al., 2013).

The quality of calculations strongly depends not only on the underlying assumptions, i.e. on the selection of chemical processes by the user, but also on the completeness and reliability of thermodynamic data used as input. The knowledge of fundamental thermodynamic properties, such as solubility products and complexation constants is required.

The development of sound thermodynamic databases (TDB) for radionuclide aqueous speciation and solid formation is therefore a prerequisite for geochemical calculations. In the last years, extensive research on the chemical thermodynamics and speciation of radionuclides in dilute, low-temperature groundwater systems has been carried out, within the OECD-NEA Thermodynamic Database (TDB) Project (www.oecd-nea.org/dbtdb/guidelines/tdb2.pdf).

The NEA compiles and evaluates existing thermodynamic data " to make available a comprehensive, internally consistent, quality-assured and internationally recognised chemical thermodynamic database of selected chemical elements in order to meet the specialised modelling requirements for safety assessments of radioactive waste disposal systems" (https://www.oecd-nea.org/dbtdb/).

The Chemical Thermodynamics Series comprises review reports with selected data for elements of interest in radioactive waste management (https://www.oecd-nea.org/dbtdb/info/publications/). This work reflects present quantitative knowledge based on the available experimental information and intends to be self-consistent.

Following the principles of NEA TDBs, some European agencies for nuclear waste managements and some research institutions develop and continuously update their own databases. This is the case of the "ThermoChimie" thermodynamic database (https://www.thermochimie-tdb.com/) initially created and developed by ANDRA (French National Radioactive Waste Management Agency (Giffaut et al., 2014)) and later joined by "Radioactive Waste Management Limited" (NDA, UK) and ONDRAF/NIRAS (National Agency for Radioactive Waste Management, Belgium). It should be mentioned that SCK•CEN developed first the MOLDATA database for NIRAS, complemented with the software called Geochemical Data Processor (GDP) enabling internal consistency checking of data for the compilation of the in-house MOLDATA database (Wang et al., 2020a; Wang et al., 2020b). Other examples are the Swiss NAGRA/PSI database (https://www.psi.ch/sites/default/files/import/les/DatabaseEN/PSI-Bericht%252014-04_final_druckerei.pdf), THEREDA – Thermodynamic reference database for nuclear waste disposal in Germany (https://www.thereda.de/de/) (Voigt et al., 2007), WEIMAR.dat (https://www.grs.de/publikationen/grs-500) database that includes relevant mineral phases of the Gorleben site (Noseck et al., 2012), or the EQ3/6 from the Lawrence Livermore National Laboratory.

Despite these important efforts, some gaps in data still exist as well as uncertainties associated with the use of the models under certain conditions. Work is ongoing internationally to further develop the thermodynamic database and to extend the ability to model chemical speciation. It must be mentioned that when dealing with natural systems some of the necessary thermodynamic data are missing or not completely reliable (many experimental data probably exist but have not been evaluated in a whole). Revisions and updates of these databases are still required, considering up-to-date experimental and theoretical studies published in peer-reviewed journals. For example, the lack of information on the kinetics of environmental processes obliges to perform calculations assuming equilibrium. New studies should focus on specific chemical conditions, like for example higher pH or high ionic strengths or on the influence of other agents, like for example organics or colloids, that may affect solubility, speciation, and sorption reactions and must be further analysed.

Laboratory experiments, chemical analysis, modelling and database maintenance and improvement are all part of an important iterative work that must be continued and even reinforced.

2.2.2.3.2 Characterisation of redox reactions from an aqueous point of view

a. Application of the K_d formalism in case of a chemical reaction involving redox phenomena

The K_d concept is based on reaction reversibility within a reactive transport conceptual model (see chapter 3 on transport). When sorption is combined with a reduction reaction coupled with an oxidation of the mineral substrate (such as magnetite, pyrite, mackinawite), the reduced RN species:

- has a much lower solubility, as pure phase (e.g. U, Se, Sb, Tc, Mo), consequently solid phases from the reduced (or oxidised) RN species can form;
- is however often present as single sorbed (e.g. U(IV), Tc(IV)) species (Chakraborty et al., 2010; Yalçıntaş et al., 2016);
- the ability of these species to return to the solution is a priori very limited, the sorption reaction being often not reversible (Couture et al., 2015; Markelova, 2017).

In the special case of RNs present in concrete pore water with Fe corrosion products (metallic canisters, steel overpacks, waste packages, reinforcement bar, …):

- the measurement of aqueous phase pH and RN total concentration and identification of the reduced species by XANES spectroscopy has led to a measure of low E_h values (around -420 mV) prevailing in those environments (Ma et al., 2018);
- however, the reductive precipitation reaction being limited in extent (e.g. by limited electron transfer within the mineral structure) when it occurs (the element of interest being often present at too low concentration to reach saturation with the solid phase), this irreversible reaction does not systematically lead to high apparent K_d values as observed at near neutral pH environments (Tsarev et al., 2016).

b. Determining and quantifying redox state of elements and speciation in solution

Spectroscopic techniques and the use of spectrochemical cells

Understanding redox reactions of radionuclides on mineral surfaces is of importance to predict their mobility in the environment. For instance, process understanding on a molecular scale is the basis for geochemical modelling calculations that is applied in calculations for safety assessment of nuclear waste repositories (Geckeis et al., 2013; Gorski et al., 2013). This understanding requires techniques such as X-ray absorption near edge structure (XANES) spectroscopy, which allow the unambiguous identification of redox states.

XANES is an X-ray absorption spectroscopy (XAS) technique, as is EXAFS (Extended X-ray Absorption Fine structure) spectroscopy. XAS is ideally suited to probe the redox state of elements in water, rocks, minerals, biota and at the respective interfaces, because it is element specific and sensitive to electronic and local structure. XAS covers almost all elements of the periodic table, but the penetration depth through water and mineral phases required for in situ redox speciation is given only for energies of a few keV, hence typically limits application of XAS to elements starting with the 3d transition metals. Since all atoms of the probed element contribute equally, and in a statistically representative way, to the measured XAS signal, the method is intrinsically suited to perform quantitative speciation analyses, without the need to account for redox-dependent absorption coefficients or spectroscopically "silent" oxidation states of a given element. These advantages are offset by a relatively poor detection limit (about 1 ppm, depending on element and matrix effects often one or two orders of magnitude higher), and an intrinsically poor spectral resolution especially for local structure analyses. In spite of these disadvantages, XAS is often the only spectroscopic method available for redox speciation, with the notable exception of Mössbauer spectroscopy, which is widely used for Fe redox speciation, but limited to only a few other elements (Sn, Sb, Te, and also possibly I and Np).

Moreover, for actinides (An), the high energy-resolution (HR-) XANES technique (see *Figure 2-5*), at the An $M_{4,5}$-edge, gives a significant advantage (Vitova et al., 2013) over the widely applied conventional An L_3-edge XANES mode to investigate oxidation states and electronic structures of the An elements (see Figure 1 and Bahl et al., 2017). It shows high sensitivity to minor contributions from An oxidation states in mixtures as it directly probes the An 5f unoccupied states, which are sensitive to changes in the chemical bonding. The synchrotron based X-ray methods in combination with optical spectroscopy ultimately provide information on the structure and bonding. As an example, UV-Vis spectroscopy as a tool for molecular speciation is sensitive to the coordination symmetry of An complexes (Meinrath, 1997).

In sorption studies with redox-sensitive An, such as Np and Pu, it is of utmost importance to achieve well-defined redox conditions. Many studies within this topic involve strict precautions to prevent the interference of minor amounts of oxygen, for example by working under inert gas atmosphere (Banik et al., 2016; Elo et al., 2017; Marsac et al., 2015). In addition, electrochemical methods give the possibility to control and thus systematically vary redox conditions. The application of an electrical field *in-situ* can attenuate potential artefacts resulting from the oxidation and subsequent alteration of the samples during sampling, storage and transportation prior to the experimental work (Pidchenko, 2016). Moreover, mechanistic understanding of the interfacial reactions within the first minutes up to hours of contact can be obtained.

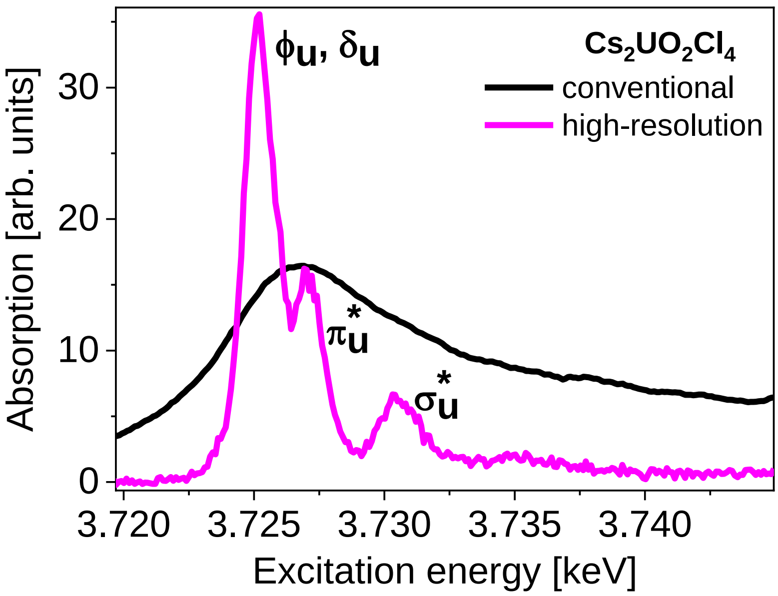

Figure 2-5 – Comparison of conventional U M_4-edge and high-resolution XANES of $Cs_2UO_2Cl_4$. Denoted are the transition to different orbitals visible as separate features in the HR-XANES (Vitova et al., 2017).

The methods of X-ray spectroscopy, optical spectroscopy and electrochemistry can be combined by designing a spectro-electrochemical cell (see *Figure 2-6*). Specific questions that were so far unsolved could be investigated with this setup. For instance, how the applied redox potential influences the surface speciation of redox sensitive radionuclides or what are the surface sites facilitating electron transfer processes (Banik et al., 2016; Marsac et al., 2015).

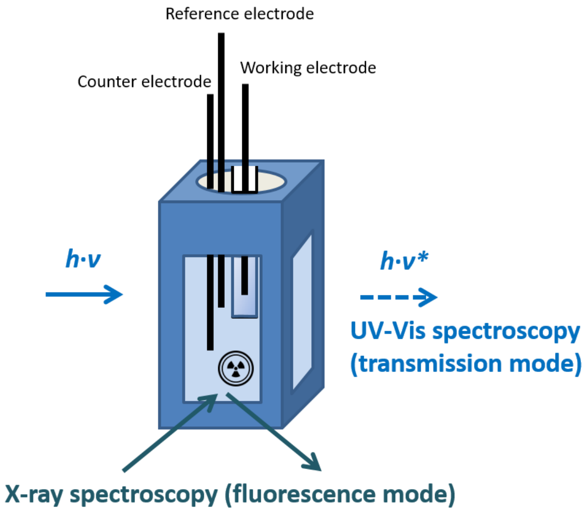

Figure 2-6 – Schematic representation of a spectroelectrochemical cell. Source: KIT-INE, based on concept of Pidchenko (2016).

2.2.2.3.3 Characterisation of redox reactions in the mineral phase

a. Determining and quantifying redox states of elements with synchrotron methods

The XANES signal arises from the transition of core electrons into free valence bands and is hence sensitive to the oxidation state of the probed element as well as to the nature of the bond towards coordinating atoms. Upon interaction of an X-ray and of a core electron (this phenomenon thus requires that the X-ray has an adequate energy), a core electron is emitted into the continuum in the photoelectric effect. The relaxation process creates an Auger electron or an outgoing photoelectric wave, the latter interacting with the electrons from neighbouring atoms. The resulting outgoing wave interferes with the photoelectron wave, causing modulations in the XAS signal. A series of numerical operations, including a Fourier transformation of the XAS signal, allows obtaining a radial distribution function (RDF) around the target element. Both methods have been widely used for redox speciation studies in the last three decades (Manceau et al., 2002), and have contributed to almost all of the results referred to in the preceding text. Only two major developments will be covered here in more detail, since they are very recent and since they remediate one of the biggest disadvantages, the poor spectral resolution of the XANES and EXAFS parts.

High-resolution XANES (HERFD-XANES)

Due to relatively long core-hole lifetimes, elements that can be probed by their K edges (up to and including period 5), allow XANES measurements with the resolution sufficient to discriminate different oxidation states even when several oxidation states of an element are present in the same sample. This has been demonstrated for instance for the 4 common oxidation states of Se (-II, 0, IV, VI) (Rojo et al., 2018; Scheinost et al., 2008). Actinides, however, are typically probed at L-edges with much shorter core-hole lifetimes and correspondingly poor resolution (> 5 eV). Furthermore, the evaluation of XANES is complicated by very diverse coordination environments, with e.g. uranium changing from yl-type at oxidation states VI and V to a highly symmetric cubic coordination for U(IV) (Hennig et al., 2007; Ikeda et al., 2007). Because of this, the more exotic pentavalent oxidation state of U has been intrinsically difficult to detect and can be easily overlooked in oxidation state mixtures. Due to the advent of secondary monochromatization with for instance bent analyser crystals in Rowland geometry, the spectral resolution can be significantly improved by high-energy-resolution fluorescence detection (HERFD) XANES (Kvashnina and Scheinost, 2016). A substantial breakthrough, however, in the detection and quantification of various U oxidation states in mixtures was obtained only after applying the HERFD-XANES technique to M edges (Butorin et al., 2017; Butorin et al., 2016a; Butorin et al., 2016b; Kvashnina et al., 2018; Kvashnina et al., 2017; Leinders et al., 2020; Prieur et al., 2018). This method has now also been applied to other actinides such as Pu and Am (Epifano et al., 2019; Kvashnina et al., 2019; Prieur et al., 2018). The detection limit depends on the element investigated, the chemical composition of the sample, and the instrumental set up (including the synchrotron source), but can reach values in the order of the ppm.

Statistical approaches for quantitative speciation with EXAFS and XANES

Besides improving the spectral resolution of XANES by employing analyser crystals, substantial progress has been made in statistical treatments of spectroscopic data in order to derive reliable speciation as well as to extract the pure spectra of the endmember components from spectral mixtures (Rossberg et al., 2003; Rossberg et al., 2009), a method also applied to derive quantitatively the structures of the different oxidation states of Se and Tc (Charlet et al., 2007; Rojo et al., 2018; Yalçıntaş et al., 2016). This method was further enhanced by coupling to Monte-Carlo simulations in order to derive the specific surface geometry of Pu(III) on magnetite (Kirsch et al., 2011; Rossberg and Scheinost, 2005). Finally, novel approaches can be used to directly derive the radial pair distribution function from EXAFS spectra, a method particularly well suited for strongly disordered structures like that of the Cm(III) aqua complex (Rossberg and Funke, 2010).

b. Models (modelling of redox reactions)

Thermodynamic models are particularly relevant and required for a comprehensive prediction of An behaviour (migration) in natural systems. Only few studies available in the literature attempt to describe redox reactions in the presence of minerals quantitatively via mechanistic surface complexation models.

Soltermann (2014) described the sorption and oxidation of Fe(II) on Wyoming montmorillonite by using the 2SPN SC/CE model and considering the formation of ferric surface complexes ($\equiv S^{S}OFe^{2+}$) along with ferrous surface complexes ($\equiv S^{S}OFe^{+}$). The developed model is capable of describing the adsorption of Fe(II) on different montmorillonites, however it does not provide a realistic mechanistic description, since it does not account for the intrinsic redox properties of the clay mineral itself.

Degueldre and Bolek (2009) discussed Pu sorption onto Al_2O_3, FeOOH and SiO_2 colloids based on a simple R_d approach. Their calculations included the effect of redox potential, which was shown to have a major impact on calculated Pu uptake data. Schwantes and Santschi (2010) proposed a surface complexation model involving all Pu redox states (from +III to +VI) to minerals and a reversible surface mediated Pu(V)–Pu(IV) reaction to explain the observed kinetics of Pu uptake. Experimentally determined redox potential (pe; E_h), oxygen partial pressures, or redox speciation are essential for the application of surface complexation models to describe sorption behaviour of redox-sensitive elements. However, in most studies mentioned above, such data are often not provided due to difficulties associated with their experimental determination (Altmaier et al., 2010; Schüring, 2000).

Marsac et al. (2015) investigated the uptake of Np(V) on illite under anaerobic conditions. Partial reduction of Np(V) to Np(IV) at the mineral surface was observed under conditions where only Np(V) was expected to be stable in aqueous solution. The result was explained by a thermodynamic sorption model, based on measured redox potentials and the high stability of inner-sphere surface complexes of tetravalent An, here Np(IV). The stability constants of such surface complexes can conveniently be estimated by analogy to other elements, here for example to Th(IV), which is not redox-sensitive. The approach was also successful in the case of Pu adsorption on illite (Banik et al., 2016; Gorski et al., 2013). Pursuing such ideas Banik et al. (2017) simulated uptake of Np, again Np(IV) and Np(V), on illite even in high salt contents. The sorption behaviour of the pure oxidation states, which are required in the model had been experimentally tested for Np(V) under oxidising conditions and for Np(IV) under inert gas atmosphere by Nagasaki et al. (Nagasaki et al., 2017; Nagasaki et al., 2016). The model of Banik et al. (2017) was supported by these independent studies, while the mechanism of the redox reactions and the origin of the negative measured E_h-values remained unclear. To understand those findings, a surface complexation model providing a more detailed molecular scale description for the macroscopic quantification of the retention of redox sensitive radionuclides under variable redox conditions should be developed. Starting from the approach by Marsac et al. (2015) and Banik et al. (2017) is probably an appropriate option since the modelling strategy was found to be successful for various actinides and covering a broad range of solution compositions.

c. Kinetics

Radionuclide redox kinetics in aqueous solutions depend on various parameters. These parameters include for example the redox potential defining the concentration of available electrons, the concentration of redox-active substances in the system under investigation, the number of electrons that need to be transferred for the specific redox reaction. Other chemical specificities can however play a role. These specificities include chemical reaction as a consequence of redox transition (e.g. the kinetically hindered reduction of PuO_2^+ to Pu(IV)) and the type of binding of the redox-sensitive radionuclide to the electron acceptor or donor (e.g. inner-sphere complexation or outer-sphere interaction) and therefore also the geochemical boundary conditions. Redox kinetics, therefore, requires a detailed understanding of ongoing reactions. Numerous respective investigations have been published (e.g. Hixon and Powell, 2018; Ma et al., 2020; Romanchuk et al., 2016).

It is also worth noting that, in natural systems, Tc(VII) reduction is found to depend strongly on the Fe(II) content of the rock (Huber et al., 2017 and references therein). The rock treatment and conditioning prior to experimental studies, for example the preservation of the rock oxidation state, is consequently of utmost importance to be able to mimic in situ conditions. Reoxidation by contacting with oxygenated groundwater simulating oxidized melt water into a granitic fracture seems to depend on the nature of granite bound Tc: Surface precipitated TcO_2 seems to reoxidize faster than surface sorbed Tc(IV). Kinetics of redox reactions have been measured for the Tc(VII)/Tc(IV) pair and correlate with the redox potential measured in solution (Kobayashi et al., 2013). Relatively rapid reduction is observed if the E_h is far below the Tc(VII)/Tc(IV) borderline. In their experiments, they found as well an acceleration of Tc(VII) reduction in the presence of Fe(II) solid phases, pointing to the possible relevance of specific surface interaction for electron transfer.

Cevirim et al. (2018) found similar dependencies of U(VI) reduction to $U(IV)O_2$ in their solubility studies. Depending on the reducing agent they applied to adjust reducing conditions, they identified the $pe_{(exp)} – pe_{(U(VI)/U(IV))}$ difference as a driving force for reduction. This explains that even when adding strongly reducing Sn(II) to a U(VI) solution at hyper alkaline conditions requires up to almost two years to reduce U(VI) quantitatively to $U(IV)O_2$ because the *pe* difference is relatively low at high pH.

2.2.3 Solid solutions

2.2.3.1 Theory and current understanding

Solid solutions are mixtures of two or more components on a molecular level existing over a range of chemical compositions. Solid solutions are ubiquitous in natural and industrial systems and play a major role in the fate and transport of elements in earth surface environments. Solid solution formation can lead to a retention of harmful ions in the environment and is included in the design of engineered barriers e.g. for the immobilization of radionuclides or industrially generated pollutants (Prieto et al., 2016). The disordered arrangement of different atoms over the same lattice is stabilized by the entropy, providing an energetic advantage compared to the pure, stoichiometric end members. The charge difference and size of the substituting atoms as well as the flexibility of the host structure, e.g. its Young´s modulus, are important for the extent of solid solution formation. The chemical composition of a solid solution can be defined in terms of fixed end-member compositions – e.g., the binary solid solution $U_{1-x}Pu_xO_2$ can exist in a range of compositions specified by the mole fraction, $XPuO_2$ of the end-member PuO_2. Solid solution formation is typically favoured between isostructural end-members, where the exchangeable atoms have the same charge and similar ionic radii. In many systems, the mixing is incomplete. In general, solid solution formation is limited at low temperatures and is favoured at higher temperatures (Bosbach et al., 2020).

A special case, relevant to nuclear waste management, is the formation of solid solutions in contact with aqueous solutions. Depending on the conditions, solid solution aqueous solution systems (SS-AS) can form by re-crystallization of pre-existing minerals or by co-precipitation from supersaturated solutions (Klinkenberg et al., 2014). These processes can compete with classical sorption processes e.g. adsorption or formation of a pure radionuclide phase. As a consequence of the uptake of radionuclides into solid solutions, these are structurally bound into a thermodynamically stable phase – sometimes leading to significantly lowered radionuclide solubility's (Bosbach et al., 2020). For example, long-term laboratory experiments of several years indicated that the ^{226}Ra uptake into $(Ba,Ra)SO_4$ may take place in time scales relevant to deep geological waste disposal (Klinkenberg et al., 2014).

2.2.3.1.1 Solid-solution formation and radionuclide retention

In the safety assessment of planned nuclear disposal sites, the co-precipitation of radionuclides with sulphates and carbonates are considered as this provides more realistic aqueous concentrations of radionuclides in pore waters of the near field of nuclear waste repositories (Curti, 1999; Curti et al., 2010). For instance, barite is widely studied in the field, as it is the main scavenger of ^{226}Ra, a long-lived radionuclide (Brandt et al., 2015; Brandt et al., 2018; Klinkenberg et al., 2018). Under repository relevant conditions, Ba and Ra released from the radioactive waste will react with porewater containing sulphate, triggering the formation of $(Ba,Ra)SO_4$ (Curti et al., 2010) or even $(Ba,Sr,Ra)SO_4$ (Klinkenberg et al., 2018). In the specific case of ^{226}Ra, the ideal solid solution with $BaSO_4$ irreversibly binds the contaminant in a well-defined, stable phase. Depending on the amount and the properties of the solid, the formation of solid solutions can become a very important retention mechanism and is therefore included in some scenarios of safety cases for deep geological repositories (NAGRA, 2002).

2.2.3.1.2 Thermodynamic and kinetic aspects of solid-solution formation

The most common tool used to rationalize the possible equilibrium states of solid solution is the Lippmann diagram (Glynn, 2000; Lippmann, 1980). The Lippmann diagram is a phase diagram whereby the solidus is a function of the solid phase mole fraction while the solutus is a function of the aqueous activity fractions. The Lipmann model introduces the concept of total activity product, ($\sum\Pi$). It is defined as the sum the of the partial activity products contributed by each component (end member) of the solid solution. Considering the Lippmann diagram of a $(Ba,Ra)SO_4$ solid solution (*Figure 2-7*a) as an example, the solidus expresses ($\sum\Pi$) as the total solubility product using equation (2-13) while the solutus expresses ($\sum\Pi$) in terms of the aqueous phase composition given in equation (2-14).

$$\sum\Pi_{eq} = K_{RaSO4}a_{RaSO4} + K_{BaSO4}a_{BASO4} = K_{RaSO4}\gamma_{RaSO4}X_{Ra} + K_{BaSO4}\gamma_{BASO4}X_{Ra} \qquad (2\text{-}13)$$

$$\sum \Pi_{eq} = \frac{1}{\frac{X_{Ra,aq}}{K_{RaSO4}\gamma_{RaSO4}} + \frac{X_{Ba,aq}}{K_{BaSO4}\gamma_{BASO4}}} \tag{2-14}$$

where $a_{Ba^{2+}}$, $a_{Ra^{2+}}$ and $a_{SO_4{}^{2-}}$ represent the activities in the free solution; K_{BaSO_4} and K_{RaSO_4}, the solubility product of the end-members $BaSO_4$ and $RaSO_4$ (with $K_{sp}(BaSO_4)=10^{-9.97}$ (Hummel et al., 2002) and $K_{sp}(RaSO_4)=10^{-10.27}$ (Langmuir and Riese, 1985) for a temperature of at 298.15 K; and X_{Ba} and X_{Ra}, the molar fraction of $BaSO_4$ and $RaSO_4$ in the solid. γ_{BaSO_4} and γ_{RaSO_4} are the activity coefficients of the end members in the solid solution. $X_{Ra,aq}$ and $X_{Ba,aq}$ are the aqueous activity fractions

The solid solution composition corresponding to an equilibrium aqueous composition is determined by a horizontal line connecting the solutus and the solidus. For instance, an aqueous solution with mole fraction of Ba in solution ($XBa^{2+}{}_{aq}$) equal to 0.7 (*Figure 2-7*) corresponds to a solid-phase composition with mole fraction of $BaSO_4$ ($XBaSO_4$) of 0.3.

While the Lippmann diagram provides the basis for understanding the equilibrium dynamics between the solid solution and the aqueous solution, it does not consider the effect of supersaturation. The key feature of a solid solution formation is that trace element contaminants can co-precipitate as solid solution even though the solution is undersaturated with respect to the pure end-member solid containing that element. The concept of supersaturation for solid solutions is extensively described in the review of Prieto (2009) and the common tools include the stoichiometric supersaturation function, (Ω_{st}) (Prieto, 2009) and the 'δ'-functions (Astilleros et al., 2003). As an example, the supersaturation function of a hypothetical solution containing 10^{-4} mol/L $Ba_{(aq)}$, 10^{-4} mol/L $SO_{4(aq)}$ and 10^{-7} mol/L $Ra_{(aq)}$ was computed and depicted in *Figure 2-7*b using equation (2-15).

$$\Omega_{st}(X_{Ba}) = \frac{(a_{Ba^{2+}})^{X_{Ba}}(a_{Ra^{2+}})^{X_{Ra}}(a_{SO_4{}^{2-}})}{(K_{BaSO_4}\gamma_{BaSO_4}X_{Ba})^{X_{Ba}}.(K_{RaSO_4}\gamma_{RaSO_4}X_{Ra})^{X_{Ra}}} \tag{2-15}$$

A supersaturation Ω equal to 1 denotes equilibrium (dashed line). Solid solutions with compositions below the dashed line are expected to dissolve, whereas solid solutions with compositions above the dashed line can precipitate with the maxima representing the solid solution composition thermodynamically favoured. The example shows that, although the solution is undersaturated with respect to pure $RaSO_4$, radium present in trace amounts is likely to be removed from the aqueous solution through the formation of a $BaSO_4$ enriched solid solution.

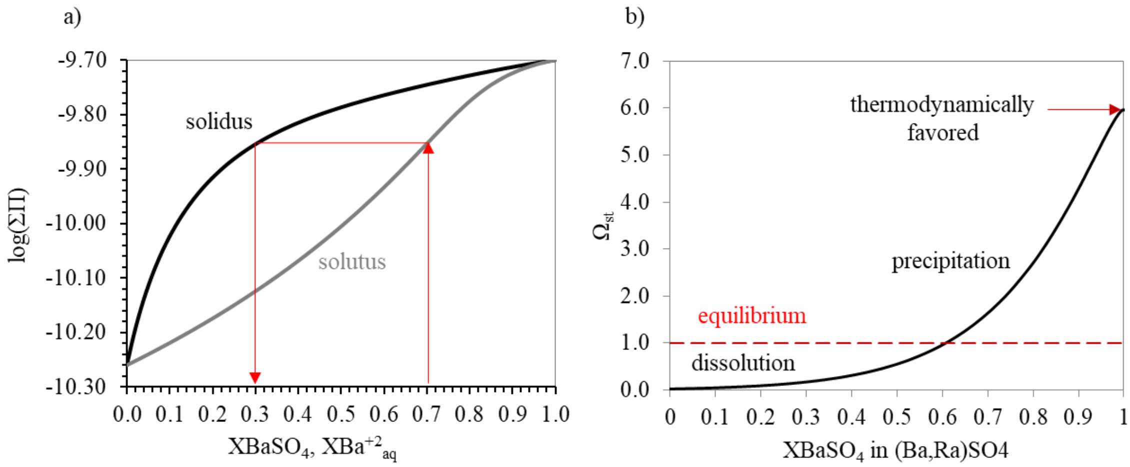

Figure 2-7 – a) Lippmann diagram (Monnin and Cividini, 2006) showing the equilibrium states for (Ba,Ra)SO₄ for the solid solution aqueous solution. b) supersaturation of (Ba,Ra)SO₄ as a function of the mole fraction of BaSO₄ (XBaSO₄). These diagrams were constructed considering a temperature of 298.15 K, a regular mixing model with enthalpy of mixing between Ra and Ba equal to 2947 J/mol (Vinograd et al., 2018).

Because of the complexity of sulphate mineral nucleation and precipitation kinetics, highly supersaturated solutions can lead to metastable phases (Poonoosamy et al., 2016; Prieto, 2014; Weber et al., 2017), and thermodynamic equilibrium calculations might not be sufficient for a reliable prediction of ^{226}Ra mobility (Curti et al., 2019). While the mathematical description of thermodynamic equilibrium behaviour of solid solutions is well-established, the implementations of kinetics still remains a challenging task (Noguera et al., 2016). The effect of kinetics of solid solution precipitation is accounted for in various works by considering the nucleation rate of the solid solutions (Noguera et al., 2016; Pina et al., 2000).

2.2.3.1.3 Nucleation of solid solutions in porous media

The understanding of nucleation processes in porous media is essential for the selection and parameterisation of mathematical equations implemented in numerical reactive transport tools. These are used to assess the geochemical long-term evolution of interfaces in deep geological nuclear waste repositories whereby precipitation and co-precipitation processes are recurrent. The nucleation mechanisms of minerals are described by (Kashchiev and van Rosmalen, 2003). In porous media, both homogeneous and heterogeneous nucleation can occur (Poonoosamy et al., 2016; Poonoosamy et al., 2020). Homogeneous nucleation occurs in the pore solution, whereas heterogeneous nucleation occurs on the surface of existing solids that provide active centres for nucleation. It is generally admitted that homogeneous and heterogeneous nucleation prevail at high and low supersaturation levels, respectively (Kashchiev and van Rosmalen, 2003; Kügler et al., 2016).

The Classical Nucleation theory (CNT) is commonly applied to describe nucleation processes in porous media or confined spaces (Poonoosamy et al., 2019; Prasianakis et al., 2017). Although the applicability of CNT is highly debated (Gebauer et al., 2014), recent studies support the applicability and validity of CNT, for sulphate minerals (Curti et al., 2019; Prieto, 2014) and even carbonates (Henzler et al., 2018). Although CNT is based on empirical formulations, it is an elegant way of integrating experimental observations on mineral precipitation and nucleation kinetics into reactive transport simulations (Poonoosamy et al., 2019).

The nucleation rate (J) depends on supersaturation and can be calculated as follows

$$J = \mathrm{r} exp\left(-\frac{\Delta G_c}{kT}\right) \tag{2-16}$$

where k is the Boltzmann constant, T is the absolute temperature, r is a pre-exponential factor related to the solubility. ΔG_c the energy required for the formation of a nucleus of critical size and is given as:

$$\Delta G_c = \frac{\beta {v_0}^2 \sigma^3}{(kT ln\Omega)^2} \tag{2-17}$$

where v_0 is the molecular volume in the solid phase, β is a geometry factor that depends on the shape of the nucleus, and σ [J/m^2] is the surface tension of the nucleating phase and the solution interface.

For a solid solution, the stoichiometric supersaturation (Ω_{st}) is considered in equations 2-16 and 2-17. Therefore the nucleation rate for (Ba,Ra)SO_4 solid solution is written as a function of the composition:

$$J(X_{RaSO_4}) = \mathrm{r}(X_{RaSO_4}) exp\left(-\frac{\Delta G_{c(X_{RaSO4})}}{kT}\right) \tag{2-18}$$

where $r(X_{RaSO4})$ and ΔG_c are function of the solid solution composition (Pina et al., 2000).

Nucleation in porous media is highly debated (Stack, 2015). Several authors, (Prieto, 2014; Putnis and Mauthe, 2001; Stack et al., 2014) have shown the dependence of nucleation kinetics on the pore size, with an inhibition of nucleation in smaller pores. Unlike a free bulk solution, a porous medium divides the fluid in a large number of pores, which act as independent volumes with respect to nucleation. Because the nucleation probability is essentially proportional to the solution volume, precipitation in small pores is most likely hindered compared to a bulk solution. This point is illustrated by the basic equation for the induction time (Kashchiev and van Rosmalen, 2003) given as:

$$t_i = \frac{1}{JV} \tag{2-19}$$

where t_i is the induction time, J is the nucleation rate (the rate of appearance of supercritical nuclei per unit solution volume) and V is the volume of fluid.

In the same line of thoughts, other authors (Emmanuel and Berkowitz, 2007) consider the solubility of minerals to be pore size dependent. This is commonly referred as the pore-size controlled solubility or PCS effect. In the PCS consideration, the effective solubility of a mineral in a given pore volume, S_e, is related to its bulk solubility, S_0, as follows:

$$\frac{S_e}{S_0} = \exp\left(\frac{-V_S^c}{mRT}\frac{2\sigma cos\theta}{r}\right) \tag{2-20}$$

where V_S^c is the molar volume of the salt, m is the number of ions per unit volume, R is the gas constant, T is the absolute temperature, σ is the surface tension, r is the radius of a cylindrical pore, and θ is the contact angle between the nucleating phase and the wall of the cylindrical pore. In most cases, $\theta > 90$, and $exp\left(\frac{-V_S^c}{mRT}\frac{2\sigma cos\theta}{r}\right) > 1$, such that the effective solubility of a mineral in a given pore volume is always higher than the solubility in bulk water, $S_e > S_0$. PCS, equation (2-20), considers that a given solution can be supersaturated in a big pore and undersaturated in a smaller pore, which can give rise to heterogeneous mineral precipitation distribution with a preferential mineralization in the larger pores.

Although many studies converge towards an inhibition of nucleation in small pores, according to the latest review on mineral crystallisation in confinement (Meldrum and O'Shaughnessy, 2020) it is not possible to make this a generality. Indeed, other studies have shown that nucleation occur uniformly over all pore sizes without size dependence (Borgia et al., 2012) or even preferentially in fine capillaries (Hedges and Whitelam, 2012). Crystallization in confinement is still an open question and require further investigation as it affect pore network alteration and transport properties of host-rock.

2.2.3.2 Research methods

Typically, SS-AS systems are studied in batch precipitation, solubility, or uptake experiments. Complementary to the evolution of the chemical composition of the solution via wet chemical and radiochemical methods (e.g. ICP-MS, liquid scintillation counting, gamma spectrometry), the solids are in-depth characterized to understand the details of the structural uptake (Brandt et al. 2015; Klinkenberg et al., 2018). A review on the characterization of SS-AS systems is provided by (Prieto et al., 2016). Classical methods for the characterization are spectroscopy such as time-resolved laser fluorescence spectroscopy (TRLFS), X-ray absorption (EXAFS, XANES) or Raman and IR-spectroscopy. Lately, methods with high spatial resolution providing chemical information have been applied to unravel the minor component's distribution in a host material, including Secondary Ion Mass Spectrometry (SIMS), Micro-X-Ray Fluorescence (µ-XRF) and electron microscopy (SEM-EDX or TEM-EDX). X-Ray and neutron diffraction were applied to assess thermodynamic quantities such as the excess mixing volume.

Complementary, theoretical methods have also successfully been applied to SS-AS systems including Density Functional Theory (DFT) (Vinograd et al., 2013) or molecular dynamics (MD) (Heberling et al., 2014).

Recently a novel microscopic method for the observation of dissolution/precipitation processes in tightly confined spaces in the nano to micrometre scale have been developed. It consists of the combination of microfluidic experiments (lab on a chip) and pore scale modelling (Poonoosamy et al. 2019). Micromodels enable the in situ live monitoring of flow and reactive transport in two dimensional geometries and have been used, for example, to study single and multiphase flow, including the effects of pore geometry, capillary pressure, and fluid phase saturation (Poonoosamy et al., 2019) and references therein). Combined with spectroscopic techniques and pore scale modelling, micromodels enable the spatio-temporal visualization of mineralogical changes and ion concentrations, resulting in supersaturation determination.

2.2.3.3 Remaining uncertainties

Uncertainties remain with respect to the competition between processes in the pore space e.g. the adsorption of ^{226}Ra within a clay rock versus the formation of secondary phases. Some clay pore waters (e.g., COx and OPA clay) contain significant amounts of Sr and sulphate, so that minor amounts of Ba and ^{226}Ra may lead to the formation of a $(Ba,Sr,Ra)SO_4$ solid solution.

Despite the extensive studies of the thermodynamic properties of $(Ba,Sr,Ra)SO_4$ solid solutions, summarized by (Vinograd et al., 2013; Vinograd et al., 2018), only a few studies (Pina et al., 2000) have been dedicated to the nucleation of solid solutions or were limited to computational investigations (Noguera et al., 2016). Still, the effect of pore size dependency on nucleation is an unresolved issue.

2.3 Upscaling – “bottom-up approach”

Sorption is a complex process, and it is rather unsatisfactory that the whole of the complexity of the radionuclide/water/rock interacting system is contained in a single empirical K_d term as is commonly used in safety assessment. The empirical approach has clear and significant disadvantages in that it has no predictive capabilities. For this reason, sorption models on pure clay minerals based on a mechanistic approach to understand and quantify the processes controlling the uptake of radionuclides were developed. Recently, Baeyens and Bradbury (2017) and Bradbury and Baeyens (2017) developed so-called thermodynamic sorption databases for montmorillonite and illite, respectively. Such databases contain mineral-specific characteristics such as site types, site capacities, protolysis constants, selectivity coefficients and surface complexation constants.

The next step is to apply the so-called composite additive (CA) or bottom-up approach to natural systems. The hypothesis upon which the bottom-up approach is based on is that the uptake of radionuclides in complex mineral/groundwater systems can be quantitatively predicted from the knowledge and understanding of the mechanistic sorption processes on single minerals, and the models developed to describe them. There are a few examples in the open literature where this approach has been tested. Bradbury and Baeyens (2011a) have studied the sorption of Cs, Co, Ni, Eu, Th and U on MX-80 bentonite and Opalinus Clay and obtained satisfactory predictions in applying the bottom up approach. In another study by Marques Fernandes et al. (2015) the bottom up approach was tested for similar radionuclides on Opalinus Clay and Boda Claystone rocks.

2.4 Sources of sorption data

This section presents an extended (but not complete) overview of available sources of sorption data, mainly K_d based, relevant for clay and crystalline host rocks for safety assessment purposes.

2.4.1 Sorption on 2:1 clay minerals

Since 1995 the Paul Scherrer Institute is performing sorption studies on montmorillonite and developing a semi-quantitative mechanistic non-electrostatic sorption model for the uptake of (radio)contaminants. The studies started by the detailed investigation of Ni and Zn sorption on montmorillonite (Baeyens and Bradbury, 1997; Bradbury and Baeyens, 1997a) and continued with a suite of elements in Bradbury and Baeyens (2005a). The same basic non-electrostatic sorption model could be implemented for the clay mineral illite and similar to montmorillonite a number of (radio)contaminants were modelled (Bradbury and Baeyens, 2009a, b). These studies formed an important basis for the development of sorption databases used in major Swiss safety assessments. Comprehensive compilations of the sorption data and modelling can be found in (Baeyens and Bradbury, 2017); Baeyens and Marques Fernandes (2018); Bradbury and Baeyens (2017) and Baeyens and Marques Fernandes (2018).

2.4.2 Sorption on argillaceous rocks

2.4.2.1 Bentonite

To support the Swiss safety case dedicated sorption studies have been performed on MX-80 bentonite. The study was specifically designed for the Swiss case and the data are published in a technical report (Bradbury and Baeyens, 2011b). The bottom-up approach was also tested on selected data sets (Bradbury and Baeyens, 2011a).

A study by Grambow et al. (2006) presents sorption data for 11 different radionuclides (Cs, Ni, Pb, Eu(III), Am(III), Cm(III), Ac(III), Tc(IV), Th, Zr and U(IV)) on MX-80 bentonite. The experimental sorption data sets were modelled, and the model uncertainty was assessed.

Comprehensive sorption studies have been carried out on FEBEX clay, a Spanish bentonite with 98% smectite content, exhaustively characterized in the frame of the Spanish nuclear waste safety case, within the homonymous projects (Huertas et al., 2000) and other international projects. Fundamental chemical parameters of FEBEX bentonite were analysed to support geochemical modelling (Fernández et al., 2004). The radionuclides whose sorption was analysed include anions like selenite (Mayordomo et al., 2016; Missana et al., 2009) and cations of different valence: Cs (Missana et al., 2014; Missana et al., 2004), Ca, Co, Sr (Mayordomo et al., 2019; Missana et al., 2009; Missana and Garcıa-Gutierrez, 2007; Missana et al., 2008b), Ga (Benedicto et al., 2014a; Benedicto et al., 2014b; Missana et al., 2009), Pu (Begg et al., 2015), Np (Benedicto et al., 2014a), U (Missana et al., 2009; Missana et al., 2004) and other elements considered as actinide analogues (Galunin et al., 2009; Galunin et al., 2010). Radionuclide sorption on FEBEX smectite was mainly described by cation exchange and surface complexation, that was interpreted considering a 2-sites (*weak,* S_wOH, and *strong,* S_sOH) non-electrostatic model (NEM). The sorption irreversibility of some radionuclides onto FEBEX bentonite was also analysed (Begg et al., 2015; Missana et al., 2004).

2.4.2.2 Opalinus Clay

Similar as in the case of bentonite for the Swiss safety case, sorption measurements have been carried out on Opalinus Clay and related formations. Reports on these studies were published by Lauber et al. (2000) and Baeyens et al. (2014a). The bottom-up approach was tested on a number of data sets (Bradbury and Baeyens, 2011a; Marques Fernandes et al., 2015)).

2.4.2.3 Boom Clay

Within the geological disposal program in Belgium (co-ordinated by ONDRAF/NIRAS), sorption studies have been performed by SCK CEN to complement the radionuclide migration studies. (Van Laer et al., 2016) give an overview of all the sorption experiments performed on Boom Clay and the main constituting minerals illite and montmorillonite. Particularly for these studies is the emphasis on the influence of Natural Organic Matter (NOM) on the radionuclide sorption behaviour. The Boom Clay contains considerable amount of organic matter that exhibits an important interaction (complexation, colloid formation) with a wide variety of radionuclides (transition metals, lanthanides, actinides) changing its sorption behaviour.

2.4.2.4 Boda Claystone

The geological disposal programme in Hungary (co-ordinated by PURAM) considers two occurrences of the Boda Claystone Formation as potential sites (Breitner et al., 2015; Németh et al., 2016). In addition to diffusion investigations, sorption studies were performed by EK on Boda Claystone involving Cs, Sr, Co and I (Mell et al., 2006a). Within the frame of a Swiss-Hungarian bilateral project, the bottom-up approach was tested for Cs, Co, Ni, Eu, Th and U in cooperation with PSI (Marques Fernandes et al., 2015). Sorption was mostly related to the illite-rich clayey matrix on the microscale (Kéri et al., 2016; Osán et al., 2014). The bottom-up approach based on illite was found to work well for Boda Claystone, despite the high hematite content due to the oxidized nature of the rock compared to the reducing properties of Opalinus Clay.

2.4.2.5 Callovo-Oxfordian argillite

Sorption studies on Callovo Oxfordian argillite have been performed by several labs.

Studies for the following species are reported: I^- (Bazer-Bachi et al., 2006; Montavon et al., 2014), SO_4^{2-} (Bazer-Bachi et al., 2007), Sr (Altmann et al., 2015), Cs (Chen et al., 2014b; Melkior et al., 2005), Ni (Chen et al., 2014a), Zn (Altmann et al., 2015), Pb (Orucoglu et al., 2018), Sn (Kedziorek et al., 2007; Latrille et al., 2006), Eu (Descostes et al., 2017), Pu (Latrille et al., 2006), organic ligands and acids (EDTA, isosaccharinate (ISA), phthalate, oxalate, polymaleic acid) (Dagnelie et al., 2018; Durce et al., 2014; Rasamimanana et al., 2017). Often these studies were combined with migration experiments.

In ANDRA's Dossier 2005 (ANDRA, 2005), K_d values on Callovo-Oxfordian argillite for safety relevant radionuclides are listed.

2.4.3 Sorption on crystalline rocks and components

Compilations of sorption distribution coefficients (K_d) for respectively Swedish (SKB) and Finnish (POSIVA) safety cases in crystalline bedrocks are available in e.g. Crawford (2010) and Hakanen et al. (2014).

Li et al. (2018); Li et al. (2020) and Puhakka et al. (2019) investigated the sorption behaviour of Se(IV) on Grimsel granodiorite (mainly plagioclase, K-feldspar, quartz and biotite) using artificial Grimsel groundwater and different concentrations of Se(IV). Fukushi et al. (2013) focused their study on Eu(III) sorption on granite. The distribution coefficients of Ba on Olkiluoto pegmatitic granite and veined gneiss, Grimsel granodiorite and their main minerals (quartz, plagioclase, K-feldspar and biotite) were obtained by batch sorption experiments (Muuri, 2019; Muuri et al., 2018).

Batch sorption experiments focused on rock-forming minerals, partially also present as fracture-filling minerals, including muscovite, orthoclase, and quartz. Various aspects of investigations comprise surface complexation modelling, thermodynamic sorption modelling, and data compilation for databases (e.g., Britz (2018); Noseck et al. (2018); Noseck et al. (2012); Richter et al. (2016); Stamberg et al. (2014); Stockmann et al. (2017); Videnska et al. (2015); Videnská et al. (2013)).

An application of the smart K_d-concept (see section 3.1.3.3) in reactive transport calculations for porous sedimentary systems is described in detail by Noseck et al. (2012).

Newly-formed sheet-silicates and other precipitates in fractures, such as sulphates (e.g., baryte, celestite) or carbonates (e.g., calcite) show remarkable retention capacities for some radionuclides, such as Ra (Brandt et al., 2015; Chagneau et al., 2015; Curti, 1999; Klinkenberg et al., 2018).

2.4.4 Sorption databases

The publication of sorption databases (K_d values) used in performance assessments are very sparse in the open literature, and if so they are mainly published in the form of technical reports. Examples are sorption databases on bentonite and argillaceous rocks which have been used in the Swiss safety cases for marl formations (Bradbury and Baeyens, 1997b); for bentonite (Bradbury and Baeyens, 2003a) and for Opalinus Clay and related formations (Baeyens et al., 2014b; Bradbury and Baeyens, 2003b).

RES³T (https://www.hzdr.de/db/res3t.login) is an acronym for the "Rossendorf Expert System for Surface and Sorption Thermodynamics" which is an open source digitized thermodynamic sorption database and comprises mineral-specific data sets for sorption modelling (e.g. surface complexation parameters, thermodynamic data, surface complexation reactions, etc.). The database covers 145 minerals, approx. 140 sorbing ligands, 2150 specific surface area measurements, 1900 surface site data sets, 6700 surface complexation reactions, and according literature references to ensure re-traceability and transparency.

3 Transport processes in host rocks

The scope of this chapter is to describe current predictive models for radionuclide (RN) migration as dissolved species (colloid related transport behaviour is not discussed here) in a fully saturated environment, the role and influence of structural properties, as well as the experimental and numerical approaches utilised for clay and crystalline host rocks. In this context, the main processes e.g. diffusion, advection, retention in clay and crystalline rocks are characterized including main components and heterogeneities along the migration path and understanding of coupled transport and retention processes.

3.1 Introduction to diffusion, advection and retention processes

3.1.1 Basics

For more in depth reading we refer to some good text books (Appelo and Postma, 2004; Crank, 1975; Cussler, 2009; Dullien, 1991; Grathwohl, 1998; Mitchell, 1993).

In porous (fully saturated) media, the net flux (J) of a solute is equal to the sum of all the fluxes induced by the different gradients that may be present in the considered system: chemical potential, hydraulic head, electrical potential, and temperature and described by the Onsager reciprocal relations. However, the two most dominant transport processes for radionuclide migration are:

- Diffusion (created by a gradient of chemical potential, hence concentration), and;
- Advection (created by a gradient of hydraulic pressure).

Diffusive flux is the net movement of dissolved species present in aqueous solution because of a difference of chemical potential (with the concentration gradient as driving force). Fick's first law describes the relationship between the diffusive flux and the concentration gradient

$$J = -D_e \frac{\partial C}{\partial x} \qquad (3\text{-}1)$$

Where J is the solute flux [mol/m²s], D_e is the effective diffusion coefficient [m²/s] of the solute in the porous medium and C is the aqueous phase solute concentration [mol/m³].

The effective diffusion coefficient (D_e) of each dissolved species directly depends on its diffusion coefficient in pure water, D_0, its diffusion accessible porosity in the medium η [-] and a geometric factor G [-] depending on the microstructure of the porous medium:

$$D_e = \eta G D_0 \qquad (3\text{-}2)$$

The geometric factor[1] is a lumping parameter that averages the complex morphology of the pore structure and typically consists of two terms: the tortuosity τ [-] and the constrictivity δ [-]. Tortuosity accounts for the effects of an increased path length of a molecule diffusing through the water-filled pores of the porous medium and is therefore larger than one. Constrictivity accounts for pore narrowing and widening but is often arbitrarily set equal to one. Both constrictivity and tortuosity cannot be measured independently. Only the lumping geometric factor can be estimated from a diffusion experiment if the porosity is known.

$$G = \frac{\delta}{\tau^2} \qquad (3\text{-}3)$$

The molecular diffusion coefficient D_0 of a dissolved species in pure water depends essentially on its chemical nature (atomic or molecular weight, hydrated radius, steric effects, electrical charge, …), the

[1] Please note that the G factor is sometimes defined differently as τ^2/δ in papers used furtheron in this report e.g. Appelo (2010), Glaus (2015a).

temperature and the viscosity of the fluid. Typical values for molecular diffusion coefficients of ions and molecules in water are in the range of 10^{-9} and 10^{-10} m^2/s (Li and Gregory, 1974).

Fick's second law describes the transient evolution of flux:

$$\frac{\partial C}{\partial t} = \frac{D_e}{\eta}\frac{\partial^2 C}{\partial x^2} \tag{3-4}$$

The radionuclide transport in a porous medium is influenced by retention processes at the water-rock interface (see previous chapter on retention processes). When these processes are rapid, linear and reversible, their effect on the transport regime can be accounted for by a retardation factor, R [-] which can be related to the solid-liquid distribution coefficient K_d [m^3/kg] (often derived from sorption experiments, see chapter 2 on retention processes):

$$R = 1 + \frac{\varrho_d K_d}{\eta} \tag{3-5}$$

with ρ_d the dry bulk density [kg/m^3].

Rewriting Fick's second law including reversible retardation one obtains:

$$\frac{\partial C}{\partial t} = \frac{D_e}{(\eta + \varrho_d K_d)}\frac{\partial^2 C}{\partial x^2} = \frac{D_e}{\eta R}\frac{\partial^2 C}{\partial x^2} = D_a\frac{\partial^2 C}{\partial x^2} \tag{3-6}$$

Other frequently used diffusion parameters[2], are the pore diffusion coefficient, D_p, and the apparent diffusion coefficient, D_a, which are related to each other in following way:

$$D_a = \frac{G}{R} D_0 \qquad \text{with} \qquad G D_0 = D_p$$

So,

$$D_e = \eta G D_0 = \eta D_p = \eta R D_a \tag{3-7}$$

The product ηR is also often referred to as the "rock capacity factor, α". The rock capacity factor, relates the concentration in the porous medium, C_{bulk}, to the concentration in the solution, C, i.e. the sum of the amount of the species in the solution and in the solid normalised to the solution and solid volumes (Tournassat and Steefel, 2015). Hence the term refers to a "storage capacity" of a porous medium for a certain species.

$$C_{bulk} = \alpha C = \eta R C = (\eta + \varrho_d K_d) C \tag{3-8}$$

[2] The correct name of each diffusion coefficient must always first been clearly and explicitly stated along with its definition to avoid confusion. Simply referring to a "diffusion coefficient" or to "diffusivity" is insufficient and can lead to serious errors when transferring/using data.

The transport of dissolved species by **advection** is the result of the movement of the pore water under the effect of a hydraulic pressure gradient. The hydraulic pressure gradient causes the water to move out of a porous medium with an average velocity, called the Darcy velocity, V_{darcy} [m/s].

The Darcy law describes the flowrate *(Q)* of water forced through a porous medium of cross section *S* [m²] and length *L* [m] by a hydraulic gradient *(ΔP/L)*:

$$Q = KS\frac{\Delta P}{L} \tag{3-9}$$

The Darcy velocity corresponds to the water flowrate *Q* divided by the cross section *S* of the considered porous volume:

$$V_{darcy} = \frac{Q}{S} = K\frac{\Delta P}{L} \tag{3-10}$$

with *Q* the flowrate [m³/s], *ΔP* the hydraulic pressure difference that is exerted over the length of the porous medium (expressed in m of water column height), and *K* a proportionality constant called the hydraulic conductivity [m/s]. While the Darcy velocity represents the velocity of water flowing out of the porous medium, the pore water velocity (V_p) takes into account that inside the porous medium, water flows only through the pore space. Both parameters are related via the water porosity or total porosity, *η*:

$$V_p = \frac{V_{darcy}}{\eta} \tag{3-11}$$

Note that, as soon as an advective flow is present, the diffusive flow also becomes affected by mechanical and hydrodynamic dispersion and becomes a dispersion coefficient (D_{disp}) which is a function of the advective velocity (a is the longitudinal dispersivity [m]):

$$D_{disp,p} = D_p + aV_{darcy} \tag{3-12}$$

Mechanical dispersion (hydrodynamic dispersion) results from ground/pore water moving at rates both greater and less than the average linear velocity (Fetter, 1992). This is caused by: 1) fluids moving faster through the center of the pores than along the edges, 2) fluids traveling shorter pathways and/or splitting or branching to the sides, and 3) fluids traveling faster through larger pores than through smaller pores (*Figure 3-1)*.

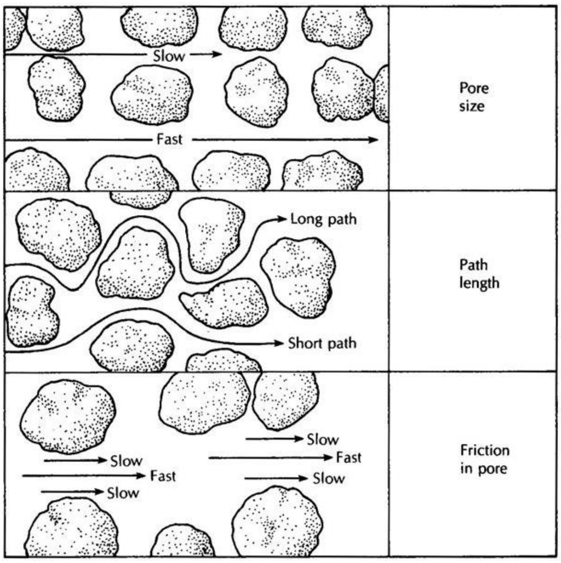

Figure 3-1 – Illustration of factors causing mechanical (hydrodynamic) dispersion (Figure taken from (Fetter, 1992)).

Because the solute-containing water does not travel at the same velocity everywhere, “mixing” occurs along flow paths. This mixing is called mechanical dispersion and results in a distribution of the solute at the advancing edge of flow. The dispersion coefficient in the transport equation accounts for the combined effects of mechanical dispersion and molecular diffusion, both of which cause spreading from highly concentrated areas toward less concentrated areas.

The ratio of the advective transport rate over the diffusive transport rate is known as the Péclet number *(P_e):*

$$P_e = \frac{L\,V}{D} \tag{3-13}$$

With L , characteristic length [m] (travelled length of the fluid), V and D respectively the water velocity and the diffusion coefficient, respectively. The Péclet number is used as a criterium to evaluate which transport mechanism is dominant. This is the general form of the Péclet number and depending on the underlying assumptions in the solute transport equation, it can have different forms (Huysmans and Dassargues, 2004).

Adding advection into the transport equation, this becomes:

$$\frac{\delta C}{\delta t} = \frac{D_{disp,p}}{R}\frac{\partial^2 C}{\partial x^2} - \frac{V_{darcy}}{\eta R}\frac{\delta C}{\delta x} \tag{3-14}$$

Taking into account that $V_{darcy}/\eta=V_p$ and introducing the notation of “apparent” coefficients to incorporate the retardation effect we obtain:

$$\frac{\delta C}{\delta t} = D_{disp,a}\,\frac{\partial^2 C}{\partial x^2} - V_a\frac{\delta C}{\delta x} \tag{3-15}$$

The classical diffusion-retardation equation considers the concentration of the solutes to be the same over the entire pore space and it accounts for linear reversible sorption processes. The latter are mainly linked to the main sorption mechanisms in clays *i.e.*, ion-exchange and surface complexation. It disregards i) the presence of the electrical double layers (EDL) which has an effect on the concentration profiles of ions within the pores and ii) non-reversible retention processes (irreversible chemisorption, surface precipitation, incorporation, solid-solution formations, precipitation,…).

3.1.2 Numerical modelling of coupled physical and chemical processes in transport

Numerical modelling of coupled physical and chemical processes of fluid flow, solute transport, and chemical reactions is vital for predicting the migration of RN in host rocks. In general, such numerical models include reactive-transport equations (Steefel and Lasaga, 1994) for solutes transport and chemical reactions and the conservation of momentum for fluid flow (Steefel et al., 2005). A multitude of reactive transport codes are available, see Steefel et al. (2014) for a non-exhaustive list of reactive transport codes like PHREEQC, PHREEQC-PHAST, HPx, HYTEC, CRUNCHFLOW, ORCHESTRA, PFLOTRAN, OpenGeoSys, TOUGHREACT, …

3.1.2.1 Reactive multi-species diffusion models (mainly applicable to clays)

For each species, diffusion is coupled to speciation reactions in solution, sorption reactions on mineral surfaces as well as mineral reactions.

1D reactive multi-species diffusion in solution may be described for *i* species in solution with concentration C_i by

$$\frac{\partial C_i}{\partial t} = D_p \frac{\partial^2 C_i}{\partial x^2} - R_i - r_i \ , i = 1,2, \dots, n_{aqueous} \qquad (3\text{-}16)$$

D_p is the pore diffusion coefficient [m²/s], R_i [mol/m³s] denotes a source/sink term due to equilibrium reactions between the solution and non-moving species sorbed on mineral surfaces according to

$$R_i = \sum_{j=1}^{n_{sorbed}} v_{i,j} \frac{1-\eta}{\eta} \rho_s \frac{\partial S_j}{\partial t} \ , i = 1,2, \dots, n_{aqueous} \qquad (3\text{-}17)$$

$n_{aqueous}$ and n_{sorbed} [-] denote the number of species in solution and sorbed, respectively and $v_{i,j}$ [-] are stoichiometric coefficients. r_i [mol/m³s] are the source/sink terms due to mineral reactions.

The mass action law or the assumed equilibrium chemistry in solution and between solution and minerals and mineral surfaces yields constraints that define the source/sink term for each species and represents the mechanistic understanding of surface and/or ion exchange reactions of the following form

$$\equiv sc_1 + c_2 \Leftrightarrow \equiv sc_2 + c_1 \qquad (3\text{-}18)$$

Mineral reactions can be kinetically or by chemical equilibrium controlled and have the following form

$$r_i = \sum_{m=1}^{N_m} v_{im} r_m \ , i = 1,2, \dots, n_{aqueous} \qquad (3\text{-}19)$$

where r_m [mol/m³s] is the net rate of precipitation ($r_m > 0$) or dissolution ($r_m < 0$) of mineral per unit volume of rock, v_{im} [-] is the number of moles of species *i* per mole of mineral *m* present in the rock.

This can be further extended by accounting for effects of electrical potentials that develop during movement of charged species (Nernst-Planck formalisms).

3.1.2.2 Reactive transport including advective fluid flow (important for crystalline rocks)

At the **pore scale,** the crystalline rock can be considered as a binary domain consisting of solid material and the pore space. Transport of (solute) species occurs in the pore space and reactive processes such as adsorption/desorption of RN and mineral dissolution/precipitation take place at the fluid-solid interfaces. The Navier-Stokes equation (NS) or the Stokes equation are employed as a momentum equation to describe fluid flow in pore space (Li et al., 2008; Molins, 2015). Interfacial reactions are usually treated as a boundary condition at the fluid-solid boundaries (Molins, 2015).

Pore-scale simulation equations:

(1) Fluid flow using NS equation:

$$\frac{\partial u}{\partial t} + (u \cdot \nabla)u = -\frac{1}{\rho}\nabla p + \nu \Delta u, \qquad \text{(3-20)}$$

$$\nabla \cdot u = 0,$$

where u is velocity vector, p is pressure, ρ is the fluid density, and ν is the kinematic viscosity of the fluid.

(2) Solute transport and chemical reactions; reactive transport equations:

$$\frac{\partial c_i}{\partial t} + \nabla \cdot (uc_i - D_i \nabla c_i) = R_i, \qquad \text{(3-21)}$$

where c_i is the molar concentration of species i in solution, D_i is the dispersion/diffusion coefficient, and R_i is the reaction term.

(3) Surface reactions:

$$-D_i \nabla c_i = \xi_{im} r_m, \qquad \text{(3-22)}$$

where r_m denotes the surface reaction rate and ξ_{im} is the stoichiometric coefficient of the component i in each surface reaction m.

At the **continuum scale**, the porous medium is typically conceptualized as a continuum with bulk parameters that characterize its physical and chemical properties. At this scale, mobile and immobile phases are assumed to coexist in each point in space. The Darcy's equation is applied as a momentum equation, while reactive transport is described by the mass balance equation of each species (Steefel and Lasaga, 1994). Reactive transport in fractured porous media can be simulated using the coupled Stokes-Brinkman equation and reactive-transport equations (Yuan et al., 2019; Yuan et al., 2016), which allows to efficiently model the alterations of rock properties caused by chemical reactions:

$$\mu K_{perm}^{-1} u + \nabla p - \mu^* \Delta u = 0 \qquad \text{(3-23)}$$

$$\nabla \cdot u = 0,$$

where K_{perm}^{-1} is a permeability tensor, u represents the physical velocity of the fluid in the fractures and the Darcy velocity in porous media, μ is the dynamic viscosity of the fluid, and μ^* is the effective dynamic viscosity.

3.1.3 Accounting for retention processes in transport: empirical and thermodynamic approaches

There are different approaches to describe sorption and desorption processes at water-rock interfaces:

a) empirical relationships such as e.g. Langmuir, Freundlich or linear sorption isotherms (Henry isotherm) and

b) conceptual thermodynamic sorption models (TSM) that describe ion-surface associations based on mechanistic approaches to characterize coordinative properties of surface complexes using e.g. the diffuse double layer (DDL) model or more sophisticated model theories (Ochs et al., 2012).

Approaches from Langmuir and Freundlich, as well as thermodynamic sorption models assume a thermodynamic equilibrium between the solid and the surrounding electrolyte. However, in comparison to empirical approaches mechanistic thermodynamic sorption models are based on the law of mass action.

3.1.3.1 Empirical – Constant K_d approach

In performance and safety assessment calculations, sorption is usually described with linear distribution coefficients (see also section 2.1) constant in space and time, *i.e.*, simple K_d-values (NAGRA, 2002; POSIVA, 2012a; SKB, 2011) and applied in the classical advection-diffusion equation (ADE) as a retardation factor *R*.

Since sorption of many elements and radionuclides strongly depends on the geochemical properties of the surrounding solution and sediments, **this approach of constant K_d-values is justified only for constant hydrogeological and geochemical conditions.**

Within large time frames or in dynamic systems a variability of geochemical conditions can be expected due to spatial heterogeneities and environmental variations. Therefore, it can be desirable to describe transport and/or sorption of potential contaminants as a function of important environmental parameters, such as pH or ionic strength.

3.1.3.2 Process understanding – Thermodynamic approaches

Reactive transport simulations typically rely on transport codes coupled with a geochemical code, capable of using thermodynamic sorption models based on mass action law equations:

$$\equiv sc_1 + c_2 \Leftrightarrow \equiv sc_2 + c_1 \tag{3-24}$$

These coupled models are useful for acquiring process and system understanding, as they are able to account for different chemical conditions in contrast to the constant K_d approach.

Different thermodynamic sorption models have been elaborated to describe the mineral-fluid interface during sorption processes (Ochs et al., 2012) (see also section 2.1.2). Thermodynamic sorption models that are used to calculate defined surface complexation processes of e.g. metal cations (Me) are called surface complexation models (SCMs). All thermodynamic sorption models are based on law of mass action and mole balance equations (Davis and Kent, 1990b), but involve different descriptions of the electric double layer (EDL), i.e. electrostatic interaction term (Davis and Kent, 1990b; Westall and Hohl, 1980). In the no EDL models (noEDLM) the electrostatic interaction term is not considered at all; thus, a diffuse double layer (DDL) is neglected. Each thermodynamic sorption model (except noEDLMs) considers different electrostatic planes that can contribute to the sorption processes.

3.1.3.3 Towards safety assessment – “Smart K_d“ approach

When it comes to simulate the impact of changing geochemical conditions over very long time frames and/or variability in composition over larger distances, as is necessary for safety assessment purposes a fully coupled reactive transport approach may result in unfeasible computation times due to the complexity of mechanistic model approaches (Noseck et al., 2014).

For safety assessment purposes it is still common practice to reduce the solute/rock interaction to a constant K_d-value being uniform in the whole transport domain and invariant in time as in Crawford (2010) or Hakanen et al. (2012). Uncertainties are accounted for by choosing a conservative K_d-value. More elaborated models can be used to underpin the selection of the K_d-value and its uncertainty.

Therefore, (Noseck et al., 2018; Noseck et al., 2012) proposed and developed the “smart K_d-concept” (http://www.smartkd-concept.de/) and implemented it in transport modelling. It combines state-of-the-art mechanistic thermodynamic sorption model theories with the traditional empirical, constant, linear, and reversible K_d-approach and presents a computation time efficient approach to simulate long-term contaminant transport over large areas and long distances.

It allows the interpolation of distribution coefficients (referred to as smart K_d-values) for any observed (or hypothetic) combination of environmental boundary conditions treating complex systems in a more rigorous way. This approach is based on surface complexation models (SCM) and considers further ion exchange, solid phase equilibria and complexation in aqueous solutions (Stockmann et al., 2017).

An application of the smart K_d-concept in reactive transport calculations for porous sedimentary systems is described in detail by Noseck et al. (2012).

3.2 Transport in clays

3.2.1 Structural aspects of clays

Argillaceous sediments are deposited in various marine (OPA, COx and Boom Clay) and lacustrine (Boda Claystone) environments. Because of water-rock interactions and microbial activity, physico-chemical changes occur in clay sediments after their deposition and they undergo diagenesis being progressively transformed in clay rocks. The diagenesis of clay sediments depends on many factors such as, depositional environment, types of clay minerals, amount of organic matter, pore water chemistry, geothermal gradient and burial history. Increasing burial depth leads to sediments compaction and chemical diagenesis which results in a systematic decrease of porosity, water expulsion, and progressive transformation reaction of smectite into illite (Velde and Meunier, 2008; Weaver, 1989).

The principal minerals in argillaceous sediments consist of clay minerals, with additional quartz, feldspars and calcite, small amounts of pyrite, Fe-carbonates and apatite. In addition, solid or immobile organic matter in form of more or less evolved kerogen may be present. When argillaceous sediments are sufficiently compacted so that they are no longer soft or plastic but still not fissile (i.e., not cleavable along weak planes as shales or metamorphic slates), they are called clay rock or mudstone. Depending on its mineralogy (smectite content), a clay sediment may exhibit swelling properties in the presence of water, which is an important aspect in the application for nuclear waste disposal as it provides self-sealing properties. Argillaceous sediments contain variable amounts of water present both in the clay mineral structures and in the nanometre pore spaces. High water contents (>20 vol%) result in soft and plastic clay (e.g. Boom Clay) whereas clay rocks/mudstones (Opalinus Clay, Callovo Oxfordian Clay, Boda Claystone) are drier (< 20 vol% pore water) and stiffer. Further compaction and water expulsion from the pores result in further alignment of clay mineral grains so that the rocks become fissile forming shales and, eventually, slates.

Clay minerals are phyllosilicates (from the Ancient Greek φύλλον "phyllon", leaf) and the principal clay minerals in argillaceous host rocks are smectite (or “swelling clay”), illite, kaolinite and chlorite. These phyllosilicates are composed of jointed octahedral (O) layers (containing Al^{3+}, Mg^{2+}, Fe^{2+}, …), and tetrahedral (T) layers (containing Si^{4+}, Al^{3+}, …) (*Figure 3-2*). Illite and montmorillonite (main smectite) are composed of TOT layer sequences while kaolinite is composed of TO sequences. Chlorite are TOT layer sequences with brucite-like interlayers with compositions near to $(Mg,Fe,Al)_3(OH)_6$.

Due to isomorphic substitution where a higher valency element is replaced by a lower valency element, Si^{4+} by Al^{3+} in the tetrahedral layer or Al^{3+} by Mg^{2+} and Fe^{2+} in the octahedral layer, permanent electrical charges are formed. These negative charges become charge balanced by (hydrated) cations in the interlayer between two TOT layers. Due to the higher negative layer charge of illite TOT layers, cations (mainly K^+) are fixed strongly in the interlayer without their hydration shell. In contrast, montmorillonite, which has a lower charge, has interlayer cations that keep their hydration shells. The TO layers of kaolinite are uncharged. An excellent overview of surface properties of clay minerals is given by (Tournassat et al., 2015). For an extensive overview on the basics of clays the reader is referred to Mitchell (1993), (Meunier and Fradin, 2005; Velde and Meunier, 2008).

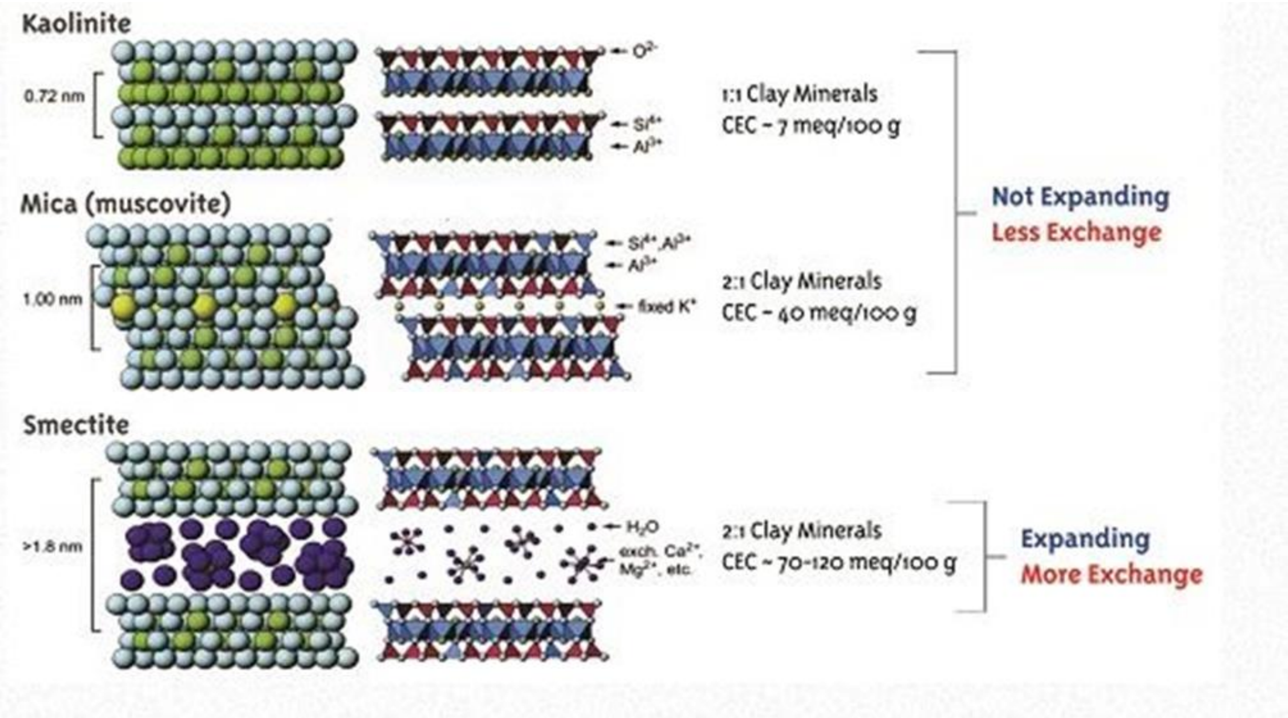

Figure 3-2 – Representation of the structures of different types of clay minerals (figure from https://www.soils4teachers.org/mineralogy).

3.2.2 Main processes controlling transport in clays

3.2.2.1 Diffusion dominated transport

In compact clay systems (natural host rocks, clay based engineered barriers) used for geological disposal of radioactive waste, diffusion is the dominant transport mechanism due to the very low hydraulic conductivities of these rocks ($<10^{-11}$ m/s).

Clay host rocks may experience tectonic disturbances, but due to the presence of swelling clays and water, they tend to self-seal relatively quick (weeks to years). The higher the amount of water and smectites, the prompter is the self-sealing response (plastic Boom Clay vs. Callovo Oxfordian Clay and Opalinus Clay host rocks). After tectonic disturbances, the intrinsic permeability of fractured clay rock is expected to return to that of the intact non-fractured rock (OECD/NEA, 1996).

Advective transport in clays due to the presence or the creation of faults and fractures (by natural processes or excavation processes) is considered negligible with respect to geological time scales because of the self-sealing properties (Bernier et al., 2007; Bock et al., 2010; Li, 2013).

3.2.2.2 Retention predominantly by ion-exchange and surface complexation

Clay minerals such as montmorillonite, illite (including illite-smectite mixed layers) are important in the disposal of radioactive waste since the former is the major clay mineral component of bentonite near-field (buffer, backfill) whereas the latter is present at significant levels in many argillaceous host rock formations under consideration.

The main sorption mechanisms of aqueous species on clay minerals are cation exchange and surface complexation. Cation exchange processes do not depend on pH and occur at the planar surfaces, while surface complexation takes place at edge sites, exhibiting ampholytic protonation behaviour, hence pH dependent. The sorption behaviour of a broad series of elements has been well investigated. See section 2.1 (Classical retention processes) for more details.

Besides these classical retention processes, redox induced precipitation is also an important retention mechanism for redox-sensitive radionuclides. On one hand, this process is due to the presence of Fe(II) bearing minerals such as pyrite or siderite in natural clay host rocks. On the other hand, this can be invoked by the presence of clay minerals containing Fe(II) in their mineral structure (see section 2.2.2 for more details).

For transition metals, another retention mechanism in clays has been observed. At higher loadings of transition metal, surface precipitation of neo-formed phyllosilicates or layered double hydroxides (LDH) may be formed (see also section 2.2.1).

Presence of carbonate and sulphate minerals in the natural clays may also lead to solid solution formation causing strong retention for some radionuclides (e.g. Ba, Sr, Ra) (see section 2.2.3, Solid solutions).

3.2.2.3 Special effect of the negatively charged clay surfaces on radionuclide transport behaviour – double layer effects

Because of the negatively charged clay mineral surfaces, the anionic, cationic and neutral species exhibit distinct diffusion behaviour.

- Anionic species become repelled by the negatively charged surface of clay minerals, which limits their accessibility to certain pores (smallest size and access restriction by constrictivity effects) and reduces their movement to a more limited zone of the bigger pores. This phenomenon is known as “anion exclusion” or “Donnan exclusion”.
- Cationic species on the contrary become attracted by the clay negative surfaces leading to interaction processes that enhance the sorption/uptake in the host rock. These interaction processes are generally expected to lead to a slowed down diffusive transport and are called retardation processes.
- Neutral species are hardly affected by the electrostatic forces.

Recent studies (EC CATCLAY project, Altmann et al. (2015)) have however revealed that uptake of cations in clays not only leads to an increase of the rock capacity factor (cf. eq. 3–7), it may also have an impact on the diffusive properties in terms of altering the D_e values. Potential explanations for this peculiarity will be outlined in the following. For this reason, the effect of nuclide uptake by the solid phase does not inevitably lead to retardation in all cases, it is rather the result of the combined impact on R and D_e (cf. eq. 3–6).

The classical description of diffusive processes of solutes interacting with surfaces according to eq. 3-6 is inherently bound to the assumption that species bound to the surface are immobile, viz. they can only change location after a desorption step (stationary and mobile phases concept borrowed from chromatography). Sorption thus only contributes as a "capacity factor" increasing the retardation of the solute. Once the sorption capacity is filled, or sorption sites are saturated, the amount of solute transported per unit of cross section area and time, viz. the diffusive flux, is exactly the same as for the case of an inert solute that does not interact with the clay surface. The only driving force for diffusion is the concentration gradient of dissolved species present in the bulk aqueous phase (cf. eq. 3-1, first Fick law). In such cases, D_e values of different solutes would only depend on their respective D_0 values, and ηG factors (eq. 3-2). The latter factor is often assumed to be identical for all aqueous species in a given porous medium (e.g. (Aldaba et al., 2014; Jacops et al., 2017b)). However, this assumption has turned out as rather invalid for the case of charged solutes in the nano-scale pore network of the negatively charged clay minerals and clay rocks (cf. *Figure 3-3*). For an overview of the literature, the reader is referred to reviews such as (Altmann et al., 2015; Bourg et al., 2003; Miller and Wang, 2012; Shackelford and Moore, 2013; Tinnacher et al., 2016). The D_e values derived with eq. 3-6 for anionic species are generally lower than those of an uncharged reference species such as HTO or D_2O, while those of cationic species are generally larger, even after normalisation for the individually different D_0 values (see *Table 3-1*). Also for non-charged species (dissolved gasses), unexpected phenomena such as a functional dependence of the "geometric factor" on the molecular size was demonstrated (Jacops et al., 2017a; Jacops et al., 2017b).

Table 3-1 – Normalisation of the effective diffusion coefficient ($D_{e,i}$) of an aqueous species i with the effective diffusion coefficient ($D_{e,HTO}$) of tritiated (HTO) or deuterated (HDO) water and the respective diffusion coefficients in bulk water (D_0). Dependence on the electrical charge of the species.

Dissolved species	$D_{e,i}/D_{e,HTO} \cdot D_{0,HTO}/D_{0,i}$
Anions	< 1
HTO or HDO	= 1
Cations	> 1

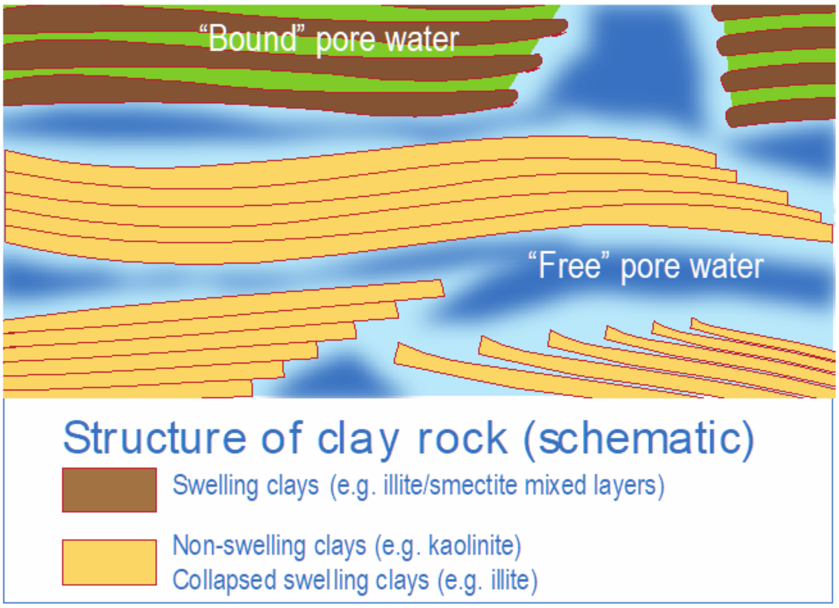

Figure 3-3 – Texture of a clay rock, illustrating the various water properties and the heterogeneity of the different types of clay minerals at the nm scale. Dark blue colours indicate water domains with bulk water properties, light blue colours indicate water domains, which are influenced by the negatively charged surfaces of the clay minerals and their electrical double layers (EDL). Depending on the amount of fixed charges of the latter, the overall charge equivalents of positively and negatively charged solutes may vary within these different water domains. The green colour represents water domains in the interlayers of swelling clays. Note that the fractional distribution of clay and water domains does not represent the reality (drawing taken from (Appelo and Wersin, 2007)).

While potential differences between geometry factors of anionic and neutral species could be a valuable explanation for the lower D_e values of anionic species in the sense of a restricted accessibility of anionic species to the pore space of negatively charged clay surfaces, called "anion exclusion" e.g. (Wigger and Van Loon, 2017), such an explanation would fail for the enhanced D_e values of cationic species. It has been demonstrated (Glaus et al., 2017) for different clay materials that the diffusion-accessible porosity for uncharged species is equal to the total water porosity. If the enhanced D_e values were related to geometry effects, the only reasonable explanation could be found in reduced tortuosity factors τ^2 (cf. eq. 3-3). Consequently one would have to assume shorter diffusion paths (Shackelford and Moore, 2013) for cationic species compared to neutral species, which cannot be justified from a physical point of view.

In view of the conceptual difficulties to explain the different diffusive behaviour of differently charged species by geometry effects solely, it appears to be more sensible to question the assumption of concentration gradients of bulk aqueous species as the only driving force for diffusion. In fact it has been demonstrated for the diffusion of cationic species in compacted smectite clay that the direction and the magnitude of the observed diffusive fluxes depends on the concentration gradients of those cationic species bound to the cation exchange sites present in the interlayer space instead of those in the aqueous phase, cf. *Figure 3-8* (Glaus et al., 2013).

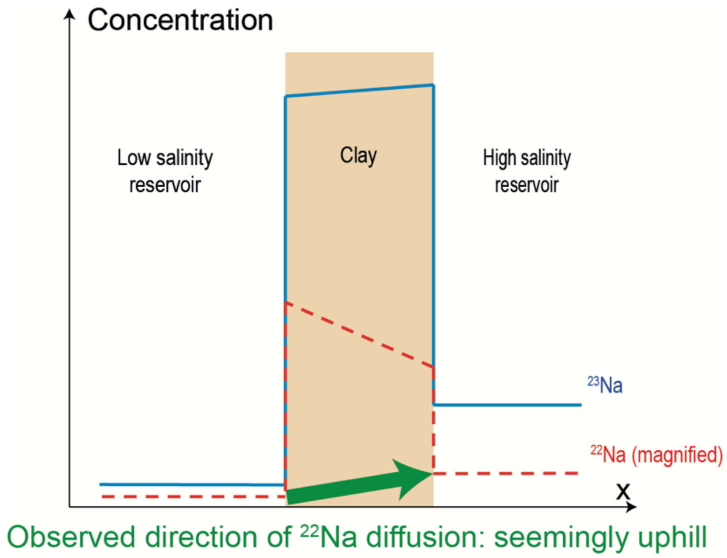

Figure 3-4 – Schematic (qualitative) representation of the concentrations in a steady-state flux situation of an uphill diffusion experiments in which a compacted montmorillonite sample was first equilibrated on both sides with electrolyte solutions differing in their salinity ($^{23}NaCl$), followed by tracer addition ($^{22}NaCl$) on both sides (after Glaus et al. (2013)). The concentrations of the stable isotope cation ($^{23}Na^+$) are shown in blue, those of the radioactive species in red. As indicated by the higher concentration of $^{22}Na^+$ in the high salinity reservoir compared to the low salinity side, this species seemingly diffuses against its own concentration gradient. This can, however, be explained, if its concentration gradient in the cation exchange sites is assumed as the dominant driving force for diffusion. Because of the higher enrichment of the clay with $^{22}Na^+$ at the low salinity side, a decreasing concentration profile of exchanged $^{22}Na^+$ from low salinity to high salinity side has built up as indicated by the dotted red line in the clay phase.

The approach to describe such phenomena on a process-based physical model is an open question and probably depends on structural characteristics of the clay material besides those of the diffusing solute. Although no direct experimental evidence exists for a Brownian type of motion of such surface-associated species, it is reasonable to assume that a similar relationship exists according to eq. 3-1 (first Fick law) between the concentration gradient of these species and their respective diffusive fluxes, as for the species in the aqueous phase. Conceptually, the overall observed diffusive flux can be described as the result of the superposition of the individual fluxes in two phases, one representing the bulk aqueous species and a second the mobile surface species (cf. eq. 3–25).

Within the scope of such a concept, the first Fick law, eq. (3-1), can be expanded to expressions like

$$J = -D_e \frac{\partial c_f}{\partial x} - D_s \frac{\partial c_s}{\partial x} \qquad (3\text{-}25)$$

where the subscripts *f* denote species in the bulk like ("free") aqueous phase and *s* those of the mobile surface species with D_s the respective effective diffusion coefficient of these surface species, hence the term "*surface diffusion*" (a summary of quantitative expressions related to D_s from key references can be found in (Maes et al., 2017a; Maes et al., 2017b)). Depending on the particular characteristics of a given case, it is possible to simplify eq. 3-25 viz. by assuming (i) that either one of the terms on the right-hand side of eq. 3-25 can be neglected and (ii) by replacing the concentration of the sorbed species by using well known thermodynamic equilibrium expressions between C_s and C_f. Just a few examples from the literature are mentioned in the following. Experimental evidence for the validity of expressions like eq. 3-25 was already found many decades ago e.g. (van Schaik et al., 1966).

Glaus et al. (2007) showed that the diffusion across the bulk aqueous phase of cationic species bound to the clay mineral surface by cation exchange (e.g. Na^+ and Sr^{2+}) in compacted montmorillonite was negligible and diffusion was dominated by cationic species present in the cation exchange sites. Cation exchange selectivity's according to the Gaines-Thomas convention were used to relate C_s and C_f.

Diffusion of cationic species across compacted montmorillonite was thus described using the assumption of the clay porosity represented as a single phase. The same approach was also applied by Birgersson and Karnland (2009), who used an electrostatic Donnan-type distribution between the clay phase and the bulk aqueous phase to describe chemical equilibration of differently charged species. These authors could successfully describe the diffusive behaviour of negatively and positively charged species in compacted smectite minerals and bentonites.

Gimmi and Kosakowski (2011) compiled a broad collection of literature data for diffusion of cationic species in clay minerals, clay rocks and argillaceous soils. They used a relationship derived from eq. 3-25 between the observed D_e values and the pertinent R_d (or K_d) values to evaluate D_s values. Thereby they could show that the resulting D_s values comprise rather limited parameter ranges for the cationic species tested in their compilation, confirming the generically applicable character of eq. 3-25.

All these studies were, however, mainly related to cationic species interacting with the clay surface by cation exchange or by electrostatic interactions, respectively. Many representatives from the transition metal and lanthanide or actinide series were shown to form strong surface complexes by chemical bonding with surface groups present at the so-called edge surfaces of clay minerals. Owing to the presumed covalent character of this type of surface bonding, it is hardly expected that such complexes exhibit an appreciable surface mobility. Recent studies by Altmann et al. (2015); Glaus et al. (2015a); Glaus et al. (2020); Montoya et al. (2018), who investigated the diffusion of Co^{2+}, Zn^{2+}, Eu^{3+} and Cs^{+} in compacted illite as a function of a broad variety of solution parameters, such as pH, ionic strength or the concentration of the respective stable isotope element, also gave evidence for surface diffusion phenomena being active in the case of these cations. Significantly larger D_e values were indeed observed for these elements than could be expected from the direct proportionalities with the respective D_0 values of an uncharged reference species. It was demonstrated that the characteristic parameter dependencies of the D_e values were not related with the formation of surface complexes at the clay edge surfaces, but rather with the species bound to planar surfaces. As an example (*Figure 3-5)*, the diffusion depths in compacted illite of bi-valent transition metals significantly increased with decreasing ionic strength (Glaus et al., 2015a), while their total concentrations in the clay at the interface between clay and solution was almost identical for all ionic strengths. This was a clear indication that the D_e values were affected by the variation of ionic strength, rather than sorption. It is well known that the uptake processes of cations at the planar surfaces are susceptible to variations of the ionic strength, while the formation of surface complexes at the edge surfaces is much less dependent on ionic strength (e.g. Bradbury and Baeyens (2005a)). It was further demonstrated in those studies that the R_d values derived from diffusion experiments exhibited the same parameter dependencies as those measured in static batch sorption experiments, in which the tracer distribution between the liquid and the clay phase is measured using dilute clay suspensions.

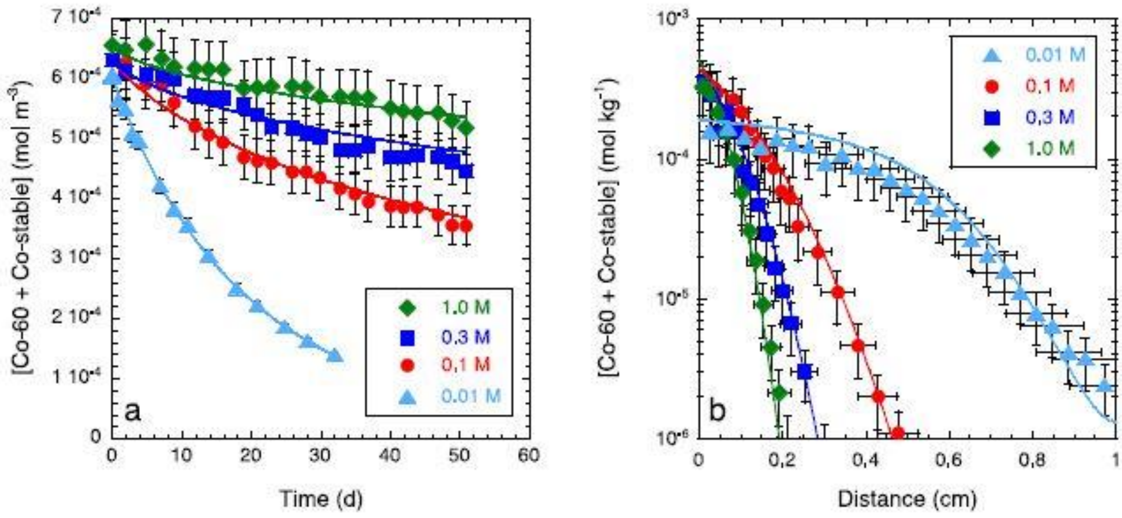

Figure 3-5 – In-diffusion experiments with $^{60}Co^{2+}$ at pH 5 in compacted Na-IdP as a function of ionic strength ($NaClO_4$). Left: the concentration decrease in the source reservoir, right: the profile in the clay (figure from Glaus et al. (2015a)).

In contrast to the very small pore sizes of smectites (order of 1 nm), the pore sizes of compacted illite may be larger by a factor of ~5–10 (Sanchez et al., 2008) and the planar surfaces may thus be in contact with bulk-type water. The distribution of charged species near such charged surfaces is frequently described using the concept of an electrical double layer (EDL) (*Figure 3-6*).

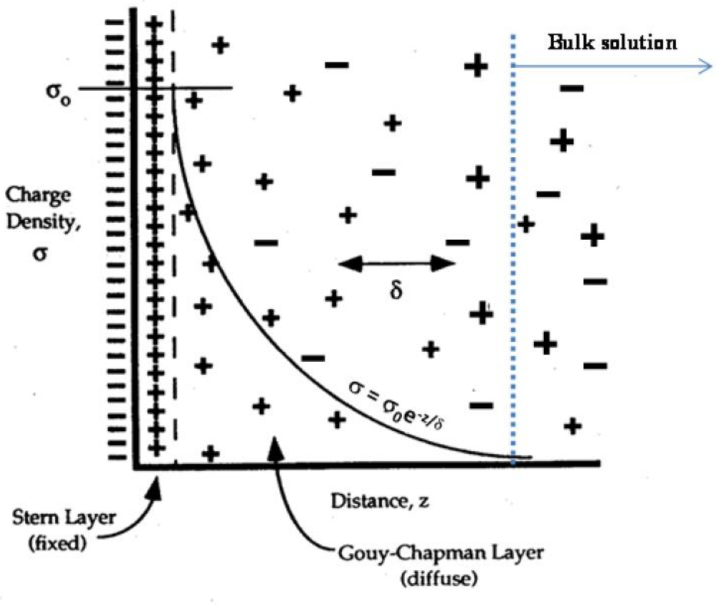

Figure 3-6 – Schematic representation of the electrical double layer (EDL) close to the negatively charged surface of clay minerals with the Stern layer (fixed) and the diffuse (Gouy-Chapman) layer. Source: Altmann et al. (2015).

The neutralisation of the negative surface charges occurs by two different types of cationic species. The first type is located directly at the clay surface and is assumed to be bonded as inner-sphere complexes and thus considered as immobile. These surface species are frequently referred to as the Stern layer species. The second type is a diffuse swarm of cations, near the surface and assumed to be mobile. Anions, accompanied by an excess of diffuse swarm cations, may also enter the EDL domain to a reduced extent. Depending on the charge density of the solid phase and various solution parameters, cationic species are thus enriched in the EDL compared to their respective concentrations in the bulk aqueous phase. If a concentration gradient parallel to the planar surfaces exists, the diffusive flux of cationic species in a charged clay will thus be larger compared to an uncharged clay, owing to the higher population of the cations in the EDL and the resulting larger concentration gradients parallel to the clay surface. Similar to cation exchange in the interlayers of smectites, the unexpectedly large fluxes of transition metal cations can be understood as an enrichment phenomenon at the planar illite surfaces.

For quantitative purposes and for simplifying the numerical procedures for diffusion calculations, the Donnan approach has been proposed to represent the local distribution of the electrical potential near the planar surfaces (Altmann et al., 2015; Appelo et al., 2010; Appelo and Wersin, 2007; Gimmi and Alt-Epping, 2018; Glaus et al., 2015a; Glaus et al., 2020). – shows a schematic representation of the equilibrium distribution of cationic and anionic species between free pore water and EDL water for a Donnan approach using a parallel clay pore geometry.

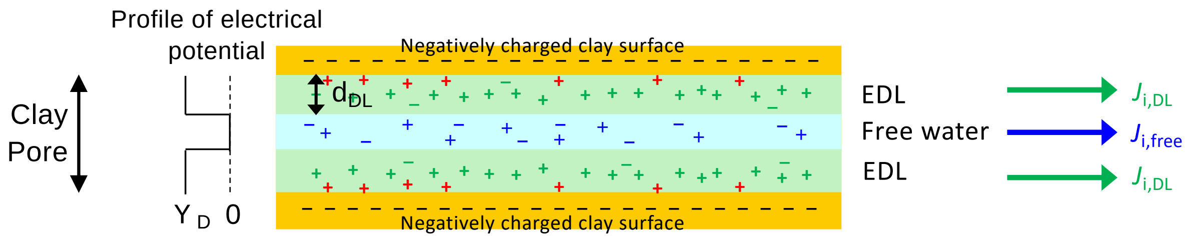

Figure 3-7 – Schematic representation of the Donnan approach for an EDL at the planar clay surfaces. Species in blue (ions in free water) and green colour (ion swarm in the Donnan volume) are assumed to be mobile, while red cationic species are present as immobile surface complexes in the Stern layer. If a concentration difference of a tracer cation species between left and right side of the clay (in analogy to Figure 3-6) is present, the individual flux contributions (J_i) would result from the local concentration gradients parallel to the clay surface in the different domains.

Similarly this concept was also used for a circular pore geometry (Glaus et al., 2015a; Glaus et al., 2020). Note that the choice of the model geometry is a rather arbitrary and an uncritical decision. In the Donnan approach, the extension of the EDL is finitely defined by the Donnan thickness, d_{DL}, exhibiting a constant potential (the Donnan potential, ψ_D) across the Donnan volume. The equilibrium distribution of cationic and anionic species between free pore water and water in the Donnan volume is governed by ψ_D, which is basically derived from the electrical potential at the surface taking into account the shielding effect of the cations in the Stern layer. ψ_D and the d_{DL} are adjustable parameters in this model.

The total flux for each species *i* ($J_{tot,i}$) is the sum of the fluxes in the free pore water ($J_{free,i}$) and the Donnan layer ($J_{DL,i}$) (Altmann et al., 2015; Appelo et al., 2010; Glaus et al., 2015a)[3]:

$$J_{free,i} = -f_{free}\eta G \frac{\partial C_i}{\partial x} D_0 \tag{3-26}$$

$$J_{DL,i} = -f_{DL}\eta G \frac{C_{DL,i}}{C_i} q_n \frac{\partial C_i}{\partial x} D_0 \tag{3-27}$$

$$J_{tot,i} = -\eta G \left(f_{free} + f_{DL}\frac{C_{DL,i}}{C_i} q_n\right) \frac{\partial C_i}{\partial x} D_0 = -D_{e;i}\frac{\partial C_i}{\partial x} \tag{3-28}$$

[3] In case of smectite type clays with accessible interlayers an extra flux, J_{IL}, is present and needs to be added to the total flux: $J_{IL,i} = -f_{IL}\eta G_{IL}\frac{C_{IL,CEC}}{z_i}\frac{\partial \beta_i}{\partial x} D_0$ with β_i the molar or equivalent fraction and $C_{IL,CEC}$ the CEC expressed in interlayer water (mol/l)

Appelo, C.A.J., Van Loon, L.R., Wersin, P., 2010. Multicomponent diffusion of a suite of tracers (HTO, Cl, Br, I, Na, Sr, Cs) in a single sample of Opalinus Clay. Geochimica Et Cosmochimica Acta 74, 1201-1219.

According to the assumed mobility of the different cationic species (bulk aqueous and diffuse layer species = mobile; Stern layer species immobile), the $D_{e,i}$ values for the situation depicted in *Figure 3-7* are calculated as follows:

$$D_{e;i} = \eta G \left(f_{free} + f_{DL} \frac{c_{DL,i}}{c_i} q_n \right) \tag{3-29}$$

η [–] is the total water accessible porosity, G [–] the geometry factor, f_{free} [–] the porosity fraction containing free pore water, f_{DL} [–] the fraction of Donnan layer porosity, D_0 [m^2/s] the diffusion coefficient in bulk water and q_n [–] the viscosity factor. The ratio c_{DL}/c represents the concentration ratio of cationic species between the diffuse layer and the bulk aqueous phase. q_n reflects changes in the surface mobility compared to the mobility in the bulk pore aqueous phase. The application of expressions like in eq. (3–29) in transport models is limited to situations in which the various parameters are independent of concentration c. This can reasonably be assumed to be the case in many examples of tracer diffusion in a given electrolyte medium.

Within the concepts of such electrostatic approaches for the description of surface uptake reactions and diffusion processes, not only the behaviour of the counter-ions, but also those of the co-ions (anions, in the case of negative charged clay surfaces) are implicitly included. A valuable overview of different models to describe the behaviour of anions in charged clays can be found in Tournassat and Appelo (2011). The picture shown in – shall not be confused with the anion exclusion concept in which the assumption is made that part of the porosity is completely inaccessible to anions (e.g. Van Loon et al. (2007)). The volume fraction of free pore water in the Donnan approach is always larger than the equivalent exclusion volume in the latter approach. The results of both approaches can, however, be mutually converted for the purpose of comparison.

The description of the diffusion of charged species in charged porous argillaceous media may thus be based on the use of lump-defined effective diffusion coefficients, comprising the characteristic geometric properties of the porous medium and the presence of multiple chemical concentration gradients, despite the comprehension that it may actually be the result of the superposition of the diffusion of individual chemical species in multiple phases. Because the local concentration gradients of those species cannot always be measured by experimental methods, the use of thermodynamic equilibrium models for the description of lump-defined effective diffusion coefficients is indispensable for the purpose. Currently, reactive transport codes as PhreeqC and Crunchflow have implemented the double layer effects on diffusion in their codes. Obviously, the diffusion model represented in eq. (3–29) uses an idealised picture of the chemical species and equilibria involved. This applies also for the assumptions regarding geometry. The model does not describe effects of the orientation of the clay particles with respect to the direction of diffusion. In this idealised picture, the concentration gradients responsible for tracer diffusion are assumed to be parallel to the clay surfaces, while the respective concentration gradients perpendicular to the surface determine the chemical species equilibration at those surfaces and thus the chemical enrichment or depletion factors.

Alternative assumptions for the equilibrium distribution can be taken, such as a Poisson type of distribution (*Figure 3-6*) instead of a discrete Donnan type distribution and resulted in similar diffusion models cf. e.g. (Ochs et al., 2001; Tachi and Yotsuji, 2014). The various ambiguities in the model assumptions can only be resolved to a limited extent by macroscopic diffusion experiments. Ambiguities remain for instance with respect to the individual species concentrations and their molecular mobility's. More elaborated methods, such as spectroscopic, diffractive and microscopic techniques (e.g. Bostick et al. (2002); Ferrage (2016); Malikova et al. (2010); Park et al. (2008); Strawn and Sparks (1999)) are required to bound critical model assumptions. Similarly holds also for the use of atomistic simulation methods which can give more insight into the detailed structural characteristics and processes related to surface reactivity of clays (Bourg et al. (2017); Bourg and Sposito (2010); Churakov (2013); Churakov and Gimmi (2011); Cygan et al. (2009); Gimmi and Churakov (2019); Holmboe and Bourg (2014); Kosakowski et al. (2008); Tinnacher et al. (2016); Tournassat et al. (2016a))

The broad variety of model concepts for describing the dynamics of diffusive transport processes in clay minerals and clay rocks renders the definition of an effective diffusion coefficient more and more complex. In fact, a confusing variety of different terminologies can be found in the literature for the exact definition of effective diffusion coefficients, which makes it sometimes difficult to compare the results of individual works. Valuable attempts to provide an overview of this situation can, however, also be found in the literature (e.g. Shackelford and Daniel (1991); Shackelford and Moore (2013)). Despite the "unphysical" nature of such coefficients, they are frequently applied for engineering purposes, because the concentration gradients in the bulk aqueous phase are the only sound basis for transport simulations. In order to attain an improved process-based understanding of the diffusion of charged species in charged porous argillaceous media, it is, however, imperative to improve the physical basis of the understanding of surface induced diffusion phenomena.

3.2.3 Research methods to extract transport parameters

Several types of migration experiments are used to investigate radionuclide transport in clays. The transport parameters that are extracted from these experiments, by solving the transport equation (section 3.1) analytically or numerically for the correct initial and boundary conditions, are D_a, D_e and the rock capacity factor ηR (porosity times retardation factor). It is worth to note that D_a, and D_e are related as $D_e = \eta R D_a$.

Already some decades ago, pioneers in the field have described experimental methods and mathematical models for deriving diffusion parameters for application in nuclear waste disposal: Crank (1975), Put and Henrion (1992); Shackelford (1991); Shackelford and Daniel (1991).

More recently, some publications with comprehensive overviews became available: Aertsens (2011); Bourg and Tournassat (2015); Van Loon et al. (2012).

In this section, the focus is set on classical mass transfer experiments as these apply in principle to all radionuclides of interest in the context of geological disposal and they can provide direct information on their transport behaviour. Detailed insight into local mobility of ions in different pores of clay materials can also be obtained by classical and ab initio molecular dynamics simulations. These simulations are particularly useful for understanding the ion transport in narrow pores close to the negatively charged surface of clay particles, viz. diffuse double layer (DDL) (see Churakov and Prasianakis (2018) and references therein). There exist techniques based on nuclear magnetic resonance (NMR) and neutron scattering, electrical conductivity (impedance spectroscopy,…) which also provide important information on transport in porous media, but they require sophisticated equipment and data treatment and are only applicable to a limited set of “tracers”. They mainly provide qualitative information on the transport mechanism and less quantitative data on the tracer transport parameters. Further information to key references on these methods are available in the papers of Bourg and Tournassat (2015); Van Loon et al. (2012).

The mass transfer-based methods most widely used nowadays are summarised in the present section highlighting recent developments.

Methods to derive migration parameters in compact clay materials can be divided in two categories:

1) transport by diffusion only (concentration gradient is the only driving force),

2) transport by a combination of diffusion and an extra flux component as result of a hydraulic or electrical driving force with percolation or electromigration experiments respectively.

The methods described here are applied for laboratory experiments performed at the cm-scale for compacted and fully saturated clay systems. These methods are summarised in a comprehensive way in *Table 3-2*.

3.2.3.1 Category 1 – Diffusion only

3.2.3.1.1 Back-to-back diffusion

This is the simplest form of a diffusion experiment in which a trace amount (below the solubility limit) of the diffusing species (radionuclide previously conditioned to be at chemical equilibrium with the clay in the case of redox-sensitive elements to avoid precipitation and reactive transport) is spiked (either directly on the surface or by means of a saturated thin porous disk, which does not interact with the tracer) between 2 clay cores in a diffusion cell which confines the system (*Figure 3-8a*). In the absence of precipitation during the transport, diffusion gives rise to a typical Gaussian shaped tracer profile in the clay core. The diffusion profile is obtained by cutting the clay core in thin slices and measuring the concentration (or the radioactivity) of the diffusing species in each slice. It is a simple technique and there is a direct contact between the diffusing species and the clay material (no disturbing influences from confining porous filters – see further 3.2.3.3). ***This technique provides the value of the apparent diffusion coefficient (D_a) only***.

Back-to-back diffusion is a technique of choice for strongly sorbing radionuclides with a simple chemistry such as caesium (Cs^+). However, with redox-sensitive radionuclides (Se, Tc, U, Np, Pu,…) the radionuclide must first be put at thermodynamic equilibrium with the clay prior starting the diffusion experiments. This is particularly important when reducing conditions are prevailing in the clay. If the redox-sensitive element is introduced in its oxidised state, it will be reduced during the transport and could precipitate. Under such an experimental setup, it is impossible to distinguish between sorption and precipitation and the modelling will lead to erroneous overestimated retardation factors (R).

3.2.3.1.2 Through-Diffusion

This is probably the most widely used method to determine diffusion parameters. A clay core is confined in a diffusion cell between 2 porous filter plates connected to water compartments (*Figure 3-8b*). One compartment contains the diffusing species (high concentration reservoir, upstream), the other compartment is free of diffusing species (low concentration reservoir, downstream). In these experiments, the flux arriving at the downstream compartment is monitored until a quasi steady-state flux regime has been attained. ***From the evolution of the flux with time, the effective diffusive coefficient (D_e) and the rock capacity factor ηR (also called α) can be determined independently***. As we have access to the ηR, these experiments can be linked to batch sorption experiments (R – K_d relation eq. 3-5). In this technique, also the decrease of the concentration of the diffusing species in the upstream compartment can be monitored as well as the concentration profile inside the clay (by post mortem slicing, idem above). The related analysis of mass balance and the observation of concentrations within the clay sample can be used to crosscheck the results obtained for mass balance and internal consistency. Depending on the experimental conditions (Variable or Constant Concentrations in the reservoirs), one defines different sub-types: CC-CC, VC-VC, VC-CC, CC-VC (Aertsens et al. (2017); Takeda et al. (2008a); Takeda et al. (2008b). It is important that the mathematical models used to interpret the measurements make use of the correct boundary conditions in line with the experiment as this can lead to significant differences in the derived parameters. The use of porous filter materials in these experiments can play an important role in the transport process. This is not so important for non sorbing tracers (anions, HTO) as long as the clay cores are sufficiently thick compared to the combined filter thickness, but they were evidenced to have a pronounced role for sorbing tracers either as an extra diffusion barrier (simple cations such as Sr^{2+}, Cs^+,… Aertsens et al. (2017); Glaus et al. (2015b)) or they have a tendency to strongly sorb the diffusing species (transition metals, lanthanides and actinides) (Altmann et al., 2015). Dierckx et al. (2000) showed the strong sorption of ^{241}Am onto stainless steel filters.

A through-diffusion (TD) experiment can be followed by out-diffusion (OD), which is a valuable technique to crosscheck the results of the TD step. Out-diffusion is measured after reaching the steady-state flux phase of a through-diffusion experiment. Both reservoirs are exchanged by solutions devoid of the diffusing species, viz. its concentration is kept at an approximate zero level on both sides of the clay sample. Out-diffusion can be used also to detect slow diffusion pathways. If their contribution to the overall flux is only a small fraction (a few percent's), such pathways cannot be directly revealed in a through-diffusion experiment. In an out-diffusion experiment they will, however, become visible as a two-phase flux behaviour (Van Loon and Jakob, 2005). Out-diffusion can also be used to reveal inconsistencies with respect to through-diffusion.

3.2.3.1.3 In-Diffusion

The in-diffusion (ID) method can be considered as a sub-type of the through-diffusion experiments. The set-up is similar (*Figure 3-8c*), but in TD it is intended to measure the flux going through the entire clay sample, while in an ID experiment not. Especially for sorbing tracers, it may take extremely long times for the tracer to diffuse through. ***In this technique the decrease of the tracer concentration in the upstream reservoir and the tracer profile in the clay are determined and the combination of this information provides information on the D_e and ηR*** (Yaroshchuk and Van Loon, 2008). As with the through-diffusion experiment, the presence of a porous filter plate may have an important effect.

The in-diffusion method is also commonly applied for in-situ tests of radionuclide transport (see 3.2.4): the DI, DI-A, DI-B and DR in-situ experiments in the Mont Terri Rock Laboratory and the DIR in-situ tests in Bure URL (overview in Delay et al. (2007); Gimmi et al. (2014); Leupin et al. (2017); Van Loon et al. (2012)). Post-mortem profile analysis is performed on a large clay core recovered by overcoring the borehole used to inject the tracer solution.

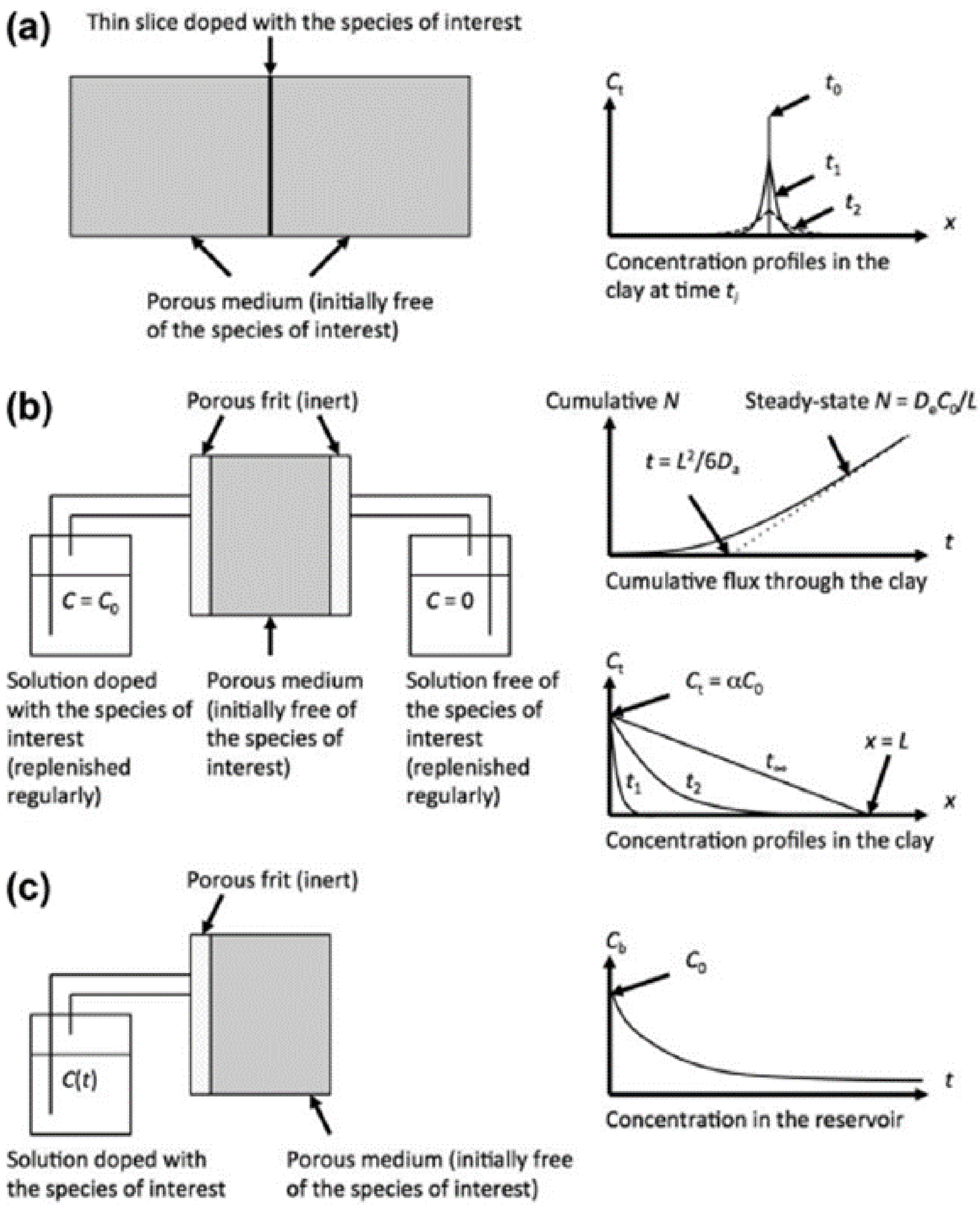

Figure 3-8 – Schematic representation of different methods used to determine diffusion parameters of radionuclides in saturated porous materials where diffusion is the only transport mechanism. Figure taken from Bourg and Tournassat (2015).

3.2.3.2 Category 2 – Diffusion + extra driving force

In this category, an extra driving force is used to speed up the transport process. These driving forces are either a hydraulic gradient (diffusion-advection experiment) or an electric field (electromigration experiment).

3.2.3.2.1 Column migration experiments applying a hydraulic gradient

In these experiments, a clay core is confined in a migration cell connected at one side (inlet) with a water vessel that is at elevated pressure so that a hydraulic gradient is applied (piston pump, HPLC pump, pressurised water barrel,…). At the inlet, a HPLC injection valve is installed from which a small pulse of tracer can be injected into the water stream in front of the clay core. This mimics a chromatographic column set-up (Put et al., 1991) (*Figure 3-9 top*). ***At the other side of the clay core (outlet), water is collected as a function of time and the amount of tracer flowing out is measured to obtain a breakthrough curve. Because of the presence of an additional hydraulic gradient, not an apparent diffusion coefficient but an apparent dispersion coefficient (*** $D_{disp,a} = D_a + aV_a$ ***) can be obtained. However, as long as the advective term remains limited, the approximation of*** $D_{disp,a} \sim D_a$ ***applies. From the ratio*** V_{darcy}/V_a ***information on the rock capacity factor*** $\alpha = \eta R$ **can be derived.** This kind of test is particularly interesting for non-sorbing (or slightly sorbing) tracers. When coupled to a manifold system, several experiments can be performed simultaneously and successive tracer injections can also be performed on the same clay core if necessary (as no long out-diffusion is required) (Aertsens et al., 2003). This method is also useful for investigating the effect of changing chemical conditions in the percolating water: different ionic strength (Aertsens et al. (2009a); Moors (2005)), influence of an alkaline plume (ECOCLAYII (2005); Wang et al. (2007)), $NaNO_3$ plume (Bleyen et al. (2018)) on transport by first analysing the diffusion behaviour in pristine pore water after which the water becomes switched to another type of water followed by new tracer injections, all on the same core.

For sorbing tracers, breakthrough may not be reached even after many years, and in that case the tracer profile determined on the clay core at the end of the experiment can provide information on the apparent diffusion coefficient D_a **only**. Similarly to the TD and ID tests, the porous filter and injection loop may cause problems when working with strongly sorbing tracers, which often sorb onto these materials (often 316 stainless steel) as well.

Here again, it is necessary to stress the importance of the chemical speciation of redox-sensitive radionuclides at the start of the percolation experiment. If a radionuclide soluble under oxidizing conditions (using radiotracers "as received") is progressively reduced during its transport in clay, it can precipitate if the solubility limit of its reduced species is exceeded. It is therefore essential to guarantee that redox-sensitive species are first in chemical equilibrium with the reducing clay before to start the experiment. Failing to properly achieve this chemical pre-equilibration step can lead to the reduction/precipitation of the redox-sensitive radionuclide during its transport and it will be difficult/impossible to derive quantitative transport parameters from it or the data become wrongly interpreted.

In order to circumvent the problem of radionuclide sorption onto the porous filter, the back-to-back configuration can be used and connected to a hydraulic gradient (*Figure 3-9 middle*). For non-sorbing or moderately sorbing tracers, the breakthrough curve can be determined. For strongly sorbing tracers, the clay core can be cut into thin slices and the radionuclide profile inside the clay can be determined to obtain D_a without the problem of sorption on the filters. In these experiments one can also use a solid phase of the tracer in equilibrium with the pore water. In this case you have a constant source (instead of a Dirac pulse) of the species controlled by the solubility.

3.2.3.2.2 Electromigration

By imposing an external electrical field to both extremities of a cylindrical clay core confined in an appropriate cell, ions present in the clay pore water are forced to move towards the electrode of opposite charge (this phenomenon is called electromigration), which seriously accelerates their transport (*Figure 3-9 bottom*). The velocity with which the charged species moves is linearly proportional to the strength of the applied electrical field. The proportionality coefficient is the ionic mobility, which is related to the apparent diffusion coefficient (D_a) of the considered ion. As an effect of the moving cations, a water flow is also created which is called electro-osmosis. The movement of water (osmosis) towards the cathode in the clay core is directly related to the movement of cations. First because cations moving in the electrical double layer (EDL) close to the clay negatively charged surface drags the free water present in the pores and also because water in the hydration shell is interacting stronger with cations than with anions due to their smaller ionic radius. Applying an electrical field to accelerate the transport is particularly interesting for strongly sorbing tracers. A method was developed by Beauwens et al. (2005); Maes et al. (1998); Maes et al. (1999); Maes. et al. (2001) to determine diffusion coefficients for radionuclides in Boom Clay. Besides using the method in a quantitative way (determination of diffusion coefficients) it can also be used to obtain information on the speciation of the moving species (Maes et al., 2002; Maes. et al., 2001) and the migration behaviour (stability) of radionuclide-Organic Matter species/colloids (Maes et al., 2004; Maes. et al., 2001). This method was later on used and adapted for compacted clays (Higashihara et al. (2004); Tanaka et al. (2011)), and granitic rocks (Li et al. (2019b); Lofgren and Neretnieks (2006) see section 3.3.3.2.2 and *Figure 3-17*). ***Information on the apparent diffusion coefficient D_a is obtained by performing multiple experiments at varying electrical field E (causing different electromigration velocity). Apparent dispersion coefficients are obtained for each electromigration velocity. To obtain the D_a the linear relationship of the determined dispersion coefficients as function of E is extrapolated to E = 0.***

Application of high electrical fields to a clay core triggers a significant heat release that may have an influence on the mobility of the diffusing species under investigation. Furthermore, it might also disturb the clay core in unexpected ways e.g. electro-consolidation due to electro-osmosis.

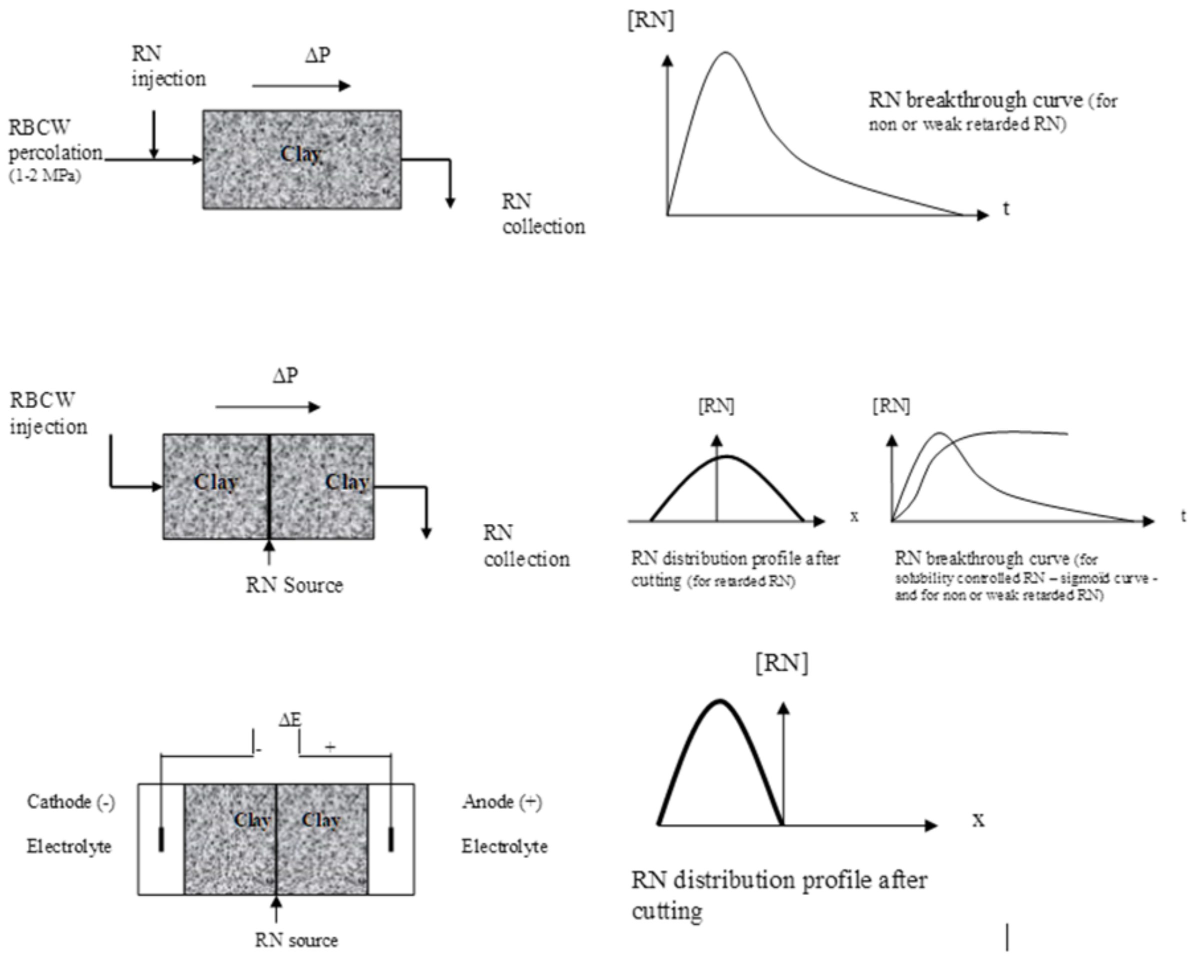

Figure 3-9 – Illustration of migration experiments where an extra hydraulic or electrical gradient is applied to accelerate the transport of the radionuclide of interest. Abbreviations: RN: radionuclide, RBCW: real Boom Clay water (Figures from Maes N.).

Table 3-2 – Summary of various laboratory techniques, based on mass transfer, for diffusion measurements (adapted from Van Loon et al. (2012)).

Technique	Features	Diffusion parameters	Suited for	Less suited for
Through-diffusion	Steady-state technique Time consuming Porous filters may be a problem	D_e, $\alpha = \eta R$	Non and weakly sorbing tracers	Strongly sorbing tracers
Out-diffusion	Steady-state technique Time consuming Porous filters may be a problem	D_e, $\alpha = \eta R$	Non and weakly sorbing tracers	Strongly sorbing tracers
In-diffusion Controlled source	Transient technique Relatively fast Porous filters may be a problem	D_e, $\alpha = \eta R$	All kind of tracers	
In-diffusion No control on source	Transient technique Relatively fast	D_a	All kind of tracers	
Back-to-Back diffusion (BtB)	Transient technique No problem with porous filters	D_a	All kind of tracers	Strongly sorbing tracers (e.g., Cs^+)
Column migration experiment – Pulse injection	Additional hydraulic gradient Clay cores can be conditioned with other pore waters Porous filters may be a problem	$D^i_a \sim D_a$, $\alpha = \eta R$, K	Non and weakly sorbing tracers	Strongly sorbing tracers
Column migration experiment – BtB	Additional hydraulic gradient No problem with porous filters	$D^i_a \sim D_a$, *($\alpha = \eta R$ only for weakly retarded tracers), K, (solubility information)*	All kind of tracers	Strongly sorbing tracers (e.g., Cs^+)
Electromigration	Additional electrical gradient (acceleration) No problem with porous filters Provides information on the chemical speciation Induces chemical changes in the system	D_a, *(ion mobility)*	Non, weak to moderately sorbing tracers,	

3.2.3.3 Experimental challenges and technical solutions

As pointed out, when a compacted clay sample is contacted with solution reservoirs, porous filter-plates are required in order to maintain the sample integrity related to the swelling behaviour of clays. These porous filter plates can introduce artefacts as they represent an additional diffusion barrier (2 – 3 mm thickness) specifically for through-diffusion (TD) and in-diffusion (ID) experiments, especially when thin clay slabs (5 – 10 mm thickness) are used (Aertsens et al. (2017); Glaus et al. (2015b); Glaus et al. (2008b); Suzuki et al. (2003)). This can be accounted for in the modelling by explicitly considering the diffusion behaviour of the filters. However, even when accounting for the filter behaviour, it increases the uncertainty of the obtained data. Glaus et al. (2015b) designed the so-called flushed filter cells in which the problem of the diffusion barrier created by the filter is strongly reduced. This design is based on the work of Jahnke and Radke (1989).

Furthermore, the porous filter plates, typically made of fritted stainless steel (to withstand the swelling pressure developed by the swelling clay) may exhibit strong sorption properties (especially for transition metals, lanthanides, and actinides at more alkaline pH). In fact, any other material that is in contact with the tracer other than the clay, such as tubing, water vessels, valves and connectors may exhibit sorption properties towards the diffusing species and as such affect the results of the experiment. It is therefore advised to test the sorption to the materials used beforehand. Other more “inert” materials such as PEEK, PTFE, organic polymeric membranes,… may provide a solution to circumvent sorption (Glaus et al., 2015b). In some cases for clay rocks, it may be possible to avoid filters by using very small specimen in direct contact with the tracer-containing solution (Van Loon and Muller, 2014).

Investigating the diffusion behaviour of strongly sorbing tracers is further challenging because of the limited travel distances, which means that experiments may need considerably long times (years) before a meaningful analysis can be performed. This entails that during the entire period, the chemical and physical conditions of the experiment should be kept stable. Even then, the diffusion profiles that develop within the clay often do not extend further than a few mm. Soft clays such as Boom Clay and Ypresian Clay, or London Clay, are easy to cut in slices of about 0.5 – 1 mm with a simple knife and a special cutting edge system equipped with a piston mounted on a screw to push the clay core out of the diffusion cell and with a Palmer to precisely adapt the slice thickness. To enable a precise determination of the shorter diffusion profile in hard and brittle clays or argilites, a more sophisticated profiling technique is needed that goes into the sub-mm range. Van Loon and Eikenberg (2005) developed the abrasive peeling method. Savoye et al. (2013) have used µ-LIBS (micro Laser induced breakdown spectroscopy) to characterise concentration profiles at submillimetre scales. Rutherford backscattering spectroscopy (RBS) used by Alonso et al. (2009) was another spectroscopic technique that even goes to lower scale (tens of nm). Also Laser Ablation Mass Spectrometry (LA-MS) is used (Wang et al. (2013); Wang et al. (2011)). These techniques are challenging (calibration, interpretation, sample pre-treatment, range of application, …) and are not commonly available.

Linked to the limited penetration depths of the diffusion profiles are the artefacts induced at the external surface of the samples. Sample preparation (and storage) will inevitably create disturbances (physical, chemical) at the external surfaces, which will be the first in contact with the tracer. Furthermore, when put in contact with water, by means of a porous filter, some swelling effects will occur disturbing the clay surface in direct contact with the filter: clay particles may be pushed into the porous filter plates and water may locally soften the clay near the contact interface resulting in an increased porosity and water content at the interface filter/clay. This will also change the porosity of the filter (clogging) and the properties of the first mm of the clay sample. This is very important when interpreting TD/ID experiments (Glaus et al. (2011); Glaus et al. (2008b)).

Besides experimental difficulties, there are also challenges on the modelling side. Even though, the principles of diffusion are well known and accepted (Crank (1975); Shackelford (1991)) and mathematical expressions have been used to obtain parameters for a range of experimental conditions since a long time, it became apparent that the number of experimental factors, which have been neglected before, do have a significant effect on the derived parameters especially for the sorbing tracers. These factors include filters, strict control of boundary conditions, induced changes at the clay matrix at the interfaces (mechanical disturbances, density and porosity changes due to clay hydration and swelling,…),…. Incorporation of all these possible influences into a consistent mathematical model has been proven to be challenging. Many TD studies (especially older studies) may provide data that were not obtained using a correct mathematical description of the experimental conditions and as a result, the values of the migration parameters are subject to a large uncertainty.

Related to this is the consistency of data obtained from different types of experiments. Several studies of Aertsens et al. (2008a); Aertsens et al. (2012); (Aertsens et al., 2020); Aertsens et al. (2009b) have indicated that using different types of experiments (ID, TD, column migration,…) not always provide consistent transport parameters. Often the derived D_a was quite consistent, but not the values for the rock capacity factor $\alpha = \eta R$. This could in part be explained by experimental factors that have an important influence on the experimental results (filters in TD), correct inclusion of the boundary conditions in the mathematical model, but also because of flaws in the conceptual mathematical description of the transport processes. Aertsens et al. (2020) have recently shown that column migration experiments (percolation experiments, or infiltration tests) do not provide a correct estimate of the diffusion accessible porosity (η) of anions as compared to pure diffusive experiments (TD). A factor two often affected the values.

As already explained previously, it is also essential to work with redox-sensitive radionuclides (Se, Tc, U, Np, Pu,…) in chemical equilibrium with the reducing conditions prevailing in situ in the clay before to start the migration experiments. Failing to pre-equilibrate a redox-sensitive element with the clay prior to start the diffusion test leads to considerable artefact making a quantitative analysis difficult/impossible.

3.2.4 Experimental approaches to upscaling

The mobility of ions in clay porous media depends on the electrostatic interactions in the diffused double layer (DDL) formed at the surface of negatively-charged clay mineral particles and on complex coupled pore scale transport phenomena controlled by the connectivity of pore space (Churakov and Prasianakis, 2018). In principle the macroscopic mobility, e.g. one measured in laboratory experiments can be obtained taking into account the local mobility of ions and the geometry of pore space. The local mobility of ions close to mineral surfaces has been extensively characterized by molecular simulations. Molecular simulations provide insights into the nature of mineral-aqueous interface and allow discriminating the effect of mean-field electrostatic interaction of ions with the surface, dynamic ion-ion correlation phenomena, and the short-range steric effects at the interface. On the larger scale, the fluid transport will be mainly determined by the texture of the rock and connectivity of the pore space. The pore scale transport simulations are performed by stochastic methods (Random Walk, Brownian dynamics) and Lattice Boltzmann simulations techniques. One of the most critical parameters for the pore scale modelling is a realistic representation of the pore scale geometry. Whereas the larger sub-micrometre pores are accessible by computerised tomography (CT)-measurements (Keller and Holzer, 2018), the smaller nanometre scale pores are envisaged by numerical modelling (Tyagi et al. (2013); Underwood and Bourg (2020)). Following the idea of a 'virtual rock laboratory', several attempts have been taken to merge atomistic and pore scale simulations to explain experimentally observed trends in water and ion transport as a function of compaction state, clay and pore water composition, and saturation degree. Simulation results show qualitative agreement with experimental observations (Churakov and Gimmi (2011); Churakov et al. (2014); Gimmi and Churakov (2019)).

The purpose of performing macroscopic diffusion/retention experiments is to obtain transport parameter values (and uncertainty ranges) that are relevant for the considered host formation to be used in safety assessment evaluations. This requires that the data obtained can be up-scaled with respect to time and space scales.

Laboratory diffusion experiments suffer from relatively short time-scale and challenging sample preparation. Total confinement pressure release may result in decompaction and irreversible distortion of the geometrical structure, which may have an impact on the transport properties. Also sample preparation, may result in artefacts and alteration in the chemical environment (e.g. pyrite and clay oxidation, CO_2 degassing, microbial perturbation, …) affecting the transport properties. Field experiments may therefore be seen to be more realistic because tracer migration occurs, after a certain distance from the borehole, in a more or less virgin environment.

Microscopic phenomena determine the behaviour of fluid dynamics in porous media. This makes the description of the pore geometry complex both at laboratory scale and at field scale. To tackle flow and transport phenomena at relevant scales (much larger than the pore scale), mass and momentum balances at the pore scale are averaged over volumes or areas containing many pores, they are considered as a continuum. This is related to the Representative Elementary Volume (REV).

For clays, typical grain size of a particle measures several tens of micrometres (excluding larger inclusions such as pyrite and carbonate concretions, septaria, fossils, worm tunnels, sand lenses, and other local heterogeneities). The dimension of a REV is in the order of several mm. Consequently for natural clay samples, most experimental and modelling scales are larger than the dimensions of a REV. Upscaling does not require to adapt hydraulic or transport parameters as far as macroscopic heterogeneities remain limited (Marivoet et al., 2006).

Within safety evaluations, clay host formations are often considered homogeneous. However, at lower scales, heterogeneity definitely exists and may have important impact on transport parameters.

There are several ways to perform upscaling and to assess the impact of heterogeneities: large-scale tests (lab and in-situ), natural tracer profiles, lab diffusion/sorption tests on cores sampled over the entire stratigraphy.

First of all, large-scale transport tests may be considered. These can be conducted in the lab using large blocks (up to several dm) or in-situ in Underground Research Labs – URL- (several dm up to several m). The latter experiments are an upscaling both in time (tens of years) and distance (up to dm and even several meters). These tests mainly make use of conservative or weakly sorbing tracers in order to obtain measurable tracer profiles over sufficiently large distances in still reasonable time frames (several years to decades).

An example of a large block experiment consist of a large cylindrical drill cores where a radiotracer source is emplaced in a hole drilled at the centre (see *Figure 3-10*). After a given time, subcores are taken to determine the 3D spatial distribution of the tracers (this mimics an in-diffusion experiment where the profile in the clay is determined). These experiments provide information about the anisotropy of the diffusion coefficients and can be compared to small-scale diffusion experiments. This kind of tests was conducted on OPA Clay samples (Cormenzana et al. (2008); García-Gutiérrez et al. (2006) and COx (Cormenzana et al. (2008)).

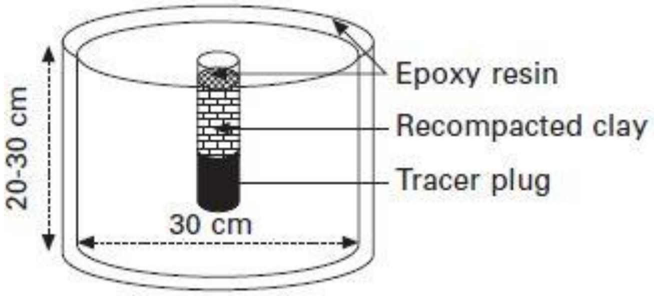

Figure 3-10 – Schematic representation of a large-block diffusion test (taken from García-Gutiérrez et al. (2006)).

A first type of *in situ* diffusion experiment can be considered as an up-scaling of the large block experiments. In this *in situ* radial diffusion test, a borehole is drilled in the clay formation (see *Figure 3-11*). A cylindrical filter screen is emplaced at the bottom of the borehole enabling circulation of water that contains the radiotracers. The borehole is sealed with a packer, an inflatable rubber element sealing the annular space between the down-hole equipment and the borehole wall. The radiotracers diffuse radially into the surrounding clay rock. After a given time, the experiment is ended, and the borehole is overcored. Subcoring of the part where the tracers were applied enables the determination of the 3D spatial distribution of the tracers. From the tracers diffusion profiles in the clay rock, combined with the change in relative concentration (C/C_0, where C_0 is the initial concentration) of the tracers in the reservoir solution as a function of time, the effective diffusion coefficient (D_e) and the rock capacity factor ($\alpha = \eta R$) can be calculated accounting for anisotropy.

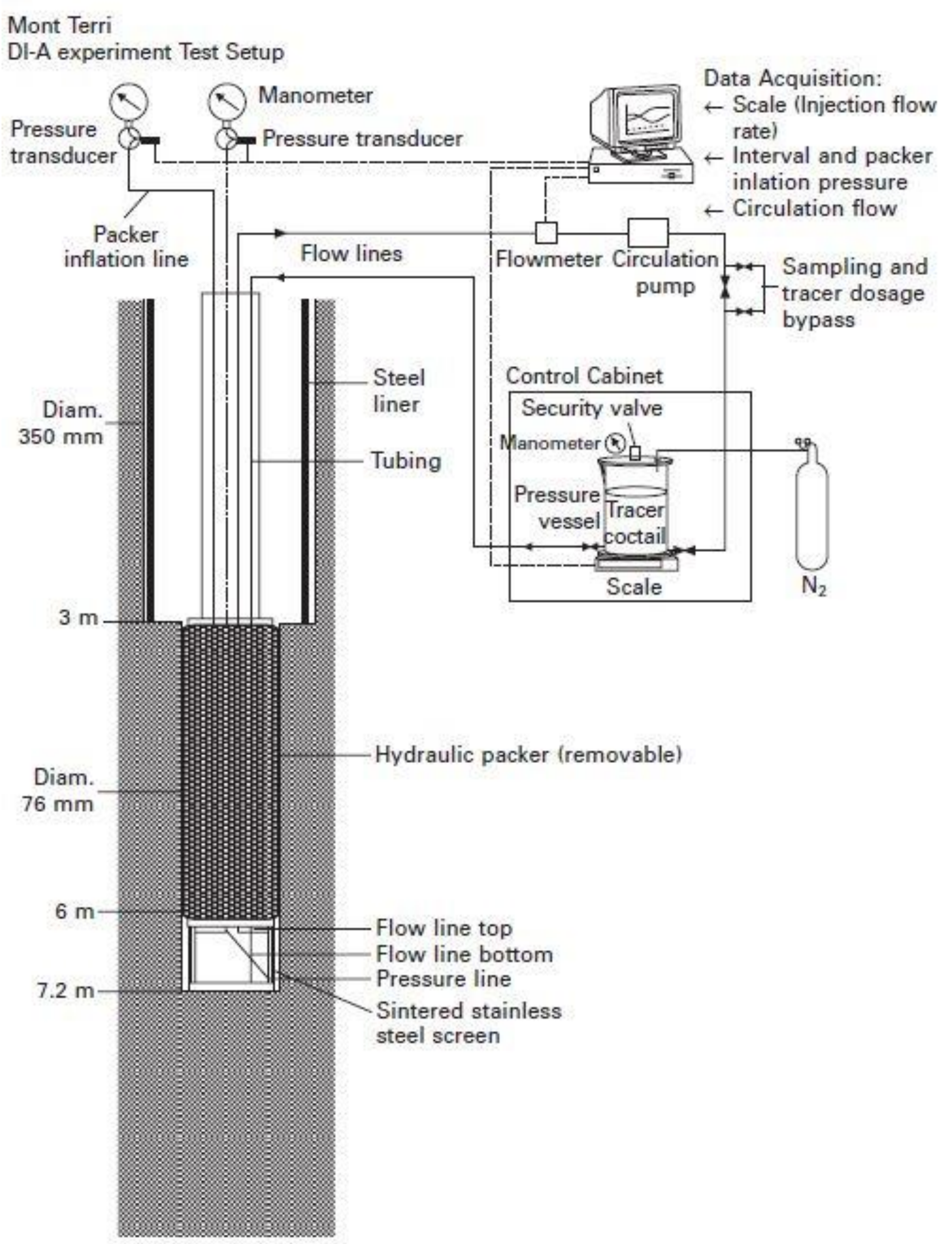

Figure 3-11 – Schematic view of a large scale in situ in-diffusion experiments in Opalinus Clay at Mont Terri Rock Laboratory (DI-A1 experiment) (Van Loon et al., 2004b).

This type of experiment is always affected by a "skin" effect due to the excavation-disturbed zone (EDZ) that exists around the borehole (BDZ). This may cause problems in the interpretation of the data and is especially a problem for sorbing tracers as their penetration depth remains limited even after several years. In general, these experimental tests still only provide information on a dm scale distance limited to the overcoring dimensions. The overcoring method also represents a considerable technical challenge and in case of failure for unexpected reasons, all the information on the tracers profile in the clay can be lost in a few minutes at the end of the experiment after several years of work (cf. cement water (CW) experiment at Mont Terri and two of the DIR experiments at Bure). Hence, there are intrinsic limitations, which are related to upscaling in space and time.

This type of tests has been conducted in Mont Terri Rock laboratory in Opalinus Clay (https://www.mont-terri.ch), the so-called DI and DR experiments and in Bure URL in Callovo-Oxfordian Clay (https://meusehautemarne.andra.fr), the so-called DIR experiments (overview in Delay et al. (2007); Gimmi et al. (2014); Leupin et al. (2017); Soler et al. (2019); Van Loon et al. (2012); (Van Loon et al., 2004b)).

A second type of large-scale *in situ* diffusion experiments makes use of multi-filter piezometers. These tests are particularly applied in the HADES URL in Boom Clay (https://www.euridice.be), due to its higher plasticity and porosity.

In these tests, a borehole is drilled with compressed air from the underground laboratory into the clay formation and a stainless steel cylindrical tube with a series of filter screens (= multi-filter piezometer) at well-known distance (up to 0.5 – 1 m apart) is emplaced into the borehole (*Figure 3-12*). After convergence of the clay, the filters are in direct contact with Boom Clay because of its high plasticity and no packer is needed to hydraulically isolate the different filter intervals. The filters are equipped with one, or sometimes two, stainless steel tubings leading to the gallery and allowing injection / withdrawal (or recirculation in case of 2 tubings) of water. In the injection filter (often the central filter), a radiotracer solution is injected/circulated and at regular time intervals, water samples are taken from the adjacent filters. This enables to establish "break-through" curves of these tracers at different distances. An extension to this test is the emplacement of different multi-filters in a 3D configuration. This also enables the sampling in neighbouring piezometer providing excellent 3D spatial information at a scale of several meters.

In Boom Clay, the *in situ* diffusion tests do not significantly suffer from a borehole disturbed zone (BDZ) as the damaged clay skin around the filters is rapidly sealed by the fast convergence / creep of the plastic clay around the piezometer casing. As it is not intended to overcore these piezometers which will remain in place, there is no time constraint and the diffusion of conservative tracers (HTO, $H^{14}CO_3^-$) develop over several meters without being affected by the already negligible BDZ. These tests have no end date and they continue to provide reliable data for several years/decades. Hence, these tests are very valuable with respect to upscaling to tens of years and up to several meters.

Examples of these tests in the HADES URL (Boom Clay) are the tests CP1, TRIBICARB, TRANCOM-R41H/V, MEGAS (Aertsens (2013); Aertsens et al. (2013); Martens et al. (2010); Weetjens et al. (2011); Weetjens et al. (2014)).

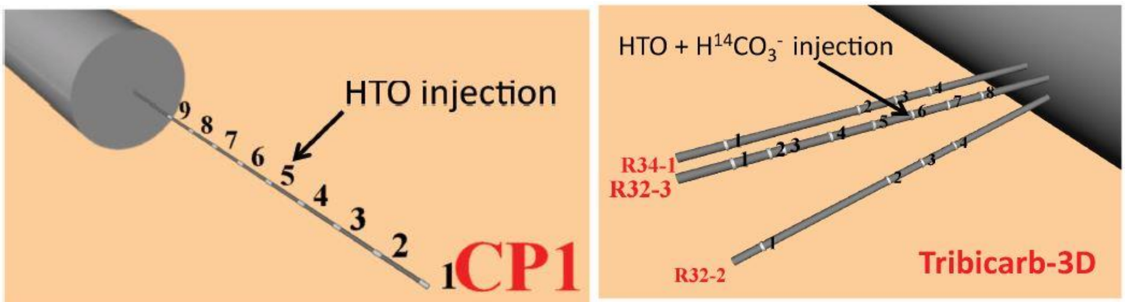

Figure 3-12 – Schematic representation of large-scale multi-filter piezometer diffusion experiments in the HADES URL.- (Left) CP1 (Concrete Plug One) single piezometer configuration, (right) TRIBICARB (tritium – bicarbonate) multiple piezometer configuration (Figure from (Aertsens et al., 2013)).

These *in situ* diffusion tests (CP1 and Tribicarb-3D) provide us with confidence that the migration of HTO and $H^{14}CO_3^-$ is correctly understood at the metric scale. Blind predictions at large scale based on migration parameters obtained at lab scale allow the validation and the verification of water flow and diffusion models. These experiments show that the applied models are consistent with our scientific understanding and adequately represent the relevant phenomena and interactions of conservative tracers at the scale of several meters (Weetjens et al. (2011); Weetjens et al. (2014)).

At the clay formation scale (several millions years and 100 m thickness), natural tracer profiles ($\delta^{18}O$, $\delta^{2}H$, He, Cl, Br, I) provide valuable information regarding migration scenarios in natural systems and dominant transport processes. Despite that the initial and boundary conditions are not well known, a careful analysis is useful to check consistency with results and conclusions from studies at smaller scale. From natural profiles we can better characterize the dominant transport processes (diffusion and advection) that have occurred during the burial period and may provide some information on the effect of larger heterogeneities (distinct clay layers) and they confirm the common up-scaling approach. A comprehensive overview of the studies of natural tracer profiles is given by Mazurek et al. (2011); Mazurek et al. (2009) in the frame of their works performed for the ClayTrac project supported by the OECD/NEA Clay Club.

In order to evaluate the impact of heterogeneities (e.g. due to layering with regular alternation of silt and clay sediments as observed in Boom Clay) on the solute transport parameters, lab migration experiments can be conducted on a series of drillcores coming from boreholes drilled in the frame of site characterisation campaigns. The general characteristics and microstructural features of a particular clay core can be related to the experimentally determined transport parameters. In this way, the effect of heterogeneities on the general solute transport mechanisms can be evaluated. Examples of such studies for Boom Clay and Ypresian Clays are reported by Aertsens et al. (2010a); Aertsens et al. (2005a); Aertsens et al. (2005b); Aertsens et al. (2010b); Aertsens et al. (2008b); Aertsens et al. (2004), Callovo-Oxfordian Clay by ANDRA (2018b, 2018a); Descostes et al. (2008); Jacquier et al. (2013); Melkior et al. (2005); Robinet et al. (2012); Van Loon et al. (2012) and for Opalinus Clay (Van Loon et al. (2012); Van Loon (2014)). New data will become available from currently on-going drillings performed in the frame of the deep boreholes TBO project of NAGRA.

The above methods are mainly applicable for conservative (i.e., non-retarded) tracers and weakly sorbing tracers. For radionuclides exhibiting strong interactions with certain mineral phases, small local variations in the clay composition (i.e., in the content of these mineral phases) may have a significant effect. Large-scale experiments for these strongly sorbing elements will not be very helpful because of their very limited diffusion distances even for very long time periods. For these elements, small-scale experiments studying the relationship between sorption and the mineralogical characteristics (variability) of the clay formation will be much more relevant. Such experiments are useful to provide reliable uncertainties on the sorption distribution coefficient (K_d) values used in safety assessment studies

(Bradbury and Baeyens, 2017). Examples of such studies are given by (Chen et al., 2014b) for the COx and by Marques Fernandes et al. (2015) for other clay rocks.

3.2.5 Sources of transport data for clay host rocks

In this section, we will provide an extensive (but not complete) overview of available sources with respect to diffusion data obtained for some well-studied clay host rocks (Opalinus Clay, Callovo-Oxfordian argillite, Boom Clay, Toarcian Clay and Boda Claystone) and single clay phases (bentonite, smectite, illite, kaolinite, …).

3.2.5.1 Opalinus Clay

The Paul Scherrer Institute (PSI) is performing diffusion studies on Opalinus Clay since 2000. The material under investigation originates from different deep boreholes in Northern Switzerland, notably from the Benken borehole in the Zürcher Weinland (BE-DBH), and from the Mont Terri Rock Laboratory, where the Opalinus Clay Formation is horizontally accessible via the safety gallery of a motorway tunnel (Transjurane highway). So far, the diffusion of HTO, D_2O, $H_2{}^{18}O$, $^{36}Cl^-$, $^{125}I^-$, $^{125}IO_3^-$, $^{35}SO_4^{2-}$, Br^-, $^{22}Na^+$, $^{85}Sr^{2+}$, $^{134}Cs^+$, $^{60}Co^{2+}$ and $^{152}Eu^{3+}$ was investigated (Glaus et al., 2008a; Jakob et al., 2009; Leupin et al., 2017; Van Loon, 2014; Van Loon et al., 2005a; Van Loon and Eikenberg, 2005; Van Loon and Jakob, 2005; Van Loon et al., 2018; Van Loon and Mibus, 2015; Van Loon et al., 2005b; Van Loon et al., 2003; Van Loon et al., 2004a; Wu et al., 2009). Further, Opalinus Clay is also being used as a reference material in different international studies, such as Joseph et al. (2013), Savoye et al. (2012c), Wigger et al. (2018), Xiang et al. (2016).

3.2.5.2 Boom Clay

SCK CEN is studying diffusion in the Boom Clay since 1978. The material under investigation is mainly originating from core material taken from the HADES URL in Mol (Belgium) and deep boreholes (e.g. Mol-1 borehole). Van Laer (2018) provides an overview of all long-term lab (Ra, Tc, Be, Ni, Zn, Pa, Zr, Am, Cm, Pu, U, Np, Pa, NOM) and in-situ (HTO, HCO_3^-, NOM, Am, Tc) migration experiments in Boom Clay. HTO, I^-, and HCO_3^- were used to investigate variability over the entire host formation using drill core samples (Aertsens et al., 2010a; Aertsens et al., 2005a; Aertsens et al., 2010b; Aertsens et al., 2008b; Aertsens et al., 2004). Transport of Dissolved Organic Matter (DOM) is particularly of interest in Boom Clay (Dierckx et al., 2000; Durce et al., 2018; Maes et al., 2011; Maes et al., 2004; Maes et al., 2006) as it may act both as a vector or a sink for radionuclides.

Also the diffusion of dissolved gases (H_2, He, Ne, Ar, CH_4, C_2H_6) has been extensively studied by Jacops et al. (2017a); Jacops et al. (2017b). Dedicated compilation reports ("Topical reports") are available which describe the current phenomenological understanding of the transport behaviour of so-called reference elements in Boom Clay based on the available sorption and diffusion experiments conducted: HTO (Bruggeman et al., 2017c), I (Bruggeman et al., 2017a), Sr (Maes et al., 2017b), Cs (Maes et al., 2017a), Se (De Canniere et al., 2010), Tc (Bruggeman et al., 2017b), Am (Bruggeman et al., 2017d), U (Salah et al., 2017), and an overview report (Bruggeman and Maes, 2017).

3.2.5.3 Callovo-Oxfordian Clay

Different labs have performed diffusion experiments on Callovo-Oxfordian Clay and Oxfordian limestone. Following elements have been studied: HTO, Cl^-, I^-, SO_4^{2-}, SeO_3^{2-}, Li^+, Na^+, K^+, Rb^+, Cs^+, Zn(II), Eu(III), organic anions, polymaleic acid (ANDRA, 2018b, a; Bazer-Bachi et al., 2007; Bazer-Bachi et al., 2006; Dagnelie et al., 2018; Descostes et al., 2008; Durce et al., 2014; Jacquier et al., 2013; Melkior et al., 2005; Melkior et al., 2007; Menut et al., 2006; Savoye et al., 2015; Savoye et al., 2012b; Savoye et al., 2013).

Also for partially saturated conditions of the Callovo-Oxfordian Clay, diffusion experiments were performed with HTO, Cl^-, I^-, Na^+, Cs^+ (Savoye et al., 2012a; Savoye et al., 2014; Savoye et al., 2017; Savoye et al., 2010).

3.2.5.4 Toarcian Clay

Diffusion experiments with HTO, Cl^-, I^- on the Toarcian argillite from Tournemire are reported in studies of Motellier et al. (2007); Savoye et al. (2006); Wittebroodt et al. (2012).

3.2.5.5 Boda Claystone

On Boda Claystone, some limited number of experiments with Cs^+, Sr^{2+}, Co^{2+}, I^-, HCO_3^- and TcO_4^- are reported by Lazar and Mathé (2012); Mell et al. (2006b).

3.2.5.6 Clay minerals

Diffusion in clay minerals (bentonite, smectite, illite, kaolinite, …) has been widely investigated.

Bourg and Tournassat (2015) provide a comprehensive literature overview on the diffusion studies on different types of bentonite (MX-80, Kunigel, Volclay KWK, Avonlea, Febex,…) and smectites (Kunipia Montmorillonite, Swy-2 Montmorillonite, Milos…). These studies were mainly using conservative tracers such as HTO/HDO, I^-/Cl^-,Br^- and ion-exchangeable cations such as Na^+, Cs^+, Sr^{2+}, (Co^{2+}). Glaus et al. (2017) published a detailed report on diffusion experiments with HTO, Na^+, Cs^+, Sr^{2+}, Cl^-, SO_4^{2-} and SeO_3^{2-} on Milos montmorillonite and Volclay KWK bentonite. They also published diffusion data for HTO, Na^+ and Cl^- on kaolinite (Glaus et al., 2010).

In the EC project CATCLAY, the diffusion of a suite of cationic species (Sr, Co, Zn, Eu) in illite (Illite du Puy) was intensively studied (Altmann et al., 2015; Glaus et al., 2015a; Glaus et al., 2020) in combination with dedicated sorption experiments.

3.3 Transport in crystalline rocks

3.3.1 Structural aspects of crystalline rocks

Crystalline formations are geological units, which consist of magmatic and/or metamorphic rocks. Metamorphic rocks have undergone changes in mineralogy, texture and/or chemical composition as a result of increasing temperature and pressure. The original rock may have been igneous, sedimentary or another metamorphic rock. Due to their evolution, metamorphic rocks (most frequent representative: gneiss) typically show an ordered and therewith anisotropic structure (foliation, schistosity). Magmatic rocks (e.g., granites) usually have a disordered and massive, more isotropic structure owing to the lack of tectonic stress during crystallization. A disordered structure is generally advantageous from the viewpoint of mechanical stability. Nevertheless, many high-grade metamorphic rocks are mechanically very stable due to their formation and recrystallization under high-pressure and high-temperature conditions.

For the mineralogical and geochemical characterization of magmatic and metamorphic rocks several classification schemes exist. Granite, diorite and gneiss as important crystalline rocks mainly consist of (Na, Ca)-feldspar (plagioclase with endmembers albite $Na[AlSi_3O_8]$, anorthite $Ca[Al_2Si_2O_8]$)], and (K, Na)-feldspar with endmembers orthoclase/microcline $K[AlSi_3O_8]$ and albite. Further constituents are biotite ($K(Mg,Fe^{2+},Mn^{2+})_3[(OH,F)_2|(Al,Fe^{3+},Ti^{3+})Si_3O_{10}]$), quartz ($SiO_2$), amphiboles (e. g., hornblende, $Ca_2(Mg,Fe,Al)_5(Al,Si)_8O_{22}(OH)_2$), calcite ($Ca[CO_3]$) and pyrite ($FeS_2$). Potential alteration processes result in albitization, biotite- and hornblende-alteration and the formation of e.g. epidote ($Ca_2(Fe^{3+},Al)Al_2[O|OH|SiO_4|Si_2O_7]$), muscovite ($KAl_2[(OH,F)_2|AlSi_3O_{10}]$), chlorite ($(Mg,Fe)_3(Si,Al)_4O_{10}(OH)_2{\cdot}(Mg,Fe)_3(OH)_6$), illite ($(K,H_3O)(Al,Mg,Fe)_2(Si,Al)_4O_{10}[(OH)_2,(H_2O)]$), smectite (e. g., montmorillonite, $(Na,Ca)_{0,3}(Al,Mg)_2Si_4O_{10}(OH)_2{\cdot}nH_2O$), kaolinite ($Al_4[(OH)_8|Si_4O_{10}]$), calcite, stilbite ($(Ca,Na)_9[(Si,Al)_{36}O_{72}]{\cdot}28H_2O$), laumontite ($Ca_4[Al_8Si_{16}O_{48}]{\cdot}18H_2O$), prehnite ($Ca_2Al[(OH)_2|AlSi_3O_{10}]$), titanite (or sphene) ($CaTi[O|SiO_4]$), hematite (Fe_2O_3) and pyrite (FeS_2) (Nishimoto and Yoshida, 2010; Niwa et al., 2016; Plumper and Putnis, 2009; Sandström and Tullborg, 2009; Stober and Bucher, 2014; Yuguchi et al., 2015). Nishimoto and Yoshida (2010) consider calcite, laumontite, chlorite, epidote and prehnite along with quartz as the most frequent fracture-filling minerals.

For the assessment of crystalline rocks as host rock for a repository for heat-generating radioactive waste, particularly its hydrogeological properties are essential. In metamorphic or magmatic crystalline rocks, the permeability of the pore network plays a minor role only. However, the groundwater flow predominantly occurs through fractures. The formation of fractures is largely controlled by tectonic processes during uplift of the rocks in depth ranges, which are suitable for radioactive waste disposal. The extent of fracture formation is mainly dependent on rock stability and regional tectonic conditions. However, due to the thermodynamic disequilibrium during uplift processes, fractures have frequently been mineralized by migrating hydrothermal solutions or groundwater. Thus, the permeability of fractures is significantly modified due to precipitation processes and infiltration of fines.

To describe transport processes in crystalline rock one has to distinguish between the unaltered and altered rock matrix (*Figure 3-13*) as well as between fractures with and without mineralization.

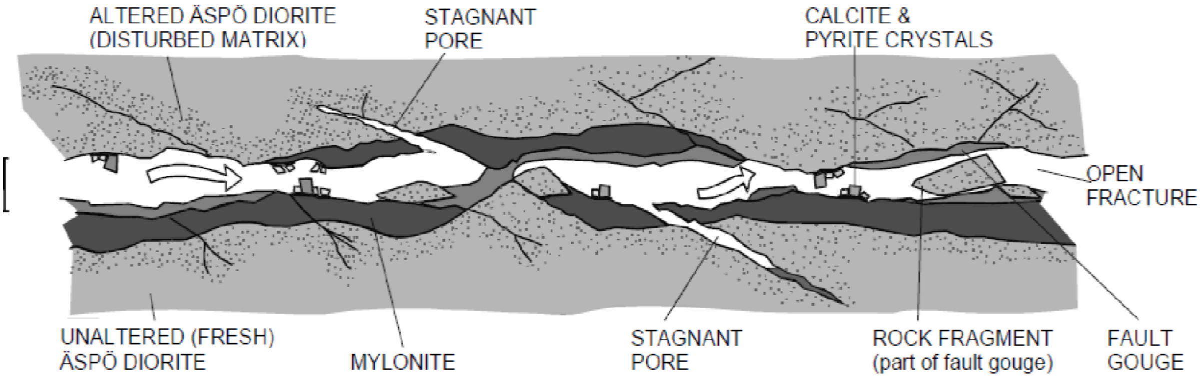

Figure 3-13 – Crystalline rock features: unaltered rock, altered rock zones, fractures with and without mineralization (Winberg et al. 2001).

Components of crystalline rock show a large variability in crystal size, often ranging from the mm- to cm-scale. Newly formed minerals and alteration products in fractures may comprise much smaller crystal sizes down to the nm-scale and show a large variability of pore diameter and volume, hence porosity (Svensson et al., 2019).

Complex flow fields evolve due to surface heterogeneity of fractures and complex geometrical fracture features, i.e., microscale roughness, reflecting the strong impact of spatial surface variability. Fracture geometry can effectively lead to retardation of solutes and colloidal phases solely on basis of hydrodynamic processes without considering physicochemical processes like matrix diffusion, sorption or reduction.

Fracture surfaces vary spatially e.g. due to fracture fillings or geometry variability (Bodin et al., 2003; Moreno et al., 1997; Moreno and Neretnieks, 1993). It was observed that water flows in narrow channels through fractures (Bodin et al., 2003; Moreno et al., 1997) which is referred to the so-called channelling effect or preferential flow paths which applies to a single fracture as well as fracture networks (Malloszewski and Zuber, 1992; Moreno et al., 2000; Park et al., 1997; Shahkarami et al., 2016; Tsang, 1984, 1992; Tsang and Tsang, 1987). Channelling can arise due to: 1) the variable aperture, 2) intersecting fractures, and 3) offset displacements of fractures (Löfgren et al., 2007) and, amongst others, affect the hydraulic properties of the crystalline rock. It also influences the fracture retention capacity since matrix diffusion processes can be affected.

3.3.2 Main processes controlling transport in crystalline rocks

Reactive transport in fractured crystalline rocks is controlled by physical and chemical properties of fractures, namely fracture walls and fracture-filling materials.

3.3.2.1 Advection in fractures is the dominant transport process

Mechanistic understanding, quantitative description, and prediction of advective transport in fractured porous media are still challenging. The surface building block size on fracture walls covers a large range of the length scale, from molecular dimension up to the characteristic extension of the fractures in the field scale (Berkowitz, 2002; Pyrak-Nolte and Nolte, 2016). The fracture geometry causes heterogeneity, such as channelling of the flow path, which furthermore is coupled to the porous and/or microfractured adjacent matrix material. Characterization of the fracture flow, its interplay with the pore space, and upscaling to the field scale relevant for performance assessment is a continuing issue (Wersin, 2017). The complexity increases still further when fracture infills (infiltration of fines) and mineralization's are considered (Antonellini et al., 2017; Soler, 2016). Fracture filling materials modify the transport conditions owing to multiple processes of precipitation/crystallization and/or particle aggregation and filtration. As a result, a large diversity of pore shapes, pore size distributions, pore network geometries, and the accessible internal surface areas is reported (James et al., 2018; Jones and Detwiler, 2016; Nollet et al., 2009; Zhang et al., 2015).

Apart from advection through fractures with apertures larger than 100 µm, additional two-dimensional tight flow pathways exist along microfractures and grain boundaries. Consequently, length-scale depending variability of permeability has been observed and compared to multi-scale porosity and pore network data using multiple methods, such as mercury intrusion porosimetry (MIP) and pore network tomography (e.g. µCT, FIB-SEM, BIB-SEM) (David et al., 2018).

3.3.2.2 Matrix diffusion

A simplified description of fluid transport in fractured crystalline rock is based on the dual porosity model (e.g., Smith et al., 1991). In the dual porosity model, diffusion into the rock material adjacent to the fractures is included via **matrix diffusion** (*Figure 3-14*). The matrix-controlled transport is determined by the sorption on solid surfaces as well as parameters controlling the diffusion process, particularly the diffusion coefficient and the matrix porosity.

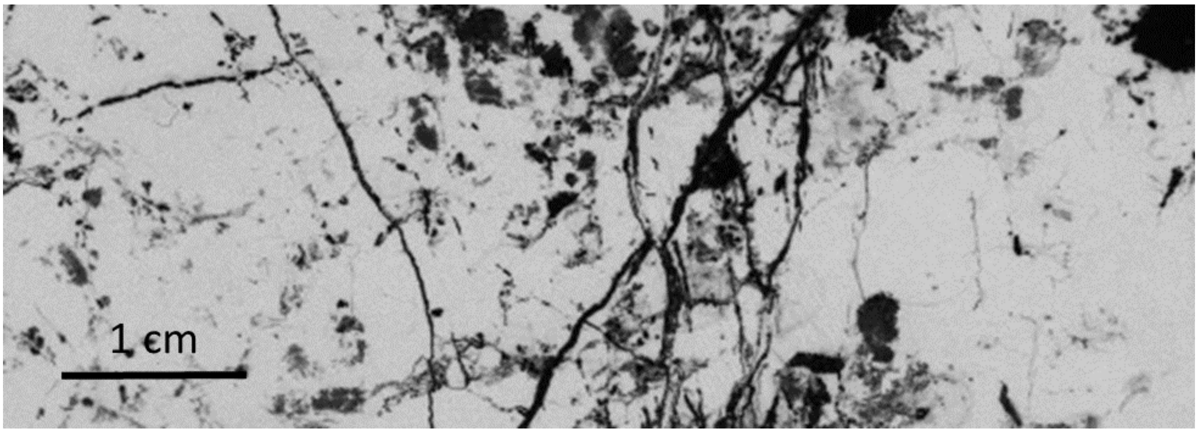

Figure 3-14 – Model representation of the dual-porosity concept of transport in fractured, low-permeability rocks. The schematic picture of a vertical cross-section of a rock core (granite from Palmottu, Finland) showing the structure of the matrix. The dark areas indicate porous phases, fissures and fractures in the rock core whereas white areas are congruent with the main minerals of the granite.

The concept of anion exclusion explains, similarly as in a clay environment (see chapter 3.2.2) charge-depending modifications of the mobility of ions. The electrostatic interactions modifying the ion mobility are dominating for pore sizes in the nm-range. While this effect has been often observed in and described for argillaceous rocks, anion exclusion can be significant in the crystalline rock matrix as well. Consequently, diffusion coefficients determined in diffusion experiments in crystalline rock matrices using anions tend to be smaller compared to cations or water (Kuva et al., 2018; Smellie et al., 2014; Tachi et al., 2015; Voutilainen et al., 2019).

3.3.2.3 Role of sorption and surface induced processes

Retention processes, having a common physical background for both clay and crystalline rock environment, are described in Chapter 2. Some specific issues, being devoted to a crystalline fractured environment, are tackled here.

3.3.2.3.1 Sorption on fracture surfaces, including fracture-filling materials

In Hakanen et al. (2014), the evaluation of data for rock material is based on laboratory-derived K_d values of crushed rocks. Based on the results of the mineral-specific sorption of radionuclides in diffusion experiments and results of sorption to rock surfaces, these distribution coefficients were converted to K_d values for intact rock. From this evaluation it was suggested that the mica minerals and other minerals with high cation exchange capacity (CEC) or high surface area dominate the sorption into intact rock.

A combination of microscopic and macroscopic investigations performed by Fukushi et al. (2013) focused on Eu(III) sorption on granite. Here, biotite has been identified as the controlling factor for sorption strength. Numerical approaches considering a single-site cation exchange reaction are able to predict the sorption behaviour at pH > 4. The results suggest that sorption on a complex mineral assemblage such as granite could be modelled by using a single most relevant mineral phase (here: biotite) representative for the bulk sorption reaction in the complex mineral assemblage.

Li et al. (2018); Li et al. (2020) and Puhakka et al. (2019) investigated the sorption behaviour of Se(IV) on Grimsel granodiorite (mainly plagioclase, K-feldspar, quartz and biotite) using artificial Grimsel groundwater and different concentrations of Se(IV). A strong Se concentration dependence of Se sorption was observed, and highest sorption values were found on biotite at low Se concentrations (< 10^{-7} mol/l). The distribution coefficients of Ba on Olkiluoto pegmatitic granite and veined gneiss, Grimsel granodiorite and their main minerals (quartz, plagioclase, K-feldspar and biotite) were obtained by batch sorption experiments (Muuri, 2019; Muuri et al., 2018). Highest sorption efficiencies were found on biotite and plagioclase. Recent results by Konevnik et al. (2017) suggest a strong increase of K_d values for Sr(II) and Am(III) for a temperature increase from 20°C to 90°C.

3.3.2.3.2 Surface induced processes and reactivity

The presence of specific minerals in crystalline rock can induce processes that lead to reactions, including radionuclide retention. A typical reaction is the species reduction due to the presence of either Fe minerals or Fe bearing minerals. Those processes are specified in detail in section 2.2.2. An example of this process is the retention of I on pyrite, biotite and magnetite (Fuhrmann et al., 1998) by surface reduction of IO_3^- to I_2 and oxidation of S^{2-}.

Similarly, selenium sorption has been studied and results suggested that Se(IV) is more readily reduced to Se(0) or Se(-II) when solution is exposed to metal or Fe containing minerals (e.g., biotite) (Hakanen et al., 2014; Stamberg et al., 2014; Videnska et al., 2015; Videnská et al., 2013). The abiotic homogeneous reduction of selenite or selenate to selenide occurs at very low rates. Thus, the reduction reaction in the environment is most probably microbe-mediated, equivalent to the reduction of sulphate to sulphide (Hakanen et al., 2014; Hockin and Gadd, 2003; Myneni, 1997). Increased Tc sorption was observed for rocks containing Cu, Fe and Pb sulphides, and additional examples of retention of radionuclides on pyrite, galena or chalcopyrite via reduction are provided in a review by Suter (1991).

3.3.2.3.3 Solid solution

Solid solutions can be formed during precipitation of mineral phases on the fracture surface and in pores close to the fracture (Poonoosamy et al., 2020). Those are typically sulphates (e.g., baryte, celestite) or carbonates (e.g., calcite) and can become an important retention mechanism for some radionuclides, such as Ra (See section 2.2.3 for more details). For example, precipitation of calcite might occur in crystalline carbonate water at higher pH. Curti (1999) reports that actinides strongly partition into calcite under reducing conditions; nickel(II) incorporation is moderate, while incorporation of ions like U(VI), Cs(I), Sr(II) and Ra(II) in calcite is weak.

3.3.3 Research methods to characterise fracture properties and radionuclide migration

3.3.3.1 Advective flow and transport properties (geoPET and PMMA)

Although methods for characterizing bulk rock properties are highly developed, the characterization of porosity in crystalline rock still remains challenging due to low pore space and a broad range of potential pore sizes (David et al., 2018). Specifically, µCT(spatial resolution in the order of 50 µm) is relevant for the transport studies in large and continuous fractures with aperture widths above the instrumental resolution. Methods, such as optical microscopy approaches for the quantification of surface roughness variability provide detailed insight into critical surface building blocks of the fracture wall (Fischer and Luttge, 2007), but require preparation of and accessibility to the fracture surface. Apart from visualization of fractures on relevant scales another challenging aspect for µCT analysis are, e.g., porous fracture fillings and intergrown minerals due to their highly porous structure that can be of negligible density contrast to the surrounding fluid (Berg et al., 2016; Menke et al., 2018). Furthermore, the C-14 PMMA method (impregnation with C-14 labelled Polymethylmethacrylate resin followed by autoradiography) was developed to obtain information about the spatial distribution of porosity on the core scale (Sammaljärvi et al., 2012). It has been successfully used to characterize the spatial distributions of porosity in REPRO samples from Olkiluoto and has been combined with other techniques (Ikonen et al., 2015), such as electron microscopy for mineralogical characterization (Sammaljärvi et al., 2017). Furthermore, CT tomography analysis can be combined with C-14-PMMA method-based porosity results and SEM-based mineralogical analysis to obtain a three-dimensional structure of crystalline rock.

Radionuclide tracer propagation through rock cores with natural or artificial fractures are studied using positron emission tomography (PET) (Kulenkampff et al., 2008). PET data analysis provides spatiotemporal images of the tracer concentration during conservative transport. In contrast, reactive (sorbing) PET tracers identify reactive sites of rock surfaces during fluid-solid interaction (Kulenkampff et al., 2018). Usually, PET techniques are combined with microcomputed tomography (µCT) data for the identification of the geometry of the fractures as well as pores and pore networks. Segmented µCT data yield a structural model for reactive transport modelling (Kahl et al., 2020). Flow field interpretations based on PET data sequences are used to identify flow heterogeneities (Lippmann-Pipke et al., 2017; Zahasky and Benson, 2018). Both parametrization and validation of numerical transport models are an important application of PET flow field and velocity data.

3.3.3.2 Matrix diffusion

3.3.3.2.1 Through-diffusion method

The most commonly used method to determine the effective diffusion coefficient (D_e) of elements in hard materials is the through-diffusion (TD) experimental method (see also 3.2.3.1.2 for clay material). In this method, the sample is placed between a tracer-spiked and a tracer-free solution. The sample is glued to a sample holder, equilibrated in a tracer-free solution, often with synthetic groundwater, and installed between the two reservoirs. The tracer concentration is monitored in the initially tracer-free reservoir (*Figure 3-15*) (Voutilainen et al., 2017). The apparent and effective diffusion coefficients as well as the geometric factors (G) can be determined from the experimental results based on Fick's second law of diffusion.

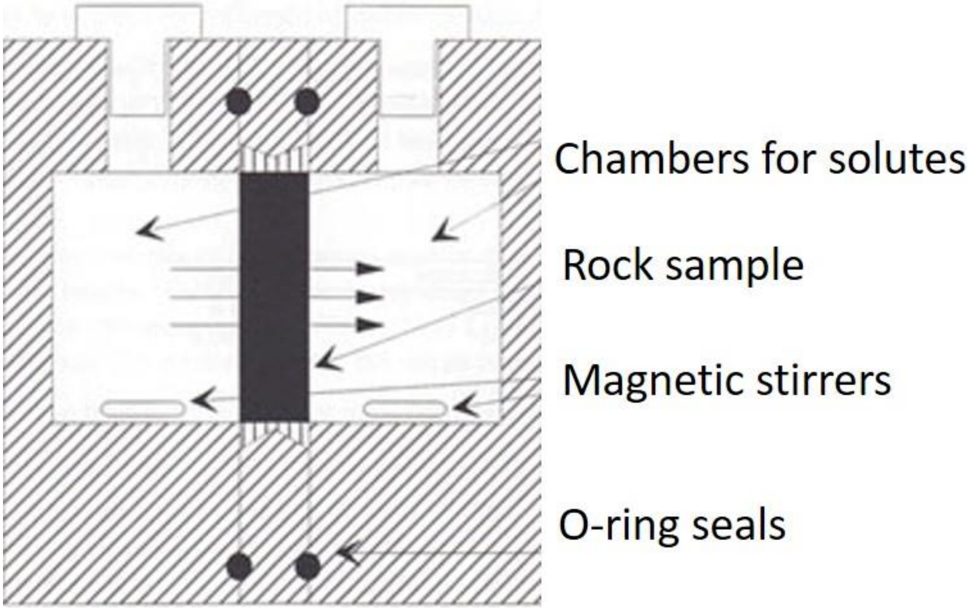

Figure 3-15 – During the through-diffusion experiment diffusion takes place in a sample placed between a tracer-containing solution and a tracer-free solution (Voutilainen et al., 2017).

Besides concentration induced diffusion experiments with aqueous solutions, through-diffusion experiments can also be performed in the gas phase. The diffusion coefficients of helium in a nitrogen filled sample is measured (Kuva et al., 2015). Results showed that helium gas molecules diffuse more than 11 000 times faster than atoms and molecules in a water phase.

The experimental arrangement of equilibration-leaching or out diffusion method can also be used to determine the pore diffusion coefficient (Smellie et al., 2014) *Figure 3-16* shows the setup of the outleaching experiment. The kinetics of tracers can be quantified by measuring the evolution of concentration in solution.

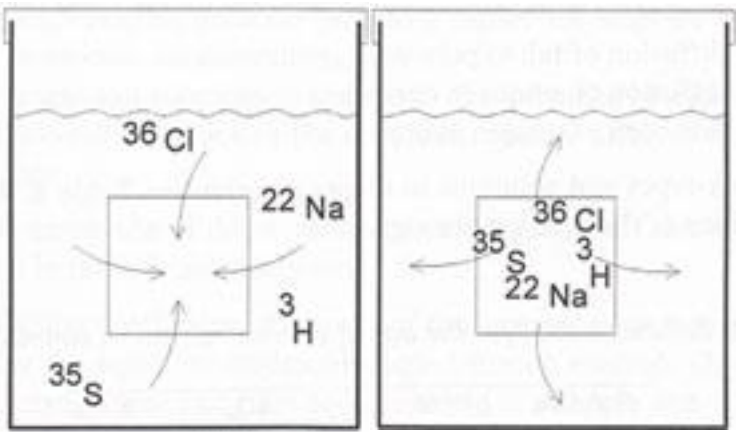

Figure 3-16 – Two phases of the equilibration-leaching experiment: A rock sample is equilibrated with the tracer-containing solution (left) and subsequently leached in a tracer-free solution (right).

3.3.3.2.2 Electromigration

The through-electromigration method (André et al., 2009; Lofgren and Neretnieks, 2006; Löfgren et al., 2009), adapted from Maes et al. (1998); Maes et al. (1999); Maes. et al. (2001), combines the principle of a TD method with the electromigration method and it provides the effective diffusion coefficient (D_e), distribution coefficient (K_d) and geometrical factor (G) for an intact crystalline rock sample in a faster way than traditional block scale diffusion experiments. It avoids the problem of rock crushing in batch sorption experiments, which can create new surfaces and significantly increases specific surface area leading to an overestimation of K_d values. The setup for electromigration experiments is schematically shown in *Figure 3-17* (Lofgren and Neretnieks, 2006). A small electric field is applied over the rock sample, which is placed between two chambers, one holding an electrolyte with high tracer concentration (source chamber) and the other holding the same electrolyte initially free of the tracer (recipient chamber). André et al. (2009) tested the migration behaviours of I^- and Cs^+ ions in samples of intact rock samples.

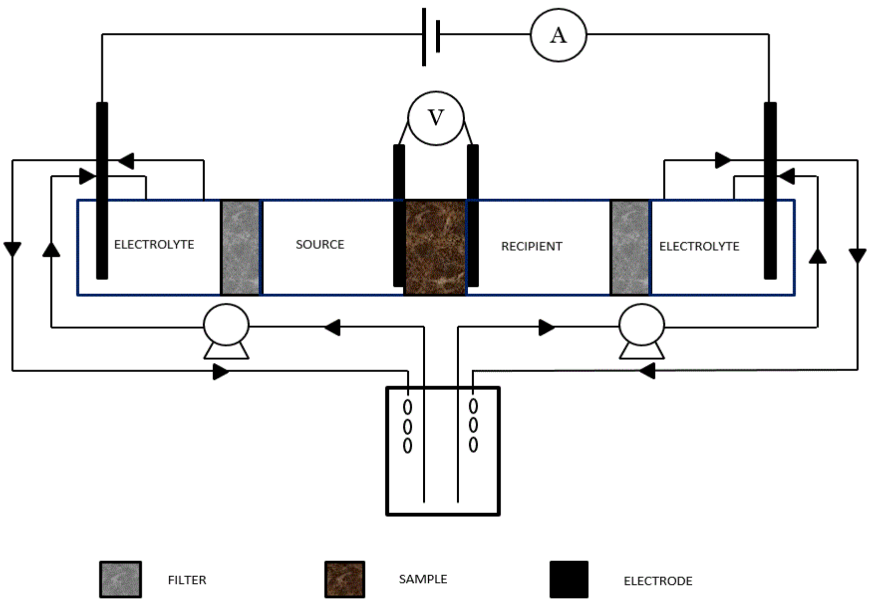

Figure 3-17 – Schematic setup for the through-electromigration experiments (Lofgren and Neretnieks, 2006).

In André et al. (2009), the device was found to have difficulties in controlling a constant electric potential over the rock sample, and thereby, making the experimental results difficult to interpret. To overcome this problem, Li et al. (2019b) upgraded this device by making use of a potentiostat instead of an ordinary power source and performed iodide (I^-) and selenite (SeO_3^{2-}) through-electromigration experiments. In addition, $NaHCO_3$ was added as buffer to the background electrolytes to stabilize the pH of the solution during the experiment. As a result, the electromigration device has the capabilities of voltage-self-controlling, continuous-current-recording and solution-pH-stabilization.

It should be noted that the classical theory for interpretation of the experimental results simply applies the ideal plug-flow model that accounts only for the effect of electromigration on ionic transport but neglects contributions of electroosmosis and dispersion. To tackle this problem, an advection-dispersion model was developed by Meng et al. (2020). The model accounts for the influences of electromigration, electroosmosis and dispersion of ion transport through the rock. The analytical solution was derived in the Laplace space and describes the transient tracer concentration variation in the recipient chamber.

3.3.3.2.3 C-14 PMMA method

As stated above (cf.3.3.3.1), the C-14 PMMA method was developed to gain information about pore networks and porosity at the core scale (Sammaljärvi et al., 2012). Such data sets act as a basis for the modelling of diffusion in crystalline rock (Kuva et al., 2018; Mazurier et al., 2016; Voutilainen et al., 2019; Voutilainen et al., 2017). Further refinement of image analysis in C-14-PMMA yields pore apertures from C-14-PMMA autoradiographs (Bonnet et al., 2020).

3.3.3.2.4 Flow field analyses: GeoPET

Quantitative insight into the flow pathway heterogeneity is provided by directly visualizing the propagation of a positron-emitting tracer such as ^{124}I and ^{22}Na with GeoPET (Kulenkampff et al., 2018; Kulenkampff et al., 2016). The method provides a suite of quantitative tomograms of the spatial tracer distribution. This allows for the derivation of a spatially resolved tensor of molecular diffusion coefficients. A robust algorithm for reconstructing the dominant pathways and flow field ("Darcy velocity") has been developed and is currently further improved.

3.3.3.2.5 In-situ vs. laboratory experiments

Since 2004 two large scale, long-term in situ diffusion experiments (LTD) have been conducted at the Grimsel Test Site, which aimed to examine in-situ matrix diffusion and pore space visualisation (Ikonen et al., 2016a; Ikonen et al., 2016b; Soler et al., 2015) – see 3.3.4.

Two in situ flow experiments have been conducted in Onkalo at the Repro site where the dominant rock type is veined gneiss. Parallel to in situ experiments the project focused on rock matrix characterisation and matrix diffusion in laboratory experiments to compare conditions such as stress relaxation, which might open the pore space and increase the diffusivity of the rock – see 3.3.4.

3.3.3.3 Sorption

Different approaches exist to characterize mineral-specific sorption relevant processes such as acid-base behaviour of surfaces and retardation, e.g., surface complexation processes, in general. To examine sorption reactions at the solid-liquid interface, commonly applied methods are classical potentiometric titration experiments, column titration experimental set-ups, so-called batch experiments and column transport experiments. These techniques are described in section 2.1.2.5.

In the following, a brief overview of titration, batch, and column experimental approaches, that are specific for crystalline rocks, is provided. Detailed information on spectroscopic methods is provided elsewhere (see section 2.1.2.5.2) and not in the scope of this chapter.

3.3.3.3.1 Titration experiments

Potentiometric mineral titration experiments in batch are appropriate to investigate solids with large specific surface areas such as clays (see section 2.1.2.5). However, especially crystalline rock samples might have very small surface areas. To collect trustworthy information on the acid-base behaviour of samples with small specific surface areas column potentiometric titration experiments may be applied (Neumann et al., 2020; Scheidegger et al., 1994). The advantage is a significantly larger solid-liquid ratio compared to batch potentiometric titrations. Hence, a larger surface area is exposed to a relatively small amount of titrant making it possible to obtain trustworthy results of changes in surface charge as a function of e.g., ionic strength, pH, ligands, etc.

3.3.3.3.2 Batch sorption experiments

Batch sorption experiments can be based on the pre-equilibration of the solid phase in an electrolyte solution before adding the radionuclide allowing it to sorb over a defined period of time and can be used for any material, e.g. for clays. It is assumed that after pre-equilibration of the solid the radionuclide sorbs onto a slightly altered surface, which is expected to represent conditions that are closer to nature, compared to surfaces that have not experienced pre-treatment. Collected batch sorption results correlate well with data found in literature and confirm the expected sorption trends that substantiates the approach. Unfortunately, pre-equilibration is time consuming and may take from several weeks up to months depending on the solid phase.

A more time efficient approach are batch experiments that are carried out without pre-equilibration of the sample. The solid is briefly suspended in an acidic electrolyte that contains the element/radionuclide. Since sorption of many relevant elements/radionuclides is pH-dependent no significant surface reactions take place under these acidic initial conditions. Via slow adjustment of the suspension's pH to higher pH conditions the radionuclide sorbs onto the surface of the solid systematically. To reach steady state conditions at surface and to be able to compare results between the two experimental set ups identical equilibration times should be allowed for the element/radionuclide to sorb at the surface. In an ongoing research project (SMILE, funding code 02 E 11668A, German Federal Ministry of Economics and Technology) it could be shown that both experimental approaches yield comparable results for quartz and feldspar surfaces. However, the second approach bears complications when using solids that own strong natural buffer capacities and that are prone to dissolution reactions in acidic conditions: Buffer reactions of the minerals' surfaces result in pH shifts when comparing initially adjusted pH values with measured pH values after equilibration of the radionuclide with the surface. Minerals that undergo unrealistic dissolution processes under acidic conditions may leach silica and other cations from the crystal lattice into the solution that later on, at higher pH might bias sorption processes and dynamics via competing surface reactions or complexing reactions in solution (formation of aqueous complexes with altered sorption tendencies).

To prevent pH shifts from buffer reactions, hence, to precisely control pH values of the solid-electrolyte suspensions artificial buffers can be added that have been shown to not interfere with sorption processes (Missana et al., 2009). This technique is often used for solids that undergo a pre-treatment, however, it may also be applied for batch sorption experiments without pre-equilibration of the surface.

Alonso et al. (2013); Alonso et al. (2014) proposed the combination of the Rutherford backscattering spectrometry (RBS) and micro particle-induced X-ray emission (μPIXE) to analyse radionuclide retention and diffusion at a mineral scale using intact crystalline rocks, thus accounting for their heterogeneity. The method has been tested with different radionuclides (or chemical analogues) and resulted especially successful in the case of uranium and selenium.

3.3.3.3.3 Dynamic column transport experiments

A different experimental set-up to gain more understanding of sorption processes at the mineral-water interface are column experiments. While batch sorption experiments represent sorption processes under static, equilibrium conditions, with column transport experiments it is possible to collect retardation data under dynamic conditions and/or under equilibrium conditions. In column experiments, a cylinder is homogeneously filled with crushed mineral/rock and closed. For saturated conditions, a background electrolyte with defined chemical conditions is percolated through the column. After the column is saturated and geochemical conditions are adjusted as required, an electrolyte spiked with the radionuclide/contaminant of interest can be introduced into the column. At the end of the column, fractions of the solution that percolated through the column are collected and information on retardation factors, retention times, mineral dissolution processes, pH evolution, ionic strength changes etc. throughout the experiment can be observed. Since any electrolyte may be introduced into the system and critical parameters such as pH, ionic strength, ligand concentrations may be changed this experimental system can be used to investigate dynamic transport and retardation processes.

As a side note it should be stated that evaluation of results collected from column experiments in general may provide transport parameters such as the retardation factors and distribution coefficients (R and K_d), Péclet number (P_e) or hydrodynamic dispersion coefficient and diffusion coefficients (Stamberg et al., 2014). However, to obtain these parameters numerical models have to be applied such as e.g. HYDRUS, STANMOD, 2D/3D transport models, etc.

3.3.4 Experimental approach to upscaling

3.3.4.1 Advective transport processes

An extensive experimental programme has been performed in several underground laboratories, namely in Äspö hard rock laboratory (Sweden) and Grimsel Test Site (Switzerland). Experiments focus on RN migration/retention and fracture properties (see e.g., an overview of tracer tests in Löfgren et al. (2007) or references at https://www.grimsel.com/). A generalised view on understanding of RN migration and retention in fractured rock was provided by projects TRUE-1 and TRUE Block Scale (Andersson et al., 2002a; Andersson et al., 2002b; Poteri et al., 2002). The projects focussed on the meter up to block (hundred meter) scale similar to the Migration project (MI) and Excavation project (EP) in Grimsel Test Site (Alexander and Frieg, 2009; Alexander et al., 2003; Smith et al., 2001). Grimsel test site project CRIEPIS´s Fractured Rock Experiment (C-FSR) yielded fundamental knowledge about the properties of fractures such as aperture, dispersivity and flow wetted surface using tracer tests and resin injection (http://www.grimsel.com/gts-phase-vi/c-frs/). Natural fracture properties are most often determined using in-situ tracer tests in underground laboratories (Löfgren et al., 2007). For practical reasons, the tests are generally performed in reasonably well connected and hydraulically conductive fractures where groundwater pumping can be performed. The rock mass surrounding the fractures is likely to be intersected by swarms or clusters of minor fractures that can only be described stochastically. Information concerning an accumulation of fractures, so-called deformation zones, and individual hydraulically conducting fractures in the rock matrix are normally obtained by drilling boreholes and examining the boreholes geologically, hydraulically, and geophysically.

3.3.4.2 Diffusive transport

Since 2004 two large scale, long-term in-situ diffusion experiments (LTD) were performed at the Grimsel Test Site which aimed to examine in-situ matrix diffusion and pore space visualisation (Ikonen et al., 2016a; Ikonen et al., 2016b; Soler et al., 2015). The full characterisation of spatial porosity distribution in the matrix, and its link to the mineralogy, in order to better identify microstructure derived diffusion was performed by Voutilainen et al. (2017) from the first LTD monopole experiment. The heterogeneous mineral and pore structure of the studied rock as well as the changing K_d of caesium was taken into account for proper interpretation of the results of in-situ experiments.

Since 2009 in-situ experiments are running within the Repro cluster in Onkalo URL (Finland) for investigating rock matrix retention properties under in situ conditions and to demonstrate that assumptions applied in the safety case are in line with evidence collected on site, in situ (Poteri et al., 2018a; Poteri et al., 2018b; Voutilainen et al., 2019). Two in situ flow experiments were conducted in Onkalo at Repro site where the dominant rock type is veined gneiss. Parallel to in situ experiments the project is focused on rock matrix characterisation and matrix diffusion in laboratory experiments to compare conditions such as stress relaxation, which might open the pore space and increase the diffusivity of the rock. In the work of Voutilainen et al. (2019) the transport of tritiated water (HTO), ^{36}Cl, and ^{22}Na was studied using laboratory and in-situ aqueous phase diffusion experiments (WPDEs).

Upscaling of the results from numerical simulations at the pore scale can be used to derive key parameters for the models at larger scales in crystalline host rocks. The volume average approach has been applied as an upscaling method for the transport processes in porous media (Molins, 2015). As the imaging techniques are progressively improving, "*digital rock physics*" becomes a useful tool to numerically investigate fluid-solid reactive transport (Grathoff et al., 2016). Consequently, the image-based upscaling approach (Keller and Holzer, 2018) can preserve the small-scale information in large-scale simulations. However, one of the challenging aspects of upscaling is whether small-scale measurements are representative for the investigated volume.

3.3.5 Sources of transport data for crystalline rocks

This section presents an extensive (but not complete) overview of available data sources for understanding transport processes specific to crystalline rocks.

3.3.5.1 Transport and retention processes

Fracture surface varies spatially e.g. due to fracture fillings or geometry variability (Bodin et al., 2003; Moreno et al., 1997; Moreno and Neretnieks, 1993). It was observed that water flows in narrow channels through fractures (Bodin et al., 2003; Moreno et al., 1997) which is referred to the so-called channelling effect or preferential flow paths which applies to a single fracture as well as fracture networks (Malloszewski and Zuber, 1992; Moreno et al., 2000; Park et al., 1997; Shahkarami et al., 2016; Tsang, 1984, 1992; Tsang and Tsang, 1987). For an overview of solute transport mechanisms in fractured rock, the RETROCK Project (Nykyri, 2004) and Neretnieks (1993) are also recommended. Detailed information on fracture heterogeneity and its influence on transport processes is described in detail by POSIVA (2012b) and Poteri et al. (2014) who describe phenomena observed at the Olkiluoto site.

An overview of tracer tests can be found in the work of Löfgren et al. (2007) or at the Grimsel Test Site publications list page at https://www.grimsel.com/.

A generalised view on understanding of RN migration and retention in fractured rock was provided by the projects TRUE-1 and TRUE Block Scale (Andersson et al., 2002a; Andersson et al., 2002b; Poteri et al., 2002). The projects focused on the meter up to the block (hundred meter) scale similar to the Migration project (MI) and Excavation project (EP) in the Grimsel Test Site (Alexander and Frieg, 2009; Alexander et al., 2003; Smith et al., 2001).

Diffusive transport is devoted to the zones adjacent to the fractures, enabling radionuclides to enter connected system of pores in the rock matrix. Recent experimental studies on potential crystalline host rocks and diffusive transport include the Grimsel LTD experiment (Havlova et al., 2013; Martin et al., 2013), investigations at the Olkiluoto site (Aromaa et al., 2019; Voutilainen et al., 2019) and Beishan granite investigations (Yang et al., 2018).

3.3.5.2 Sorption processes

Many studies were focused on specific aspects of sorption in crystalline rock, generally using batch sorption experimental set-ups. A wide range of papers dedicated to batch sorption experiments can be found in section 2.4.3 (sorption on crystalline rocks and components).

Detailed experimental set-ups of dynamic sorption column experiment can be obtained from e.g., Britz (2018), Dangelmayr et al. (2017); Höltä et al. (1997); Hölttä et al. (1996); Li et al. (2009); Missana et al. (2008a); Palágyi and Stamberg (2010); Palágyi et al. (2012); Palágyi and Vodičková (2009); Porro et al. (2000); Stamberg et al. (2014); Videnska et al. (2015); Videnská et al. (2013).These papers present experimental data, different model approaches, advantages as well as drawbacks compared to batch experiments.

More information on column titration as one of the methods for the determination of retention properties experiments is provided by e.g., García et al. (2019); Stolze et al. (2020); Svecova et al. (2008).

3.3.5.3 Data used in safety assessment

With respect to sorption on crystalline rock material, compilations of sorption distribution coefficients (K_d) including uncertainties to be used in transport calculations for safety assessment are available in e.g. Crawford (2010); Hakanen et al. (2014). In Hakanen et al. (2014), the evaluation of data for rock material is based on laboratory-derived K_d values of crushed rocks. Based on the results of the mineral-specific sorption of radionuclides in diffusion experiments and results of sorption to rock surfaces, these distribution coefficients determined on crushed rocks were converted to K_d values for intact rock.

4 Remaining Research Questions and Needs

There has been research on the various topics of radionuclide migration for more than 35 years, often co-funded by the European Commission (EC). Within the EC JOPRAD project "Towards a joint programme on radioactive waste disposal" (www.joprad.eu), a consortium of WMO (waste management organisation), TSO (technical support organisation), RE (research entity) and Actor groups representative organisations from European member states identified research development and demonstration (RD&D) priorities of common interest. These RD&D priorities are based on commonly defined remaining key uncertainties and research needs and it forms the basis of a Strategic Research Agenda (SRA) that is used to coordinate, plan and conduct future waste disposal related research in Europe, the so-called European Joint Projects (EJP). Within the SRA (JOPRAD, 2018), different sub-domains were defined prioritising the future research needs.

The overview on remaining research questions and needs provided in this report, starts from those defined in the SRA (divided in sub-domains) and were extended, or more detailed, where appropriate. These added parts are highlighted *in italic* hereafter.

Geochemistry of host rock (intact and disturbed)

The mobility, or the retention, of radionuclides is the result of their interactions with the liquid and the solid phases of the rock under intact in-situ, or altered, conditions. It is therefore important to properly constrain the porewater chemistry and to adequately define reference and bounding ground waters, buffer and backfill pore waters for the safety studies.

For the clay pore water chemistry, the main remaining uncertainties still concern the correct measurements/determination under undisturbed in-situ conditions of non-preservable parameters: pCO_2, pH and E_h. The conditions for the formation of solid solutions of carbonate and sulfate phases are also an open question.

Furthermore the impact of "perturbations" like pyrite oxidation, radiolysis, CO_2 degassing, alkaline plume, iron/clay interactions,… are still poorly understood.

Chemical thermodynamics

Assessment of the long-term performance of the disposal system relies on the understanding and quantification of the thermodynamic driving forces for degradation of waste matrices and mobilization and retention of radionuclides. High quality thermodynamic data are generally usable beyond a given disposal configuration and if one is able to base long-term performance assessments largely on such data, one can create high credibility and confidence. This can be linked to the NEA-thermodynamic database (TDB) approach, which provides high quality assurance and clear identification of priorities.

There is a need to further develop transparent and quality assured thermodynamic databases for use in performance assessment studies. This entails determining thermodynamic data for key radionuclides, principal elements of the disposal system, secondary phases and solid solutions, *realistic representation of natural processes,* filling gaps for specific environments *and specific species (e.g. organic matter, humic acids, Fe-hydroxides, etc.)*, improving the treatment of uncertainties in thermodynamic data.

Another important aspect is related to the database completeness, since the absence of relevant data in any high quality database, inevitably leads to incorrect predictions.

Sorption, site competition, speciation and transport

Radionuclide transport in pore water or groundwater of porous and fractured media is the principal process challenging the long-term isolation and confinement of radionuclides in deep geological formations. The transport rate of species in groundwater is strongly reduced (1) by retention of radionuclides on sorption sites present at the surface of minerals and engineered barrier materials and their alteration products, and (2) *in fractured media by diffusion into the low permeable rock matrix ("rock matrix diffusion").* The extent of sorption depends on the radionuclide, its speciation in solution, the geochemical boundary conditions and *on the heterogeneity of surface reactivity and permeability* of the solid phases. Competition for sorption sites between radionuclides and the main elements (Ca^{2+}, Fe^{2+}, Mn^{2+}, …) naturally present in pore and ground water may reduce the number of sites available for radionuclides.

Sorption mechanisms (such as surface complexation) should be further characterised to improve coupled chemistry/transport models for various media.

Deepening our understanding of surface complexation sorption mechanism

- *Focus on mechanistic understanding: complexation constants, spectroscopy and atomistic modelling to unravel the surface complexes,… → feeding thermodynamic databases.*
- *Impact of competing elements in sorption.*
- *Reversibility of the sorption process (adsorption vs. incorporation).*
- *Transfer of data from "simple to complex" systems: from dilute to compacted systems, from single mineral phases to polymineral host rocks.*
- *Integration of the models into reactive transport models to account for the evolution of reactive surface areas.*

To represent heterogeneous media (cement-based materials, clay-rock, crystalline rocks, bentonite, corrosion products…) in speciation, sorption (considering competitive effects) and transport models considering the variability of barrier properties at all relevant scales. This will elucidate the influence of 3D-rock anisotropy/heterogeneity on radionuclide migration.

Complex evaluation of dependence of sorption process on system constituents and boundary conditions is needed in order to reflect realistically system heterogeneity.

To further develop models, which are able to take into account the behaviour of radionuclides in complex systems (including the effects of organic and inorganic ligands, redox transitions, etc.).

Extending the classical transport models for porous media to include the effect of mobile surface species on overall diffusion rates of cations and (include) effects of anion exclusion

- *Coupling the sorption and diffusion models.*
- *Linking batch sorption data to transport experiments (attention to sorption competition effects) reflecting pore system heterogeneity by conventional description of diffusion process.*
- *Coupling physico-chemical alterations (mineral assemblage, pore structure geometry) in the repository near- and far-field to diffusive species transport.*
- *Appropriately using diffusion databases in safety assessment models.*

Incorporation of radionuclides in solid phases

In contrast to radionuclide retention by sorption, the incorporation of radionuclides in solid phases in waste matrices and along migration paths provides a different and very powerful retention mechanism. This is because incorporated radionuclides are not necessarily released upon contact of the solid with groundwater. This leads to partially irreversible entrapment as a strong safety factor for the repository system*, if colloidal transport can be excluded.* Important solids in this context are spent fuel and glass, and their alteration products, as well as slowly forming and dissolving mineral phases (carbonates, sulfates, …) in the far-field.

The mechanisms for irreversible entrapment need to be further and better characterized and modelled enabling a quantification of the long-term entrapment of key radionuclides (^{14}C, Se, U). Strong need for understanding both thermodynamics and kinetics and how to incorporate these aspects in reactive transport models.

Redox influence on radionuclide migration

Redox conditions influence radionuclide migration. Most repository concepts are based on a reducing environment. Under these conditions actinides and technetium are merely present in a tetravalent redox state. Much higher solubility is expected under oxidizing conditions. This is the principal reason why actinides only contribute for a small amount to the overall radiological risk from a geological disposal facility.

Redox conditions can however be influenced by waste compounds introduced to the near field (e.g. nitrates, organic matter) and in this context micro-organisms can play an important role.

Post-closure safety case uncertainty would be reduced by improving the understanding of:

(i) The temporal and spatial evolution of redox conditions in engineered barrier systems (for instance around metallic containers and overpacks and around steel reinforcement in concrete).

(ii) The effect of redox perturbations (e.g. arising from the presence of nitrates / organic matter) able to modify the expected oxidation states and the mobility of radionuclides.

(iii) The role of kinetics of radionuclide reduction/oxidation.

(iv) The effect of radiolysis on the transport of radionuclides in the near-field of a disposal facility. Spatial extension and time evolution of the zone affected by radiolytic processes.

(v) The role of redox active system constituents (e.g. minerals) on radionuclide mobility

(v) The knowledge of the chemical speciation in the source term.

Further research should involve:

Development of geochemical models for identifying, simulating and spatial monitoring of local and global anoxic conditions and/or redox transitions, including the associated modelling and transfer to realistic conditions.

Characterising the mobility of radionuclides under well controlled redox conditions and complex conditions (pCO_2, pH, nitrate, etc.). *Need for well controlled chemical preparation techniques (reducing agents, purification methods, electrochemical techniques, use of potentiostat, …) and speciation characterisation methods for chemically conditioning radionuclides and tracer sources to be used for redox-sensitive elements before to start sorption and diffusion experiments.*

Improve and extend our understanding of coupled sorption and electron transfer interface reactions governing the retention of redox-sensitive RN on Fe(II)/Fe(III) bearing minerals, including:

- *Complement thermodynamic databases, using realistic data.*
- *Improve capacity to model.*
- *Correlation of mineral properties to their retention capacity and reactivity.*
- *Transfer of data from "simple to complex" systems: from dilute to compacted systems, from single minerals to natural host rocks.*
- *Integration into reactive transport codes addressing also heterogeneous reactivity.*

Transport of strongly sorbing radionuclides

Strongly sorbing radionuclides are expected to only move on a very short distance over geological time periods. Typical strongly sorbing nuclides are tri-and tetravalent actinides and tetravalent technetium. The actual migration distance is difficult to assess and requires sophisticated solid-state analytical techniques. Migration distances can increase by complexation with organic ligands originating from the waste, complexation/colloid formation with naturally present dissolved organic matter, even though retention remains very strong.

Even if strongly sorbing radionuclides in a deep geologic repository constitute only a small risk to the environment, more understanding is desirable to increase confidence, exploring for instance the chemical degradation of the cement-based materials, the presence of organic molecules, saline groundwaters, etc.).

To determine and to better:

- Represent heterogeneous media (cement-based materials, clay-rock, crystalline rocks, bentonite, corrosion products, etc.).
- Simulate anoxic environmental conditions in the experiments.
- Predict the transport of strongly sorbing nuclides*, which is commonly based on the use of so-called effective diffusion coefficients (D_e) and sorption distribution coefficients (R_d). Recent experimental evidence has demonstrated that D_e values may depend on various characteristics of the mineral surfaces and the pertinent pore water composition, as is the case for R_d values. It is therefore imperative to further improve the physico-chemical basis for the use of appropriate D_e values in safety assessment studies.*
- Characterize the retention of redox-sensitive radionuclides or toxic elements.

Retardation by isotopic exchange

e.g., the case of $H^{14}CO_3^-$ with calcite and other carbonates.

The first question to answer is the following: can this isotopic exchange process be treated as pure sorption/retardation (linear and reversible equilibrium, K_d approach?) or is it a true incorporation in solid phase because of precipitation/dissolution equilibrium controlling the ^{14}C-incorporation?

Effects of microbial perturbations on radionuclide migration

Microbes and fungal activity can influence radionuclide migration by biosorption, metabolic processes, formation of biofilms, etc. By release of organic molecules (siderophores), microbes can produce soluble radionuclide complexes. Microbial activity can also influence the chemical environment and in particular the redox state of radionuclides. Nitrates may influence the fate of microbes. In the absence of microorganisms, the transformation of sulphate to sulphide is, e.g. extremely slow, while it is fast in presence of sulphate-reducing bacteria. There is a lot of sulphate in typical repository environments and sulphide formation may strongly influence the geochemical near-field environment. The geochemical environment and the presence of gases (H_2, CH_4, alkanes, …) will strongly influence microbial populations and activities.

Based on previous and ongoing work (e.g. EC MIND project) the role of microbes is typically addressed in implementers' safety cases by bounding assumptions.

Bounding conditions for predictions of microbial activity may be required for performance assessments. Quantitative information on microbe populations, energy and carbon source availability (site specific, waste specific) would be beneficial in this context.

The impact of microbes on the chemical environment needs to be considered as a function of time to understand and quantify the fate and impact of microbial activity on radionuclide migration.

Assessment of the influence of gas on geochemistry and microbial activity in the near-field, considering void spaces, release of hydrogen, organic ligands, nitrates, sulphides, and methane to assess the impact on barrier performance and radionuclide migration.

It would be beneficial to develop methods to upscale from phenomenological descriptions to mechanistic models.

Organic-radionuclide migration

It is likely that a variety of organic substances will be part of any disposal concept, either from the waste inventory, or as superplasticiser or admixtures for concrete structures, or from pre-existing organic matter in the geological formation. It is possible to consider a variety of substances, likely to be present and known for their stability, mobility and radionuclide complexation in laboratory (and *in situ*) transport experiments and models. An example of a very organic-rich waste type is bituminized waste. Organic matter can influence radionuclide migration by creating soluble or colloidal complexes with radionuclides, which would otherwise be insoluble, or by blocking sorption sites. Hyperalkaline water may increase the solubility and the mobility of organic matter (R–COOH and Ø–OH dissociation at high pH) along with entrained admixture compounds (superplasticizers…) arising from cementitious systems. In compact clay rocks present at depth only small organic molecules can be transported, larger ones are filtered in clay pores.

Further research is required to enhance the understanding of the role of organics (either naturally occurring in the clay formation or introduced in the wastes and in the engineered barriers materials) and their influence on radionuclide migration.

(i) the nature of the organic molecules generated by the organic waste or admixture degradation, (ii) their stability with time, (iii) their effects on radionuclide migration (speciation, solubility, retention, diffusion as a complex organic/radionuclide), (iv) the effect of cocktail of organic molecules, (v) the nature and release rate of organic compounds resulting from polymers radiolysis and hydrolysis, and (vi) implementation in a reactive transfer model.

Acquisition of Thermodynamic data for feeding into databases.

Colloid influence on radionuclide migration

Colloids can be organic or inorganic. Their size is typically smaller than 0.5 µm so that they do not settle during groundwater transport. In a repository, colloids may pre-exist in the groundwater system, or may be generated by interaction of groundwater with repository components. Important examples are smectite colloids formed by interaction of glacial melt water with bentonites (peptisation at low ionic strength). Clay rock and swelling clay backfills are filters against colloid transport and this is well documented (BELBaR EC project). If colloids are filtered, they do not contribute to radionuclide migration. If colloids are mobile, colloidal transport is particularly important for radionuclide migration, especially for radionuclides, which are sparingly soluble and strongly sorbed.

An improved understanding of the role of colloid generation and transport for different host rocks is required to increase confidence in post-closure safety cases.

Colloid influence on RN migration:

- *Mechanistic description of the RN-colloid interaction (kinetics of complexation, stability,…).*
- *Colloid interaction with the solid (sorption like).*
- *Colloid straining/filtering behaviour: size dependent transport.*
- *Reactive transport modeling of colloid migration and retention: Implementation of new insights into the enhanced / inhibited particle retention on rough mineral/ rock surfaces.*

Temperature influence on radionuclide migration

Elevated temperature may change the migration behaviour of radionuclides by changing sorption constants, by changing diffusion coefficients in porous media or by influencing the stability of organic matter or of minerals. There are only a few studies on the effect of a temperature increase on radionuclide migration and sorption.

There is a need to support concept optimisation by studying temperature effects on groundwater composition, solid phase transformations and for some key radionuclides the effects of elevated temperature on radionuclide speciation and solubility, sorption and diffusion.

Fracture filling

Most groundwater flow and thus radionuclide migration in higher-strength rocks takes place through a network of interconnected fractures. Fractures will be filled with precipitating minerals over time. How this happens will depend on various factors, including temperature and time. This could influence the porosity, permeability, organic surface coating, microbial community, and eventually the sorption of long-lived radionuclides on mineral surfaces.

A thorough understanding of the processes of fracture filling by precipitating minerals *with a focus on precipitation kinetics* is required to support the safety case for a geological disposal facility in higher strength rock.

Moreover, fracture system characterisation, including pore distribution and sorption properties, in both fracture filling and crystalline host rock is necessary in order to reflect realism of transport pathway properties. Evaluation of system heterogeneity in connection with retention process is inevitable.

Investigation of pore network and surface topography / rugosity of fractured crystalline rock samples with mineral infills:

- *Impact of surface potential variability, the role of grain boundaries, the effect of water saturation, content and chemistry (pH, ionic strength) as well as the impact of pore size variability (nanometre pore scale: meso-/ macropores).*
- *Analysis of the velocity field (diffusive vs. advective transport) in and close to fractures by using PET techniques.*
- *Derivation and quantification of parameter uncertainties to be used in transport modelling in fractured rock.*

Rock matrix diffusion

For long-term safety relevant radionuclides it would be beneficial in the development of safety cases to gain improved understanding of the impact of rock-matrix diffusion on travel time through the geosphere*, including anion exclusion effect. Moreover, realistic reflection of system heterogeneity would be desirable.*

Heterogeneity

The near and far field surrounding a Geological Disposal Facility is likely to be subject to heterogeneities which are unlikely to be fully represented in models, e.g. from a flow point of view, heterogeneities are either generated by the construction of the repository (voids, EDZ, etc.) or exist locally in the geological environment. Integrated modelling taking into account the heterogeneities can provide significant benefits:

- To undertake phenomenological and safety studies to take into account heterogeneities of the system (mineralogy, hydrology, water composition, permeability, porosity, fracture networks).
- To provide a modelling capability which can integrate available site data to account for heterogeneities in the near field.

Performance assessment tools

Modern numerical simulations are an efficient tool to address the complexity of flow and transport of radionuclides in porous media at large time and space scales. However, the quality of the results depend on the accuracy of the input data and the influence of each input parameter can also be difficult to quantify (sensitivity analysis, uncertainties). As a consequence, many mathematical methods to treat parameter sensitivity / uncertainties have been developed, which should be assessed and possibly improved in view of performance assessment calculations.

The research should aim at:

- improving mathematical methods to: (i) analyse the importance of model input parameters of a simulation on the relevant output of the simulation (sensitivity analysis) and (ii) quantify the effect of uncertainties on these outputs (uncertainty analysis).
- developing a tool which includes algorithms that can be coupled to any kind of numerical code and provide relevant indicators.
- developing a systematic procedure to analyse the data quality and to quantify the input data uncertainty in order to assess the confidence level of the model results.

Upscaling in support of performance assessment

Upscaling strategies (including bottom-up approaches) are developed to support and justify hypotheses, parameters and models used in performance assessment calculations. They are based on the understanding and modelling of the fundamental processes from the micro to macroscopic scale taking into account spatial heterogeneity, including multi-scale structuration of rocks/materials.

Upscaling strategy development should aim toward:

- understanding the role of physical/chemical processes at different scales and linking bottom-up and top-down approaches in performance assessments.
- extending upscaling to the materials involved in radioactive waste disposal, e.g. cementitious-based materials.
- to develop multi-scale approaches for coupled processes (including chemistry, hydraulic, mechanics, etc.).
- developing multi-scale strategies to represent complex phenomena (redox processes, microbial activity, mineral transformation, etc.).

References

Aeppli, M., Voegelin, A., Gorski, C.A., Hofstetter, T.B., Sander, M., 2018. Mediated Electrochemical Reduction of Iron (Oxyhydr-)Oxides under Defined Thermodynamic Boundary Conditions. Environmental Science & Technology 52, 560-570.

Aertsens, M., Put, M., Dierckx, A., 2003. An analytical model for the interpretation of pulse injection experiments performed for testing the spatial variability of clay formations. Journal of Contaminant Hydrology 61, 423-436.

Aertsens, M., Wemaere, I., Wouters, L., 2004. Spatial variability of transport parameters in the Boom Clay. Applied Clay Science 26, 37-45.

Aertsens, M., Dierckx, A., Put, M., Moors, H., Janssen, K., Van Ravestyn, L., Van Gompel, M., Van Gompel, M., De Cannière, P., 2005a, Determination of the hydraulic conductivity, the product ηR of the porosity η and the retardation factor R, and the apparent diffusion coefficient Dp on Boom Clay cores from the Mol-1 drilling, SCK•CEN-R-3503, SCK-CEN, Mol, Belgium.

Aertsens, M., Dierckx, A., Put, M., Moors, H., Janssen, K., Van Ravestyn, L., Van Gompel, M., Van Gompel, M., De Cannière, P., 2005b, Determination of the hydraulic conductivity, ηR and the apparent diffusion coefficient on Ieper Clay and Boom Clay cores from the Doel-1 and Doel-2b drillings, SCK-CEN-R3589, Mol, Belgium.

Aertsens, M., De Canniere, P., Lemmens, K., Maes, N., Moors, H., 2008a. Overview and consistency of migration experiments in clay. Physics and Chemistry of the Earth 33, 1019-1025.

Aertsens, M., Van Gompel, M., De Canniere, P., Maes, N., Dierckx, A., 2008b. Vertical distribution of (HCO3-)-C-14 transport parameters in Boom Clay in the Mol-1 borehole (Mol, Belgium). Physics and Chemistry of the Earth 33, S61-S66.

Aertsens, M., De Cannière, P., Moors, H., Van Gompel, M., 2009a. Effect of ionic strength on the transport parameters of tritiated water, iodide and $H^{14}CO_3^-$ in Boom Clay, in: Burakov, B.E., Aloy, A.S. (Eds.), Scientific Basis for Nuclear Waste Management XXXIII, St. Petersburg, pp. 497-504.

Aertsens, M., Maes, N., Van Gompel, M., 2009b. Consistency of the strontium transport parameters in Boom Clay obtained from different types of migration experiments, in: Burakov, B.E., Aloy, A.S. (Eds.), Scientific Basis for Nuclear Waste Management XXXIII, St. Petersburg, pp. 421-428.

Aertsens, M., Dierckx, A., Moors, H., De Canniere, P., Maes, N., 2010a, Vertical distribution of H14CO3- transport parameters in Boom Clay in the Mol-1 borehole (Mol, Belgium) and comparison with data from independent measurements, SCK-CEN-ER-66, SCK-CEN, Mol, Belgium.

Aertsens, M., Maes, N., Labat, S., Van Gompel, M., Maes, T., 2010b, Vertical distribution of HTO and 125I- transport parameters in Boom Clay in the Essen-1 borehole (Belgium), SCK-CEN-ER-67, SCK-CEN, Mol, Belgium.

Aertsens, M., Govaerts, J., Maes, N., Van Laer, L., 2012. Consistency of the strontium transport parameters in Boom Clay obtained from different types of experiments: accounting for the filter plates. MRS Proceedings 1475, 583-588.

Aertsens , M., 2013, Overview of migration experiments in the HADES Underground Research Facility at Mol, SCK-CEN-ER164, SCK-CEN, Mol, belgium.

Aertsens, M., Maes, N., Van Ravestyn, L., Brassinnes, S., 2013. Overview of radionuclide migration experiments in the HADES Underground Research Facility at Mol (Belgium). Clay Minerals 48, 153-166.

Aertsens, M., Van Laer, L., Maes, N., Govaerts, J., 2017. An improved model for through-diffusion experiments: application to strontium and tritiated water (HTO) diffusion in Boom Clay and compacted illite. Geological Society, London, Special Publications 443, 205-210.

Aertsens, M., Maes, N., Govaerts, J., Durce, D., 2020. Why tracer migration experiments with a pressure gradient do not always allow a correct estimation of the accessible porosity in clays. Applied Geochemistry 120.

Ahmed, I.A.M., Hudson-Edwards, K.A., 2017. Redox-reactive Minerals: Properties, Reactions and Applications in Clean Technologies. Mineralogical Society of Great Britain and Ireland.

Aldaba, D., Glaus, M., Leupin, O., Van Loon, L., Vidal, M., Rigol, A., 2014. Suitability of various materials for porous filters in diffusion experiments. Radiochimica Acta 102.

Alexander, W.R., Ota, K., Frieg, B., 2003, The Nagra-JNC in situ study of safety relevant radionuclide retardation in fractured crystalline rock. II: the RRP project methodology development, field and laboratory tests, 1015-2636,

Alexander, W.R., Frieg, B., 2009, Grimsel test site investigation Phase IV The Nagra-JAEA in situ study of safety relevant radionuclide retardation in fractured crystalline rock III: The RRP project final report, NTB-00-07, NAGRA, Switzerland.

Alexandrov, V., Rosso, K.M., 2013. Insights into the Mechanism of Fe(II) Adsorption and Oxidation at Fe–Clay Mineral Surfaces from First-Principles Calculations. The Journal of Physical Chemistry C 117, 22880-22886.

Allison, J.D., Brown, D.S., Novo-Gradac, K.J., 1991, MINTEQA2/PRODEFA2, a geochemical assessment model for environmental systems: Version 3. 0 user's manual, PB-91-182469/XAB; EPA-600/3-91/021 United States NTIS GRA English,

Alonso, U., Missana, T., Garcia-Gutierrez, M., Patelli, A., Siitari-Kauppi, M., Rigato, V., 2009. Diffusion coefficient measurements in consolidated clay by RBS micro-scale profiling. Applied Clay Science 43, 477-484.

Alonso, U., Missana, T., Garcia-Gutierrez, M., Patelli, A., Rigato, V., Ceccato, D., 2013. Ion beam analyses of radionuclide migration in heterogeneous rocks, in: Ricci, R.A., Rigato, V., Mazzoldi, P. (Eds.), Multidisciplinary Applications of Nuclear Physics with Ion Beams. Amer Inst Physics, Melville, pp. 87-94.

Alonso, U., Missana, T., Patelli, A., Ceccato, D., Garcia-Gutierrez, M., Rigato, V., 2014. Se(IV) uptake by Aspo diorite: Micro-scale distribution. Applied Geochemistry 49, 87-94.

Altmaier, M., Gaona, X., Fellhauer, D., Buckau, G., 2010, Intercomparison of Redox determination methods on designed and near-natural aqueous systems : FP 7 EURATOM Collaborative Project "Redox Phenomena Controlling Systems" (KIT Scientific Reports ; 7572),

Altmann, S., Aertsens, M., Appelo, C.A.J., Bruggeman, C., Gaboreau, S., Glaus, M.A., Jacquier, P., Kupcik, T., Maes, N., Montoya, V., Rabung, T., Robinet, J.C., Savoye, S., Schaefer, C.E., Tournassat, C., van Laer, L., Van Loon, L., 2015, Processes of cation migration in clayrocks: Final scientific report of the CatClay European Project, Rapport CEA-R6410, CEA, F., France.

Andersson, P., Byegaard, J., Dershowitz, B., Doe, T., Hermanson, J., Meier, P., Tullborg, E.-L., 2002a, Final report of the TRUE Block Scale project 1 Characterisation and model development, SKB-TR-02-13, SKB, Sweden.

Andersson, P., Byegaard, J., Winberg, A., 2002b, Final report of the TRUE Block Scale project 2 Tracer tests in the block scale, SKB-TR-02-14, SKB, Sweden.

ANDRA, 2005, Dossier 2005 Argile: Safety evaluation of a geological repository, ANDRA, Paris.

ANDRA, 2018a, Les propriétés de transfert naturel des solutés dans le Callovo-Oxforiden, Fiche Bilan CG.FI.ASTR.18.0007, ANDRA,

ANDRA, 2018b, La migration des radionucléides et des toxiques chimiques dans le Callovo-Oxfordien, Fiche Bilan CG.FI.ASTR.18.0010, ANDRA,

André, M., Malmström, M.E., Neretnieks, I., 2009. Determination of sorption properties of intact rock samples: New methods based on electromigration. Journal of Contaminant Hydrology 103, 71-81.

Antonellini, M., Mollema, P.N., Del Sole, L., 2017. Application of analytical diffusion models to outcrop observations: Implications for mass transport by fluid flow through fractures. Water Resour. Res. 53, 5545-5566.

Appelo, C.A.J., Postma, D., 2004. Geochemistry, Groundwater and Pollution. CRC Press.

Appelo, C.A.J., Wersin, P., 2007. Multicomponent diffusion modeling in clay systems with application to the diffusion of tritium, iodide, and sodium in opalinus clay. Environmental Science & Technology 41, 5002-5007.

Appelo, C.A.J., Van Loon, L.R., Wersin, P., 2010. Multicomponent diffusion of a suite of tracers (HTO, Cl, Br, I, Na, Sr, Cs) in a single sample of Opalinus Clay. Geochimica Et Cosmochimica Acta 74, 1201-1219.

Aqvist, J., 1990. Ion-water interaction potentials derived from free energy perturbation simulations. Journal of Physical Chemistry 94, 8021 - 8024.

Aromaa, H., Voutilainen, M., Ikonen, J., Yli-Kaila, M., Poteri, A., Siitari-Kauppi, M., 2019. Through diffusion experiments to study the diffusion and sorption of HTO, Cl, Ba and Cs in crystalline rock. Journal of Contaminant Hydrology 222, 101-111.

Astilleros, J.M., Pina, C.M., Fernández-Díaz, L., Putnis, A., 2003. Supersaturation functions in binary solid solution–aqueous solution systems. Geochimica et Cosmochimica Acta 67, 1601-1608.

Bach, D., Christiansen, B.C., Schild, D., Geckeis, H., 2014. TEM study of Green Rust Sodium Sulphate ($GR_{Na,SO4}$) Interacted with Neptunyl Ions (NpO_2^+). Radiochimica Acta 102, 279-289.

Badaut, V., Schlegel, M.L., Descostes, M., Moutiers, G., 2012. In Situ Time-Resolved X-ray Near-Edge Absorption Spectroscopy of Selenite Reduction by Siderite. Environmental Science & Technology 46, 10820-10826.

Baeyens, B., Bradbury, M.H., 1995, A quantitative mechanistic description of Ni, Zn and Ca sorption on Na-Montmorillonite. Part I: Physico-chemical characterisation and titration measurements, PSI Bericht 95-10 / NAGRA NTB 95-04, PSI-NAGRA, Swizerland.

Baeyens, B., Bradbury, M.H., 1997. A mechanistic description of Ni and Zn sorption on Na-montmorillonite Part I: Titration and sorption measurements. Journal of Contaminant Hydrology 27, 199-222.

Baeyens, B., Marques Fernandes, M., Bradbury, M.H., 2014a, Comparison of sorption measurements on argillaceous rocks and bentonite with predictions using the SGT-E2 Approach to derive sorption data bases, NAGRA NTB 12-05, NAGRA, Switzerland.

Baeyens, B., Thoenen, T., Bradbury, M., Marques Fernandes, M., 2014b, Sorption data bases for the host rocks and lower confining units and bentonite for provisional safety analysis for SGT-E2, NAGRA NTB 12-04, NAGRA, Switzerland.

Baeyens, B., Bradbury, M.H., 2017, The development of a thermodynamic sorption database for montmorillonite and the application to bentonite, PSI Bricht 17-05 / NAGRA NTB 17-13, PSI-NAGRA, Switzerland

Baeyens, B., Marques Fernandes, M., 2018. Adsorption of heavy metals including radionuclides, Developments in Clay Science. Elsevier, pp. 125-172.

Bahl, S., Peuge, S., Pidchenko, I., Pruessmarm, T., Rothe, J., Dardenne, K., Delrieu, J., Fellhauer, D., Jegou, C., Geckeis, H., Vitova, T., 2017. Pu Coexists in Three Oxidation States in a Borosilicate Glass: Implications for Pu Solubility. Inorg Chem 56, 13982-13990.

Banik, N.L., Marsac, R., Lutzenkirchen, J., Diascorn, A., Bender, K., Marquardt, C.M., Geckeis, H., 2016. Sorption and Redox Speciation of Plutonium at the Illite Surface. Environmental Science & Technology 50, 2092-2098.

Banik, N.L., Marsac, R., Lutzenkirchen, J., Marquardt, C.M., Dardenne, K., Rothe, J., Bender, K., Geckeis, H., 2017. Neptunium sorption and redox speciation at the illite surface under highly saline conditions. Geochimica Et Cosmochimica Acta 215, 421-431.

Barbier, F., Duc, G., Petit-Ramel, M., 2000. Adsorption of lead and cadmium ions from aqueous solution to the montmorillonite/water interface. Colloids and Surfaces A: physicochemical and engineering aspects 166, 153-159.

Batrice, R.J., Wacker, J.N., E., K.K., 2016. Speciation of Actinide Complexes, Clusters, and Nanostructures in Solution, Experimental and Theoretical Approaches to Actinide Chemistry, pp. 53-127.

Bazer-Bachi, F., Tevissen, E., Descostes, M., Grenut, B., Meier, P., Simonnot, M.O., Sardin, M., 2006. Characterization of iodide retention on Callovo-Oxfordian argillites and its influence on iodide migration. Physics and Chemistry of the Earth 31, 517-522.

Bazer-Bachi, F., Descostes, M., Tevissen, E., Meier, P., Grenut, B., Simonnot, M.O., Sardin, M., 2007. Characterization of sulphate sorption on Callovo-Oxfordian argillites by batch, column and through-diffusion experiments. Physics and Chemistry of the Earth 32, 552-558.

Beauwens, T., De Canniere, P., Moors, H., Wang, L., Maes, N., 2005. Studying the migration behaviour of selenate in Boom Clay by electromigration. Eng. Geol. 77, 285-293.

Begg, J.D., Zavarin, M., Tumey, S.J., Kersting, A.B., 2015. Plutonium sorption and desorption behavior on bentonite. Journal of environmental radioactivity 141, 106-114.

Bender, W.M., Becker, U., 2019. Quantum-mechanical investigation of the structures and energetics of uranium and plutonium incorporated into the magnetite (Fe_3O_4 lattice. ACS Earth and Space Chemistry 3, 637-651.

Benedicto, A., Begg, J.D., Zhao, P., Kersting, A.B., Missana, T., Zavarin, M., 2014a. Effect of major cation water composition on the ion exchange of Np (V) on montmorillonite: NpO2+–Na+–K+–Ca2+–Mg2+ selectivity coefficients. Applied Geochemistry 47, 177-185.

Benedicto, A., Degueldre, C., Missana, T., 2014b. Gallium sorption on montmorillonite and illite colloids: Experimental study and modelling by ionic exchange and surface complexation. Applied geochemistry 40, 43-50.

Benedicto, A., Missana, T., Fernández, A.M., 2014c. Interlayer collapse affects on cesium adsorption onto illite. Environmental science & technology 48, 4909-4915.

Benson, L., 1982. A tabulation and evaluation of ion exchange data on smectites. Environmental Geology 4, 23-29.

Berg, S., Rücker, M., Ott, H., Georgiadis, A., van der Linde, H., Enzmann, F., Kersten, M., Armstrong, R.T., de With, S., Becker, J., Wiegmann, A., 2016. Connected pathway relative permeability from pore-scale imaging of imbibition. Advances in Water Resources 90, 24-35.

Berkowitz, B., 2002. Characterizing flow and transport in fractured geological media: A review. Advances in Water Resources 25, 861-884.

Bernier, F., li, X.L., Bastiaens, W., Ortiz, L., Van Geet, M., Wouters, L., Frieg, B., Blümling, P., Desrues, J., Viaggiani, G., Coll, C., Chanchole, S., De Greef, V., Hamza, R., Malinski, L., Vervoort, A., Vanbrabant, Y., Debecker, B., Verstraelen, J., Govaerts, A., Wevers, M., Labiouse, V., Escoffier, S., Mathier, J.F., Gastaldo, L., Bühler, C., 2007, Fractures and Self-healing within the Excavation Disturbed Zone in Clays (SELFRAC), EUR 22585, EC,

Bethke, C., Yeakel, S., 2016. The Geochemist's Workbench: Release 11 - GWB Essentials Guide., Champain, Illinois, USA.

Bickmore, B.R., Bosbach, D., Hochella Jr, M.F., Charlet, L., Rufe, E., 2001. In situ atomic force microscopy study of hectorite and nontronite dissolution: Implications for phyllosilicate edge surface structures and dissolution mechanisms. American Mineralogist 86, 411-423.

Bildstein, O., Claret, F., 2015. Stability of Clay Barriers Under Chemical Perturbations, in: Tournassat, C., Steefel, C.I., Bourg, I.C., Bergaya, F. (Eds.), Natural and Engineerd Clay Barriers. Elsevier, Amsterdam, pp. 155-188.

Birgersson, M., Karnland, O., 2009. Ion equilibrium between montmorillonite interlayer space and an external solution-Consequences for diffusional transport. Geochimica Et Cosmochimica Acta 73, 1908-1923.

Bishop, M.E., Dong, H., Kukkadapu, R.K., Liu, C., Edelmann, R.E., 2011. Bioreduction of Fe-bearing clay minerals and their reactivity toward pertechnetate (Tc-99). Geochimica et Cosmochimica Acta 75, 5229-5246.

Bleyen, N., Marien, A., Valcke, E., 2018, The geochemical perturbations of Boom Clay due to the $NaNO_3$ plume released from Eurobitumen bituminised radioactive waste: status 2013, SCK-CEN-ER0221, SCK-CEN, Mol, Belgium.

Bock, H., Dehandschutter, B., Martin, C., Mazurek, M., De Haller, A., Skoczylas, F., Davy, C., 2010, Self-sealing of fractures in argillaceous formations in the context of geological disposal of radioactive waste, NEA report 6184, OECD, Bodin, J., Delay, F., de Marsily, G., 2003. Solute transport in a single fracture with negligible matrix permeability: 1. fundamental mechanisms. Hydrogeology Journal 11, 418-433.

Boland, D.D., Collins, R.N., Payne, T.E., Waite, T.D., 2011. Effect of Amorphous Fe(III) Oxide Transformation on the Fe(II)-Mediated Reduction of U(VI). Environmental Science & Technology 45, 1327-1333.

Bonen, D., 1992. Composition and Appearance of Magnesium Silicate Hydrate and Its Relation to Deterioration of Cement-Based Materials. Journal of the American Ceramic Society 75, 2904-2906.

Bonnet, M., Sardini, P., Billon, S., Siitari-Kauppi, M., Kuva, J., Fonteneau, L., Caner, L., 2020. Determining Crack Aperture Distribution in Rocks Using the 14 C-PMMA Autoradiographic Method: Experiments and Simulations. Journal of Geophysical Research: Solid Earth 125.

Borgia, A., Pruess, K., Kneafsey, T.J., Oldenburg, C.M., Pan, L., 2012. Numerical simulation of salt precipitation in the fractures of a CO2-enhanced geothermal system. Geothermics 44, 13-22.

Börsig, N., Scheinost, A.C., Shaw, S., Schild, D., Neumann, T., 2018. Retention and multiphase transformation of selenium oxyanions during the formation of magnetite via iron(II) hydroxide and green rust. Dalton Transactions 47, 11002-11015.

Bosbach, D., Brandt, F., Bukaemskiy, A., Deissmann, G., Kegler, P., Klinkenberg, M., Kowalski, P.M., Modolo, G., Niemeyer, I., Neumeier, S., Vinograd, V., 2020. Research for the Safe Management of Nuclear Waste at Forschungszentrum Jülich: Materials Chemistry and Solid Solution Aspects. Advanced Engineering Materials, 1901417-1901417.

Bossart, P., Bernier, F., Birkholzer, J., Bruggeman, C., Connolly, P., Dewonck, S., Fukaya, M., Herfort, M., Jensen, M., Matray, J.M., Mayor, J.C., Moeri, A., Oyama, T., Schuster, K., Shigeta, N., Vietor, T., Wieczorek, K., 2017. Mont Terri rock laboratory, 20 years of research: introduction, site characteristics and overview of experiments. Swiss Journal of Geosciences 110, 3-22.

Bostick, B.C., Vairavamurthy, M.A., Karthikeyan, K.G., Chorover, J., 2002. Cesium adsorption on clay minerals: An EXAFS spectroscopic investigation. Environmental Science & Technology 36, 2670-2676.

Boult, K., Cowper, M., Heath, T., Sato, H., Shibutani, T., Yui, M., 1998. Towards an understanding of the sorption of U (VI) and Se (IV) on sodium bentonite. Journal of Contaminant Hydrology 35, 141-150.

Bourg, I.C., Bourg, A.C.M., Sposito, G., 2003. Modeling diffusion and adsorption in compacted bentonite: a critical review. Journal of Contaminant Hydrology 61, 293-302.

Bourg, I.C., Sposito, G., Bourg, A.C., 2007. Modeling the acid–base surface chemistry of montmorillonite. Journal of Colloid and Interface Science 312, 297-310.

Bourg, I.C., Sposito, G., 2010. Connecting the Molecular Scale to the Continuum Scale for Diffusion Processes in Smectite-Rich Porous Media. Environmental Science & Technology 44, 2085-2091.

Bourg, I.C., Tournassat, C., 2015. Chapter 6 - Self-Diffusion of Water and Ions in Clay Barriers, in: Tournassat, C., Steefel, C.I., Bourg, I.C., Bergaya, F. (Eds.), Developments in Clay Science. Elsevier, pp. 189-226.

Bourg, I.C., Lee, S.S., Fenter, P., Tournassat, C., 2017. Stern Layer Structure and Energetics at Mica-Water Interfaces. J. Phys. Chem. C 121, 9402-9412.

Bradbury, M., Baeyens, B., 2017, The development of a thermodynamic sorption data base for illite and the application to argillaceous rocks, PSI Bericht 17-06 / Nagra NTB 17-14, PSI-NAGRA, Switzerland.

Bradbury, M.H., Baeyens, B., 1997a. A mechanistic description of Ni and Zn sorption on Na-montmorillonite Part II: modelling. Journal of Contaminant Hydrology 27, 223-248.

Bradbury, M.H., Baeyens, B., 1997b, Far-field sorption database for performance assessment of a L/ILW repository in an undisturbed Palfris Marl host rock, NAGRA NTB 96-05, NAGRA, Switzerland.

Bradbury, M.H., Baeyens, B., 2000. A generalised sorption model for the concentration dependent uptake of caesium by argillaceous rocks. Journal of Contaminant Hydrology 42, 141-163.

Bradbury, M.H., Baeyens, B., 2003a, Near-field sorption database for compacted MX-80 bentonite for performance assessment of a high-level radioactive waste repository in Opalinus Clay host rock, NAGRA NTB 02-18, NAGRA, Switzerland.

Bradbury, M.H., Baeyens, B., 2003b, Far field sorption data bases for performance assessment of a high-level radioactive waste repository in an undisturbed Opalinus Clay host rock, PSI Bericht 03-08, PSI, Switzerland.

Bradbury, M.H., Baeyens, B., 2005a. Modelling the sorption of Mn(II), Co(II), Ni(II), Zn(II), Cd(II), Eu(III), Am(III), Sn(IV), Th(IV), Np(V) and U(VI) on montmorillonite: Linear free energy relationships and estimates of surface binding constants for some selected heavy metals and actinides. Geochimica et Cosmochimica Acta 69, 875-892.

Bradbury, M.H., Baeyens, B., 2005b. Erratum to Michael H. Bradbury and Bart Baeyens (2005) “Modelling the sorption of Mn(II), Co(II), Ni(II), Zn(II), Cd(II), Eu(III), Am(III), Sn(IV), Th(IV), Np(V) and U(VI) on montmorillonite: Linear free energy relationships and estimates of surface binding constants for some selected heavy metals and actinides”, Geochimica et Cosmochimica Acta 69, 875–892. Geochimica et Cosmochimica Acta 69, 5391-5392.

Bradbury, M.H., Baeyens, B., 2009a. Sorption modelling on illite Part I: Titration measurements and the sorption of Ni, Co, Eu and Sn. Geochimica et Cosmochimica Acta 73, 990-1003.

Bradbury, M.H., Baeyens, B., 2009b. Sorption modelling on illite. Part II: Actinide sorption and linear free energy relationships. Geochimica et Cosmochimica Acta 73, 1004-1013.

Bradbury, M.H., Baeyens, B., 2011a. Predictive sorption modelling of Ni(II), Co(II), Eu(IIII), Th(IV) and U(VI) on MX-80 bentonite and Opalinus Clay: A “bottom-up” approach. Applied Clay Science 52, 27-33.

Bradbury, M.H., Baeyens, B., 2011b, Physico-chemical characterisation data and sorption measurements of Cs, Ni, Eu, Th, U, Cl, I and Se on MX-80 Bentonite, PSI Bericht 11-05 / NAGRA NTB 09-08, NAGRA, P., Switzerland.

Brandt, F., Curti, E., Klinkenberg, M., Rozov, K., Bosbach, D., 2015. Replacement of barite by a (Ba,Ra)SO4 solid solution at close-to-equilibrium conditions: A combined experimental and theoretical study. Geochimica et Cosmochimica Acta 155, 1-15.

Brandt, F., Klinkenberg, M., Poonoosamy, J., Weber, J., Bosbach, D., 2018. The Effect of Ionic Strength and Sraq upon the Uptake of Ra during the Recrystallization of Barite. Minerals 8, 502-502.

Breitner, D., Osán, J., Fábián, M., Zagyvai, P., Szabó, C., Dähn, R., Fernandes, M.M., Sajó, I.E., Máthé, Z., Török, S., 2015. Characteristics of uranium uptake of Boda Claystone Formation as the candidate host rock of high level radioactive waste repository in Hungary. Environmental Earth Sciences 73, 209-219.

Breynaert, E., Bruggeman, C., Maes, A., 2008. XANES-EXAFS analysis of se solid-phase reaction products formed upon contacting Se(IV) with FeS2 and FeS. Environmental Science & Technology 42, 3595-3601.

Breynaert, E., Scheinost, A.C., Dom, D., Rossberg, A., Vancluysen, J., Gobechiya, E., Kirschhock, C.E.A., Maes, A., 2010. Reduction of Se(IV) in Boom Clay: XAS solid phase speciation. Environmental Science & Technology 44, 6649-6655.

Britz, S., 2018. Europium sorption experiments with muscovite, orthoclase, and qartz: Modeling of surface complexation and reactive transport. PhD Thesis. TUBraunschweig, Braunschweig, Germany, p. 284.

Brookshaw, D.R., Pattrick, R.A.D., Bots, P., Law, G.T.W., Lloyd, J.R., Mosselmans, J.F.W., Vaughan, D.J., Dardenne, K., Morrie, K., 2015. Redox Interactions of Tc(VII), U(VI), and Np(V) with Microbially Reduced Biotite and Chlorite. Environmental Science & Technology 49, 13139-13148.

Brouwer, E., Baeyens, B., Maes, A., Cremers, A., 1983. Cesium and rubidium ion equilibria in illite clay. J. Phys. Chem. 87, 1213-1219.

Bruggeman, C., 2006. Assessment of the geochemical behaviour of selenium oxyanions under Boom Clay geochemical conditions. PhD Thesis, Bio-ingeneurswetenschappen. KULeuven Leuven, Belgium, p. 137.

Bruggeman, C., Maes, A., Vancluysen, J., 2007. The identification of FeS_2 as a sorption sink for Tc(IV). Physics and Chemistry of the Earth 32, 573-580.

Bruggeman, C., Maes, N., 2010. Uptake of Uranium(VI) by Pyrite under Boom Clay Conditions: Influence of Dissolved Organic Carbon. Environmental Science & Technology 44, 4210-4216.

Bruggeman, C., Maes, N., Christiansen, B.C., Stipp, S.L.S., Breynaert, E., Maes, A., Regenspurg, S., Malström, M.E., Liu, X., Grambow, B., Schäfer, T., 2012. Redox-active phases and radionuclide equilibrium valence state in subsurface environments – New insights from 6th EC FP IP FUNMIG. Applied Geochemistry 27, 404-413.

Bruggeman, C., Aertsens, M., Maes, N., Salah, S., 2017a, Iodine retention and migration behaviour in Boom Clay, SCK-CEN-ER0409, SCK-CEN, Mol, Belgium.

Bruggeman, C., Maes, N., 2017, Radionuclide migration and retention in Boom Clay, SCK-CEN-ER0345, SCK-CEN, Mol, Belgium.

Bruggeman, C., Maes, N., Aertsens, M., Govaerts, J., Martens, E., Jacops, E., Van Gompel, M., Durce, D., 2017b, Technetium retention and migration behaviour in Boom Clay, SCK-CEN-ER0403, SCK-CEN, Mol, Belgium.

Bruggeman, C., Maes, N., Aertsens , M., Salah, S., 2017c, Tritiated water retention and migration behaviour in Boom Clay, SCK-CEN-ER0408, SCK-CEN, Mol, Belgium.

Bruggeman, C., Salah, S., Maes, N., Durce, D., 2017d, Americium retention and migration behaviour in Boom Clay, SCK-CEN-ER0396, SCK-CEN, Mol, Belgium.

Bruggenwert, M., Kamphorst, A., 1982. Survey of experimental information on cation exchange in soil systems, in: G.H., B. (Ed.), Developments in Soil Science. Elsevier, pp. 141-203.

Burgos, W.D., 2016, Reactivity of iron-rich clays with uranium through redox transition zones,

Butorin, S.M., Kvashnina, K.O., Smith, A.L., Popa, K., Martin, P.M., 2016a. Crystal-Field and Covalency Effects in Uranates: An X-ray Spectroscopic Study. Chemistry-a European Journal 22, 9693-9698.

Butorin, S.M., Kvashnina, K.O., Vegelius, J.R., Meyer, D., Shuh, D.K., 2016b. High-resolution X-ray absorption spectroscopy as a probe of crystal-field and covalency effects in actinide compounds. Proceedings of the National Academy of Sciences of the United States of America 113, 8093-8097.

Butorin, S.M., Kvashnina, K.O., Prieur, D., Rivenet, M., Martin, P.M., 2017. Characteristics of chemical bonding of pentavalent uranium in La-doped UO2. Chemical Communications 53, 115-118.

Byrne, J.M., van der Laan, G., Figueroa, A.I., Qafoku, O., Wang, C., Pearce, C.I., Jackson, M., Feinberg, J., Rosso, K.M., Kappler, A., 2016. Size dependent microbial oxidation and reduction of magnetite nano- and micro-particles. Scientific Reports 6, 30969.

Cevirim-Papaioannou, N., Yalcintas, E., Gaona, X., Dardenne, K., Altmaier, M., Geckeis, H., 2018. Redox chemistry of uranium in reducing, dilute to concentrated NaCl solutions. Applied Geochemistry 98, 286-300.

Chagneau, A., Claret, F., Enzmann, F., Kersten, M., Heck, S., Madé, B., Schäfer, T., 2015. Mineral precipitation-induced porosity reduction and its effect on transport parameters in diffusion-controlled porous media. Geochemical transactions 16, 13-13.

Chakraborty, S., Favre, F., Banerjee, D., Scheinost, A.C., Mullet, M., Ehrhardt, J.-J., Brendlé, J., Vidal, L., Charlet, L., 2010. U(VI) Sorption and Reduction by Fe(II) Sorbed on Montmorillonite. Environmental Science & Technology 44, 3779-3785.

Chang, F.-R.C., Sposito, G., 1994. The electrical double layer of a disk-shaped clay mineral particle: Effect of particle size. Journal of Colloid and Interface Science 163, 19-27.

Chang, F.-R.C., Sposito, G., 1996. The electrical double layer of a disk-shaped clay mineral particle: Effects of electrolyte properties and surface charge density. Journal of Colloid and Interface Science 178, 555-564.

Charlet, L., Tournassat, C., 2005. Fe (II)-Na (I)-Ca (II) cation exchange on montmorillonite in chloride medium: evidence for preferential clay adsorption of chloride–metal ion pairs in seawater. Aquatic Geochemistry 11, 115-137.

Charlet, L., Scheinost, A.C., Tournassat, C., Greneche, J.M., Gehin, A., Fernandez-Martinez, A., Coudert, S., Tisserand, D., Brendle, J., 2007. Electron transfer at the mineral/water interface: Selenium reduction by ferrous iron sorbed on clay. Geochimica Et Cosmochimica Acta 71, 5731-5749.

Charlet, L., Kang, M., Bardelli, F., Kirsch, R., Géhin, A., Grenèche, J.-M., Chen, F., 2012. Nanocomposite Pyrite–Greigite Reactivity toward Se(IV)/Se(VI). Environmental Science & Technology 46, 4869-4876.

Chen, Z., Montavon, G., Guo, Z., Wang, X., Razafindratsima, S., Robinet, J.C., Landesman, C., 2014a. Approaches to surface complexation modeling of Ni(II) on Callovo-Oxfordian clayrock. Applied Clay Science 101, 369-380.

Chen, Z., Montavon, G., Ribet, S., Guo, Z., Robinet, J.C., David, K., Tournassat, C., Grambow, B., Landesman, C., 2014b. Key factors to understand in-situ behavior of Cs in Callovo–Oxfordian clay-rock (France). Chemical Geology 387, 47-58.

Chisholm-Brause, C.J., Conradson, S.D., Buscher, C.T., Eller, P.G., Morris, D.E., 1994. Speciation of uranyl sorbed at multiple binding sites on montmorillonite. Geochimica et Cosmochimica Acta 58, 3625-3631.

Christiansen, B.C., Geckeis, H., Marquardt, C.M., Bauer, A., Römer, J., Wiss, T., Schild, D., Stipp, S.L.S., 2011. Neptunyl (NpO_2^+) interaction with green rust, $GR_{Na,SO4}$. Geochimica et Cosmochimica Acta 75, 1216-1226.

Churakov, S.V., 2006. Ab initio study of sorption on pyrophyllite: Structure and acidity of the edge sites. The Journal of Physical Chemistry B 110, 4135-4146.

Churakov, S.V., 2007. Structure and dynamics of the water films confined between edges of pyrophyllite: A first principle study. Geochimica et Cosmochimica Acta 71, 1130-1144.

Churakov, S.V., Gimmi, T., 2011. Up-Scaling of Molecular Diffusion Coefficients in Clays: A Two-Step Approach. J. Phys. Chem. C 115, 6703-6714.

Churakov, S.V., Daehn, R., 2012. Zinc Adsorption on Clays Inferred from Atomistic Simulations and EXAFS Spectroscopy. Environmental Science and Technology 46, 5713−5719.

Churakov, S.V., 2013. Mobility of Na and Cs on montmorillonite surface under partially saturated conditions. Environ Sci Technol 47, 9816-9823.

Churakov, S.V., Gimmi, T., Unruh, T., Van Loon, L.R., Juranyi, F., 2014. Resolving diffusion in clay minerals at different time scales: Combination of experimental and modeling approaches. Applied Clay Science 96, 36-44.

Churakov, S.V., Liu, X., 2018. Quantum-chemical modelling of clay mineral surfaces and clay mineral–surface–adsorbate interactions, Developments in Clay Science. Elsevier, pp. 49-87.

Churakov, S.V., Prasianakis, N.I., 2018. Review of the current status and challenges for a holistic process-based description of mass transport and mineral reactivity in porous media. American Journal of Science 318, 921-948.

Cormenzana, J., Garcia-Gutierrez, M., Missana, T., Alonso, U., 2008. Modelling large-scale laboratory HTO and strontium diffusion experiments in Mont Terri and Bure clay rocks. Physics and Chemistry of the Earth 33, 949-956.

Couture, R.-M., Charlet, L., Markelova, E., Madé, B.t., Parsons, C.T., 2015. On–Off Mobilization of Contaminants in Soils during Redox Oscillations. Environmental Science & Technology 49, 3015-3023.

Crank, J., 1975. The mathematics of diffusion, 2nd edition. oxford university press.

Crawford, J., 2010, Bedrock Kd data and uncertainty assessment for application in SR-Site geosphere transport calculations, SKB R-10-48, SKB, Sweden.

Cui, D., Eriksen, T.E., 1996, Reduction of Tc(VII) and Np(V) in solution by ferrous iron A laboratory study of homogeneous and heterogeneous redox processes, SKB-TR-96-03, Sweden.

Curti, E., 1999. Coprecipitation of radionuclides with calcite: estimation of partition coefficients based on a review of laboratory investigations and geochemical data. Applied Geochemistry 14, 433-445.

Curti, E., Fujiwara, K., Iijima, K., Tits, J., Cuesta, C., Kitamura, A., Glaus, M.A., Müller, W., 2010. Radium uptake during barite recrystallization at 23±2°C as a function of solution composition: An experimental 133Ba and 226Ra tracer study. Geochimica et Cosmochimica Acta 74, 3553-3570.

Curti, E., Aimoz, L., Kitamura, A., 2013. Selenium uptake onto natural pyrite. Journal of Radioanalytical and Nuclear Chemistry 295, 1655-1665.

Curti, E., Xto, J., Borca, C.N., Henzler, K., Huthwelker, T., Prasianakis, N.I., 2019. Modelling Ra-bearing baryte nucleation/precipitation kinetics at the pore scale: application to radioactive waste disposal. European Journal of Mineralogy 31, 247-262.

Cussler, E.L., 2009. Diffusion: mass transfer in fluid systems, 3rd edition. Cambridge university press, Cambridge.

Cygan, R.T., Liang, J.-J., Kalinichev, A.G., 2004. Molecular Models of Hydroxide, Oxyhydroxide, and Clay Phases and the Development of a General Force Field. Journal of Physical Chemistry B 108, 1255-1266.

Cygan, R.T., Greathouse, J.A., Heinz, H., Kalinichev, A.G., 2009. Molecular models and simulations of layered materials. J. Mater. Chem. 19, 2470-2481.

Dagnelie, R.V.H., Rasamimanana, S., Blin, V., Radwan, J., Thory, E., Robinet, J.C., Lefevre, G., 2018. Diffusion of organic anions in clay-rich media: Retardation and effect of anion exclusion. Chemosphere 213, 472-480.

Dähn, R., Scheidegger, A.M., Manceau, A., Schlegel, M.L., Baeyens, B., Bradbury, M.H., 2001. Ni clay neoformation on montmorillonite surface. Journal of Synchrotron Radiation 8, 533-535.

Dähn, R., Scheidegger, A.M., Manceau, A., Schlegel, M.L., Baeyens, B., Bradbury, M.H., Morales, M., 2002. Neoformation of Ni phyllosilicate upon Ni uptake on montmorillonite: A kinetics study by powder and polarized extended X-ray absorption fine structure spectroscopy. Geochimica et Cosmochimica Acta 66, 2335-2347.

Dähn, R., Scheidegger, A.M., Manceau, A., Schlegel, M.L., Baeyens, B., Bradbury, M.H., Chateigner, D., 2003. Structural evidence for the sorption of Ni(II) atoms on the edges of montmorillonite clay minerals. A polarized X-ray absorption fine structure study. Geochimica et Cosmochimica Acta 67, 1-15.

Dähn, R., Baeyens, B., Bradbury, M.H., 2011. Investigation of the different binding edge sites for Zn on montmorillonite using P-EXAFS – the strong/weak site concept in the 2SPNE SC/CE sorption model. Geochimica et Cosmochimica Acta 75, 5154-5168.

Dangelmayr, M.A., Reimus, P.W., Wasserman, N.L., Punsal, J.J., Johnson, R.H., Clay, J.T., Stone, J.J., 2017. Laboratory column experiments and transport modeling to evaluate retardation of uranium in an aquifer downgradient of a uranium in-situ recovery site. Applied Geochemistry 80, 1-13.

Dauzères, A., Achiedo, G., Nied, D., Bernard, E., Alahrache, S., Lothenbach, B., 2016. Magnesium perturbation in low-pH concretes placed in clayey environment - solid characterisations and modelling. Cement and Concrete Research 79, 137-150.

David, C., Wassermann, J., Amann, F., Klaver, J., Davy, C., Sarout, J., Esteban, L., Rutter, E.H., Hu, Q., Louis, L., Delage, P., Lockner, D.A., Selvadurai, A.P.S., Vanorio, T., Amann Hildenbrand, A., Meredith, P.G., Browning, J., Mitchell, T.M., Madonna, C., Billiotte, J., Reuschlé, T., Lasseux, D., Fortin, J., Lenormand, R., Loggia, D., Nono, F., Boitnott, G., Jahns, E., Fleury, M., Berthe, G., Braun, P., Grégoire, D., Perrier, L., Polito, P., Jannot, Y., Sommier, A., Krooss, B., Fink, R., Clark, A., 2018. KG²B, a collaborative benchmarking exercise for estimating the permeability of the Grimsel granodiorite—Part 2: modelling, microstructures and complementary data. Geophysical Journal International 215, 825-843.

Davis, J., Kent, D., 1990a. Surface complexation modelling in aqueous geochemistry. Pp. 177À260 in: Mineral-Water Interface Geochemistry (MF Hochella and AF White, editors). Reviews in Mineralogy 23.

Davis, J.A., Kent, D., 1990b. Surface complexation modeling in aqueous geochemistry. Reviews in Mineralogy and Geochemistry 23, 177-260.

De Canniere, P., Maes, A., Wimiams, S., Bruggeman, C., Beauwens, T., Maes, N., Cowper, M., 2010, Behaviour of Selenium in Boom Clay. State-of-the-art report, SCK-CEN-ER-120, SCK-CEN, Mol, Belgium.

Debure, M., Tournassat, C., Lerouge, C., Madé, B., Robinet, J.-C., Fernández, A.M., Grangeon, S., 2018. Retention of arsenic, chromium and boron on an outcropping clay-rich rock formation (the Tégulines Clay, eastern France). Science of The Total Environment 642, 216-229.

Degueldre, C., Baeyens, B., Goerlich, W., Riga, J., Verbist, J., Stadelmann, P., 1989. Colloids in water from a subsurface fracture in granitic rock, Grimsel Test Site, Switzerland. Geochimica et Cosmochimica Acta 53, 603-610.

Degueldre, C., Bolek, M., 2009. Modelling colloid association with plutonium: The effect of pH and redox potential. Applied Geochemistry 24, 310-318.

Delay, J., Distinguin, M., Dewonck, S., 2007. Characterization of a clay-rich rock through development and installation of specific hydrogeological and diffusion test equipment in deep boreholes. Physics and Chemistry of the Earth, Parts A/B/C 32, 393-407.

Delhorme, M., Labbez, C., Caillet, C., Thomas, F., 2010. Acid-Base Properties of 2:1 Clays. I. Modeling the Role of Electrostatics. Langmuir 26, 9240-9249.

Descostes, M., Blin, V., Bazer-Bachi, F., Meier, P., Grenut, B., Radwan, J., Schlegel, M.L., Buschaert, S., Coelho, D., Tevissen, E., 2008. Diffusion of anionic species in Callovo-Oxfordian argillites and Oxfordian limestones (Meuse/Haute-Marne, France). Applied Geochemistry 23, 655-677.

Descostes, M., Pointeau, I., Radwan, J., Poonoosamy, J., Lacour, J.L., Menut, D., Vercouter, T., Dagnelie, R.V.H., 2017. Adsorption and retarded diffusion of Eu-III-EDTA(-) through hard clay rock. Journal of Hydrology 544, 125-132.

Dierckx, A., Put, M., De Cannière, P., Maes, N., Aertsens, M., Maes, A., Vancluysen, J., Verdickt, W., Gielen, R., Christiaens, M., Warwick, P., Hall, A., Van der Lee, J., 2000, TRANCOM-CLAY: transport of radionuclides due to complexation with organic matter in clay formations, EUR 19135 EN, Commission, E., Luxembourg.

Dong, H., Fredrickson, J.K., Kennedy, D.W., Zachara, J.M., Kukkadapu, R.K., Onstott, T.C., 2000. Mineral transformations associated with the microbial reduction of magnetite. Chemical Geology 169, 299-318.

Dong, H., Kukkadapu, R.K., Fredrickson, J.K., Zachara, J.M., Kennedy, D.W., Kostandarithes, H.M., 2003. Microbial Reduction of Structural Fe(III) in Illite and Goethite. Environmental Science & Technology 37, 1268-1276.

Dong, H., Jaisi, D.P., Kim, J., Zhang, G., 2009. Microbe-clay mineral interactions. American Mineralogist 94, 1505-1519.

Duc, M., Gaboriaud, F., Thomas, F., 2005. Sensitivity of the acid–base properties of clays to the methods of preparation and measurement: 1. Literature review. Journal of colloid and interface science 289, 139-147.

Dullien, F., 1991. Fluid tansport and pore structure Academic press.

Dumas, T., Fellhauer, D., Schild, D., Gaona, X., Altmaier, M., Scheinost, A.C., 2019. Plutonium retention mechanisms by magnetite under anoxic conditions: Entrapment versus sorption. ACS Earth and Space Chemistry 3, 2197-2206.

Durce, D., Landesman, C., Grambow, B., Ribet, S., Giffaut, E., 2014. Adsorption and transport of polymaleic acid on Callovo-Oxfordian clay stone: batch and transport experiments. J Contam Hydrol 164, 308-322.

Durce, D., Aertsens, M., Jacques, D., Maes, N., Van Gompel, M., 2018. Transport of dissolved organic matter in Boom Clay: Size effects. J Contam Hydrol 208, 27-34.

Durrant, C.B., Begg, J.D., Kersting, A.B., Zavarin, M., 2018. Cesium sorption reversibility and kinetics on illite, montmorillonite, and kaolinite. Science of the Total Environment 610, 511-520.

Dzombak, D.A., Morel, F.M., 1990. Surface complexation modeling: hydrous ferric oxide. John Wiley & Sons.

ECOCLAYII, 2005, ECOCLAY II: Effects of cement on clay barrier performance., EUR21921, Commision, E.,

El Hajj, H., Abdelouas, A., El Mendili, Y., Karakurt, G., Grambow, B., Martin, C., 2013. Corrosion of carbon steel under sequential aerobic-anaerobic environmental conditions. Corrosion Science 76, 432-440.

El Mendili, Y., Abdelouas, A., Chaou, A.A., Bardeau, J.F., Schlegel, M.L., 2014. Carbon steel corrosion in clay-rich environment. Corrosion Science 88, 56-65.

Elo, O., Muller, K., Ikeda-Ohno, A., Bok, F., Scheinost, A.C., Holtta, P., Huittinen, N., 2017. Batch sorption and spectroscopic speciation studies of neptunium uptake by montmorillonite and corundum. Geochimica Et Cosmochimica Acta 198, 168-181.

Emmanuel, S., Berkowitz, B., 2007. Effects of pore-size controlled solubility on reactive transport in heterogeneous rock. Geophysical Research Letters 34, L06404-L06404.

Emmanuel, S., Ague, J.J., 2009. Modeling the impact of nano-pores on mineralization in sedimentary rocks. Water Resour. Res. 45.

Emmanuel, S., Ague, J.J., Walderhaug, O., 2010. Interfacial energy effects and the evolution of pore size distributions during quartz precipitation in sandstone. Geochimica Et Cosmochimica Acta 74, 3539-3552.

Epifano, E., Naji, M., Manara, D., Scheinost, A.C., Hennig, C., Lechelle, J., Konings, R.J.M., Guéneau, C., Prieur, D., Vitova, T., Dardenne, K., Rothe, J., Martin, P.M., 2019. Extreme multi-valence states in mixed actinide oxides. Communications Chemistry 2, 1-11.

Faucher, J.A., Thomas, H.C., 1954. Adsorption Studies on Clay Minerals. IV. The System Montmorillonite-Cesium-Potassium. The Journal of Chemical Physics 22, 258-261.

Fernández, A.M., Baeyens, B., Bradbury, M., Rivas, P., 2004. Analysis of the porewater chemical composition of a Spanish compacted bentonite used in an engineered barrier. Physics and Chemistry of the Earth, Parts A/B/C 29, 105-118.

Ferrage, E., 2016. Investigation of the interlayer organization of water and ions in smectite from the combined use of diffraction experiments and molecular simulations. a review of methodology, applications, and perspectives. Clays and Clay Minerals 64, 348-373.

Fetter, C.W., 1992. Contaminant Hydrology. Macmillan Publishing Company, New York.

Finck, N., Dardenne, K., Bosbach, D., Geckeis, H., 2012. Selenide Retention by Mackinawite. Environmental Science & Technology 46, 10004-10011.

Finck, N., 2020. Iron speciation in Opalinus clay minerals. Applied Clay Science 193, 105679.

Fischer, C., Luttge, A., 2007. Converged surface roughness parameters A new tool to quantify rock surface morphology and reactivity alteration. American Journal of Science 307, 955-973.

Ford, R.G., Scheinost, A.C., Sparks, D.L., 2001. Frontiers in metal sorption/precipitation mechanisms on soil mineral surfaces. Avances in Agronomy 74, 41-62.

Fox, P.M., Davis, J.A., Kukkadapu, R., Singer, D.M., Bargar, J., Williams, K.H., 2013. Abiotic U(VI) reduction by sorbed Fe(II) on natural sediments. Geochimica et Cosmochimica Acta 117, 266-282.

Frohlich, D.R., Amayri, S., Drebert, J., Grolimund, D., Huth, J., Kaplan, U., Krause, J., Reich, T., 2012. Speciation of Np(V) uptake by Opalinus Clay using synchrotron microbeam techniques. Analytical and Bioanalytical Chemistry 404, 2151-2162.

Fuhrmann, M., Bajt, S.a., Schoonen, M.A.A., 1998. Sorption of iodine on minerals investigated by X-ray absorption near edge structure (XANES) and 125I tracer sorption experiments. Applied Geochemistry 13, 127-141.

Fukushi, K., Hasegawa, Y., Maeda, K., Aoi, Y., Tamura, A., Arai, S., Yamamoto, Y., Aosai, D., Mizuno, T., 2013. Sorption of Eu(III) on Granite: EPMA, LA–ICP–MS, Batch and Modeling Studies. Environmental Science & Technology 47, 12811-12818.

Fuller, A.J., Shaw, S., Ward, M.B., Haigh, S.J., Mosselmans, J.F.W., Peacock, C.L., Stackhouse, S., Dent, A.J., Trivedi, D., Burke, I.T., 2015. Caesium incorporation and retention in illite interlayers. Applied Clay Science 108, 128-134.

Gailhanou, H., Lerouge, C., Debure, M., Gaboreau, S., Gaucher, E.C., Grangeon, S., Greneche, J.M., Kars, M., Made, B., Marty, N.C.M., Warmont, F., Tournassat, C., 2017. Effects of a thermal perturbation on mineralogy and pore water composition in a clay-rock: An experimental and modeling study. Geochimica Et Cosmochimica Acta 197, 193-214.

Gaines, G.L., Thomas, H.C., 1953. Adsorption Studies on Clay Minerals. II. A Formulation of the Thermodynamics of Exchange Adsorption. The Journal of Chemical Physics 21, 714-718.

Gaines, G.L., Thomas, H.C., 1955. Adsorption Studies on Clay Minerals. V. Montmorillonite-Cesium-Strontium at Several Temperatures. The Journal of Chemical Physics 23, 2322-2326.

Galunin, E., Alba, M.D., Avilés, M.A., Santos, M.J., Vidal, M., 2009. Reversibility of La and Lu sorption onto smectites: implications for the design of engineered barriers in deep geological repositories. Journal of hazardous materials 172, 1198-1205.

Galunin, E., Alba, M.D., Santos, M.J., Abrao, T., Vidal, M., 2010. Lanthanide sorption on smectitic clays in presence of cement leachates. Geochimica et Cosmochimica Acta 74, 862-875.

García-Gutiérrez, M., Cormenzana, J.L., Missana, T., Mingarro, M., Martín, P.L., 2006. Large-scale laboratory diffusion experiments in clay rocks. Physics and Chemistry of the Earth, Parts A/B/C 31, 523-530.

García, D., Lützenkirchen, J., Petrov, V., Siebentritt, M., Schild, D., Lefèvre, G., Rabung, T., Altmaier, M., Kalmykov, S., Duro, L., Geckeis, H., 2019. Sorption of Eu(III) on quartz at high salt concentrations. Colloids and Surfaces A: Physicochemical and Engineering Aspects 578, 123610-123610.

Gaucher, E., Robelin, C., Matray, J.M., Négrel, G., Gros, Y., Heitz, J.F., Vinsot, A., Rebours, H., Cassagnabère, A., Bouchet, A., 2004. ANDRA underground research laboratory: interpretation of the mineralogical and geochemical data acquired in the Callovian–Oxfordian formation by investigative drilling. Physics and Chemistry of the Earth, Parts A/B/C 29, 55-77.

Gebauer, D., Kellermeier, M., Gale, J.D., Bergström, L., Cölfen, H., 2014. Pre-nucleation clusters as solute precursors in crystallisation. Chem. Soc. Rev. 43, 2348-2371.

Geckeis, H., Lützenkirchen, J., Polly, R., Rabung, T., Schmidt, M., 2013. Mineral–Water Interface Reactions of Actinides. Chemical Reviews 113, 1016-1062.

Giffaut, E., Grivé, M., Blanc, P., Vieillard, P., Colàs, E., Gailhanou, H., Gaboreau, S., Marty, N., Madé, B., Duro, L., 2014. Andra thermodynamic database for performance assessment: ThermoChimie. Applied Geochemistry 49, 225-236.

Gimmi, T., Kosakowski, G., 2011. How Mobile Are Sorbed Cations in Clays and Clay Rocks? Environmental Science & Technology 45, 1443-1449.

Gimmi, T., Leupin, O.X., Eikenberg, J., Glaus, M.A., Van Loon, L.R., Waber, H.N., Wersin, P., Wang, H.A.O., Grolimund, D., Borca, C.N., Dewonck, S., Wittebroodt, C., 2014. Anisotropic diffusion at the field scale in a 4-year multi-tracer diffusion and retention experiment – I: Insights from the experimental data. Geochimica et Cosmochimica Acta 125, 373-393.

Gimmi, T., Alt-Epping, P., 2018. Simulating Donnan equilibria based on the Nernst-Planck equation. Geochimica et Cosmochimica Acta 232, 1-13.

Gimmi, T., Churakov, S.V., 2019. Water retention and diffusion in unsaturated clays: Connecting atomistic and pore scale simulations. Applied Clay Science 175, 169-183.

Glaus, M., Frick, S., Van Loon, L., 2017, Diffusion of selected cations and anions in compacted montmorillonite and bentonite, PSI Bericht 17-08, PSI, Villigen PSI, Switzerland.

Glaus, M.A., Baeyens, B., Bradbury, M.H., Jakob, A., Van Loon, L.R., Yaroshchuk, A., 2007. Diffusion of Na-22 and Sr-85 in montmorillonite: Evidence of interlayer diffusion being the dominant pathway at high compaction. Environmental Science & Technology 41, 478-485.

Glaus, M.A., Muller, W., Van Loon, L.R., 2008a. Diffusion of iodide and iodate through Opalinus Clay: Monitoring of the redox state using an anion chromatographic technique. Applied Geochemistry 23, 3612-3619.

Glaus, M.A., Rosse, R., Van Loon, L.R., Yaroshchuk, A.E., 2008b. TRACER DIFFUSION IN SINTERED STAINLESS STEEL FILTERS: MEASUREMENT OF EFFECTIVE DIFFUSION COEFFICIENTS AND IMPLICATIONS FOR DIFFUSION STUDIES WITH COMPACTED CLAYS. Clays and Clay Minerals 56, 677-685.

Glaus, M.A., Frick, S., Rosse, R., Van Loon, L.R., 2010. Comparative study of tracer diffusion of HTO, Na-22 (+) and Cl-36 (-) in compacted kaolinite, illite and montmorillonite. Geochimica Et Cosmochimica Acta 74, 1999-2010.

Glaus, M.A., Frick, S., Rosse, R., Van Loon, L.R., 2011. Consistent interpretation of the results of through-, out-diffusion and tracer profile analysis for trace anion diffusion in compacted montmorillonite. Journal of Contaminant Hydrology 123, 1-10.

Glaus, M.A., Birgersson, M., Karnland, O., Van Loon, L.R., 2013. Seeming steady-state uphill diffusion of 22Na+ in compacted montmorillonite. Environ Sci Technol 47, 11522-11527.

Glaus, M.A., Aertsens, M., Appelo, C.A.J., Kupcik, T., Maes, N., Van Laer, L., Van Loon, L.R., 2015a. Cation diffusion in the electrical double layer enhances the mass transfer rates for Sr2+, Co2+ and Zn2+ in compacted illite. Geochimica Et Cosmochimica Acta 165, 376-388.

Glaus, M.A., Aertsens, M., Maes, N., Van Laer, L., Van Loon, L.R., 2015b. Treatment of boundary conditions in through-diffusion: A case study of Sr-85(2+) diffusion in compacted illite. Journal of Contaminant Hydrology 177, 239-248.

Glaus, M.A., Frick, S., Van Loon, L.R., 2020. A coherent approach for cation surface diffusion in clay minerals and cation sorption models: Diffusion of Cs+ and Eu3+ in compacted illite as case examples. Geochimica et Cosmochimica Acta 274, 79-96.

Glynn, P., 2000. Solid-Solution Solubilities and Thermodynamics: Sulfates, Carbonates and Halides. Reviews in Mineralogy and Geochemistry 40, 481-511.

Goldberg, S., Sposito, G., 1984. A chemical model of phosphate adsorption by soils: I. Reference oxide minerals. Soil Science Society of America Journal 48, 772-778.

Goldberg, S., Glaubig, R., 1986. Boron Adsorption and Silicon Release by the Clay Minerals Kaolinite, Montmorillonite, and Illite 1. Soil Science Society of America Journal 50, 1442-1448.

Goldberg, S., Glaubig, R., 1988a. Anion sorption on a calcareous, montmorillonitic soil—arsenic. Soil Science Society of America Journal 52, 1297-1300.

Goldberg, S., Glaubig, R., 1988b. Anion sorption on a calcareous, montmorillonitic soil-selenium. Soil Science Society of America Journal 52, 954-958.

Gorski, C.A., Aeschbacher, M., Soltermann, D., Voegelin, A., Baeyens, B., Marques Fernandes, M., Hofstetter, T.B., Sander, M., 2012a. Redox Properties of Structural Fe in Clay Minerals. 1. Electrochemical Quantification of Electron-Donating and -Accepting Capacities of Smectites. Environmental Science & Technology 46, 9360-9368.

Gorski, C.A., Klüpfel, L., Voegelin, A., Sander, M., Hofstetter, T.B., 2012b. Redox Properties of Structural Fe in Clay Minerals. 2. Electrochemical and Spectroscopic Characterization of Electron Transfer Irreversibility in Ferruginous Smectite, SWa-1. Environmental Science & Technology 46, 9369-9377.

Gorski, C.A., Klüpfel, L.E., Voegelin, A., Sander, M., Hofstetter, T.B., 2013. Redox Properties of Structural Fe in Clay Minerals: 3. Relationships between Smectite Redox and Structural Properties. Environmental Science & Technology 47, 13477-13485.

Gorski, C.A., Edwards, R., Sander, M., Hofstetter, T.B., Stewart, S.M., 2016. Thermodynamic Characterization of Iron Oxide–Aqueous Fe2+ Redox Couples. Environmental Science & Technology 50, 8538-8547.

Grambow, B., Smailos, E., Geckeis, H., Müller, R., Hentschel, H., 1996. Sorption and Reduction of Uranium(VI) on Iron Corrosion Products under Reducing Saline Conditions. Radiochimica Acta 74, 149-154.

Grambow, B., Fattahi, M., Montavon, G., Moisan, C., Giffaut, E., 2006. Sorption of Cs, Ni, Pb, Eu (III), Am (III), Cm, Ac (III), Tc (IV), Th, Zr, and U (IV) on MX 80 bentonite: an experimental approach to assess model uncertainty. Radiochimica Acta 94, 627-636.

Grambow, B., 2016. Geological Disposal of Radioactive Waste in Clay. Elements 12, 239-245.

Grangeon, S., Vinsot, A., Tournassat, C., Lerouge, C., Giffaut, E., Heck, S., Groschopf, N., Denecke, M.A., Wechner, S., Schäfer, T., 2015. The influence of natural trace element distribution on the mobility of radionuclides. The exemple of nickel in a clay-rock. Applied Geochemistry 52, 155-173.

Grathoff, G.H., Peltz, M., Enzmann, F., Kaufhold, S., 2016. Porosity and permeability determination of organic-rich Posidonia shales based on 3-D analyses by FIB-SEM microscopy. Solid Earth 7, 1145-1156.

Grathwohl, P., 1998. diffusion in natural porous media: contaminant transport, sorption,/desorption and dissolution kinetics. Kluwer academic publishers.

Grimm, R.E., 1953. Clay Mineralogy. McGraw-hill, New York.

Guillaumont, R., Fanghänel, T., Fuger, J., Grenthe, I., Neck, V., Palmer, D.A., Rand, M.H., 2003. Update on the Chemical Thermodynamics of Uranium, Neptunium, Plutonium, Americium and Technetium. Elsevier, Amsterdam.

Guillot, B., 2002. A reappraisal of what we have learnt during three decades of computer simulations on water. Journal of Molecular Liquids 101, 219-260.

Hakanen, M., Ervanne, H., Puukko, E., 2012, Safety Case for the Disposal of Spent Nuclear Fuel at Olkiluoto: Radionuclide Migration Parameters for the Geosphere, POSIVA Report 2012-41, Helsinki, Finland.

Hakanen, M., Ervanne, H., Puukko, E., 2014, Safety Case for the Disposal of Spent Nuclear Fuel at Olkiluoto: Radionuclide Migration Parameters for the Geosphere, POSIVA 2012-41, Posiva Oy, H., Helsinki, Finland.

Han, D.S., Batchelor, B., Abdel-Wahab, A., 2011. Sorption of selenium(IV) and selenium(VI) to mackinawite (FeS): Effect of contact time, extent of removal, sorption envelopes. Journal of Hazardous Materials 186, 451-457.

Han, D.S., Batchelor, B., Abdel-Wahab, A., 2012. Sorption of selenium(IV) and selenium(VI) onto synthetic pyrite (FeS2): Spectroscopic and microscopic analyses. Journal of Colloid and Interface Science 368, 496-504.

Havlova, V., Martin, A., Landa, J., Sus, F., Siitari-Kauppi, M., Eikenberg, J., Soler, P., Miksova, J., 2013. Long term diffusion experiment LTD Phase I: Evaluation of results and modelling, Brighton, UK, pp. 188-189.

Hayes, K.F., Redden, G., Ela, W., Leckie, J.O., 1991. Surface complexation models: an evaluation of model parameter estimation using FITEQL and oxide mineral titration data. Journal of colloid and interface science 142, 448-469.

Heberling, F., Vinograd, V.L., Polly, R., Gale, J.D., Heck, S., Rothe, J., Bosbach, D., Geckeis, H., Winkler, B., 2014. A thermodynamic adsorption/entrapment model for selenium(IV) coprecipitation with calcite. Geochimica et Cosmochimica Acta 134, 16-38.

Hedges, L.O., Whitelam, S., 2012. Patterning a surface so as to speed nucleation from solution. Soft Matter 8, 8624-8624.

Heinz, H., Lin, T.J., Mishra, R.K., Emami, F.S., 2013. Thermodynamically Consistent Force Fields for the Assembly of Inorganic, Organic, and Biological Nanostructures: The INTERFACE Force Field. Langmuir 29, 1754-1765.

Hennig, C., Schmeide, K., Brendler, V., Moll, H., Tsushima, S., Scheinost, A.C., 2007. EXAFS investigation of U(VI), U(IV), and Th(IV) sulfato complexes in aqueous solution. Inorg Chem 46, 5882 - 5892.

Henzler, K., Fetisov, E.O., Galib, M., Baer, M.D., Legg, B.A., Borca, C., Xto, J.M., Pin, S., Fulton, J.L., Schenter, G.K., Govind, N., Siepmann, J.I., Mundy, C.J., Huthwelker, T., De Yoreo, J.J., 2018. Supersaturated calcium carbonate solutions are classical. Science Advances 4, 6283.

Heron, G., Crouzet, C., Bourg, A.C.M., Christensen, T.H., 1994. Speciation of Fe(II) and Fe(III) in Contaminated Aquifer Sediments Using Chemical Extraction Techniques. Environmental Science & Technology 28, 1698-1705.

Hiemstra, T., Venema, P., Riemsdijk, W.V., 1996. Intrinsic proton affinity of reactive surface groups of metal (hydr) oxides: The bond valence principle. Journal of colloid and interface science 184, 680-692.

Higashihara, T., Kinoshita, K., Sato, S., Kozaki, T., 2004. Electromigration of sodium ions and electro-osmotic flow in water-saturated, compacted Na-montmorillonite. Applied Clay Science 26, 91-98.

Hixon, A.E., Hu, Y.-J., Kaplan, D., Kukkadapu, R.K., Nitsche, H., Qafoku, O., Powell, B.A., 2010. Influence of iron redox transformations on plutonium sorption to sediments. Radiochimica Acta 98, 685.

Hixon, A.E., Powell, B.A., 2018. Plutonium environmental chemistry: mechanisms for the surface-mediated reduction of Pu(v/vi). Environ Sci-Proc Imp 20, 1306-1322.

Hockin, S.L., Gadd, G.M., 2003. Linked redox precipitation of sulfur and selenium under anaerobic conditions by sulfate-reducing bacterial biofilms. Applied and environmental microbiology 69, 7063-7072.

Holmboe, M., Bourg, I.C., 2014. Molecular Dynamics Simulations of Water and Sodium Diffusion in Smectite Interlayer Nanopores as a Function of Pore Size and Temperature. J. Phys. Chem. C 118, 1001-1013.

Höltä, P., Siitari-Kauppi, M., Hakanen, M., Huitti, T., Hautojärvi, A., Lindberg, A., 1997. Radionuclide transport and retardation in rock fracture and crushed rock column experiments. Journal of Contaminant Hydrology 26, 135-145.

Hölttä, P., Hakanen, M., Hautojärvi, A., Timonen, J., Väätäinen, K., 1996. The effects of matrix diffusion on radionuclide migration in rock column experiments. Journal of Contaminant Hydrology 21, 165-173.

Hoving, A.L., Sander, M., Bruggeman, C., Behrends, T., 2017. Redox properties of clay-rich sediments as assessed by mediated electrochemical analysis: Separating pyrite, siderite and structural Fe in clay minerals. Chemical Geology 457, 149-161.

Huber, F., Schild, D., Vitova, T., Rothe, J., Kirsch, R., Schafer, T., 2012. U(VI) removal kinetics in presence of synthetic magnetite nanoparticles. Geochimica et Cosmochimica Acta 96, 154-173.

Huber, F.M., Totskiy, Y., Marsac, R., Schild, D., Pidchenko, I., Vitova, T., Kalmykov, S., Geckeis, H., Schafer, T., 2017. Tc interaction with crystalline rock from Aspo (Sweden): Effect of in-situ rock redox capacity. Applied Geochemistry 80, 90-101.

Huertas, F., Fuentes-Santillana, J., Jullien, F., Rivas, P., Linares, P., 2000, Full scale engineered barriers experiment for a deep geological repository for high-level radioactive waste in crystalline host rock, EUR 19147

Hummel, W., Berner, U., Curti, E., Pearson, F.J., Thoenen, T., 2002. Nagra / PSI Chemical Thermodynamic Data Base 01/01; Nagra technical report 02-16.

Huo, L., Xie, W., Qian, T., Guan, X., Zhao, D., 2017. Reductive immobilization of pertechnetate in soil and groundwater using synthetic pyrite nanoparticles. Chemosphere 174, 456-465.

Huysmans, M., Dassargues, A., 2004. Review of the use of Péclet numbers to determine the relative importance of advection and diffusion in low permeability environments. Hydrogeology Journal 13, 895-904.

Ikeda, A., Hennig, C., Tsushima, S., Takao, K., Ikeda, Y., Scheinost, A.C., Bernhard, G., 2007. Comparative study of uranyl(VI) and -(V) carbonato complexes in an aqueous solution. Inorg Chem 46, 4212-4219.

Ikonen, J., Sammaljärvi, J.V.M., Kuva, J., Siitari-Kauppi, M.L.A., Timonen, J., 2015, Investigation of Rock Matrix Retention Properties, Supporting laboratory studies I: Mineralogy, porosity and pore structure, Posiva Working Report 2014-86, Helsinki, Finland.

Ikonen, J., Sardini, P., Jokelainen, L., Siitari-Kauppi, M., Martin, A., Eikenberg, J., 2016a. The tritiated water and iodine migration in situ in Grimsel granodiorite. Part I: determination of the diffusion profiles. Journal of Radioanalytical and Nuclear Chemistry 310, 1041-1048.

Ikonen, J., Sardini, P., Siitari-Kauppi, M., Martin, A., 2016b. In situ migration of tritiated water and iodine in Grimsel granodiorite, part II: assessment of the diffusion coefficients by TDD modelling. Journal of Radioanalytical and Nuclear Chemistry 311, 339-348.

Ilgen, A.G., Kukkadapu, R.K., Leung, K., Washington, R.E., 2019. “Switching on” iron in clay minerals. Environmental Science: Nano 6, 1704-1715.

Ilton, E.S., Boily, J.-F., Buck, E.C., Skomurski, F.N., Rosso, K.M., Cahill, C.L., Bargar, J.R., Felmy, A.R., 2010. Influence of Dynamical Conditions on the Reduction of UVI at the Magnetite−Solution Interface. Environmental Science & Technology 44, 170-176.

Ithurbide, A., Peulon, S., Miserque, F., Beaucaire, C., Chausse, A., 2009. Interaction between uranium(VI) and siderite (FeCO3) surfaces in carbonate solutions. Radiochimica Acta 97, 177-180.

Ithurbide, A., Peulon, S., Miserque, F., Beaucaire, C., Chaussé, A., 2010. Retention and redox behaviour of uranium(VI) by siderite (FeCO3). Radiochimica Acta 98, 563-568.

Jacops, E., Aertsens, M., Maes, N., Bruggeman, C., Krooss, B.M., Amann-Hildenbrand, A., Swennen, R., Littke, R., 2017a. Interplay of molecular size and pore network geometry on the diffusion of dissolved gases and HTO in Boom Clay. Applied Geochemistry 76, 182-195.

Jacops, E., Aertsens, M., Maes, N., Bruggeman, C., Swennen, R., Krooss, B., Amann-Hildenbrand, A., Littke, R., 2017b. The Dependency of Diffusion Coefficients and Geometric Factor on the Size of the Diffusing Molecule: Observations for Different Clay-Based Materials. Geofluids, 16.

Jacquier, P., Hainos, D., Robinet, J.C., Herbette, M., Grenut, B., Bouchet, A., Ferry, C., 2013. The influence of mineral variability of Callovo-Oxfordian clay rocks on radionuclide transfer properties. Applied Clay Science 83-84, 129-136.

Jahnke, F.M., Radke, C.J., 1989. A radially perfused cell for measuring diffusion in compacted, highly sorbing media. Industrial & Engineering Chemistry Research 28, 347-355.

Jaisi, D.P., Kukkadapu, R.K., Eberl, D.D., Dong, H., 2005. Control of Fe(III) site occupancy on the rate and extent of microbial reduction of Fe(III) in nontronite. Geochimica et Cosmochimica Acta 69, 5429-5440.

Jaisi, D.P., Dong, H., Plymale, A.E., Fredrickson, J.K., Zachara, J.M., Heald, S., Liu, C., 2009. Reduction and long-term immobilization of technetium by Fe(II) associated with clay mineral nontronite. Chemical Geology 264, 127-138.

Jakob, A., Pfingsten, W., Van Loon, L., 2009. Effects of sorption competition on caesium diffusion through compacted argillaceous rock. Geochimica et Cosmochimica Acta 73, 2441-2456.

James, S.C., Wang, L., Chrysikopoulos, C.V., 2018. Modeling colloid transport in fractures with spatially variable aperture and surface attachment. Journal of Hydrology 566, 735-742.

Jenni, A., Mäder, U., Lerouge, C., Gaboreau, S., Schwyn, B., 2014. In situ interaction between different concretes and Opalinus Clay. Physics and chemistry of the Earth Parts A/B/C, 71-83.

Jeon, B.-H., Dempsey, B.A., Burgos, W.D., Barnett, M.O., Roden, E.E., 2005. Chemical Reduction of U(VI) by Fe(II) at the Solid−Water Interface Using Natural and Synthetic Fe(III) Oxides. Environmental Science & Technology 39, 5642-5649.

Joe-Wong, C., Brown, G.E., Maher, K., 2017. Kinetics and Products of Chromium(VI) Reduction by Iron(II/III)-Bearing Clay Minerals. Environmental Science & Technology 51, 9817-9825.

Jones, A.M., Murphy, C.A., Waite, T.D., Collins, R.N., 2017. Fe(II) Interactions with Smectites: Temporal Changes in Redox Reactivity and the Formation of Green Rust. Environmental Science & Technology 51, 12573-12582.

Jones, T.A., Detwiler, R.L., 2016. Fracture sealing by mineral precipitation: The role of small-scale mineral heterogeneity. Geophysical Research Letters 43, 7564-7571.

JOPRAD, 2018, Programme Document - The Scientific and Technical Basis for a Future Joint Programme on Radioactive Waste Management and Disposal - Deliverable 4.4, JOPRAD-D4.4, EC,

Jorgensen, W.L., Tirado-Rives, J., 1988. The OPLS [optimized potentials for liquid simulations] potential functions for proteins, energy minimizations for crystals of cyclic peptides and crambin. Journal of the American Chemical Society 110, 1657 - 1666.

Joseph, C., Van Loon, L.R., Jakob, A., Steudtner, R., Schmeide, K., Sachs, S., Bernhard, G., 2013. Diffusion of U(VI) in Opalinus Clay: Influence of temperature and humic acid. Geochimica Et Cosmochimica Acta 109, 74-89.

Kahl, W.-A., Yuan, T., Bollermann, T., Bach, W., Fischer, C., 2020. Crystal surface reactivity analysis using a combined approach of X-ray micro-computed tomography and vertical scanning interferometry. American Journal of Science 320, 27-52.

Kang, M., Chen, F., Wu, S., Yang, Y., Bruggeman, C., Charlet, L., 2011. Effect of pH on Aqueous Se(IV) Reduction by Pyrite. Environmental Science & Technology 45, 2704-2710.

Kang, M., Ma, B., Bardelli, F., Chen, F., Liu, C., Zheng, Z., Wu, S., Charlet, L., 2013. Interaction of aqueous Se(IV)/Se(VI) with FeSe/FeSe2: Implication to Se redox process. Journal of Hazardous Materials 248-249, 20-28.

Kars, M., Lerouge, C., Grangeon, S., Aubourg, C., Tournassat, C., Madé, B., Claret, F., 2015. Identification of nanocrystalline goethite in reduced clay formations: Application to the Callovian-Oxfordian formation of Bure (France). American Mineralogist 100, 1544-1553.

Kashchiev, D., van Rosmalen, G.M., 2003. Review: Nucleation in solutions revisited. Crystal Research and Technology 38, 555-574.

Kedziorek, M.A.M., Bourg, A.C.M., Giffaut, E., 2007. Hydrogeochemistry of Sn(IV) in the context of radioactive waste disposal: Solubility and adsorption on MX-80 bentonite and Callovo-Oxfordian argilite. Physics and Chemistry of the Earth 32, 568-572.

Keller, L.M., Holzer, L., 2018. Image-Based Upscaling of Permeability in Opalinus Clay. Journal of Geophysical Research: Solid Earth 123, 285-295.

Keri, A., Dahn, R., Marques Fernandes, M., Scheinost, A.C., Krack, M., Churakov, S.V., 2020. Iron adsorption on clays inferred from atomistic simulations and XAS studies. Environmental science & technology, 10.1021/acs.est.1029b07962.

Kéri, A., Osán, J., Fábián, M., Dähn, R., Török, S., 2016. Combined X-ray microanalytical study of the Nd uptake capability of argillaceous rocks. X-Ray Spectrometry 45, 54-62.

Kirsch, R., Fellhauer, D., Altmaier, M., Neck, V., Rossberg, A., Fanghänel, T., Charlet, L., Scheinost, A.C., 2011. Oxidation state and local structure of plutonium reacted with magnetite, mackinawite and chukanovite. Environmental Science & Technology 45, 7267–7274.

Klinkenberg, M., Brandt, F., Breuer, U., Bosbach, D., 2014. Uptake of Ra during the Recrystallization of Barite: A Microscopic and Time of Flight-Secondary Ion Mass Spectrometry Study. Environmental science & technology 48, 6620-6627.

Klinkenberg, M., Weber, J., Barthel, J., Vinograd, V., Poonoosamy, J., Kruth, M., Bosbach, D., Brandt, F., 2018. The solid solution–aqueous solution system (Sr,Ba,Ra)SO4 + H2O: A combined experimental and theoretical study of phase equilibria at Sr-rich compositions. Chemical Geology 497, 1-17.

Kobayashi, T., Scheinost, A.C., Fellhauer, D., Gaona, X., Altmaier, M., 2013. Redox behavior of Tc(VII)/Tc(IV) under various reducing conditions in 0.1 M NaCl solutions. Radiochimica Acta 101, 323-332.

Konevnik, Y.V., Zakharova, E.V., Martynov, K.V., Andryushchenko, N.D., Proshin, I.M., 2017. Influence of temperature on the sorption properties of rocks from the Nizhnekansky massif. Radiochemistry 59, 313-319.

Kosakowski, G., Churakov, S.V., Thoenen, T., 2008. Diffusion of Na and Cs in montmorillonite. Clays and Clay Minerals 56, 190-206.

Kostka, J.E., Haefele, E., Viehweger, R., Stucki, J.W., 1999. Respiration and Dissolution of Iron(III)-Containing Clay Minerals by Bacteria. Environmental Science & Technology 33, 3127-3133.

Kowal-Fouchard, A., Drot, R., Simoni, E., Ehrhardt, J., 2004a. Use of spectroscopic techniques for uranium (VI)/montmorillonite interaction modeling. Environmental science & technology 38, 1399-1407.

Kowal-Fouchard, A., Drot, R., Simoni, E., Marmier, N., Fromage, F., Ehrhardt, J.-J., 2004b. Structural identification of europium (III) adsorption complexes on montmorillonite. New Journal of Chemistry 28, 864-869.

Kraepiel, A.M., Keller, K., Morel, F.M., 1998. On the acid− base chemistry of permanently charged minerals. Environmental science & technology 32, 2829-2838.

Kraepiel, A.M., Keller, K., Morel, F.M., 1999. A model for metal adsorption on montmorillonite. Journal of Colloid and Interface Science 210, 43-54.

Kraevsky, S.V., Tournassat, C., Vayer, M., Warmont, F., Grangeon, S., Wakou, B.F.N., Kalinichev, A.G., 2020. Identification of montmorillonite particle edge orientations by atomic-force microscopy. Applied Clay Science 186, 105442.

Kremleva, A., Kruger, S., Rosch, N., 2011. Uranyl adsorption at (010) edge surfaces of kaolinite: A density functional study Geochimica et Cosmochimica Acta 75 706-718.

Kremleva, A., Martorell, B., Kruger, S., Rosch, N., 2012. Uranyl adsorption on solvated edge surfaces of pyrophyllite: a DFT model study. Physical Chemistry Chemical Physics 14, 5815-5823.

Kremleva, A., Kruger, S., Rosch, N., 2015a. Uranyl adsorption at solvated edge surfaces of 2: 1 smectites. A density functional study. Physical Chemistry Chemical Physics 17, 13757-13768.

Kremleva, A., Krüger, S., Rösch, N., 2015b. Toward a reliable energetics of adsorption at solvated mineral surfaces: A computational study of uranyl (VI) on 2: 1 clay minerals. The Journal of Physical Chemistry C 120, 324-335.

Kügler, R.T., Beißert, K., Kind, M., 2016. On heterogeneous nucleation during the precipitation of barium sulfate. Chemical Engineering Research and Design 114, 30-38.

Kulenkampff, J., Gründig, M., Richter, M., Enzmann, F., 2008. Evaluation of positron-emission-tomography for visualisation of migration processes in geomaterials. Physics and Chemistry of The Earth 33, 937-942.

Kulenkampff, J., Zakhnini, A., Gründig, M., Lippmann-Pipke, J., 2016. Quantitative experimental monitoring of molecular diffusion in clay with positron emission tomography. Solid Earth 7, 1207-1215.

Kulenkampff, J., Stoll, M., Gründig, M., Mansel, A., Lippmann-Pipke, J., Kersten, M., 2018. Time-lapse 3D imaging by positron emission tomography of Cu mobilized in a soil column by the herbicide MCPA. Scientific reports 8, 7091-7091.

Kulik, D.A., Aja, S.U., Sinitsyn, V.A., Wood, S.A., 2000. Acid–base surface chemistry and sorption of some lanthanides on K+-saturated Marblehead illite: II. A multisite–surface complexation modeling. Geochimica et Cosmochimica Acta 64, 195-213.

Kulik, D.A., Wagner, T., Dmytrieva, S.V., Kosakowski, G., Hingerl, F.F., Chudnenko, K.V., Berner, U., 2013. GEM-Selektor geochemical modeling package: revised algorithm and GEMS3K numerical kernel for coupled simulation codes. Computational Geosciences 17, 1-24.

Kurganskaya, I., Luttge, A., 2013. A comprehensive stochastic model of phyllosilicate dissolution: Structure and kinematics of etch pits formed on muscovite basal face. Geochimica Et Cosmochimica Acta 120, 545-560.

Kuva, J., Voutilainen, M., Kekäläinen, P., Siitari-Kauppi, M., Timonen, J., Koskinen, L., 2015. Gas Phase Measurements of Porosity, Diffusion Coefficient, and Permeability in Rock Samples from Olkiluoto Bedrock, Finland. Transport in Porous Media 107, 187-204.

Kuva, J., SammaljÄRvi, J., Parkkonen, J., Siitari-Kauppi, M., Lehtonen, M., Turpeinen, T., Timonen, J., Voutilainen, M., 2018. Imaging connected porosity of crystalline rock by contrast agent-aided X-ray microtomography and scanning electron microscopy. Journal of Microscopy 270, 98-109.

Kvashnina, K., Romanchuk, A., Pidchenko, I., Amidani, L., Gerber, E., Trigub, A., Rossberg, A., Weiss, S., Popa, K., Walter, O., Caciuffo, R., Scheinost, A.C., Butorin, S., Kalmykov, S., 2019. A novel meta-stable pentavalent plutonium solid phase on the pathway from aqueous Pu(VI) to PuO_2 nanoparticles. Angewandte Chemie 58, 17558-17562.

Kvashnina, K.O., Scheinost, A.C., 2016. A Johann-type X-ray emission spectrometer at the Rossendorf beamline. Journal of Synchrotron Radiation 23, 836-841.

Kvashnina, K.O., Walker, H.C., Magnani, N., Lander, G.H., Caciuffo, R., 2017. Resonant x-ray spectroscopy of uranium intermetallics at the M-4,M-5 edges of uranium. Physical Review B 95.

Kvashnina, K.O., Kowalski, P.M., Butorin, S.M., Leinders, G., Pakarinen, J., Bes, R., Li, H., Verwerft, M., 2018. Trends in the valence band electronic structures of mixed uranium oxides. Chemical communications (Cambridge, England) 54, 9757-9760.

Lammers, L.N., Bourg, I.C., Okumura, M., Kolluri, K., Sposito, G., Machida, M., 2017. Molecular dynamics simulations of cesium adsorption on illite nanoparticles. Journal of Colloid and Interface Science 490, 608-620.

Landstroem, O., Tullborg, E.L., 1995, Interactions of trace elements with fracture filling minerals from the Äspö Hard Rock Laboratory, SKB-TR-95-13, Sweden.

Langmuir, D., Riese, A.C., 1985. The thermodynamic properties of radium. Geochimica et Cosmochimica Acta 49, 1593-1601.

Latrille, C., Ly, J., Herbette, M., 2006. Retention of Sn(IV) and Pu(IV) onto four argillites from the Callovo-Oxfordian level at Bure (France) from eight equilibrated sedimentary waters. Radiochimica Acta 94, 421-427.

Latta, D.E., Boyanov, M.I., Kemner, K.M., O'Loughlin, E.J., Scherer, M.M., 2012. Abiotic reduction of uranium by Fe(II) in soil. Applied Geochemistry 27, 1512-1524.

Latta, D.E., Neumann, A., Premaratne, W.A.P.J., Scherer, M.M., 2017. Fe(II)–Fe(III) Electron Transfer in a Clay Mineral with Low Fe Content. ACS Earth and Space Chemistry 1, 197-208.

Lauber, M., Baeyens, B., H, B.M., 2000, Physico-chemical characterisation and sorption measurements of Cs, Sr, Ni, Eu, Th, Sn and Se on Opalinus Clay from Mont Terri, PSI Bericht 00-10 / Nagra NTB 00-11, PSI, Switzerland.

Lazar, K., Mathé, Z., 2012. Claystone as a Potential Host Rock for Nuclear Waste Storage, Clay Minerals in Nature - Their Characterization, Modification and Application - chapter 10.

Lee, S., Anderson, P.R., Bunker, B.A., Karanfil, C., 2004. EXAFS study of Zn sorption mechanisms on montmorillonite. Environmental Science & Technology 38, 5426-5432.

Leinders, G., Bes, R., Kvashnina, K., Verwerft, M., 2020. Local structure in U(IV) and U(V) environments: The case of U_3O_7 Inorg Chem 59, 4576-4587.

Lerouge, C., Grangeon, S., Claret, F., Gaucher, E., Blanc, P., Guerrot, C., Flehoc, C., Wille, G., Mazurek, M., 2014. Mineralogical and Isotopic Record of Diagenesis from the Opalinus Clay Formation at Benken, Switzerland: Implications for the Modeling of Pore-Water Chemistry in a Clay Formation. Clays and Clay Minerals 62, 286-312.

Lerouge, C., Gaboreau, S., Grangeon, S., Claret, F., Warmont, F., Jenni, A., Cloet, V., Mäder, U., 2017. In situ interactions between Opalinus Clay and Low Alkali Concrete. Physics and Chemistry of the Earth, Parts A/B/C 99, 3-21.

Leupin, O.X., Van Loon, L.R., Gimmi, T., Wersin, P., Soler, J.M., 2017. Exploring diffusion and sorption processes at the Mont Terri rock laboratory (Switzerland): lessons learned from 20 years of field research. Swiss Journal of Geosciences 110, 391-403.

Li, L., Steefel, C.I., Yang, L., 2008. Scale dependence of mineral dissolution rates within single pores and fractures. Geochimica et Cosmochimica Acta 72, 360-377.

Li, M.-H., Wang, T.-H., Teng, S.-P., 2009. Experimental and numerical investigations of effect of column length on retardation factor determination: A case study of cesium transport in crushed granite. Journal of Hazardous Materials 162, 530-535.

Li, X., Puhakka, E., Ikonen, J., Söderlund, M., Lindberg, A., Holgersson, S., Martin, A., Siitari-Kauppi, M., 2018. Sorption of Se species on mineral surfaces, part I: Batch sorption and multi-site modelling. Applied Geochemistry 95, 147-157.

Li, X., Liu, L., Wu, Y., Liu, T., 2019a. Determination of the Redox Potentials of Solution and Solid Surface of Fe(II) Associated with Iron Oxyhydroxides. ACS Earth and Space Chemistry 3, 711-717.

Li, X., Meng, S., Puhakka, E., Ikonen, J., Liu, L., Siitari-Kauppi, M., 2019b. A modification of the electromigration device and modelling methods for diffusion and sorption studies of radionuclides in intact crystalline rocks. J Contam Hydrol, 103585.

Li, X., Puhakka, E., Liu, L., Zhang, W., Ikonen, J., Lindberg, A., Siitari-Kauppi, M., 2020. Multi-site surface complexation modelling of Se(IV) sorption on biotite. Chemical Geology 533, 119433-119433.

Li, X.L., 2013. TIMODAZ: A successful international cooperation project to investigate the thermal impact on the EDZ around a radioactive waste disposal in clay host rocks. journal of rock mechanics and geotechnical engineering 8, 231-242.

Li, Y.H., Gregory, S., 1974. Diffusion of Ions in Sea-Water and in Deep-Sea Sediments. Geochimica Et Cosmochimica Acta 38, 703-714.

Liger, E., Charlet, L., Van Cappellen, P., 1999. Surface catalysis of uranium(VI) reduction by iron(II). Geochimica et Cosmochimica Acta 63, 2939-2955.

Lippmann-Pipke, J., Gerasch, R., Schikora, J., Kulenkampff, J., 2017. Benchmarking PET for geoscientific applications: 3D quantitative diffusion coefficient determination in clay rock. Computers and Geosciences 101, 21-27.

Lippmann, F., 1980. Phase diagrams depicting the aqeous solubility of binary mineral systems. N Jahrb Mineral Abh 139, 1-25.

Liu, X., Fattahi, M., Montavon, G., Grambow, B., 2008. Selenide retention onto pyrite under reducing conditions. Radiochimica Acta 96, 473-479.

Liu, X., Lu, X., Wang, R., Meijer, E.J., Zhou, H., 2011. Acidities of confined water in interlayer space of clay minerals. Geochimica Et Cosmochimica Acta 75, 4978-4986.

Liu, X., Jan Meijer, E., Lu, X., Wang, R., 2012a. First-Principles Molecular Dynamics Insight Into Fe2+ Complexes Adsorbed on Edge Surfaces of Clay Minerals. Clays and clay minerals 60, 341-347.

Liu, X., Lu, X., Meijer, E.J., Wang, R., Zhou, H., 2012b. Atomic-scale structures of interfaces between phyllosilicate edges and water. Geochimica et Cosmochimica Acta 81, 56-68.

Liu, X., Lu, X., Sprik, M., Cheng, J., Meijer, E.J., Wang, R., 2013. Acidity of edge surface sites of montmorillonite and kaolinite. Geochimica et Cosmochimica Acta 117, 180-190.

Liu, X., Cheng, J., Sprik, M., Lu, X., Wang, R., 2014a. Surface acidity of 2:1-type dioctahedral clay minerals from first principles molecular dynamics simulations. Geochimica Et Cosmochimica Acta 140, 410-417.

Liu, X., Cheng, J., Sprik, M., Lu, X., Wang, R., 2015a. Interfacial structures and acidity of edge surfaces of ferruginous smectites. Geochimica Et Cosmochimica Acta 168, 293-301.

Liu, X., Lu, X., Cheng, J., Sprik, M., Wang, R., 2015b. Temperature dependence of interfacial structures and acidity of clay edge surfaces. Geochimica et Cosmochimica Acta 160, 91-99.

Liu, X.D., Cheng, J., Sprik, M., Lu, X.C., Wang, R.C., 2014b. Surface acidity of 2:1-type dioctahedral clay minerals from first principles molecular dynamics simulations. Geochimica Et Cosmochimica Acta 140, 410-417.

Livens, F.R., Jones, M.J., Hynes, A.J., Charnock, J.M., Mosselmans, J.F.W., Hennig, C., Steele, H., Collison, D., Vaughan, D.J., Pattrick, R.A.D., Reed, W.A., Moyes, L.N., 2004. X-ray absorption spectroscopy studies of reactions of technetium, uranium and neptunium with mackinawite. Journal of Environmental Radioactivity 74, 211-219.

Llorens, I., Fattahi, M., Grambow, B., 2007. New synthesis route and characterization of siderite (FeCO3) and coprecipitation of 99Tc, in: Dunn, D., Poinssot, C., Begg, B. (Eds.), Scientific Basis for Nuclear Waste Management Xxx, pp. 419-+.

Lofgren, M., Neretnieks, I., 2006. Through-electromigration: a new method of investigating pore connectivity and obtaining formation factors. J Contam Hydrol 87, 237-252.

Löfgren, M., Crawford, J., Elert, M., 2007, Tracer tests - possibilities and limitations. Experience from SKB fieldwork: 1977-2007, SKB report P-07-39, Stockholm, Sweden.

Löfgren, M., Vecernik, P., Havlova, V., 2009, Studying the influence of pore water electrical conductivity on the formation factor, as estimated based on electrical methods, SKB-R-09-57, SKB, Sweden.

Luan, F., Gorski, C.A., Burgos, W.D., 2014. Thermodynamic Controls on the Microbial Reduction of Iron-Bearing Nontronite and Uranium. Environmental Science & Technology 48, 2750-2758.

Ma, B., Fernandez-Martinez, A., Madé, B., Findling, N., Markelova, E., Salas-Colera, E., Maffeis, T.G.G., Lewis, A.R., Tisserand, D., Bureau, S., Charlet, L., 2018. XANES-Based Determination of Redox Potentials Imposed by Steel Corrosion Products in Cement-Based Media. Environmental Science & Technology 52, 11931-11940.

Ma, B., Charlet, L., Fernandez-Martinez, A., Kang, M., Madé, B., 2019. A review of the retention mechanisms of redox-sensitive radionuclides in multi-barrier systems. Applied Geochemistry 100, 414-431.

Ma, B., Fernandez-Martinez, A., Wang, K.F., Made, B., Henocq, P., Tisserand, D., Bureau, S., Charlet, L., 2020. Selenite Sorption on Hydrated CEM-V/A Cement in the Presence of Steel Corrosion Products: Redox vs Nonredox Sorption. Environmental Science & Technology 54, 2344-2352.

Mäder, U., Jenni, A., Lerouge, C., Gaboreau, S., Miyoshi, S., Kimura, Y., Shibata, M., 2018. 5-year chemico-physical evolution of concrete-claystone interfaces, Mont Terri rock laboratory (Switzerland), Mont Terri Rock Laboratory, 20 years. Birkhäuser.

Maes, A., Peigneur, P., Cremers, A., 1975. Thermodynamics of transition metal ion exchange in montmorillonite, Proc. Int. Clay Conf., pp. 319-333.

Maes, N., Moors, H., De Canniere, P., Aertsens, M., Put, M., 1998. Determination of the diffusion coefficient of ionic species in boom clay by electromigration: Feasibility study. Radiochimica Acta 82, 183-189.

Maes, N., Moors, H., Dierckx, A., De Canniere, P., Put, M., 1999. The assessment of electromigration as a new technique to study diffusion of radionuclides in clayey soils. Journal of Contaminant Hydrology 36, 231-247.

Maes, N., Moors, H., Wang, L., Delécaut, G., De Canniere, P., put, M., 2002. The use of electromigration as a qualitative technique to study the migration behaviour and speciation of uranium in Boom Clay. Radiochimica Acta 90, 741-746.

Maes, N., Wang, L., Delécaut, G., Beauwens, T., Van Geet, M., Put, M., Weetjens, E., Marivoet, J., Van der Lee, J., Warwick, P., Hall, A., Walker, G., Maes, A., Bruggeman, C., Bennett, D., Hicks, H., Galson, D., 2004, Migration case study: Transport of radionuclides in a reducing clay sediment (Trancom-II), EUR 21022 EN, EC, Luxembourg.

Maes, N., Wang, L., Hicks, T., Bennett, D., Warwick, P., Hall, T., Walker, G., Dierckx, A., 2006. The role of natural organic matter in the migration behaviour of americium in the Boom Clay - Part I: Migration experiments. Physics and Chemistry of the Earth 31, 541-547.

Maes, N., Bruggeman, C., Govaerts, J., Martens, E., Salah, S., Van Gompel, M., 2011. A consistent phenomenological model for natural organic matter linked migration of Tc (IV), Cm (III), Np (IV), Pu (III/IV) and Pa (V) in the Boom Clay. Physics and Chemistry of the Earth 36, 1590-1599.

Maes, N., Salah, S., Bruggeman, C., Aertsens, M., 2017a, Caesium retention and migration behaviour in Boom Clay, SCK-CEN-ER0387, SCK-CEN, Mol, Belgium.

Maes, N., Salah, S., Bruggeman, C., Aertsens, M., Martens, E., Van Laer, L., 2017b, Strontium retention and migration behaviour in Boom Clay, SCK-CEN-ER0394, SCK-CEN, Mol, Belgium.

Maes., N., Moors, H., Dierckx, A., Aertsens, M., Wang, L., De Cannière, P., Put, M., 2001. Studying the migration behaviour of radionuclides in Boom Clay by electromigration, in: Czurda, C., Haus, R., Kappeler, C., Zorn, R. (Eds.), EREM2001, 3rd symposium and status report on electrokinetic remediation, EREM2001 ed. Schriftenreihe angewandte geologie Karlsruhe, Universität Karlsruhe, Karlsruhe, pp. 35/31-21.

Malikova, N., Dubois, E., Marry, V., Rotenberg, B., Turq, P., 2010. Dynamics in Clays - Combining Neutron Scattering and Microscopic Simulation. Z. Phys. Chemie-Int. J. Res. Phys. Chem. Chem. Phys. 224, 153-181.

Malloszewski, P., Zuber, A., 1992. On the calibration and validation of mathematical models for the interpretation of tracer experiments in groundwater. Advances in Water Resources 15, 47-62.

Manceau, A., Drits, V.A., Silvester, E., Bartoli, C., Lanson, B., 1997. Structural mechanism of Co^{2+} oxidation by the phyllomanganate buserite. American Mineralogist 82, 1150-1175.

Manceau, A., Chateigner, D., Gates, W.P., 1998. Polarized EXAFS, distance-valence least-squares modeling (DVLS) and quantitive texture analysis approaches to the structural refinement of Garfield nontronite. Physics and Chemistry of Minerals 25, 347-365.

Manceau, A., Schlegel, M.L., Nagy, K.L., Charlet, L., 1999. Evidence for the formation of trioctahedral clay upon sorption of Co2+ on quartz. Journal of Colloid and Interface Science 220, 181-197.

Manceau, A., Lanson, B., Schlegel, M.L., Hargé, J.C., Musso, M., Eybert-Bérard, L., Hazemann, J.L., Chateigner, D., Lamble, G.M., 2000. Quantitative Zn speciation in smelter-contaminated soils by EXAFS spectroscopy. American Journal of Science 300, 289-343.

Manceau, A., Marcus, M.A., Tamura, N., 2002. Quantitative speciation of heavy metals in soils and sediments by synchrotron X-ray techniques, in: Fenter, P.A., Rivers, M.L., Sturchio, N.C., Sutton, S.R. (Eds.), Applications of Synchrotron Radiation in Low-Temperature Geochemistry and Environmental Sciences. Mineralogical Soc Amer & Geochemical Soc, Chantilly, pp. 341-428.

Manning, B.A., Goldberg, S., 1996. Modeling arsenate competitive adsorption on kaolinite, montmorillonite and illite. Clays and clay minerals 44, 609-623.

Marivoet, J., Jacques, D., Van Geet, M., Bastiaens, W., Wemaere, I., 2006, Considerations on up-scaling of hydraulid and transport parameters for clay formations. IP-FUNMIG Project Internal Deliverable PID3.4.4, SCK-CEN Report 06/JMa/P-13, SCK-CEN, Mol, Belgium.

Markelova, E., 2017. Interpretation of redox potential and assessment of oxyanion (As, Sb, Cr) mobility during oxic-anoxic oscillations. UWSpace.

Marques Fernandes, M., Baeyens, B., Beaucaire, C., 2012. 8 - Radionuclide retention at mineral–water interfaces in the natural environment, Radionuclide Behaviour in the Natural Environment. Woodhead Publishing, pp. 261-301.

Marques Fernandes, M., Ver, N., Baeyens, B., 2015. Predicting the uptake of Cs, Co, Ni, Eu, Th and U on argillaceous rocks using sorption models for illite. Applied Geochemistry 59, 189-199.

Marsac, R., Banik, N.L., Lutzenkirchen, J., Marquardt, C.M., Dardenne, K., Schild, D., Rothe, J., Diascorn, A., Kupcik, T., Schafer, T., Geckeis, H., 2015. Neptunium redox speciation at the illite surface. Geochimica Et Cosmochimica Acta 152, 39-51.

Marshall, T.A., Morris, K., Law, G.T.W., Mosselmans, J.F.W., Bots, P., Parry, S.A., Shaw, S., 2014. Incorporation and Retention of 99-Tc(IV) in Magnetite under High pH Conditions. Environmental Science & Technology 48, 11853-11862.

Martens, E., Maes, N., Weetjens, E., Van Gompel, M., Van Ravestyn, L., 2010. Modelling of a large-scale in-situ migration experiment with C-14-labelled natural organic matter in Boom Clay. Radiochimica Acta 98, 695-701.

Martin, A., Siitari-Kauppi, M., Havlova, V., Tachi, Y., Miksova, J., 2013. An overview of the long-term diffusion test, Grimsel Test Site, Switzerland., Migration conference 2013, Brighton, UK, pp. 313-314.

Mathurin, F.A., Drake, H., Tullborg, E.-L., Berger, T., Peltola, P., Kalinowski, B.E., Åström, M.E., 2014. High cesium concentrations in groundwater in the upper 1.2km of fractured crystalline rock – Influence of groundwater origin and secondary minerals. Geochimica et Cosmochimica Acta 132, 187-213.

Mayordomo, N., Alonso, U., Missana, T., 2016. Analysis of the improvement of selenite retention in smectite by adding alumina nanoparticles. Science of The Total Environment 572, 1025-1032.

Mayordomo, N., Alonso, U., Missana, T., 2019. Effects of γ-alumina nanoparticles on strontium sorption in smectite: Additive model approach. Applied Geochemistry 100, 121-130.

Mazurek, M., Alt-Epping, P., Gimi, T., Niklaus Waber, H., Bath, A., Gimmi, T., 2009. Natural tracer profiles across argillaceous formations: the Claytrac project. Organisation for Economic Co-Operation and Development Nuclear Energy Agency, Nuclear Energy Agency of the OECD (NEA).

Mazurek, M., Alt-Epping, P., Bath, A., Gimmi, T., Waber, H.N., Buschaert, S., De Canniere, P., De Craen, M., Gautschi, A., Savoye, S., Vinsot, A., Wemaere, I., Wouters, L., 2011. Natural tracer profiles across argillaceous formations. Applied Geochemistry 26, 1035-1064.

Mazurier, A., Sardini, P., Rossi, A.M., Graham, R.C., Hellmuth, K.-H., Parneix, J.-C., Siitari-Kauppi, M., Voutilainen, M., Caner, L., 2016. Development of a fracture network in crystalline rocks during weathering: Study of Bishop Creek chronosequence using X-ray computed tomography and14C-PMMA impregnation method. Geological Society of America Bulletin 128, 1423-1438.

McBeth, J.M., Lloyd, J.R., Law, G.T.W., Livens, F.R., Burke, I.T., Morris, K., 2011. Redox interactions of technetium with iron-bearing minerals. Mineralogical Magazine 75, 2419-2430.

McKinley, J.P., Zachara, J.M., Smith, S.C., Turner, G.D., 1995. The influence of uranyl hydrolysis and multiple site-binding reactions on adsorption of U (VI) to montmorillonite. Clays and clay minerals 43, 586-598.

Means, J.L., Crerar, D.A., Borcsik, M.P., Duguid, J.O., 1978. Radionuclide adsorption by manganese oxides and implications for radioactive waste disposal. Nature 274, 44-47.

Meena, A.H., Arai, Y., 2017. Environmental geochemistry of technetium. Environmental Chemistry Letters 15, 241-263.

Meinrath, G., 1997. Uranium(VI) speciation by spectroscopy. Journal of Radioanalytical and Nuclear Chemistry 224, 119-126.

Meldrum, F.C., O'Shaughnessy, C., 2020. Crystallization in Confinement. Advanced Materials 32, 2001068.

Melkior, T., Yahiaoui, S., Motellier, S., Thoby, D., Tevissen, E., 2005. Cesium sorption and diffusion in Bure mudrock samples. Applied Clay Science 29, 172-186.

Melkior, T., Yahiaoui, S., Thoby, D., Motellier, S., Barthes, V., 2007. Diffusion coefficients of alkaline cations in Bure mudrock. Physics and Chemistry of the Earth 32, 453-462.

Mell, P., Megyeri, J., Riess, L., Máthé, Z., Csicsák, J., Lázár, K., 2006a. Sorption of Co, Cs, Sr and I onto argillaceous rock as studied by radiotracers. Journal of radioanalytical and nuclear chemistry 268, 405-410.

Mell, P., Megyeri, J., Riess, L., Máthé, Z., Hámos, G., Lázár, K., 2006b. Diffusion of Sr, Cs, Co and I in argillaceous rock as studied by radiotracers</p> </p>. Journal of Radioanalytical and Nuclear Chemistry 268, 411-417.

Meng, S., Li, X., Siitari-Kauppi, M., Liu, L., 2020. Development and application of an advection-dispersion model for data analysis of electromigration experiments with intact rock cores. Journal of Contaminant Hydrology 231, 103618-103618.

Menke, H.P., Reynolds, C.A., Andrew, M.G., Pereira Nunes, J.P., Bijeljic, B., Blunt, M.J., 2018. 4D multi-scale imaging of reactive flow in carbonates: Assessing the impact of heterogeneity on dissolution regimes using streamlines at multiple length scales. Chemical Geology 481, 27-37.

Menut, D., Descostes, M., Meier, P., Radwan, J., Mauchien, P., Poinssot, C., 2006. Europium migration in argilaceous rocks : On the use of micro laser-induced breakdown spectroscopy (micro LIBS) as a microanalysis tool, in: VanIseghem, P. (Ed.), Scientific Basis for Nuclear Waste Management Xxix, pp. 913-+.

Meunier, A., Fradin, N., 2005. Clays. Springer.

Miller, A.W., Wang, Y., 2012. Radionuclide interaction with clays in dilute and heavily compacted systems: a critical review. Environ Sci Technol 46, 1981-1994.

Missana, T., Maffiotte, C., García-Gutiérrez, M., 2003. Surface reactions kinetics between nanocrystalline magnetite and uranyl. Journal of Colloid and Interface Science 261, 154-160.

Missana, T., Garcıa-Gutiérrez, M., Alonso, U., 2004. Kinetics and irreversibility of cesium and uranium sorption onto bentonite colloids in a deep granitic environment. Applied clay science 26, 137-150.

Missana, T., Garcıa-Gutierrez, M., 2007. Adsorption of bivalent ions (Ca (II), Sr (II) and Co (II)) onto FEBEX bentonite. Physics and Chemistry of the Earth, Parts A/B/C 32, 559-567.

Missana, T., Alonso, Ú., García-Gutiérrez, M., Mingarro, M., 2008a. Role of bentonite colloids on europium and plutonium migration in a granite fracture. Applied Geochemistry 23, 1484-1497.

Missana, T., Garcia-Gutierrez, M., Alonso, U., 2008b. Sorption of strontium onto illite/smectite mixed clays. Physics and Chemistry of the Earth, Parts A/B/C 33, S156-S162.

Missana, T., Alonso, U., García-Gutiérrez, M., 2009. Experimental study and modelling of selenite sorption onto illite and smectite clays. Journal of Colloid and Interface Science 334, 132-138.

Missana, T., Benedicto, A., García-Gutiérrez, M., Alonso, U., 2014. Modeling cesium retention onto Na-, K-and Ca-smectite: Effects of ionic strength, exchange and competing cations on the determination of selectivity coefficients. Geochimica et Cosmochimica Acta 128, 266-277.

Mitchell, J.K., 1993. Fundamentals of Soil Behavior. Wiley.

Molins, S., 2015. Reactive Interfaces in Direct Numerical Simulation of Pore-Scale Processes. Reviews in Mineralogy and Geochemistry 80, 461-481.

Monnin, C., Cividini, D., 2006. The saturation state of the world's ocean with respect to (Ba, Sr) SO4 solid solutions. geochimica Et Cosmochimica Acta 70, 3290-3298.

Montavon, G., Sabatie-Gogova, A., Ribet, S., Bailly, C., Bessaguet, N., Durce, D., Giffaut, E., Landesman, C., Grambow, B., 2014. Retention of iodide by the Callovo-Oxfordian formation: An experimental study. Applied Clay Science 87, 142-149.

Montoya, V., Baeyens, B., Glaus, M.A., Kupcik, T., Fernandes, M.M., Van Laer, L., Bruggeman, C., Maes, N., Schäfer, T., 2018. Sorption of Sr, Co and Zn on illite: Batch experiments and modelling including Co in-diffusion measurements on compacted samples. Geochimica et Cosmochimica Acta 223, 1-20.

Moors, H., 2005, Topical report on the effect of the ionic strength on the diffusion accessible porosity of Boom Clay, SCK-CEN-ER02, SCK-CEN, Mol, Belgium.

Morad, S., Sirat, M., El-Ghali, M.A.K., Mansurbeg, H., 2018. Chloritization in Proterozoic granite from the Äspö Laboratory, southeastern Sweden: record of hydrothermal alterations and implications for nuclear waste storage. Clay Minerals 46, 495-513.

Moreno, L., Neretnieks, I., 1993. Fluid flow and solute transport in a network of channels. Journal of Contaminant Hydrology 14, 163-192.

Moreno, L., Gylling, B., Neretnieks, I., 1997. Solute transport in fractured media — the important mechanisms for performance assessment. Journal of Contaminant Hydrology 25, 283-298.

Moreno, L., Svensson, E., Neretnieks, I., 2000. Determination of the Flow-Wetted Surface in Fractured Media. MRS Proceedings 663.

Morton, J.D., Semrau, J.D., Hayes, K.F., 2001. An X-ray absorption spectroscopy study of the structure and reversibility of copper adsorbed to montmorillonite clay. Geochimica et Cosmochimica Acta 65, 2709-2722.

Motellier, S., Devol-Brown, I., Savoye, S., Thoby, D., Alberto, J.C., 2007. Evaluation of tritiated water diffusion through the Toarcian clayey formation of the Tournemire experimental site (France). Journal of Contaminant Hydrology 94, 99-108.

Motta, M.M., Miranda, C., 1989. Molybdate adsorption on kaolinite, montmorillonite, and illite: Constant capacitance modeling. Soil Science Society of America Journal 53, 380-385.

Moyes, L.N., Jones, M.J., Reed, W.A., Livens, F.R., Charnock, J.M., Mosselmans, J.F.W., Hennig, C., Vaughan, D.J., Pattrick, R.A.D., 2002. An X-ray absorption spectroscopy study of neptunium(V) reactions with mackinawite (FeS). Environmental Science & Technology 36, 179-183.

Muller, F., Besson, G., Manceau, A., Drits, V.A., 1997. Distribution of isomorphous cations within octahedral sheets in montmorillonite from Camp-Bertaux. Physics and Chemistry of Minerals 24, 159-166.

Muuri, E., Matara-aho, M., Puhakka, E., Ikonen, J., Martin, A., Koskinen, L., Siitari-Kauppi, M., 2018. The sorption and diffusion of 133Ba in crushed and intact granitic rocks from the Olkiluoto and Grimsel in-situ test sites. Applied Geochemistry 89, 138-149.

Muuri, E., 2019. Migration of barium in crystalline rock: interpretation of in situ experiments, Department of Chemistry. University of Helsinki, Helsinki, pp. 59-59.

Myneni, S.C., 1997. Abiotic Selenium Redox Transformations in the Presence of Fe(II,III) Oxides. Science 278, 1106-1109.

Nagasaki, S., Saito, T., Yang, T.T., 2016. Sorption behavior of Np(V) on illite, shale and MX-80 in high ionic strength solutions. Journal of Radioanalytical and Nuclear Chemistry 308, 143-153.

Nagasaki, S., Riddoch, J., Saito, T., Goguen, J., Walker, A., Yang, T.T., 2017. Sorption behaviour of Np(IV) on illite, shale and MX-80 in high ionic strength solutions. Journal of Radioanalytical and Nuclear Chemistry 313, 1-11.

NAGRA, 2002, Project Opalinus Clay -- Safety report -- Demonstration of disposal feasibility for spent fuel, vitrified high-level waste and long-lived intermediate-level waste (Entsorgungsnachweis), NAGRA NTB 02-05, Wettingen, Switzerland.

Naveau, A., Monteil-Rivera, F., Guillon, E., Dumonceau, J., 2007. Interactions of Aqueous Selenium (−II) and (IV) with Metallic Sulfide Surfaces. Environmental Science & Technology 41, 5376-5382.

Necib, S., Linard, Y., Crusset, D., Michau, N., Daumas, S., Burger, E., Romaine, A., Schlegel, M.L., 2016. Corrosion at the carbon steel-clay borehole water and gas interfaces at 85 degrees C under anoxic and transient acidic conditions. Corrosion Science 111, 242-258.

Németh, T., Máthé, Z., Pekker, P., Dódony, I., Kovács-Kis, V., Sipos, P., Cora, I., Kovács, I., 2016. Clay mineralogy of the Boda Claystone Formation (Mecsek Mts., SW Hungary). Open Geosciences 8, 259-274.

Neretnieks, I., 1993. Solute Transport in Fractured Rock — Applications to Radionuclide Waste Repositories. Elsevier, pp. 39-127.

Neumann, A., Hofstetter, T.B., Lüssi, M., Cirpka, O.A., Petit, S., Schwarzenbach, R.P., 2008. Assessing the Redox Reactivity of Structural Iron in Smectites Using Nitroaromatic Compounds As Kinetic Probes. Environmental Science & Technology 42, 8381-8387.

Neumann, A., Sander, M., Hofstetter, T.B., 2011. Redox Properties of Structural Fe in Smectite Clay Minerals, Aquatic Redox Chemistry. American Chemical Society, pp. 361-379.

Neumann, J., Brinkmann, H., Britz, S., Lützenkirchen, J., Bok, F., Stockmann, M., Brendler, V., Stumpf, T., Schmidt, M., 2020. A comprehensive study of the sorption mechanism and thermodynamics of f-element sorpiton onto K-feldspar. Journal of Colloid and Interface Science under review.

Newton, A.G., Sposito, G., 2015. Molecular dynamics simulations of pyrophyllite edge surfaces: structure, surface energies, and solvent accessibility. Clays and Clay Minerals 63, 277-289.

Nilsson, N., Persson, P., Lövgren, L., Sjöberg, S., 1996. Competitive surface complexation of o-phthalate and phosphate on goethite (α-FeOOH) particles. Geochimica et cosmochimica acta 60, 4385-4395.

Nishimoto, S., Yoshida, H., 2010. Hydrothermal alteration of deep fractured granite: Effects of dissolution and precipitation. Lithos 115, 153-162.

Niwa, M., Shimada, K., Tamura, H., Shibata, K., Sueoka, S., Yasue, K.-i., Ishimaru, T., Umeda, K., 2016. Thermal Constraints on Clay Growth in Fault Gouge and Their Relationship with Fault-zone Evolution and Hydrothermal Alteration: Case Study of Gouges in the Kojaku Granite, Central Japan. Clays and Clay Minerals 64, 86-107.

Noguera, C., Fritz, B., Clément, A., 2016. Kinetics of precipitation of non-ideal solid-solutions in a liquid environment. Chemical Geology 431, 20-35.

Nollet, S., Koerner, T., Kramm, U., Hilgers, C., 2009. Precipitation of fracture fillings and cements in the Buntsandstein (NW Germany). Geofluids 9, 373-385.

Noseck, U., Fluegge, J., Britz, S., Schneider, A., Brendler, V., Stockmann, M., Schikora, J., Lampe, M., 2012, Realistic integration of sorption processes in transport codes for long-term safety assessments, GRS-297, GRS, Germany.

Noseck, U., Britz, S., Flügge, J., Mönig, J.B.V.S.M., 2014. New Methodology For Realistic Integration Of Sorption Processes In Safety Assessments, Phoenix, Arizona, USA.

Noseck, U., Brendler, V., Britz, S., Stockmann, M., Fricke, J., Richter, C., Lampe, M., Gehrke, A., Flügge, J., 2018, Smart Kd-Concept for Long-term Safety Assessments - Extension towards more Complex Applications, GRS Series, GRS-500; Braunschweig, Gremany.

Nykyri, M., 2004, RETROCK Project Treatment of geosphere retention phenomena in safety assessments Scientific basis of retention processes and their implementation in safety assessment models (WP2) Work Package 2 report of the RETROCK Concerted Action, 1402-3091, Sweden.

O'Loughlin, E.J., Kelly, S.D., Cook, R.E., Csencsits, R., Kemner, K.M., 2003. Reduction of Uranium(VI) by Mixed Iron(II)/Iron(III) Hydroxide (Green Rust): Formation of UO2 Nanoparticles. Environmental Science & Technology 37, 721-727.

O'Loughlin, E.J., Kelly, S.D., Kemner, K.M., 2010. XAFS Investigation of the Interactions of U-VI with Secondary Mineralization Products from the Bioreduction of Fe-III Oxides. Environmental Science & Technology 44, 1656-1661.

Ochs, M., Lothenbach, B., Wanner, H., Sato, H., Yui, M., 2001. An integrated sorption-diffusion model for the calculation of consistent distribution and diffusion coefficients in compacted bentonite. Journal of Contaminant Hydrology 47, 283-296.

Ochs, M., Payne, T.E., Brendler, V., 2012, NEA sorption project. Phase III: thermodynamic sorption modelling in support of radioactive waste disposal safety cases, NEA OECD publication No. 6914.

OECD/NEA, 1996. Fluid Flow through faults and fractures in argillaceous formations, Joint NEA/EC workshop on fluid flow through faults and fractures in argillaceous formations. OECD/NEA, Berne.

Okumura, M., Sassi, M., Rosso, K.M., Machida, M., 2017. Origin of 6-fold coordinated aluminum at (010)-type pyrophyllite edges. Aip Advances 7, 055211-055219.

Olin, A., Nolang, B., Osadchii, E.G., Ohman, L.-O., Rosén, E., 2005. Chemical thermodynamics of selenium. Elsevier, Amsterdam; London.

ONDRAF/NIRAS, 2001, SAFIR 2: Safety Assessment and Feasibility Interim Report 2, Report NIROND 2001-05E, Brussels, Belgium.

ONDRAF/NIRAS, 2013, ONDRAF/NIRAS Research, Development and Demonstration (RD&D) Plan for the geological disposal of high-level and/or long-lived radioactive waste including irradiated fuel if considered as waste, NIROND-TR 2013-12 E,

Orucoglu, E., Tournassat, C., Robinet, J.C., Made, B., Lundy, M., 2018. From experimental variability to the sorption related retention parameters necessary for performance assessment models for nuclear waste disposal systems: The example of Pb adsorption on clay minerals. Applied Clay Science 163, 20-32.

Osán, J., Kéri, A., Breitner, D., Fábián, M., Dähn, R., Simon, R., Török, S., 2014. Microscale analysis of metal uptake by argillaceous rocks using positive matrix factorization of microscopic X-ray fluorescence elemental maps. Spectrochimica Acta Part B: Atomic Spectroscopy 91, 12-23.

Pabalan, R.T., Turner, D.R., 1996. Uranium (6+) sorption on montmorillonite: Experimental and surface complexation modeling study. Aquatic Geochemistry 2, 203-226.

Palágyi, S., Stamberg, K., 2010. Modeling of transport of radionuclides in beds of crushed crystalline rocks under equilibrium non-linear sorption isotherm conditions. Radiochimica Acta 98, 359-365.

Palágyi, Š., Vodičková, H., 2009. Sorption and desorption of 125I-, 137Cs+, 85Sr2+ and 152,154Eu3+ on disturbed soils under dynamic flow and static batch conditions. Journal of Radioanalytical and Nuclear Chemistry 280, 3-14.

Palágyi, Š., Štamberg, K., Havlova, V., Vodičková, H., 2012. Effect of grain size on the 85Sr2+ sorption and desorption in columns of crushed granite and infill materials from granitic water under dynamic conditions. Journal of Radioanalytical and Nuclear Chemistry 297, 33-39.

Park, C.-K., Vandergraaf, T.T., Drew, D.J., Hahn, P.-S., 1997. Analysis of the migration of nonsorbing tracers in a natural fracture in granite using a variable aperture channel model. Journal of Contaminant Hydrology 26, 97-108.

Park, C., Fenter, P.A., Sturchio, N.C., Nagy, K.L., 2008. Thermodynamics, Interfacial Structure, and pH Hysteresis of Rb+ and Sr2+ Adsorption at the Muscovite (001)-Solution Interface. Langmuir 24, 13993-14004.

Parkhurst, D.L., Thorstenson, D.C., Plummer, N., 1980, PHREEQE : a computer program for geochemical calculations, 80-96, USGS,

Parkhurst, D.L., Appelo, C.A.J., 2013, Description of input and examples for PHREEQC version 3: a computer program for speciation, batch-reaction, one-dimensional transport, and inverse geochemical calculations, 6-A43, USGS, Reston, VA.

Pearce, C.I., Rosso, K.M., Pattrick, R.A.D., Felmy, A.R., Ahmed, I.A.M., Hudson-Edwards, K.A., 2017. Impact of iron redox chemistry on nuclear waste disposal, Redox-reactive Minerals: Properties, Reactions and Applications in Clean Technologies. Mineralogical Society of Great Britain and Ireland, p. 0.

Pearce, C.I., Icenhower, J.P., Asmussen, R.M., Tratnyek, P.G., Rosso, K.M., Lukens, W.W., Qafoku, N.P., 2018. Technetium Stabilization in Low-Solubility Sulfide Phases: A Review. Acs Earth and Space Chemistry 2, 532-547.

Pearce, C.I., Moore, R.C., Morad, J.W., Asmussen, R.M., Chatterjee, S., Lawter, A.R., Levitskaia, T.G., Neeway, J.J., Qafoku, N.P., Rigali, M.J., Saslow, S.A., Szecsody, J.E., Thallapally, P.K., Wang, G.H., Freedman, V.L., 2020. Technetium immobilization by materials through sorption and redox-driven processes: A literature review. Science of the Total Environment 716.

Pentráková, L., Su, K., Pentrák, M., Stucki, J.W., 2013. A review of microbial redox interactions with structural Fe in clay minerals. Clay Minerals 48, 543-560.

Peretyazhko, T., Zachara, J.M., Heald, S.M., Jeon, B.H., Kukkadapu, R.K., Liu, C., Moore, D., Resch, C.T., 2008. Heterogeneous reduction of Tc(VII) by Fe(II) at the solid–water interface. Geochimica et Cosmochimica Acta 72, 1521-1539.

Peretyazhko, T.S., Zachara, J.M., Kukkadapu, R.K., Heald, S.M., Kutnyakov, I.V., Resch, C.T., Arey, B.W., Wang, C.M., Kovarik, L., Phillips, J.L., Moore, D.A., 2012. Pertechnetate ($TcO4^-$) reduction by reactive ferrous iron forms in naturally anoxic, redox transition zone sediments from the Hanford Site, USA. Geochimica et Cosmochimica Acta 92, 48-66.

Pidchenko, I., 2016. Characterization of structural properties of U and Pu in model systems by advanced synchrotron based X-ray spectroscopy. PhD thesis. KIT, Karlsruhe, Germany.

Pidchenko, I., Kvashnina, K.O., Yokosawa, T., Finck, N., Bahl, S., Schild, D., Polly, R., Bohnert, E., Rossberg, A., Gottlicher, J., Dardenne, K., Rothe, J., Schafer, T., Geckeis, H., Vitova, T., 2017. Uranium Redox Transformations after U(VI) Coprecipitation with Magnetite Nanoparticles. Environmental Science & Technology 51, 2217-2225.

Pina, C.M., Enders, M., Putnis, A., 2000. The composition of solid solutions crystallising from aqueous solutions: the influence of supersaturation and growth mechanisms. Chemical Geology 168, 195-210.

Plumper, O., Putnis, A., 2009. The Complex Hydrothermal History of Granitic Rocks: Multiple Feldspar Replacement Reactions under Subsolidus Conditions. Journal of Petrology 50, 967-987.

Poinssot, C., Baeyens, B., Bradbury, M.H., 1999. Experimental and modelling studies of caesium sorption on illite. Geochim. Cosmochim. Acta 63, 3217-3227.

Poonoosamy, J., Curti, E., Kosakowski, G., Grolimund, D., Van Loon, L.R., Mäder, U., 2016. Barite precipitation following celestite dissolution in a porous medium: A SEM/BSE and µ-XRD/XRF study. Geochimica et Cosmochimica Acta 182, 131-144.

Poonoosamy, J., Westerwalbesloh, C., Deissmann, G., Mahrous, M., Curti, E., Churakov, S.V., Klinkenberg, M., Kohlheyer, D., von Lieres, E., Bosbach, D., Prasianakis, N.I., 2019. A microfluidic experiment and pore scale modelling diagnostics for assessing mineral precipitation and dissolution in confined spaces. Chemical Geology 528, 119264-119264.

Poonoosamy, J., Klinkenberg, M., Deissmann, G., Brandt, F., Bosbach, D., Mäder, U., Kosakowski, G., 2020. Effects of solution supersaturation on barite precipitation in porous media and consequences on permeability: Experiments and modelling. Geochimica et Cosmochimica Acta 270, 43-60.

Porro, I., Newman, M.E., Dunnivant, F.M., 2000. Comparison of batch and column methods for determining strontium distribution coefficients for unsaturated transport in basalt. Environmental Science & Technology 34, 1679-1686.

POSIVA, 2012a, Safety case for the disposal of spent nuclear fuel at Olkiluoto Description of the disposal system 2012, POSIVA-12-5, POSIVA, Finland.

POSIVA, 2012b, Olkiluoto site description 2011, POSIVA-11-2, POSIVA, Finland.

Poteri, A., Billaux, D., Dershowitz, W., Gomez-Hernandez, J., Cvetkovic, V., Hautojaervi, A., Holton, D., Medina, A., 2002, Final report of the TRUE Block Scale project 3 Modelling of flow and transport, SKB-TR-02-15, SKB, Sweden.

Poteri, A., Nordman, H., Pulkkanen, V.M., Smith, P., 2014, Radionuclide transport in the repository near-field and far-field, POSIVA-14-02, POSIVA, Finland.

Poteri, A., Andersson, P., Nilsson, K., Byegård, J., Skålberg, M., Siitari-Kauppi, M.K., Helariutta, A.M.K., Voutilainen, M.A., Kekäläinen, P.J., 2018a, The Second Matrix Diffusion Experiment in the Water Phase of the Repro Project: WPDE 2, Posiva Working Report 2017-24, POSIVA, Finland.

Poteri, A., Andersson, P., Nilsson, K., Johan, B., Skålberg, M., Siitari-Kauppi, M.K., Au - Helariutta, A.M.K., Voutilainen, M.A., Kekäläinen, P.J., Ikonen, J.O., Sammaljärvi, J.K.W., Antero, L., Timonen, J., Kuva, J., Koskinen, L., 2018b, The First Matrix Diffusion Experiment in the Water Phase of the REPRO Project: WPDE 1, POSIVA Working Report 2017-23, POSIVA, Finland.

Powell, B.A., Fjeld, R.A., Kaplan, D.I., Coates, J.T., Serkiz, S.M., 2005. Pu(V)O2+ Adsorption and Reduction by Synthetic Hematite and Goethite. Environmental Science & Technology 39, 2107-2114.

Prasianakis, N.I., Curti, E., Kosakowski, G., Poonoosamy, J., Churakov, S.V., 2017. Deciphering pore-level precipitation mechanisms. Scientific Reports 7, 13765-13765.

Prieto, M., 2009. Thermodynamics of Solid Solution-Aqueous Solution Systems. Reviews in Mineralogy and Geochemistry 70, 47-85.

Prieto, M., 2014. Nucleation and supersaturation in porous media (revisited). Mineralogical Magazine 78, 1437-1447.

Prieto, M., Heberling, F., Rodríguez-Galán, R.M., Brandt, F., 2016. Crystallization behavior of solid solutions from aqueous solutions: An environmental perspective. Progress in Crystal Growth and Characterization of Materials 62, 29-68.

Prieur, D., Martel, L., Vigier, J.-F., Scheinost, A.C., Kvashnina, K.O., Somers, J., Martin, P.M., 2018. Aliovalent cation substitution in UO_2: Electronic and local structures of $U_{1-y}La_yO_{2\pm x}$ solid solutions. Inorg Chem 57, 1535-1544.

Puhakka, E., Li, X., Ikonen, J., Siitari-Kauppi, M., 2019. Sorption of selenium species onto phlogopite and calcite surfaces: DFT studies. Journal of Contaminant Hydrology 227.

Put, M., Monsecour, M., Foneyne, A., Yoshida, H., 1991. Estimation of the migration parameters for the Boom Clay formation by percolation experiments on undisturbed clay cores. Materials Research Society symposium proceedings 212, 823-829.

Putnis, A., Mauthe, G., 2001. The effect of pore size on cementation in porous rocks. Geofluids 1, 37-41.

Pyrak-Nolte, L.J., Nolte, D.D., 2016. Approaching a universal scaling relationship between fracture stiffness and fluid flow. Nature communications 7, 10663-10663.

Rasamimanana, S., Lefevre, G., Dagnelie, R.V.H., 2017. Various causes behind the desorption hysteresis of carboxylic acids on mudstones. Chemosphere 168, 559-567.

Richter, C., Müller, K., Drobot, B., Steudtner, R., Großmann, K., Stockmann, M., Brendler, V., 2016. Macroscopic and spectroscopic characterization of uranium(VI) sorption onto orthoclase and muscovite and the influence of competing Ca2+. Geochimica et Cosmochimica Acta 189, 143-157.

Roberts, H.E., Morris, K., Law, G.T.W., Mosselmans, J.F.W., Bots, P., Kvashnina, K., Shaw, S., 2017. Uranium(V) Incorporation Mechanisms and Stability in Fe(II)/Fe(III) (oxyhydr)Oxides. Environmental Science & Technology Letters 4, 421-426.

Roberts, H.E., Morris, K., Mosselmans, J.F.W., Law, G.T.W., Shaw, S., 2019. Neptunium Reactivity During Co-Precipitation and Oxidation of Fe(II)/Fe(III) (Oxyhydr)oxides. Geosciences 9, 27.

Robinet, J.C., Sardini, P., Coelho, D., Parneix, J.C., Pret, D., Sammartino, S., Boller, E., Altmann, S., 2012. Effects of mineral distribution at mesoscopic scale on solute diffusion in a clay-rich rock: Example of the Callovo-Oxfordian mudstone (Bure, France). Water Resour. Res. 48, 17.

Roden, E.E., 2003. Fe(III) Oxide Reactivity Toward Biological versus Chemical Reduction. Environmental Science & Technology 37, 1319-1324.

Rodriguez, D.M., Mayordomo, N., Scheinost, A.C., Schild, D., Brendler, V., Müller, K., Stumpf, T., 2020. New insights into 99Tc(VII) removal by pyrite: a spectroscopic approach. Environmental Science & Technology 54, 2678-2687.

Rojo, H., Scheinost, A.C., Lothenbach, B., Laube, A., Wieland, E., Tits, J., 2018. Retention of selenium by calcium aluminate hydrate (AFm) phases under strongly reducing radioactive waste repository conditions. Dalton Transactions 47, 4209-4218.

Romanchuk, A.Y., Kalmykov, S.N., Kersting, A.B., Zavarin, M., 2016. Behaviour of plutonium in the environment. Russ Chem Rev+ 85, 995-1010.

Roosz, C., Grangeon, S., Blanc, P., Montouillout, V., Lothenbach, B., Henocq, P., Giffaut, E., Vieillard, P., Gaboreau, S., 2015. Crystal structure of magnesium silicate hydrates (M-S-H): The relation with 2:1 Mg–Si phyllosilicates. Cement and Concrete Research 73, 228-237.

Rossberg, A., Reich, T., Bernhard, G., 2003. Complexation of uranium(VI) with protocatechuic acid - application of iterative transformation factor analysis to EXAFS spectroscopy. Analytical and Bioanalytical Chemistry 376, 631-638.

Rossberg, A., Scheinost, A.C., 2005. Three-dimensional modeling of EXAFS spectral mixtures by combining Monte Carlo simulations and target transformation factor analysis. Analytical and Bioanalytical Chemistry 383, 56-66.

Rossberg, A., Ulrich, K.-U., Weiss, S., Tsushima, S., Hiemstra, T., Scheinost, A.C., 2009. Identification of uranyl surface complexes on ferrihydrite: Advanced EXAFS data analysis and CD-MUSIC modeling. Environmental Science & Technology 43, 1400–1406.

Rossberg, A., Funke, H., 2010. Determining the radial pair distribution function from X-ray absorption spectra by use of the Landweber iteration method. Journal of Synchrotron Radiation 17, 280-288.

Rotenberg, B., Morel, J.-P., Marry, V., Turq, P., Morel-Desrosiers, N., 2009. On the driving force of cation exchange in clays: Insights from combined microcalorimetry experiments and molecular simulation. Geochimica Et Cosmochimica Acta 73, 4034-4044.

Rovira, M., De Pablo, J., El Amrani, S., Duro, L., Grivé, M., Bruno, J., 2003, Study of the role of magnetite in the immobilisation of U(VI) by reduction to U(IV) under the presence of H2(g) in hydrogen carbonate medium, SKB technical report 03-04, SKB, Sweden.

Salah, S., Bruggeman, C., Maes, N., 2017, Uranium retention and migration behaviour in Boom Clay, SCK-CEN-ER0410, SCK-CEN, Mol, Belgium.

Sammaljärvi, J., Jokelainen, L., Ikonen, J., Siitari-Kauppi, M., 2012. Free radical polymerisation of MMA with thermal initiator in brick and Grimsel granodiorite. Eng. Geol. 135-136, 52-59.

Sammaljärvi, J., Lindberg, A., Voutilainen, M., Ikonen, J., Siitari-Kauppi, M., Pitkänen, P., Koskinen, L., 2017. Multi-scale study of the mineral porosity of veined gneiss and pegmatitic granite from Olkiluoto, Western Finland. Journal of Radioanalytical and Nuclear Chemistry 314, 1557-1575.

Sanchez, F.G., Van Loon, L.R., Gimmi, T., Jakob, A., Glaus, M.A., Diamond, L.W., 2008. Self-diffusion of water and its dependence on temperature and ionic strength in highly compacted montmorillonite, illite and kaolinite. Applied Geochemistry 23, 3840-3851.

Sander, M., Hofstetter, T.B., Gorski, C.A., 2015. Electrochemical Analyses of Redox-Active Iron Minerals: A Review of Nonmediated and Mediated Approaches. Environmental Science & Technology 49, 5862-5878.

Sandström, B., Tullborg, E.-L., 2009. Episodic fluid migration in the Fennoscandian Shield recorded by stable isotopes, rare earth elements and fluid inclusions in fracture minerals at Forsmark, Sweden. Chemical Geology 266, 126-142.

Savoye, S., Michelot, J.L., Wittebroodt, C., 2006. Evaluation of the reversibility of iodide uptake by argillaceous rocks by the radial diffusion method. Radiochimica Acta 94, 699-704.

Savoye, S., Page, J., Puente, C., Imbert, C., Coelho, D., 2010. New Experimental Approach for Studying Diffusion through an Intact and Unsaturated Medium: A Case Study with Callovo-Oxfordian Argillite. Environmental Science & Technology 44, 3698-3704.

Savoye, S., Beaucaire, C., Fayette, A., Herbette, M., Coelho, D., 2012a. Mobility of Cesium through the Callovo-Oxfordian Claystones under Partially Saturated Conditions. Environmental Science & Technology 46, 2633-2641.

Savoye, S., Frasca, B., Grenut, B., Fayette, A., 2012b. How mobile is iodide in the Callovo-Oxfordian claystones under experimental conditions close to the in situ ones? J Contam Hydrol 142-143, 82-92.

Savoye, S., Michelot, J.L., Matray, J.M., Wittebroodt, C., Mifsud, A., 2012c. A laboratory experiment for determining both the hydraulic and diffusive properties and the initial pore-water composition of an argillaceous rock sample: A test with the Opalinus clay (Mont Terri, Switzerland). Journal of Contaminant Hydrology 128, 47-57.

Savoye, S., Lacour, J.L., Fayette, A., Beaucaire, C., 2013. Mobility of Zinc in the Callovo-Oxfordian Claystone. Procedia Earth and Planetary Science 7, 774-777.

Savoye, S., Imbert, C., Fayette, A., Coelho, D., 2014. Experimental study on diffusion of tritiated water and anions under variable water-saturation and clay mineral content: comparison with the Callovo-

Oxfordian claystones, in: Norris, S., Bruno, J., Cathelineau, M., Delage, P., Fairhurst, C., Gaucher, E.C., Hohn, E.H., Kalinichev, A., Lalieux, P., Sellin, P. (Eds.), Clays in Natural and Engineered Barriers for Radioactive Waste Confinement. Geological Soc Publishing House, Bath, pp. 579-588.

Savoye, S., Beaucaire, C., Grenut, B., Fayette, A., 2015. Impact of the solution ionic strength on strontium diffusion through the Callovo-Oxfordian clayrocks: An experimental and modeling study. Applied Geochemistry 61, 41-52.

Savoye, S., Lefevre, S., Fayette, A., Robinet, J.-C., 2017. Effect of Water Saturation on the Diffusion/Adsorption of 22Na and Cesium onto the Callovo-Oxfordian Claystones. Geofluids 2017, 1-17.

Schaefer, M.V., Gorski, C.A., Scherer, M.M., 2011. Spectroscopic Evidence for Interfacial Fe(II)-Fe(III) Electron Transfer in a Clay Mineral. Environmental Science & Technology 45, 540-545.

Schecher, W.D., McAvoy, D.C., 1992. MINEQL+: A software environment for chemical equilibrium modeling. Computers, Environment and Urban Systems 16, 65-76.

Scheidegger, A., C.S., B., Borkovec, M., Sticher, H., Meeussen, J.C.L., van Riemsdijk, W., 1994. Convective transport of acids and bases in porous media. Water Resour. Res. 30, 2937-2944.

Scheidegger, A.M., Lamble, G.M., Sparks, D.L., 1997. Spectroscopic evidence for the formation of mixed-cation hydroxide phases upon metal sorption on clays and aluminum oxides. Journal of Colloid and Interface Science 186, 118-128.

Scheidegger, A.M., Strawn, D.G., Lamble, G.M., Sparks, D.L., 1998. The kinetics of mixed Ni-Al hydroxide formation on clay and aluminum oxide minerals: A time-resolved XAFS study. Geochimica et Cosmochimica Acta 62, 2233-2245.

Scheinost, A.C., Charlet, L., 2008. Selenite reduction by mackinawite, magnetite and siderite: XAS characterization of nanosized redox products. Environmental Science & Technology 42, 1984-1989.

Scheinost, A.C., Kirsch, R., Banerjee, D., Fernandez-Martinez, A., Zaenker, H., Funke, H., Charlet, L., 2008. X-ray absorption and photoelectron spectroscopy investigation of selenite reduction by Fe-II-bearing minerals. Journal of Contaminant Hydrology 102, 228-245.

Scheinost, A.C., Steudtner, R., Hübner, R., Weiss, S., Bok, F., 2016. Neptunium^{V} retention by siderite under anoxic conditions: Precipitation of NpO_2−like nanoparticles and of Np^{IV} pentacarbonate. Environmental Science & Technology 50, 10413-10420.

Schlegel, M.L., Manceau, A., Charlet, L., Chateigner, D., Hazemann, J.L., 2001a. Sorption of metal ions an clay minerals. 3. Nucleation and epitaxial growth of Zn phyllosilicate on the edges of hectorite. Geochimica et Cosmochimica Acta 65, 4155-4170.

Schlegel, M.L., Manceau, A., Charlet, L., Hazemann, J.L., 2001b. Adsorption mechanisms of Zn on hectorite as a function of time, pH, and ionic strength. American Journal of Science 301, 798-830.

Schlegel, M.L., Bataillon, C., Blanc, C., Pret, D., Foy, E., 2010. Anodic activation of iron corrosion in clay media under water-saturated conditions at 90 degrees C: Characterization of the corrosion interface. Environmental Science & Technology 44, 1503-1508.

Schlegel, M.L., Bataillon, C., Brucker, F., Blanc, C., Pret, D., Foy, E., Chorro, M., 2014. Corrosion of metal iron in contact with anoxic clay at 90 degrees C: Characterization of the corrosion products after two years of interaction. Applied Geochemistry 51, 1-14.

Schliemann, R., Churakov, S.V., 2021. Atomic scale mechanism of clay minerals dissolution revealed by ab initio simulations. Geochimica et Cosmochimica Acta 293, 438-460.

Schulthess, C., Sparks, D., 1986. Backtitration Technique for Proton Isotherm Modeling of Oxide Surfaces 1. Soil Science Society of America Journal 50, 1406-1411.

Schüring, J., 2000. Redox : fundamentals, processes, and applications. Springer, Berlin.

Schwantes, J.M., Santschi, P.H., 2010. Mechanisms of plutonium sorption to mineral oxide surfaces: new insights with implications for colloid-enhanced migration. Radiochimica Acta 98, 737-742.

Seabaugh, J.L., Dong, H., Kukkadapu, R.K., Eberl, D.D., Morton, J.P., Kim, J., 2006. Microbial reduction of Fe(III) in the Fithian and Muloorina illites: Contrasting extents and rates of bioreduction. Clays and Clay Minerals 54, 67-79.

Shackelford, C.D., 1991. Laboratory diffusion testing for waste disposal - A review. Journal of Contaminant Hydrology 7, 177-217.

Shackelford, C.D., Daniel, D.E., 1991. Diffusion in Saturated Soil .1. Background. Journal of Geotechnical Engineering-Asce 117, 467-484.

Shackelford, C.D., Moore, S.M., 2013. Fickian diffusion of radionuclides for engineered containment barriers: Diffusion coefficients, porosities, and complicating issues. Eng. Geol. 152, 133-147.

Shahkarami, P., Liu, L., Moreno, L., Neretnieks, I., 2016. The effect of stagnant water zones on retarding radionuclide transport in fractured rocks: An extension to the Channel Network Model. Journal of Hydrology 540, 1122-1135.

Singhal, J., Kumar, D., 1975. Thermodynamics of ion exchange equilibria involving Fe2+ ion on Na+-montmorillonite.

Sinitsyn, V., Aja, S., Kulik, D., Wood, S., 2000. Acid–base surface chemistry and sorption of some lanthanides on K+-saturated Marblehead illite: I. Results of an experimental investigation. Geochimica et Cosmochimica Acta 64, 185-194.

SKB, 2011, Long-term safety for the final repository for spent nuclear fuel at Forsmark Main report of the SR-Site project, SKB-TR-11-01, SKB, Sweden.

Smellie, J., Pitkänene, P., Koskinen, L., Aaltonen, I., Eichinger, F., Waber, N., Sahlstedt, E., Siitari-Kauppi, M., Karhu, J., Löfman, J., Poteri, J., 2014, Evolution of Olkiluoto Site: Paleohydrogeochemical Considerations, Posiva Working Report 2014-17, POSIVA, Finland.

Smith, P., Hadermann, J., Bischoff, K., 1991. Dual-porosity modelling of infiltration experiments on fractured granite, Safety Assessment of Radioactive Waste Repositories.

Smith, P.A., Alexander, W.R., Heer, W., Fierz, T., Meier, P.M., Bayerns, B., Bradbury, M.H., Mazurek, M., McKinley, I.G., 2001, Grimsel Test Site – Investigation Phase IV (1994-1996): The Nagra-JAEA in situ study of safety relevant radionuclide retardation in fractured crystalline rock I: Radionuclide migration experiment – Overview 1990 – 1996, NAGRA Technical Report NTB 00-09; Wettingen, Switzerland.

Soler, J.M., Landa, J., Havlova, V., Tachi, Y., Ebina, T., Sardini, P., Siitari-Kauppi, M., Eikenberg, J., Martin, A., 2015. Comparative modeling of an in situ diffusion experiment in granite at the Grimsel Test Site. Journal of Contaminant Hydrology 179.

Soler, J.M., 2016. Two-dimensional reactive transport modeling of the alteration of a fractured limestone by hyperalkaline solutions at Maqarin (Jordan). Applied Geochemistry 66, 162-173.

Soler, J.M., Steefel, C.I., Gimmi, T., Leupin, O.X., Cloet, V., 2019. Modeling the Ionic Strength Effect on Diffusion in Clay. The DR-A Experiment at Mont Terri. ACS Earth and Space Chemistry 3, 442-451.

Soltermann, D., Fernandes, M.M., Baeyens, B., Dähn, R., Miehé-Brendlé, J., Wehrli, B., Bradbury, M.H., 2013a. Fe(II) Sorption on a Synthetic Montmorillonite. A Combined Macroscopic and Spectroscopic Study. Environmental Science & Technology 47, 6978-6986.

Soltermann, D., Marques, M.F., Baeyens, B., Dähn, R., Brendlé, J.M., Wehrli, B., Bradbury, M.H., 2013b. Fe(II) sorption on a synthetic clay mineral without structural Fe. A wet chemistry and spectroscopic study. Environmental Science & Technology 47, 6978-6986.

Soltermann, D., 2014. Ferrous Iron Uptake Mechanisms at the Montmorillonite-Water Interface under Anoxic and Electrochemically Reduced Conditions. PhD thesis. ETH-Zürich.

Soltermann, D., Baeyens, B., Bradbury, M.H., Fernandes, M.M., 2014a. Fe(II) Uptake on Natural Montmorillonites. II. Surface Complexation Modeling. Environmental Science & Technology 48, 8698-8705.

Soltermann, D., Marques, M.F., Baeyens, B., Brendlé, J.M., Dähn, R., 2014b. Competitive Fe(II)–Zn(II) uptake on a synthetic montmorillonite. Environmental Science & Technology 48, 190-198.

Soltermann, D., Marques, M.F., Baeyens, B., Dähn, R., Joshi, P.A., Scheinost, A.C., Gorski, A., 2014c. Fe(II) uptake on natural montmorillonites. I. Macroscopic and spectroscopic characterization. Environmental Science & Technology 48, 8688–8697.

Sparks, D.L., 2003. Environmental soil chemistry. Elsevier.

Sposito, G., 1984. The Surface Chemistry of Soils. Oxford University Press, New York.

Stack, A.G., Fernandez-Martinez, A., Allard, L.F., Bañuelos, J.L., Rother, G., Anovitz, L.M., Cole, D.R., Waychunas, G.A., 2014. Pore-Size-Dependent Calcium Carbonate Precipitation Controlled by Surface Chemistry. Environmental Science & Technology 48, 6177-6183.

Stack, A.G., 2015. Precipitation in Pores: A Geochemical Frontier. Reviews in Mineralogy and Geochemistry 80, 165-190.

Stamberg, K., Palagyi, S., Videnska, K., Havlova, V., 2014. Interaction of H-3(+) (as HTO) and Cl-36(-) (as (NaCl)-Cl-36) with crushed granite and corresponding fracture infill material investigated in column experiments. Journal of Radioanalytical and Nuclear Chemistry 299, 1625-1633.

Stanfors, R., Rhén, I., Tullborg, E.-L., Wikberg, P., 1999. Overview of geological and hydrogeological conditions of the Äspö hard rock laboratory site. Applied Geochemistry 14, 819-834.

Steefel, C., Depaolo, D., Lichtner, P., 2005. Reactive transport modeling: An essential tool and a new research approach for the Earth sciences. Earth and Planetary Science Letters 240, 539-558.

Steefel, C.I., Lasaga, A.C., 1994. A coupled model for transport of multiple chemical species and kinetic precipitation/dissolution reactions with application to reactive flow in single phase hydrothermal systems. American Journal of Science 294, 529-592.

Steefel, C.I., Appelo, C.A.J., Arora, B., Jacques, D., Kalbacher, T., Kolditz, O., Lagneau, V., Lichtner, P.C., Mayer, K.U., Meeussen, J.C.L., Molins, S., Moulton, D., Shao, H., Šimůnek, J., Spycher, N., Yabusaki, S.B., Yeh, G.T., 2014. Reactive transport codes for subsurface environmental simulation. Computational Geosciences 19, 445-478.

Stober, I., Bucher, K., 2014. Hydraulic conductivity of fractured upper crust: insights from hydraulic tests in boreholes and fluid-rock interaction in crystalline basement rocks. Geofluids 15, 161-178.

Stockmann, M., Schikora, J., Becker, D.A., Flügge, J., Noseck, U., Brendler, V., 2017. Smart Kd-values, their uncertainties and sensitivities - Applying a new approach for realistic distribution coefficients in geochemical modeling of complex systems. Chemosphere 187, 277-285.

Stolze, L., Wagner, J.B., Damsgaard, C.D., Rolle, M., 2020. Impact of surface complexation and electrostatic interactions on pH front propagation in silica porous media. Geochimica et Cosmochimica Acta 277, 132-149.

Strawn, D.G., Sparks, D.L., 1999. The use of XAFS to distinguish between inner- and outer-sphere lead adsorption complexes on montmorillonite. Journal of Colloid and Interface Science 216, 257-269.

Stucki, J.W., 2011. A review of the effects of iron redox cycles on smectite properties. Comptes Rendus Geoscience 343, 199-209.

Stumm, W., Sulzberger, B., 1992. The cycling of iron in natural environments: Considerations based on laboratory studies of heterogeneous redox processes. Geochimica et Cosmochimica Acta 56, 3233-3257.

Suter, D., 1991, Chemistry of the redox sensitive elements Literature review, NAGRA NTB-91-32, Switzerland.

Suzuki, S., Sato, H., Tachi, Y., 2003. A Technical Problem in the Through-Diffusion Experiments for Compacted Bentonite. Journal of Nuclear Science and Technology 40, 698-701.

Svecova, L., Cremel, S., Sirguey, C., Simonnot, M.-O., Sardin, M., Dossot, M., Mercier-Bion, F., 2008. Comparison between batch and column experiments to determine the surface charge properties of rutile TiO2 powder. Journal of Colloid and Interface Science 325, 363-370.

Svensson, U., Voutilainen, M., Muuri, E., Ferry, M., Gylling, B., 2019. Modelling transport of reactive tracers in a heterogeneous crystalline rock matrix. J Contam Hydrol 227, 103552.

Tachi, Y., Yotsuji, K., 2014. Diffusion and sorption of Cs+, Na+, I− and HTO in compacted sodium montmorillonite as a function of porewater salinity: Integrated sorption and diffusion model. Geochimica et Cosmochimica Acta 132, 75-93.

Tachi, Y., Ebina, T., Takeda, C., Saito, T., Takahashi, H., Ohuchi, Y., Martin, A.J., 2015. Matrix diffusion and sorption of Cs+, Na+, I– and HTO in granodiorite: Laboratory-scale results and their extrapolation to the in situ condition. Journal of Contaminant Hydrology 179, 10-24.

Takeda, M., Nakajima, H., Zhang, M., Hiratsuka, T., 2008a. Laboratory longitudinal diffusion tests: 1. Dimensionless formulations and validity of simplified solutions. J Contam Hydrol 97, 117-134.

Takeda, M., Zhang, M., Nakajima, H., Hiratsuka, T., 2008b. Laboratory longitudinal diffusion tests: 2. Parameter estimation by inverse analysis. J Contam Hydrol 97, 100-116.

Tanaka, S., Noda, N., Sato, S., Kozaki, T., Sato, H., Hatanaka, K., 2011. Electrokinetic Study of Migration of Anions, Cations, and Water in Water-Saturated Compacted Sodium Montmorillonite. Journal of Nuclear Science and Technology 48, 454-462.

Tazi, S., Rotenberg, B., Salanne, M., Sprik, M., Sulpizi, M., 2012. Absolute acidity of clay edge sites from ab-initio simulations. Geochimica et Cosmochimica Acta 94, 1-11.

Tesson, S., Salanne, M., Rotenberg, B., Tazi, S., Marry, V., 2016. Classical Polarizable Force Field for Clays: Pyrophyllite and Talc. J. Phys. Chem. C 120, 3749-3758.

Thompson, H.A., Parks, G.A., Brown Jr., G.E., 1999a. Ambient-temperature synthesis, evolution, and characterization of cobalt-aluminum hydrotalcite-like solids. Clays and Clay Minerals 47, 425-438.

Thompson, H.A., Parks, G.A., Brown Jr., G.E., 1999b. Dynamic interactions of dissolution, surface adsorption, and precipitation in an aging cobalt(II)-clay-water system. Geochimica et Cosmochimica Acta 63, 1767-1779.

Tinnacher, R.M., Holmboe, M., Tournassat, C., Bourg, I.C., Davis, J.A., 2016. Ion adsorption and diffusion in smectite: Molecular, pore, and continuum scale views. Geochimica Et Cosmochimica Acta 177, 130-149.

Tournassat, C., Ferrage, E., Poinsignon, C., Charlet, L., 2004a. The titration of clay minerals: II. Structure-based model and implications for clay reactivity. Journal of Colloid and Interface Science 273, 234-246.

Tournassat, C., Greneche, J.-M., Tisserand, D., Charlet, L., 2004b. The titration of clay minerals: I. Discontinuous backtitration technique combined with CEC measurements. Journal of colloid and interface science 273, 224-233.

Tournassat, C., Gailhanou, H., Crouzet, C., Braibant, G., Gautier, A., Lassin, A., Blanc, P., Gaucher, E.C., 2007. Two cation exchange models for direct and inverse modelling of solution major cation composition in equilibrium with illite surfaces. Geochimica et Cosmochimica Acta 71, 1098-1114.

Tournassat, C., Lerouge, C., Blanc, P., Brendlé, J., Greneche, J.-M., Touzelet, S., Gaucher, E.C., 2008. Cation exchanged Fe (II) and Sr compared to other divalent cations (Ca, Mg) in the bure Callovian–Oxfordian formation: implications for porewater composition modelling. Applied Geochemistry 23, 641-654.

Tournassat, C., Gailhanou, H., Crouzet, C., Braibant, G., Gautier, A., Gaucher, E.C., 2009. Cation exchange selectivity coefficient values on smectite and mixed-layer illite/smectite minerals. Soil Science Society of America Journal 73, 928-942.

Tournassat, C., Appelo, C.A.J., 2011. Modelling approaches for anion-exclusion in compacted Na-bentonite. Geochimica Et Cosmochimica Acta 75, 3698-3710.

Tournassat, C., Bizi, M., Braibant, G., Crouzet, C., 2011. Influence of montmorillonite tactoid size on Na–Ca cation exchange reactions. Journal of Colloid and Interface Science 364, 443-454.

Tournassat, C., grangeon, S., Leroy, P., Giffaut, E., 2013. modeling specific pH dependent sorption of divalent metals on montmorillonite surfaces. A review of pitfalls, recent achievements and current challenges. American Journal of Science 313, 385-451.

Tournassat, C., Bourg, I.C., Steefel, C.I., Bergaya, F., 2015. Chapter 1 - Surface Properties of Clay Minerals, in: Tournassat, C., Steefel, C.I., Bourg, I.C., Bergaya, F. (Eds.), Developments in Clay Science. Elsevier, pp. 5-31.

Tournassat, C., Steefel, C.I., 2015. Ionic Transport in Nano-Porous Clays with Consideration of Electrostatic Effects. Reviews in Mineralogy and Geochemistry 80, 287-329.

Tournassat, C., Bourg, I.C., Holmboe, M., Sposito, G., Steefel, C.I., 2016a. MOLECULAR DYNAMICS SIMULATIONS OF ANION EXCLUSION IN CLAY INTERLAYER NANOPORES. Clays and Clay Minerals 64, 374-388.

Tournassat, C., Davis, J.A., Chiaberge, C., Grangeon, S., Bourg, I.C., 2016b. Modeling the acid–base properties of montmorillonite edge surfaces. Environmental science & technology 50, 13436-13445.

Tournassat, C., Tinnacher, R.M., Grangeon, S., Davis, J.A., 2018. Modeling uranium (VI) adsorption onto montmorillonite under varying carbonate concentrations: A surface complexation model accounting for the spillover effect on surface potential. Geochimica et Cosmochimica Acta 220, 291-308.

Towle, S.N., Bargar, J.R., Brown Jr., G.E., Parks, G.A., 1997. Surface precipitations of Co(II) on Al_2O_3. Journal of Colloid and Interface Science 187, 62-82.

Tsang, Y.W., 1984. The Effect of Tortuosity on Fluid Flow Through a Single Fracture. Water Resour. Res. 20, 1209-1215.

Tsang, Y.W., Tsang, C.F., 1987. Channel model of flow through fractured media. Water Resour. Res. 23, 467-479.

Tsang, Y.W., 1992. Usage of “Equivalent apertures” for rock fractures as derived from hydraulic and tracer tests. Water Resour. Res. 28, 1451-1455.

Tsarev, S., Waite, T.D., Collins, R.N., 2016. Uranium Reduction by Fe(II) in the Presence of Montmorillonite and Nontronite. Environmental Science & Technology 50, 8223-8230.

Turner, D.R., Pabalan, R.T., Bertetti, F.P., 1998. Neptunium (V) sorption on montmorillonite: An experimental and surface complexation modeling study. Clays and Clay Minerals 46, 256-269.

Tyagi, M., Gimmi, T., Churakov, S.V., 2013. Multi-scale micro-structure generation strategy for up-scaling transport in clays. Advances in Water Resources 59, 181-195.

Um, W., Chang, H.S., Icenhower, J.P., Lukens, W.W., Serne, R.J., Qafoku, N.P., Westsik, J.H., Buck, E.C., Smith, S.C., 2011. Immobilization of 99-technetium (VII) by Fe(II)-goethite and limited reoxidation. Environmental Science & Technology 45, 4904-4913.

Um, W., Luksic, S.A., Wang, G.H., Saslow, S., Kim, D.S., Schweiger, M.J., Soderquist, C.Z., Bowden, M.E., Lukens, W.W., Kruger, A.A., 2017. Enhanced Tc-99 retention in glass waste form using Tc(IV)-incorporated Fe minerals. Journal of Nuclear Materials 495, 455-462.

Underwood, T.R., Bourg, I.C., 2020. Large-Scale Molecular Dynamics Simulation of the Dehydration of a Suspension of Smectite Clay Nanoparticles. The Journal of Physical Chemistry C 124, 3702-3714.

Van der Lee, J., de Windt, L., 2002. CHESS Tutorial and Cookbook. Update for Version 3. User Manual, Fontainebleu, France.

Van Laer, L., Durce, D., Salah, S., Maes, N., 2016, Sorption studies on Boom Clay and Clay minerals - status 2016, SCK-CEN-ER0346, SCK-CEN, Mol, Belgium.

Van Laer, L., 2018, Long-term laboratory and in-situ migration experiments in Boom Clay - status 2017, SCK-CEN-ER0390, SCK-CEN, Mol, Belgium.

Van Loon, L., Glaus, M., Ferry, C., Latrille, C., 2012. Studying radionuclide migration on different scales: the complementary roles of laboratory and in situ experiments, Radionuclide Behaviour in the Natural Environment, pp. 446-483.

Van Loon, L., 2014, Effective diffusion coefficients and porosity values for argillacous rocks and bentonite: measured and estimated values for the provisional safety analysis for SGT-02, NAGRA NTB 12-03, NAGRA, Switzerland.

Van Loon, L.R., Soler, J.M., Jakob, A., Bradbury, M.H., 2003. Effect of confining pressure on the diffusion of HTO, Cl-36 (-) and I-125 (-) in a layered argillaceous rock (Opalinus Clay): diffusion perpendicular to the fabric. Applied Geochemistry 18, 1653-1662.

Van Loon, L.R., Soler, J.M., Muller, W., Bradbury, M.H., 2004a. Anisotropic diffusion in layered argillaceous rocks: A case study with opalinus clay. Environmental Science & Technology 38, 5721-5728.

Van Loon, L.R., Wersin, P., Soler, J.M., Eikenberg, J., Gimmi, T., Hernan, P., Dewonck, S., Savoye, S., 2004b. In-situ diffusion of HTO, Na-22 (+), Cs+ and I- in Opalinus Clay at the Mont Terri underground rock laboratory. Radiochimica Acta 92, 757-763.

Van Loon, L.R., Baeyens, B., Bradbury, M.H., 2005a. Diffusion and retention of sodium and strontium in Opalinus clay: Comparison of sorption data from diffusion and batch sorption measurements, and geochemical calculations. Applied Geochemistry 20, 2351-2363.

Van Loon, L.R., Eikenberg, J., 2005. A high-resolution abrasive method for determining diffusion profiles of sorbing radionuclides in dense argillaceous rocks. Appl Radiat Isot 63, 11-21.

Van Loon, L.R., Jakob, A., 2005. Evidence for a second transport porosity for the diffusion of tritiated water (HTO) in a sedimentary rock (Opalinus clay-OPA): Application of through- and out-diffusion techniques. Transport in Porous Media 61, 193-214.

Van Loon, L.R., Muller, W., Iijima, K., 2005b. Activation energies of the self-diffusion of HTO, Na-22 (+) and Cl-36 (-) in a highly compacted argillaceous rock (Opalinus Clay). Applied Geochemistry 20, 961-972.

Van Loon, L.R., Glaus, M.A., Muller, W., 2007. Anion exclusion effects in compacted bentonites: Towards a better understanding of anion diffusion. Applied Geochemistry 22, 2536-2552.

Van Loon, L.R., Muller, W., 2014. A modified version of the combined in-diffusion/abrasive peeling technique for measuring diffusion of strongly sorbing radionuclides in argillaceous rocks: a test study on the diffusion of caesium in Opalinus Clay. Appl Radiat Isot, 197-202.

Van Loon, L.R., Mibus, J., 2015. A modified version of Archie's law to estimate effective diffusion coefficients of radionuclides in argillaceous rocks and its application in safety analysis studies. Applied Geochemistry 59, 85-94.

Van Loon, L.R., Leupin, O.X., Cloet, V., 2018. The diffusion of SO42− in Opalinus Clay: Measurements of effective diffusion coefficients and evaluation of their importance in view of microbial mediated reactions in the near field of radioactive waste repositories. Applied Geochemistry 95, 19-24.

Van Olphen, H., 1963. An introduction to clay colloid chemistry. Interscience, New York-London.

van Schaik, J.C., Kemper, W.D., Olsen, S.R., 1966. Contribution of Adsorbed Cations to Diffusion in Clay-Water Systems. Soil Science Society of America 30, 17-22.

Vanselow, A.P., 1932. Equilibria of the base-exchange reactions of bentonites, permutites, soil colloids, and zeolites. Soil Science 33, 95-114.

Velde, B.B., Meunier, A., 2008. The Origin of Clay Minerals in Soils and Weathered Rocks. Springer Berlin Heidelberg.

Vespa, M., Manceau, A., Lanson, M., 2010. Natural attenuation of zinc pollution in smelter-affected soil. Environmental Science & Technology 44, 7814-7820.

Videnska, K., Gondolli, J., Stamberg, K., Havlova, V., 2015. Retention of selenium and caesium on crystalline rock: the effect of redox conditions and mineralogical composition. Journal of Radioanalytical and Nuclear Chemistry 304, 417-423.

Videnská, K., Palágyi, Š., Štamberg, K., Vodičková, H., Havlova, V., 2013. Effect of grain size on the sorption and desorption of SeO4 2− and SeO3 2− in columns of crushed granite and fracture infill from granitic water under dynamic conditions. Journal of Radioanalytical and Nuclear Chemistry 298, 547-554.

Vinograd, V.L., Brandt, F., Rozov, K., Klinkenberg, M., Refson, K., Winkler, B., Bosbach, D., 2013. Solid-aqueous equilibrium in the BaSO4-RaSO4-H2O system: First-principles calculations and a thermodynamic assessment. Geochimica et Cosmochimica Acta 122, 398-417.

Vinograd, V.L., Kulik, D.A., Brandt, F., Klinkenberg, M., Weber, J., Winkler, B., Bosbach, D., 2018. Thermodynamics of the solid solution - Aqueous solution system (Ba,Sr,Ra)SO4 + H2O: I. The effect of strontium content on radium uptake by barite. Applied Geochemistry 89, 59-74.

Vitova, T., Denecke, M.A., Gottlicher, J., Jorissen, K., Kas, J.J., Kvashnina, K., Prussmann, T., Rehr, J.J., Rothe, J., 2013. Actinide and lanthanide speciation with high-energy resolution X-ray techniques. J Phys Conf Ser 430.

Vitova, T., Pidchenko, I., Fellhauer, D., Bagus, P.S., Joly, Y., Pruessmann, T., Bahl, S., Gonzalez-Robles, E., Rothe, J., Altmaier, M., Denecke, M.A., Geckeis, H., 2017. The role of the 5f valence orbitals of early actinides in chemical bonding. Nature Communications 8, 1-9.

Voigt, W., Brendler, V., Marsh, K., Rarey, R., Wanner, H., Gaune-Escard, M., Cloke, P., Vercouter, T., Bastrakov, E., Hagemann, S., 2007. Quality assurance in thermodynamic databases for performance assessment studies in waste disposal. Pure and Applied Chemistry 79, 883-894.

Voutilainen, M., Kekäläinen, P., Siitari-Kauppi, M., Sardini, P., Muuri, E., Timonen, J., Martin, A., 2017. Modeling Transport of Cesium in Grimsel Granodiorite With Micrometer Scale Heterogeneities and Dynamic Update of Kd. Water Resour. Res. 53, 9245-9265.

Voutilainen, M., Kekäläinen, P., Poteri, A., Siitari-Kauppi, M., Helariutta, K., Andersson, P., Nilsson, K., Byegård, J., Skålberg, M., Yli-Kaila, M., Koskinen, L., 2019. Comparison of water phase diffusion experiments in laboratory and in situ conditions. Journal of Hydrology 575, 716-729.

Wang, H.A.O., Grolimund, D., Van Loon, L.R., Barmettler, K., Borca, C.N., Aeschimann, B., Gunther, D., 2011. Quantitative Chemical Imaging of Element Diffusion into Heterogeneous Media Using Laser Ablation Inductively Coupled Plasma Mass Spectrometry, Synchrotron Micro-X-ray Fluorescence, and Extended X-ray Absorption Fine Structure Spectroscopy. Analytical Chemistry 83, 6259-6266.

Wang, H.A.O., Grolimund, D., Giesen, C., Borca, C.N., Shaw-Stewart, J.R.H., Bodenmiller, B., Gunther, D., 2013. Fast Chemical Imaging at High Spatial Resolution by Laser Ablation Inductively Coupled Plasma Mass Spectrometry. Analytical Chemistry 85, 10107-10116.

Wang, L., Jacques, D., De Canniere, P., 2007, Effects of an alkaline plume on the Boom Clay as a otential host formation for geological disposal of radioactive waste. First full draft - v1.0, SCK-CEN-ER-28, SCK-CEN, Mol, Belgium.

Wang, L., Salah, S., De Soete, H., 2020a, MOLDATA: A thermochemical data base for phenomenological and safety assessment studies for disposal of radioactive waste in Belgium – Data Compilation Strateg, SCK-CEN-ER-820, SCK-CEN, Mol, Belgium.

Wang, L., Salah, S., De Soete, H., 2020b, MOLDATA: A thermochemical data base for phenomenological and safety assessment studies for disposal of radioactive waste in Belgium – Selected data and argumentations Release 2.0, SCK-CEN-ER-813, SCK-CEN, Mol, Belgium.

Wanner, H., Albinsson, Y., Karnland, O., Wieland, E., Charlet, L., Wersin, P., 1994. The acid/base chemistry of montmorillonite. Radiochimica Acta 66, 157-162.

Weaver, C.E., 1989. Clays, Muds, and Shales. Elsevier Science.

Weber, J., Barthel, J., Klinkenberg, M., Bosbach, D., Kruth, M., Brandt, F., 2017. Retention of 226Ra by barite: The role of internal porosity. Chemical Geology 466, 722-732.

Weetjens, E., Govaerts, J., Aertsens, M., 2011, Model and parameter validation based on in situ experiments in Boom Clay, SCK-CEN-ER-171, SCK-CEN, Mol, Belgium.

Weetjens, E., Maes, N., Van Ravestyn, L., 2014. Model validation based on in situ radionuclide migration tests in Boom Clay: status of a large-scale migration experiment, 24 years after injection. Geological Society, London, Special Publications 400, 613-623.

Wersin, P., 2017, Topics and processes dealt with in the IP FUNMIG and their treatment in the Safety Case of geologic repositories for radioactive waste, NAGRA Technical Report NTB 09-01; Wettingen, Switzerland.

Westall, J., Hohl, H., 1980. Comparison of electrostatic models for the oxide-solution interface. Advances in Colloid and Interface Science 12, 265-294.

Westall, J.C., Zachary, J.L., Morel, F., Massachusetts Institute of, T., Department of Civil, E., Ralph, M.P.L.f.W.R., Hydrodynamics, Massachusetts Institute of, T., Water Quality, L., 1976. MINEQL : a computer program for the calculation of chemical equilibrium composition of aqueous systems. Water Quality Laboratory, Ralph M. Parsons Laboratory for Water Resources and Environmental Engineering [sic], Dept. of Civil Engineering, Massachusetts Institute of Technology, Cambridge, Mass.

Wharton, M.J., Atkins, B., Charnock, J.M., Livens, F.R., Pattrick, R.A.D., Collison, D., 2000. An X-ray absorption spectroscopy study of the coprecipitation of Tc and Re with mackinawite (FeS). Applied Geochemistry 15, 347-354.

Wick, S., Baeyens, B., Fernandes, M.M., Voegelin, A., 2018. Thallium Adsorption onto Illite. Environmental Science & Technology 52, 571-580.

Wigger, C., Van Loon, L.R., 2017. Importance of Interlayer Equivalent Pores for Anion Diffusion in Clay-Rich Sedimentary Rocks. Environ Sci Technol 51, 1998-2006.

Wigger, C., Kennell-Morrison, L., Jensen, M., Glaus, M., Van Loon, L., 2018. A comparative anion diffusion study on different argillaceous, low permeability sedimentary rocks with various pore waters. Applied Geochemistry 92, 157-165.

Winkel, L.H.E., Johnson, C.A., Lenz, M., Grundl, T., Leupin, O.X., Amini, M., Charlet, L., 2012. Environmental Selenium Research: From Microscopic Processes to Global Understanding. Environmental Science & Technology 46, 571-579.

Wittebroodt, C., Savoye, S., Frasca, B., Gouze, P., Michelot, J.L., 2012. Diffusion of HTO, Cl-36 (-) and I-125 (-) in Upper Toarcian argillite samples from Tournemire: Effects of initial iodide concentration and ionic strength. Applied Geochemistry 27, 1432-1441.

Wolery, T.J., Daveler, S.A., 1992, EQ6, a computer program for reaction path modeling of aqueous geochemical systems: Theoretical manual, user`s guide, and related documentation (Version 7.0); Part 4, United States.

Wu, T., Amayri, S., Drebert, J., Van Loon, L.R., Reich, T., 2009. Neptunium (V) Sorption and Diffusion in Opalinus Clay. Environmental Science & Technology 43, 6567-6571.

Wylie, E.M., Olive, D.T., Powell, B.A., 2016. Effects of Titanium Doping in Titanomagnetite on Neptunium Sorption and Speciation. Environmental Science & Technology 50, 1853-1858.

Xiang, Y., Al, T., Mazurek, M., 2016. Effect of confining pressure on diffusion coefficients in clay-rich, low-permeability sedimentary rocks. Journal of Contaminant Hydrology 195, 1-10.

Yalçıntaş, E., Scheinost, A.C., Gaona, X., Altmaier, M., 2016. Systematic XAS study on the reduction and uptake of Tc by magnetite and mackinawite. Dalton Transactions 45, 17874-17885.

Yang, G., Prasianakis, N.I., S.V., C., 2020. Comparative modeling of ions and solvent properties in Ca-Na montmorillonite by atomistic simulations and fluid density functional theory. Clays and Clay Minerals.

Yang, J., Kukkadapu, R.K., Dong, H., Shelobolina, E.S., Zhang, J., Kim, J., 2012. Effects of redox cycling of iron in nontronite on reduction of technetium. Chemical Geology 291, 206-216.

Yang, X., Ge, X., He, J., Wang, C., Qi, L., Wang, X., Liu, C., 2018. Effects of Mineral Compositions on Matrix Diffusion and Sorption of 75Se(IV) in Granite. Environmental Science & Technology 52, 1320-1329.

Yaroshchuk, A.E., Van Loon, L.R., 2008. Improved interpretation of in-diffusion measurements with confined swelling clays. Journal of Contaminant Hydrology 97, 67-74.

Yuan, Wei, Zhang, Qin, 2019. A Numerical Simulator for Modeling the Coupling Processes of Subsurface Fluid Flow and Reactive Transport Processes in Fractured Carbonate Rocks. Water 11, 1957-1957.

Yuan, T., Ning, Y., Qin, G., 2016. Numerical Modeling and Simulation of Coupled Processes of Mineral Dissolution and Fluid Flow in Fractured Carbonate Formations. Transport in Porous Media 114, 747-775.

Yuguchi, T., Sasao, E., Ishibashi, M., Nishiyama, T., 2015. Hydrothermal chloritization processes from biotite in the Toki granite, Central Japan: Temporal variations of of the compositions of hydrothermal fluids associated with chloritization. American Mineralogist 100, 1134-1152.

Zachara, J.M., Heald, S.M., Jeon, B.-H., Kukkadapu, R.K., Liu, C., McKinley, J.P., Dohnalkova, A.C., Moore, D.A., 2007. Reduction of pertechnetate [Tc(VII)] by aqueous Fe(II) and the nature of solid phase redox products. Geochimica et Cosmochimica Acta 71, 2137–2157.

Zahasky, C., Benson, S., 2018. Micro-Positron Emission Tomography for Measuring Sub-core Scale Single and Multiphase Transport Parameters in Porous Media. Advances in Water Resources 115.

Zeelmaekers, E., Honty, M., Derkowski, A., Srodon, J., De Craen, M., Vandenberghe, N., Adriaens, R., Ufer, K., Wouters, L., 2015. Qualitative and quantitative mineralogical composition of the Rupelian Boom Clay in Belgium. Clay Minerals 50, 249-272.

Zhang, C., Liu, X., Lu, X., Meijer, E.J., Wang, K., He, M., Wang, R., 2016. Cadmium(ii) complexes adsorbed on clay edge surfaces: insight from first principles molecular dynamics simulation. Clays and Clay Minerals 64, 337-347.

Zhang, C., Liu, X.D., Lu, X.C., He, M.J., Meijer, E.J., Wang, R.C., 2017. Surface complexation of heavy metal cations on clay edges: insights from first principles molecular dynamics simulation of Ni(II). Geochimica Et Cosmochimica Acta 203, 54-68.

Zhang, W., Tang, X.-Y., Weisbrod, N., Zhao, P., Reid, B.J., 2015. A coupled field study of subsurface fracture flow and colloid transport. Journal of Hydrology 524, 476-488.

Zhu, Y., Elzinga, E.J., 2014. Formation of Layered Fe(II)-Hydroxides during Fe(II) Sorption onto Clay and Metal-Oxide Substrates. Environmental Science & Technology 48, 4937-4945.